

Technische Universität München TUM School of Natural Sciences

Field theoretical approaches to tensor network theory

Albert Gasull Celades

Vollständiger Abdruck der von der TUM School of Natural Sciences der Technischen Universität München zur Erlangung eines

Doktors der Naturwissenschaften (Dr. rer. nat.)

genehmigten Dissertation.

Vorsitz: Prof. Dr. Stefan Filipp

Prüfende der Dissertation: 1. Hon-Prof. Ignacio Cirac, Ph.D.

2. Prof. Dr. Frank Pollmann

Die Dissertation wurde am 30.10.2024 bei der Technischen Universität München eingereicht und durch die TUM School of Natural Sciences am 13.11.2024 angenommen.

ABSTRACT

This thesis focuses on the exact analytical description of quantum states, in either 1-or 2-dimensional systems, that are either proven or conjectured to be out of reach for tensor network (TN) techniques. In order to provide such analytical descriptions we introduce a new ansatz, which we call field tensor network states (fTNS), where we exploit the connection that these complicated states have with conformal field theory (CFT). The wavefunctions of both critical 1-dimensional systems and 2-dimensional chiral gapped topological order can be understood as correlators computed in an underlying CFT whose properties match those of the states via its conformal data. fTNS are a modification of TNs such that these CFT correlations can be exactly reproduced.

Firstly, we present the fTNS approach to describing phases of matter, as well as our main example throughout the whole thesis, the free boson fTNS. We begin by discussing all the intrinsic features of this ansatz, such as regularizations and gauge transformations. We then proceed to showcase the free boson fMPS and fPEPS, as the TN equivalent fTNS that recover the previously out-of-reach states. Afterwards, we present the most currently advanced form of the proof for the most important property of this tensors, which is their exact contractibility. Coupled to this concept, we also show how contracting the network of fTNS in different topologies has severe implications for the properties of the resulting states.

Secondly, we study how much of the analytical properties of 1-dimensional TNs can be translated to the free boson fMPS, specifically tackling the question of phase classification. To do so, we describe the structure of symmetries for the free boson fMPS, and provide an example in which the analogous theorem of SPT classification of TNs holds for fMPS. We then use this result to distinguish amongst the two topologically distinct groundstates of the critical point of the Majumdar-Ghosh model.

Thirdly, we showcase our study of the properties of another field theoretical approach to TNs, known as continuous TNs (cTNS). While this ansatz posesses a very clean and intuitive theoretical approach, its optimal use case scenarios are far from understood. By studying a property known as bulk-boundary correspondence of TNs, we provide an example in which a cTNS description provides an advantage in the description of a complicated field theory. Inspired by this result, we show the current state of our proof for a classification of the possible interesting scenarios that can arise within this formalism.

In summary, this thesis provides a collection of results that showcase the usage of field theoretical techniques in the context of tensor networks, providing a new avenue with which to describe physical states exactly that were previously out of reach for TNs.

ZUSAMMENFASSUNG

Diese Arbeit konzentriert sich auf die exakte analytische Beschreibung von Quantenzuständen in 1- oder 2-dimensionalen Systemen, die nachweislich oder mutmaßlich außerhalb der Reichweite von Tensornetzwerktechniken (TN) liegen. Um solche analytischen Beschreibungen zu liefern, führen wir einen neuen Ansatz ein, den wir Feld-Tensor-Netzwerk-Zustände (fTNS) nennen, wobei wir die Verbindung ausnutzen, die diese komplizierten Zustände mit der konformen Feldtheorie (CFT) haben. Die Wellenfunktionen sowohl kritischer eindimensionaler Systeme als auch zweidimensionaler chiraler lückenhafter topologischer Ordnungen können als Korrelatoren verstanden werden, die in einer zugrundeliegenden CFT berechnet werden, deren Eigenschaften mit denen der Zustände über deren konforme Daten übereinstimmen. fTNS sind eine Modifikation von TNs, so dass diese CFT-Korrelationen exakt reproduziert werden können.

Zunächst stellen wir den fTNS-Ansatz zur Beschreibung von Materiephasen vor, sowie unser Hauptbeispiel in der gesamten Arbeit, das freie Boson fTNS. Wir beginnen mit der Erörterung aller wesentlichen Merkmale dieses Ansatzes, wie Regularisierungen und Eichtransformationen. Anschließend stellen wir die freien Bosonen fMPS und fPEPS als TN-äquivalente fTNS vor, die die zuvor unerreichbaren Zustände wiederherstellen. Anschließend präsentieren wir die derzeit fortgeschrittenste Form des Beweises für die wichtigste Eigenschaft dieser Tensoren, nämlich ihre exakte Kontraktibilität. In Verbindung mit diesem Konzept zeigen wir auch, wie die Kontraktion des Netzes von fTNS in verschiedenen Topologien schwerwiegende Auswirkungen auf die Eigenschaften der resultierenden Zustände hat.

Zweitens untersuchen wir, inwieweit sich die analytischen Eigenschaften von eindimensionalen TNs auf das freie Boson fMPS übertragen lassen, wobei wir insbesondere die Frage der Phasenklassifikation angehen. Dazu beschreiben wir die Struktur der Symmetrien für das freie Boson fMPS und geben ein Beispiel, in dem das analoge Theorem der SPT-Klassifikation von TNs für fMPS gilt. Dieses Ergebnis nutzen wir dann, um zwischen den beiden topologisch unterschiedlichen Grundzuständen des kritischen Punktes des Majumdar-Ghosh-Modells zu unterscheiden.

Drittens stellen wir unsere Untersuchung der Eigenschaften eines anderen feldtheoretischen Ansatzes für TNs vor, der als kontinuierliche TNs (cTNS) bekannt ist. Während dieser Ansatz einen sehr sauberen und intuitiven theoretischen Ansatz darstellt, sind seine optimalen Anwendungsszenarien noch lange nicht verstanden. Durch die Untersuchung einer Eigenschaft, die als Korrespondenz zwischen Volumen und Grenzen von TNs bekannt ist, liefern wir ein Beispiel, in dem eine cTNS-Beschreibung einen Vorteil bei der Beschreibung einer komplizierten Feldtheorie bietet. Inspiriert von diesem Ergebnis zeigen wir den aktuellen Stand unserer Beweise für eine Klassifizierung der möglichen interessanten Szenarien, die innerhalb dieses Formalismus auftreten können.

Zusammenfassend bietet diese Arbeit eine Sammlung von Ergebnissen, die die Verwendung von feldtheoretischen Techniken im Kontext von Tensornetzwerken aufzei-

| gen und einen neuen Weg zur genauen Beschreibung physikalischer Zustände eröffnen, die zuvor für TNs unerreichbar waren. | | | | | | |
|--|--|--|--|--|--|--|
| | | | | | | |
| | | | | | | |
| | | | | | | |
| | | | | | | |
| | | | | | | |
| | | | | | | |
| | | | | | | |
| | | | | | | |
| | | | | | | |
| | | | | | | |
| | | | | | | |
| | | | | | | |
| | | | | | | |
| | | | | | | |
| | | | | | | |
| | | | | | | |
| | | | | | | |
| | | | | | | |
| | | | | | | |
| | | | | | | |
| | | | | | | |

LIST OF PUBLICATIONS

PUBLICATIONS AND PREPRINTS RELATED TO THIS THESIS

[1] Field Tensor Networks: Theorems, proofs and an exact representation of a 2 dimensional chiral gapped state.

A. Gasull, J. Ignacio Cirac, and Germán Sierra In preparation. See chapter 3.

[2] *Symmetries and field tensor network states* **A. Gasull**, Antoine Tilloy, J. Ignacio Cirac, and Germán Sierra Phys. Rev. B 107, 155102 (2023).
See chapter 4.

[3] Bulk-boundary correspondence of continuous Tensor Network states A. Gasull, A. Bochniak and J. Ignacio Cirac In preparation.
See chapter 5.

FURTHER PUBLICATIONS

[4] Crossdimensional universality classes in static and periodically driven Kitaev models Paolo Molignini, A. Gasull, R. Chitra, and Wei Chen Phys. Rev. B 103, 184507 (2021).

CONTENTS

| Al | ostrac | et | | iii |
|----|--------|---------|--|-----|
| Zι | ısamı | menfas | sung | iv |
| 1 | Intr | oductio | on | 1 |
| | 1.1 | Outlin | ne | 3 |
| 2 | Bac | kgroun | nd concepts and results | 5 |
| | 2.1 | Backg | round concepts on many-body theory | 5 |
| | | 2.1.1 | Gaps, phases and ground states | 5 |
| | | 2.1.2 | Entanglement in many-body ground states | 7 |
| | | 2.1.3 | Symmetries in many-body physics | 8 |
| | | 2.1.4 | An example of 1-dimensional SPT order | 10 |
| | | 2.1.5 | A short overview of quantum Hall physics | 12 |
| | 2.2 | Backg | round concepts on Tensor Network theory | 15 |
| | | 2.2.1 | Tensor Network states and diagrammatic notation | 15 |
| | | 2.2.2 | Matrix Product States and their limitations | 17 |
| | | 2.2.3 | Projected Entangled Pair States and chirality | 20 |
| | 2.3 | Backg | round concepts on Conformal field theory | 22 |
| | | 2.3.1 | Basics of conformal field theory | 23 |
| | | 2.3.2 | Modular Invariance | 31 |
| | | 2.3.3 | Boundary CFT | 32 |
| | | 2.3.4 | WZW models | 33 |
| 3 | Gen | eric fT | NS | 36 |
| | 3.1 | Gener | ic fTNS | 37 |
| | | 3.1.1 | From TNS to fTNS | 37 |
| | | 3.1.2 | Field-theoretical construction of the fTNS tensor | 39 |
| | | 3.1.3 | The free boson fTNS | 41 |
| | 3.2 | The fr | ree boson fMPS | 52 |
| | | | Explicit construction of the fMPS tensor | 52 |
| | | 3.2.2 | The fMPS tensor in momentum space | 54 |
| | 3.3 | The fr | ree boson fPEPS | 57 |
| | | 3.3.1 | Explicit construction of the PEPS functional | 57 |
| | | 3.3.2 | Regularization of the PEPS functional | 62 |
| | | 3.3.3 | The MPS functional as a limit of the PEPS functional | 65 |
| | | 3.3.4 | Chiral truncation of the generic and PEPS functional | 67 |
| | 3.4 | The se | ewing condition for the free boson | 68 |
| | 3.5 | | losing condition for the free boson | 84 |
| | 3.6 | | ok | 91 |

| 4 | fMP | S and symmetries | 94 |
|----|-------|---|-----|
| | 4.1 | Symmetries as fTNS | 94 |
| | | 4.1.1 Symmetries of the free boson fMPS | 95 |
| | | 4.1.2 Virtual symmetries as fMPSs | 98 |
| | 4.2 | The push-through relation of the free boson fMPS | 102 |
| | 4.3 | Application to the Majumdar-Gosh model and SPT phases | |
| | 4.4 | Outlook | 118 |
| 5 | cTN | S results | 120 |
| | 5.1 | Definition of continuous TNS | 121 |
| | 5.2 | The bulk-boundary correspondence of cTNS | 125 |
| | | 5.2.1 Fixed points of the transfer operator and its Lindblad form | 125 |
| | | 5.2.2 The transfer operator in Hamiltonian form | 128 |
| | | 5.2.3 A generic approach to the bulk-boundary problem | |
| | 5.3 | Outlook | 140 |
| Ac | knov | wledgments | 142 |
| Bi | bliog | raphy | 145 |

1 Introduction

Theoretical physics hopes to provide analytical descriptions of Nature derived from a basic set of principles in order to provide predictions and deepen our understanding. Throughout history, progress in our understanding has been driven by either theoretical predictions left to be confirmed by experimentalists across the globe, or by an experimental result left to be explained by theorists. As both the technical prowess of experimentalists grows across the world, finer and finer details of the underlying rules of Nature are brought to light. Equivalently, as theorists keep solving and understanding new problems, new languages and formalisms arise to explain more and more complicated phenomena. Very often these theoretical developments come forth due to the cross-over of ideas between different fields or mathematical formalisms. One such surprising cross-over has been the understanding of physics in terms of their computational complexity [5], which could be summarized as how hard would a given problem be for a computational machine with a given set of rules. Studying general problems under this viewpoint has allowed theoretical physicists to identify what seem to be the limits of what can be analytically and numerically solved.

One such limit is known as the many-body problem, in which one attempts to describe the properties of a system containing a number of N particles, where this number can be taken to be arbitrarily large. This problem is paramount, as it is present in most areas of physics, ranging from black hole physics, high-energy physics, molecular physics, biophysics and the most interesting for us, quantum physics and condensed matter physics. The many-body problem presents a major obstruction to providing theoretical predictions that begin from a microscopic description, as both our analytical and numerical techniques become completely impractical as N grows [6]. In the case of quantum physics, this is due to the exponential growth of the underlying Hilbert space used to describe our system. In other words, as the space in which our quantum states live grows, so do the possible patterns of the main ingredient of quantumness, entanglement.

Entanglement is the key property behind quantum mechanics [7], and the root of most of the interesting quantum collective phenomena that we can observe in Nature, albeit it also constitutes the main limiting factor behind our predictive power. While our formalism allows for very arbitrary patterns of entanglement, most interestingly the systems we encounter more often in Nature turn out to be simpler. This is due to the fact that Nature seems to tend towards certain organizations and/or patterns that establish certain preferred entanglement structures. This preferences arise in our formalism in the form of properties such as symmetries or locality constraints that limit the entanglement and therefore allow us to obtain a better handle in our descriptive power. Luckily, one of the most important situations in Nature, that of the ground state of a local system, has a very a "low" and controllable amount of entanglement [8]. This situation yields the following question: Do we really need the completely generic formalism to tackle this problem? In light of this question, the field of tensor networks was born, whose goal was to borrow tools from the field of quantum information,

designed to precisely understand entanglement, to more accurately describe scenarios in which the underlying entanglement structure of the system can be controlled and exploited.

Tensor Networks (TN) have provided a playground for theoretical physicists to gain further insight into the ground states, and low-lying excited states of several many-body systems that are often found in Nature [9–12]. Although not without its limitations, they have provided a very generic open window into the physics of low-dimensional systems, their dynamics and properties [13–17]. At their very core, TNs are a completely generic ansatz whose goal is to control the amount of entanglement present in the system as a fundamental property, which allows us to retain analytical control over the state. By demanding that this generic guess minimizes the energy of the system, one can find, accurately and with guarantees, the ground state of the system. This can be done in most cases approximately with numerical techniques, and in some cases even analytically, usually aided by symmetries or other constraints of the system.

Unfortunately, not all scenarios and systems in physics have such a benevolent entanglement structure that is adequate for a TN description, one such example being a critical system [18–20]. In a 1-dimensional critical system, the amount of entanglement grows beyond what the most basic tensor network can control efficiently [21], necessitating new tools in order to retain an analytical description of the system. New TN structures were designed to describe precisely this scenario [22], sacrificing the intuitive local structure of previous designs in order to increase the complexity of the output state. In a 2-dimensional system, describing the correlations of a critical system is well within the scope of the most basic TN structures. In this scenario, the challenge is to provide an exact description of a specific kind of systems called chiral gapped topologically ordered , which are a very important kind of state present in the field of quantum Hall physics [23–25]. While some numerical approaches have been put forward, a completely exact analytical description remains out of reach .

Quantum Hall physics is a very rich field, where the goal is to provide the wavefunction of the state of an interacting electron gas, usually subjected to a magnetic field [26–31]. Many consider the discovery of the quantization of the Hall effect as the first instance of topological order in physics. Not only do Hall systems have an inherent scientific interest due to the very rich physics that they host, but topological physics have found an increasing amount of applications for information-theoretic tasks. The potential use of this physics in the context of robust quantum information processing [32] sparked a new wave of interest in the quantum information community, and even the very recent realization of one such system in a state-of-the-art quantum simulator [33].

At this point, it seems that we have run into a crossroads. We can either sacrifice the analytically and numerically controllable structure of TNs in order to accommodate for the increasing complexity present in the Hall or critical physics, or we modify our TNs in a subtle way such that we can target these interesting states while still retaining analytical control. But how does one go about finding such an extension, specially given the currently known no-go results [34, 35] that point towards a potential inherent impossibility to describe Hall physics with TNs?

The answer comes from outside the field of quantum information, when Moore and Read realized that the wavefunctions present in the fractional quantum Hall effect (FQHE) could be obtained via a computation much more common in high energy physics [36]. They found that the wavefunctions of Hall physics could be exactly

described by a correlator of field operators for a very special field theory, known as a conformal field theory [37]. This insight drove the research in FQHE physics for a long time, extending our knowledge of both these systems and of topological quantum field theories and their relations to conformal field theories [38–41]. This discovery constitutes one of the earliest realizations of a concept that today is known as a bulk-boundary correspondence. The bulk-boundary correspondence is one of the most important features in the field of topological order, and its most important insight is that sometimes the theory that to describe a system can be shown to be dual, or equivalent, to a different theory on the boundary of the system, and thus in one less dimension. Sometimes, either the bulk or the boundary theory is easier to manage, and driven by this insight, newer and more exotic realizations of topological order were found [42]. Such an intriguing connection is also behind one of the most important theoretical advancements of the last decades in high energy physics, where this set of ideas takes the name of the holographic principle or the AdS/CFT correspondance [43].

We have finally reached the main insight from which this thesis arises. Is it possible to harness the power of conformal field theory, to extend the analytical power of tensor networks, such that we can exactly describe a wavefunction that demands an entanglement structure beyond of what is presently available? The original insight is due to Sierra and Cirac [44], where this question was originally postulated and resolved, showing that in some cases they had a perfect description via numerical techniques. From that point onwards, there have been many contributions that have set many stepping stones solidifying the use of conformal field theory in the description of many-body systems [45–50], both critical and chiral. Most of these developments fully rely on the formalism of conformal field theory itself, drawing ideas from TNs to achieve new results.

This thesis aims to provide such a new TN formalism, which we call field TNS (fTNS) which can help us in understanding these systems from the TNs prespective. fTNS constitute a generalization of standard TNs in which we allow for the correlations between the different constituents of the system to be controlled by an underlying conformal field theory. This means that now the different parts of the system can interact through the Hilbert space of a field theory, which in stark contrast to standard TNs, is an infinite dimensional space. An immediate consequence of this choice, is that we will not be able to describe any state of the generic many-body Hilbert space with fTNS, but only those that fall under the description of the conformal field theory as well. While this may seem like a problem a priori, this is precisely the compromise that allows us to retain the analytical control over the state. This analytical control is guaranteed by conformal field theory, which allows us to provide exact TNs-like representations of previously analytically unreachable states via standard TN techniques.

1.1 OUTLINE

This thesis is organized as follows. In Chapter 2 we begin with a broad overview of the different kinds of many-body phenomena that are relevant for us, focusing mainly on the difference between gapped and gapless Hamiltonians. We also provide a couple of examples of systems that are relevant for us, such as a symmetry protected topological state in a 1-dimensional system and some of the basics of Hall physics. We then move on to provide a short overview and introduction to tensor networks, while

also presenting the main results and theorems that are relevant for latter chapters of this thesis. Finally we present a brief introduction to conformal field theory, such that some of the concepts that inspired fTNS can be more easily understood.

In Chapter 3 we present field tensor network states, our new ansatz for many-body states. We focus on the first known example of fTNS, the free boson fTNS. We begin by deriving the free boson fTNS from first principles and showcase how to understand and remove all potential divergences from the tensor. As we wish to always target chiral states, we show how to perform a chiral truncation of the tensor and also show that Möbius transformations act as a gauge freedom of the tensor. We then move on to present the free boson fTNS for a critical 1-dimensional system, which we call the free boson fMPS, alongside its momentum space representation. Our next step is then to provide an extensive study of its 2-dimensional equivalent fTNS, the free boson fPEPS, which is a candidate for an exact description of gapped chiral topological order. We study its regularization structure, as well as its connection to the fMPS tensor and its chiral truncation. The most important part of this chapter is the proof of the arbitrary sewing condition, which deals with exact contraction between any two compatible free boson fTNS. As an application of the sewing condition, one can fully contract an fTNS to obtain back a chiral wavefunction with different topologies.

In Chapter 4 we provide evidence that the theory of 1-dimensional TNS can be translated to fMPS, allowing to preserve our intuition from TNS in a realm in which it was previously impossible to do so analytically. To establish a parallel with the standard theory of phase classification in 1-dimensional TNS, we derive the relation between the finite representation of SU(2) on the physical index of a fTNS and its corresponding representation as functional conformal charges on the virtual space. We also use this construction to identify the different topological properties of the two distinct ground states of the Majumdar-Ghosh point of the J_1-J_2 model.

In Chapter 5 we present a different field-theoretical ansatz called continuous Tensor Networks (cTNS), as an ansatz designed to tackle physical quantum field theories by coupling them to a virtual quantum field theory in the same spirit as TNs. We then focus our efforts to theoretically studying when using a cTNS can be advantageous in order to provide predictions for complicated QFTs. Guided by an example related to the sine-Gordon theory, in which a correlator of a complicated coupled physical bosonic field theory can be computed as a fixed-point correlator of a specific cTNS, we attempt to understand the general structure behind the bulk-boundary correspondance of cTNS.

2 BACKGROUND CONCEPTS AND RESULTS

In this Chapter, we will introduce most of the relevant terminology and background concepts used throughout the thesis. As discussed in the introduction, this thesis lies at the intersection between many-body theory, tensor networks, and conformal field theory. Naturally, we will provide the necessary context from each of these disciplines to elucidate the forthcoming chapters

2.1 BACKGROUND CONCEPTS ON MANY-BODY THEORY

In this thesis, we will use highly correlated quantum spin Hamiltonians as the main subject of study. We wish to consider these systems an effective description for a real material, atomic gas or even a quantum field theory. The quantum spin Hamiltonian arises then as a discretization of the continuous Hilbert space where a lattice is defined, and a tensor product structure is endowed on every site to represent the localized degrees of freedom. These degrees of freedom can range from spins, fermions, localized orbitals such as Wannier modes [51], or more complex algebraic structures. Therefore, the problem reduces to solving an effective Hamiltonian that acts on such a tensor product structure of the local modes.

Suppose the local Hilbert space associated with every site is the one of a spin representation with a local Hilbert space dimension j. In that case, the total Hilbert is given by $\bigotimes_{i=1}^N \mathbb{C}^j$ where N is the total number of lattice sites. This entails an exponential growth of the Hilbert space as N approaches the thermodynamic limit, which makes it a completely intractable problem. Not only is it QMA hard for a classical computer to find the ground state of the system [52], but even approximating it with a quantum computer is a hard task [53]. Furthermore, the problem of computing correlation functions or dynamics of the system is also generically hard, even for probabilistic simulations [54].

As the generic non-local problem will tend to be unmanageable, it is mandatory that we start performing sensible approximations that reduce the complexity down to a more tractable scenario. The first and most natural approximation is to demand locality of the quantum Hamiltonian. This property is enough to allow us to begin classifying the different kinds of states that exist within the many-body Hilbert space.

2.1.1 GAPS, PHASES AND GROUND STATES

A very common starting point for physics is to begin the exploration of the physical system from the Hamiltonian. We define a local quantum spin Hamiltonian on a lattice Λ with sites Λ_s as

$$H_{\Lambda} = \sum_{X \in \Lambda_s} h_X \tag{2.1}$$

where X is a set with compact support, and h_X is a local Hamiltonian on the compact support with either power-law or exponentially decaying correlations as in [8]. If all the different h_X can be minimized independently, we call the system frustration-free. Under these assumptions, it is possible to classify quantum Hamiltonians according to their spectral properties, as seen in [55, 56]. Informally, one classifies a Hamiltonian as gapped if there exists a spectral gap between the potentially degenerate ground state sector and the rest of the spectrum as one approaches the thermodynamic limit $N \to \infty$. If no such gap exists in the thermodynamic limit, then we call the Hamiltonian gapless.

The notion of a gap of local Hamiltonians is crucial in understanding the properties of the ground state of the system. The major consequence of such a gap is that any correlation function between two operators that are far apart will always show an exponential decay with respect to the distance between them, a property known as exponential clustering [57]. On the other hand, an algebraic decay of correlations is a sign of gapless behavior [37].

Although we may have knowledge about the entire spectrum, the central object of interest in any quantum spin system is the ground state, as quantum features are most pronounced at low temperatures. The structure of the ground state wave function dictates the features of the elementary excitations or particles, which can then be observed in experiments. Yet, and as explained above, finding any such generic ground state is a difficult task, even though local systems force a special structure on the ground state that allows us to target it with tensor network techniques [10].

The locality of the Hamiltonian forces the other eigenvectors with low energy to be simple local perturbations of the ground state [58], and this feature is responsible for the existence of localized elementary excitations. We usually observe these states as single-particle excitations above the ground states, and thus we further cement why the ground state is such a relevant object even if the system under consideration is not at zero temperature. This has to be contrasted to a generic eigenvalue problem where knowledge of the extremal eigenvector does not give any information about the other eigenvectors except for the fact that they are orthogonal to it. Without locality, physics would be even more wild and uncontrollable from a theoretical standpoint.

Because ground states are one of the main objects of interest for the purpose of many-body physics, it seems natural to shift the focus away from the Hamiltonian as the central object and instead develop a theory that focuses on the states themselves as the central objects. One can define a state $|\psi\rangle$ to be gapped if and only if there exists a gapped Hamiltonian H according to the previous definition for which $|\psi\rangle$ acts as a ground state, which we call the parent Hamiltonian. Accordingly, a state will be called gapless if one such gapped Hamiltonian can not be found. The main caveat of this definition is that $|\psi\rangle$ can simultaneously be the ground state of other Hamiltonians as well, and some of those may be gapless and are usually referred to as uncle Hamiltonians, as shown in [59, 60].

With the focus now on the ground states themselves, we can now group different states to form a phase of matter. Historically, the most successful theory of quantum phase transitions was developed by Landau in 1937 [61], which relied on the notion of symmetry-breaking through group theory. This successful theory led to the complete classification of most classical solid phases of matter, as well as gas and liquid ones. In Landau's theory, one understands the notion of a phase by the collection of states that either preserve or break a given symmetry. However, with the discovery of the Berezinskii-Kosterlitz-Thouless transition [62] in 1973 and the fractional quantum Hall

effect [63] in 1982, it became clear that there were phases of matter beyond the Landau paradigm. In 1989, the missing pieces were provided by a new framework for gapped quantum phases, whose name became topological phases, which includes phases with and without symmetry-breaking [64–66].

The suitable definition of a phase of matter that accommodates topological physics is as follows:

Gapped Phase of Matter: Two gapped local Hamiltonians H and H' are in the same gapped phase of matter if and only if there exists a path of local gapped Hamiltonians H_{γ} with $\gamma \in [0,1]$ such that $H_0 = H$ and $H_1 = H'$.

In other words, two states belong to the same phase if their respective Hamiltonians can be continuously connected without closing the gap along the way. A closure of the gap is then what signifies the phase transition. We will usually denote the trivial phase as whichever phase contains product states. Equipped with a notion of phases, we can now begin further coarsening this classification according to the entanglement signatures of the states.

2.1.2 Entanglement in many-body ground states

So far, we have seen that ground states of frustration-free gapped local Hamiltonians are able to minimize all the local terms of the Hamiltonian h_X simultaneously. We can therefore exchange the question of finding the ground state by diagonalization of H_Λ for the question of finding a density matrix ρ_Λ whose marginals simultaneously extremizes all the terms ${\rm Tr}\,[h_X\rho_\Lambda]$. Sadly, this is a problem known as the N-representability theorem [67], which is also known to be untractable generically [68].

While not surprising, this teaches us something important about ground states, which is that all the global features of the state, such as correlation lengths, topological order, entanglement, and excitations, all follow from this set of local conditions. Global features of the state have to be encoded locally in the state, and it turns out that this situation corresponds to states that have very little quantum entanglement [69–72].

Entanglement is the key property that is particular to quantum systems only. We can intuitively think of entanglement, the shared resource of a quantum state that correlates the different parties beyond what is classically possible. If one considers a quantum spin system whose ground state is given by $|\psi\rangle$, one can partition the system in disjoint connected regions A and B, such that ρ_A and ρ_B are the corresponding ground state reduced density matrices. One can quantify the entanglement between these two regions by means of the Von-Neumann entanglement entropy [73] as

$$S(\rho_A) = S(\rho_B) = \operatorname{Tr}\left[\rho_A \log \rho_A\right], \tag{2.2}$$

where ρ_A stands for the reduced density matrix, albeit there are many distinct ways with which one can quantify entanglement [74]. The existence of measures with which to quantify entanglement naturally leads to the notion of states that maximize them, known as maximally entangled states [75]. A surprising feature of quantum mechanics is that it seems that entanglement is a monogamous quantity [76], and therefore, if a subregion A is maximally entangled within itself, it will share no entanglement with the complement B. If we translate this concept to a system of spins, the more a spin can interact with other ones, the less entanglement it can share simultaneously with

all of them. This result is formalized in the quantum De Finetti theorem [77], and it is the underlying reason why mean field theory works increasingly well in higher dimensional systems.

We have finally reached a point in which we can understand what we meant with the statement that ground states of local gapped frustration-free have little entanglement. In classical systems, the competition between entropy and energy gives rise to phase transitions and collective phenomena. In quantum physics, the competition between monogamy of entanglement and the minimization of all the extremals ${\rm Tr}\,[h_X\rho]$ is what leads to quantum collective phenomena.

The key is, therefore, to understand how entanglement is being shared amongst the different degrees of freedom of the quantum state. Intuitively, for a given spin, it is of no use to have strong correlations with far-away spins, as this will only bring the marginals further away from the extremal points. The strongest (quantum) correlations it needs to have are with those spins with which the locality of the Hamiltonian forces it to interact with. It is then natural to imagine that the entanglement between a bipartition of a big system in two regions is proportional to the surface between them, and this area law for entanglement is exactly the notion of little entanglement that gapped states have. In equation form, ground states of gapped local frustration-free Hamiltonians obey the area law of entanglement [8, 78], in which the entanglement entropy between a region A and its complement behaves as

$$S(\rho_A) \le f \partial A \tag{2.3}$$

where ∂A is the boundary of the region A, and f is a generic numerical function determined by the specifics of the geometry. This property is in stark contrast to the situation for a generic state of the many-body Hilbert space, which in general exhibits a volume law entanglement [79].

So far, we have left gapless states and systems on the side, and the underlying reason is that they are significantly more complicated than gapped ones. From the gapped phases of matter perspective, we have associated gapless states with the phase transition points, and therefore, these will be states that will, in general, not obey the area law. In general, these states tend more towards logarithmic-like laws, as shown in [80]. The one particular example that is well understood is the critical point of 1-dimensional spin systems, in which the entanglement entropy for a region of length L scales as [21, 81]

$$S_L \sim \frac{c}{3} \log L,\tag{2.4}$$

where \sim stands for equality up to L-independent constant corrections, and c corresponds to the central charge of the associated conformal field theory of the critical point. Because the area law for 1-dimensional systems means that any subregion can have, at most, a constant amount of entanglement, critical states have, in general, more entanglement than their gapped counterparts and are, therefore, more complicated to study.

2.1.3 Symmetries in Many-Body Physics

We will now briefly present the results of [82], in which an even more coarse classification of gapped phases of matter was provided. The first distinction that the authors make is between the notions of short-range and long-range entangled order.

The definition of a gapped phase of matter established an equivalence class between gapped states that were connected via a path of local gapped Hamiltonians. One can show that this criterion is equivalent to the statement that there exists a local unitary (LU) evolution that connects both states, as given by the adiabatic theorem [83]. Because an LU evolution can remove entanglement from the system in a local way, we call a state short-range entangled if and only if it can be transformed via an LU to an unentangled state, a direct product state.

Conversely, a state is long-range entangled if no LU evolution can reduce it to an unentangled state. Topological order, in fact, provides all the equivalence classes defined by LU evolutions. According to this criterion, it would seem that there are only two possible phases of matter within the realm of gapped phases. However, the story changes the moment that we introduce symmetries.

We know that group theory and the notion of symmetries are the backbone behind Landau's paradigm of phases of matter. In the previous definition, the LU evolution is, in general, able to connect any two states that may be ground states of Hamiltonians with completely different symmetries. This is very different from the situation in Landau's paradigm, in which the different phases were characterized by a progressive breaking of the symmetry group. This motivates the study of the problem of phase classification under a different criterion, which is that of symmetric LU or, conversely, under paths of gapped symmetric Hamiltonians. According to this criterion, neither the gap is able to close, nor the symmetry can be broken along the path that connects any two states.

In 1-dimensional systems, it turns out that there is only a single gapped phase under LU, the trivial phase. However, under symmetric LU, one can distinguish between the trivial phase and the simplest form of short-ranged topological order, symmetry-protected topological states (SPT) [84]. Particular of 1-dimensional systems is the fact that no long-ranged entangled order can exist, which leads to the sometimes confusing notion that there is no topological order in 1 dimension.

SPT order was originally found in the Haldane chain model [85–89], which is a nearest-neighbor odd-spin system protected by spin rotation symmetry given by the group SO(3). An important signature of such phases is that they sometimes exhibit gapless protected edge states, which are robust under any perturbation that does not break the symmetry of the model. SPT phases are very well understood and have been classified in many different dimensionalities, as shown in [90–92]. Of special importance for this thesis is the result shown in [93], in which tensor networks are used as a very natural language with which to fully classify SPT order in one dimension. Most interestingly, a complete classification can be found even in the thermodynamic limit, as shown in [94]. We will showcase an example of a model hosting SPT order in the next sections.

For systems in two dimensions and beyond, long-range entangled topological order can emerge, both under an LU or a symmetric LU criterion. This is the family of states, which is known as true topological order. While providing an exhaustive collection of all the different kinds of known topological order is beyond the scope of this summary, we will focus our attention in the upcoming sections on what is considered to be the first discovery of topological order, the fractional quantum Hall effect. For a complete classification of long-ranged gapped topological order in terms of category theory, we refer the reader to the literature on string-net models [95], and note that an equivalent formulation in terms of tensor networks is also known [96].

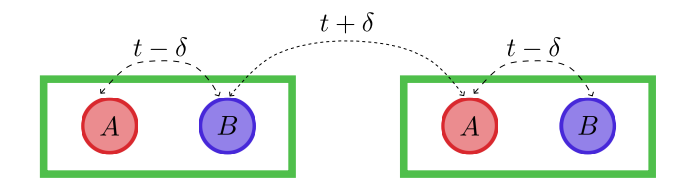


Figure 2.1: Schematic drawing of the SSH Hamiltonian, where both unit cells as well as the different interactions are depicted.

We have seen how the different patterns of entanglement are related to the different phases of matter that we find in Nature. We have also seen that these gapped phases of matter do not have a particularly large amount of entanglement, which is the insight that inspired the variational class of tensor network states. As we will see in the upcoming sections, tensor networks provide a natural language with which to study the ground state of the many-body problem, both analytically and numerically. For the remainder of the section, we will briefly showcase both an SPT state in one dimension, as well as some of the main features that surround the topological order associated with the fractional quantum Hall effect.

2.1.4 AN EXAMPLE OF 1-DIMENSIONAL SPT ORDER

In this section, we will study the SSH model as a paradigmatic example of SPT order in 1 dimension. This model was originally proposed in [97], and the authors originally interpreted the modern notions of SPT order as solitonic excitations of the spin-chain.

The SSH model describes the hopping of spinless fermions on a 1-dimensional chain whose unit lattice contains two sites, which we will denote by A and B. On a chain with N sites and open boundary conditions, the Hamiltonian is given by

$$\mathcal{H}_{\text{SSH}} = (1 - \delta) \sum_{j=0}^{N-1} \left(c_{A,j}^{\dagger} c_{B,j} + \text{h.c.} \right) + (1 + \delta) \sum_{j=0}^{N-2} \left(c_{B,j}^{\dagger} c_{A,j+1} + \text{h.c.} \right) \tag{2.5}$$

where $c_{A,j}$ and $c_{B,j}$ are the creation and annihilation operators on either sub-lattice A or B at unit cell j, and δ is the parameter of the model which we call the dimerization parameter. The intuitive understanding of this model is that fermions hop between different unit cells with strength $1-\delta$ and within the same unit cell with strength $1+\delta$, as shown in Figure 2.1.

Thus, depending on the sign and strength of δ the fermions will prefer to move within or between unit cells. In the first example, we will end up with a more localized pattern of entanglement, whilst in the second one with a pattern much more spread across the entire chain.

One can easily diagonalize this Hamiltonian imposing under periodic boundary conditions by means of the Fourier transform of the fermionic operators

$$c_{A,k}^{\dagger} = \frac{1}{\sqrt{N}} \sum_{j=0}^{N-1} e^{-ijk} c_{A,j}^{\dagger}$$
 (2.6)

where k is the label of the momentum modes, which takes values in $k = \frac{2\pi n}{N}$ with n = 0, ..., N-1. After Equation (2.6) is used for both sub-lattice modes (2.5) one

reaches the following Bloch Hamiltonian

$$\begin{split} \mathcal{H}_{\text{SSH}} &= \sum_{k} \vec{c}_{k} h_{\text{SSH}}(k) \vec{c}_{k}^{\dagger} \\ h_{\text{SSH}}(k) &= \sigma^{x} \left((1-\delta) + \cos(k)(1+\delta) \right) + \sigma^{y}(1+\delta) \sin(k) \end{split} \tag{2.7}$$

where $\vec{c}(k)$ is a 2-dimensional vector that groups the momentum operators for both sub-lattices. The energy bands $\pm \epsilon(k)$ of this Hamiltonians can be computed to obtain

$$\epsilon(k) = \sqrt{2}\sqrt{(1+\delta^2) + \cos(k)(1-\delta^2)}.$$
 (2.8)

We see that this dispersion relation can only be gapless if and only if $\delta=0$, where the gap closes at momentum $k=-\pi$. The gap closure signifies that this is the phase transition between the two potentially different gapped phases of this model. To see the difference between these two regions, we must examine the model once again with open boundary conditions.

As we only need to characterize one point within the phase, we choose the simplest possible points in each of the phases, corresponding to $\delta=\pm 1$.

We begin with $\delta=-1$, where the second term of the Hamiltonian in Equation (2.5) disappears, and therefore only intra-cell hopping is present in the model. We call this phase the fully dimerized phase, as only two fermions can place themselves in each unit cell, therefore forming an array of pairs within cells. Furthermore, in this limit, the Hamiltonian with open boundary conditions is identical to the one with periodic boundary conditions and, therefore, a fully gapped system with N levels at energy +2 and another N more at energy -2.

On the other hand, at the point $\delta=1$, only inter-cell hopping is present in the SSH Hamiltonian. In the bulk of the SSH chain, two sites in adjacent unit cells form pairs that decouple themselves energetically from the rest of the system. In analogy to the case $\delta=-1$, they lead to N-1 levels at energy +2 and N-1 levels at energy -2 in the single particle energy spectrum. However, the mode operators for the fermions at the two ends of the chain, $c_{A,0}^{\dagger}$ and $c_{B,N-1}^{\dagger}$, do not appear in the Hamiltonian. Hence, these operators create excitations with zero energy, which are fully localized on the two ends of the chain.

The appearance of gapless edge modes is the key difference between both phases, and we will denote the trivial phase as the one without them. This model very clearly exemplifies the competition between locality and monogamy entanglement. In the trivial phase, all unit cells are able to simultaneously satisfy a monogamous entanglement setting within each cell, essentially leading to a product state in the basis of unit cells. Yet, in the SPT phase, prioritizing the formation of the maximally entangled pairs leaves the edges unable to pair due to the locality constraints of the interaction.

It is possible to define for this kind of models a genuine order-parameter that captures the different topological features of each phase called a winding number for 1-dimensional systems, and Chern number for higher dimensional systems. If one writes any Bloch Hamiltonian in the form

$$h(k) = \hat{n}(k) \cdot \vec{\sigma} \tag{2.9}$$

where $\hat{n}(k)$ is a unit normal momentum-dependent vector that also defines the dispersion relation as $\epsilon(k) = \hat{n}(k)^2$. One then defines the winding number of the system as

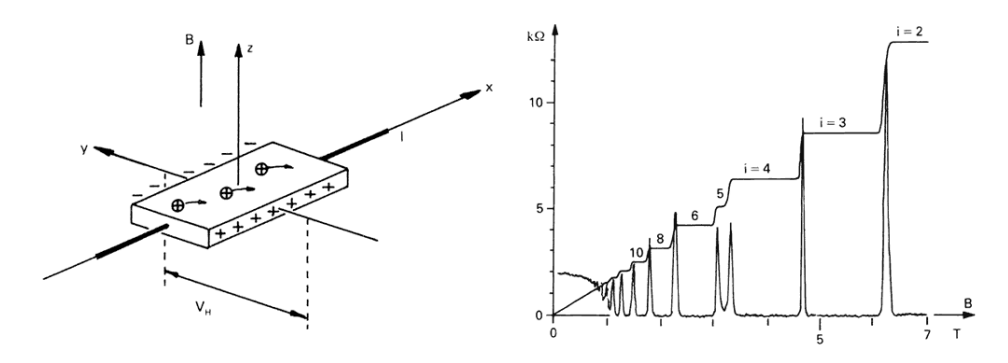


Figure 2.2: (left) Schematic of an experimental setup for observing the quantum Hall effect. (right) Hall resistance and longitudinal resistance as a function of magnetic field B in the integer QHE. The plateaus in the Hall resistance with vanishing longitudinal resistance are clearly visible. From the 1998 Press Release of the Swedish Academy of Sciences.

the integral

$$w = \frac{1}{2\pi} \int_0^{2\pi} dk \, \hat{n}(k) \cdot (\nabla \times \hat{n}(k))$$
 (2.10)

which is guaranteed to be an integer due to the fact that this is an underlying topological invariant of the vector Bloch bundle [98]. For a complete classification of topological insulators and superconductors as well as a presentation of their topological invariants, the 10-fold AZ classification in [99, 100].

2.1.5 A SHORT OVERVIEW OF QUANTUM HALL PHYSICS.

As mentioned in the introduction, the discovery of the quantum Hall effect (QHE) [63, 101] is considered to be the original discovery of topological order. This effect is observed in 2-dimensional electron gases at very low temperatures that are subject to a strong transverse magnetic field B. Such a setup is shown in Figure 2.2, where the electron gas lies in the xy-plane and the magnetic field points in the positive z-axis. An electrical current in the positive x then causes the appearance of the Hall voltage V_H in the y-direction between the edges of the sample. Following Ohm's law, classical physics would predict that the resistance R_H associated with this voltage difference would grow linearly with the magnetic field. However, the great discovery found in [101] was that at very low temperatures and strong magnetic fields, R_H displays plateaus where the resistance remained constant independently of the magnetic field and the longitudinal resistance vanishes! This is shown in the right of Figure 2.2. The even more surprising observation is that the Hall conductivity, defined as the inverse $\sigma_H = \frac{1}{R_H}$ was given, to an astonishing accuracy, by,

$$\sigma_H = \nu \frac{e^2}{h},\tag{2.11}$$

where e and h are fundamental constants, and $\nu \in \mathbb{N}_{>0}$. This phenomenon is commonly referred to as the Integer QHE (IQHE), and it was this discovery that sparked the field of topological phases of matter. As changing the value of the magnetic field does not break any symmetry, the transitions between the different plateaus had to have a description beyond the Landau paradigm. To understand this problem further, and

its relation with the Laughlin wave function, let us start with a short derivation of the IQHE.

We begin from a 2-dimensional gas of electrons of charge e and mass m in the x-y plane subjected to a strong magnetic field pointing in the positive z-direction, whose Hamiltonian is

$$\mathcal{H}_{\text{IQHE}} = \frac{1}{2m} \left[\left(-i\hbar \partial_x - \frac{e}{c} A_x \right)^2 + \left(-i\hbar \partial_y - \frac{e}{c} A_y \right)^2 \right], \tag{2.12}$$

where \vec{A} is the vector potential associated to the magnetic field, c is the speed of light. We will work with the geometry of a disk, such that the components of the vector potential are given by $A_x = -y\frac{B}{2}$ and $A_y = x\frac{B}{2}$. One can then diagonalize this Hamiltonian due to rotational invariance and obtain the spectrum of eigenenergies, usually called Landau levels

$$E_n = \hbar \omega_c \left(n + \frac{1}{2} \right), \tag{2.13}$$

where $n \in \mathbb{N}_{>0}$ is the Landau level, ω_c is the cyclotron frequency, and all the different eigenenergies are highly degenerate [102].

The set of degenerate states, also called single-particle orbitals, at each Landau level n can be labeled by their angular momentums, according to the rule that $L_z=m\hbar$ with an integer $m\geq -n$. If we denote by N_ϕ the total number of states at the $n^{\rm th}$ Landau level, then the filling fraction is defined as

$$\nu = \frac{N}{N_{\phi}},\tag{2.14}$$

where N is the number of filled single-particle orbitals. If we assume that $\nu \leq 1$, then only the levels within the lowest Landau level (LLL) can be occupied. Then, in the LLL the single-particle orbitals are described by the wave function

$$\psi_m(z) = z^m e^{-\frac{|z|^2}{(4l_0)^2}},\tag{2.15}$$

where z=x+iy, l_0 is a parameter called the magnetic length, which is controlled by the strength of the magnetic field as $l_0\sim \frac{1}{\sqrt{B}}$. If the disk has radius R, then the total number of states is given by

$$N_{\phi} = \frac{R^2}{2l_0^2}. (2.16)$$

Let us now explore the situation in which we keep increasing the magnetic field B, such that the Fermi energy of the system sits between the LLL and the next Landau level. It is usually assumed that under such magnetic fields, the electrons become completely polarized, and therefore, their behavior is simplified to be that of spinless fermions.

In this case, the many-body ground state is given by filling the N_ϕ states of the LLL only once, meaning that $\nu=1$. The final wave function is then simply given by the Slater determinant

$$\psi_{\nu=1}(z_1, ..., z_n) = \prod_{1 \le i < j \le N} (z_i - z_j) e^{-\frac{1}{4t_0^2} \sum_{i=1}^N |z_i|^2}, \tag{2.17}$$

as required per the Pauli principle. If one repeats this analysis for a toroidal geometry, one can find that the Hall conductivity of this system is given by precisely a topological invariant, the Chern number [103, 104]. This places the IQHE as a topological insulator, and therefore, it does not host true topological order. In order to host true topological order, the system needs to both show excitations that posses anyonic behavior as well as a groundstate degeneracy that reflects the underlying topology of the manifold [32, 105].

The reason why the QHE is so prominent in the field of topological physics is because many years after the discovery of the IQHE, the fractional quantum Hall effect (FQHE) was discovered [63]. New plateaus were found at filling fractions such as $\nu=\frac{1}{3}$ or $\nu=\frac{2}{5}$. These plateaus host all the elementary excitations associated with true topological order and their fractional excitations and statistics. Not only has this phenomenon been theoretically predicted, but the fractional charges of the excitations have been experimentally observed [105, 106] and even more recently, their exchange statistics [107–111].

The understanding of these plateaus necessitates very strong interactions among the electrons. Due to the strong interaction effects, the ground states of realistic microscopic models hosting intrinsic topological order are generally very difficult to compute. Instead, one frequently relies on model wave functions which are easier to analyze and capture the essential properties of the phase. Here, we will focus on one specific class of model wave functions: the Laughlin states [112]. These wavefunctions were originally designed to capture the many-body ground states of the FQHE at filling fractions $\nu = \frac{1}{q}$ with q odd.

The fermionic wavefunction that Laughlin proposed is given by

$$\psi_{\nu = \frac{1}{q}}(z_1, ..., z_n) = \prod_{1 \le i < j \le N} (z_i - z_j)^q e^{-\frac{1}{4l_0^2} \sum_{i=1}^N |z_i|^2}, \tag{2.18}$$

where the crucial difference is the appearance of the power q in the polynomial. While this wavefunction is not the ground state of any realistic Hamiltonian, it has a surprising overlap with the wavefunctions obtained from exact diagonalization studies [44, 113]. An intuitive reason behind this is that $\psi_{\frac{1}{q}}$ is the exact groundstate of a short-range Hamiltonian, and knowing that electrons have a strong short-range repulsion, it seems that this wavefunction is mainly capturing this feature.

The FQHE is not a consequence of the fermionic character of the constituents but a new phenomenon brought forth by the degeneracies of the different Landau levels. When one attempts to write down an effective field theory that captures the essential features of fractional charges and statistics for the excitations, one rediscovers a well-known action of high-energy physics, the Chern-Simons theory [114].

The Chern-Simons theory belongs to a family of field theories known as topological quantum field theories (TQFT) [115]. While an extremely interesting topic in their own right due to their intricate connections to modular theory or modular fusion tensor categories [116, 117], these theories are important for the description of topological theories as they provide a natural representation of the fusion and braiding mechanism that define the excitations of the FQHE.

In 1991, inspired by this connection with field theory, Moore and Read [36, 118] had the fundamental insight that the polynomial part of the wavefunction found in Equation (2.18) could be written as a conformal block of a 2-dimensional conformal

field theory (CFT). This insight held for both the fermionic and bosonic FQHE and sprung forward a new wave of research that began exploring the connection between these states and CFT, even reaching string theory versions of the FQHE [119]. Years later, with the discovery of the Chern-Simons/Wess-Zumino-Witten duality, it was finally understood why the CFT wavefunctions were so good at recovering the properties of the TQFT, they were, in fact, dual to one another [120, 121].

The essential insight of Moore and Read is that the polynomial part of the wavefunction of the FQHE could be, in many instances, written as

$$\psi(z_1, ..., z_n) = \langle \phi_1(z_1), ..., \phi_n(z_n) \rangle_{\text{CFT}}, \tag{2.19}$$

where $\phi_i(z_j)$ is a given set of primary and/or descendant fields of the CFT, which will be properly defined in the following sections. This insight is also the main piece of information that we need for the rest of the thesis and the one upon which we will base our new ansatz.

2.2 BACKGROUND CONCEPTS ON TENSOR NETWORK THEORY

We have seen so far that ground states of quantum gapped local Hamiltonians reside in a smaller subset of the generic quantum many-body Hilbert space as they must obey the area-law of entanglement. In order to efficiently describe these states with low entanglement, originally called finitely correlated states [9], a new language was introduced and its what today we call Tensor Network States (TNS). Their popularity rose up as a strong numerical tool for 1-dimensional systems thanks to the density matrix renormalization group algorithm by White [122], and nowadays they are well established both as a numerical technique for arbitrary dimensionalities as well as an analytical tool. There are many excellent reviews on TNS available in the literature, amongst which we recommend [12] and [11] for newcomers. For the more mathematically inclined reader, we recommend the more recent [10].

2.2.1 Tensor Network states and diagrammatic notation

As previously discussed, the goal is to provide the wavefunction of a generic many-body state, which for the sake of simplicity we will assume to consist of n local Hilbert spaces of dimension d. The most natural example of such a setting would be a system consisting of N spins. The wavefunction of such a system is generically given by

$$|\psi\rangle = \sum_{s_1,...,s_n} \psi_{s_1,...,s_n} |s_1\rangle \otimes,..., \otimes |s_n\rangle, \tag{2.20}$$

where s_i is the label of the local Hilbert space basis. We will group the d^n coefficients ψ_{s_1,\dots,s_n} in a single object which we will call a tensor. For us, a tensor is nothing but a multidimensional array of complex numbers with labeled entries, contrary to the usual definition of the word tensor used in linear algebra. We will denote one such tensor diagrammatically with

$$\psi_{s_1,\dots,s_n} = \psi \qquad (2.21)$$

where each leg of the box correspond to each of the open indices of the tensor. Every open leg of the tensor is thus labeled by the index of the basis of the local Hilbert space, and therefore can take values $s_i=1,...,d$. It is useful to think of the legs of the tensors as the diagrammatic representation of vector spaces themselves, such that then we have the following diagrammatic identifications

vector matrix tensor
$$j \longrightarrow i$$
 $j \longrightarrow i$ $A_{ij}|i\rangle\langle j|$ $A_{ijkl}|i\rangle\langle jkl|$, (2.22)

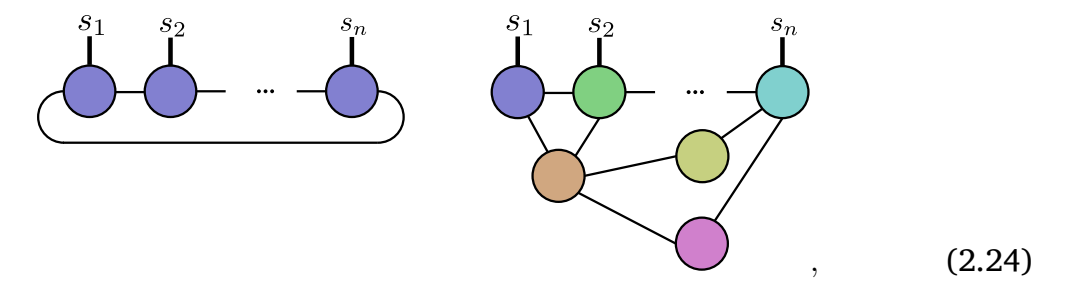
where it is important to note that we have used the right/left leg to denote the vector space and its dual. Alternative representations of this notion can also be found in the literature with arrows that either point towards or outwards from the tensor [10]. In the case of the wavefunction of Equation (2.20), the legs of Equation (2.21) point all in the same direction as they all represent each of the identical local Hilbert spaces. We also define the contraction of any two tensors by the diagram that joins their legs to represent the sum over that shared index. In the diagramatic example of matrices

Leg contraction

$$j - \underbrace{\qquad \qquad }_{\sum_{k} A_{ik} A_{kj} | i \rangle \langle j |} \qquad (2.23)$$

which concludes the basic diagrammatic rules.

A Tensor Network ansatz consists in decomposing the exponentially big coefficient tensor ψ of Equation (2.21) into a contraction of smaller tensors that have a smaller amount of parameters. Examples of possible decompositions could be



where the left example would correspond to a TN that repeats the same tensor for each open leg and only contracts with its direct neighbours. The example of the right of Equation (2.24) is a much more complicated network but serves to portray the many choices one can make with this ansatz. The different colors indicate that each of the tensors can, in general, be different and the much more complicated connectivity serves to illustrate an increase in the complexity of this ansatz.

When breaking down the big tensor in Equation (2.21), more legs and therefore vector spaces will appear in the network. It is important to keep a distinction between the original physical legs, labeled by s_i , and the new legs of the tensors that are fully contracted in the network, which we will call the virtual legs. We will reserve bolder lines for the physical d-dimensional legs/indices/spaces, and generally depict them

pointing upwards. The virtual legs/indices/spaces will in general correspond to a different arbitrary vector space with dimensionality D, which we call the bond/virtual dimension. With the general philosophy of Tensor Networks set in stone, let us now explore the most important TN ansatz for 1 and 2-dimensional systems

2.2.2 MATRIX PRODUCT STATES AND THEIR LIMITATIONS

The most important TNS for 1-dimensional systems is the Matrix Product State (MPS) ansatz. This ansatz splits the wavefunction in Equation (2.20) as

$$\psi_{s_1,...,s_n} = \sum_{\alpha_1,...,\alpha_n}^{D} A_{\alpha_1,\alpha_2}^{s_1} A_{\alpha_2,\alpha_3}^{s_2},..., A_{\alpha_n,\alpha_1}^{s_n},$$
 (2.25)

where the three-legged tensors $A^{s_i}_{\alpha_i,\alpha_{i+1}}$ are repeated at every site. If we write these tensors explicitely as matrices $A^{s_i} = \sum_{\alpha,\beta=1}^D A^{s_i}_{\alpha\beta} |\alpha\rangle\langle\beta|$, then the coefficient takes the form

$$\psi_{s_1,...,s_n} = \text{Tr}\left[A^{s_1}A^{s_2}...A^{s_n}\right],\tag{2.26}$$

which makes its name evident. Diagrammatically, an MPS is represented by the left diagram of Equation (2.24), and therefore each of the tensors is given diagrammatically by

$$A_{\alpha\beta}^{s_i} = \alpha - \beta. \tag{2.27}$$

It is possible to obtain a generic MPS representation of a 1-dimensional quantum state by performing successive Schmidt decompositions, where the Schmidt rank across a given cut becomes the bond dimension across that cut [123]. For a generic state, this will lead to an MPS whose bond dimension D grows exponentially with the number of sites n. However, most states fulfilling the area-law turn out to be exactly described by an MPS whose bond dimension grows at most polynomially in n [71]. Intuitively, this is because, for states that satisfy an area law, the Schmidt coefficients decay quickly enough to allow one to throw away all but polynomially many of them without significantly changing the quantum state. This result means that we can represent MPS states with only ndD^2 coefficients, which is an immense improvement over the previous exponential scaling. Interestingly, states that obey a logarithmic entanglement law, like critical states, can be well-approximated by MPS, but not exactly represented, as shown in [124]. This is one of the main motivations for this thesis, as we wish to provide such exact representations that still mimic the structure of MPS. As we will see in the following chapter, we will need to introduce tools from field theory to achieve this goal.

In preparation for Chapter 5, let us discuss a generic feature of TNS in the context of MPS, the bulk-boundary correspondance [125]. This correspondance states that if we divide the system into two connected subsystems A and B, the reduced density matrix ρ_A has the same spectrum as another matrix σ that can be viewed as living on the virtual indices on the boundary between A and B.

To see this, let us write a quantum state represented by the following open-boundary conditions MPS as

$$|\psi\rangle = -$$
 ... (2.28)

where we omit explicit indexes for the sake of notation and the green tensors are the open boundary conditions. We compute its density matrix diagrammaticaly as

where the downwards facing physical legs refer to the "bra" part of the density matrix. To compute the reduced density matrix ρ_A we are instructed to contract all the physical legs in the complement region B as follows

$$\rho_A = \underbrace{\begin{array}{c} \bullet & \bullet & \cdots & \bullet \\ \bullet & \bullet & \cdots & \bullet \\ \hline A & & B \end{array}}_{A}. \tag{2.30}$$

If one focuses exclusively on the contracted network in subregion B, it is easy to see that there are only two leftover legs that connect it with the region A, and therefore one can change this whole diagram by a matrix σ_R as follows

$$\rho_A = \bigcap_{R} \bigcap_{R$$

In order to deal with the information of the subsystem A, one begins by defining a linear map \mathcal{L} from the virtual index at the boundary of A and B to the physical legs as

$$\mathcal{L} = \underbrace{\hspace{1cm}}_{(2.32)}$$

We can then apply the polar decomposition to $\mathcal L$ to write it as $\mathcal L=\mathcal V\mathcal P$ where $\mathcal P=\sqrt{\mathcal L^\dagger\mathcal L}$ is a positive matrix and $\mathcal V$ is an isometry from the virtual to the physical legs obeying $\mathcal V\mathcal V^\dagger=\mathbb I_{D\times D}$. One can graphically write $\mathcal L^\dagger\mathcal L$ as

which allows to identify $\mathcal{P} = \sqrt{\sigma_L}$. Putting everything together one reaches, in equation form,

$$\rho_A = \mathcal{V}^{\dagger} \sqrt{\sigma_L^T} \sigma_R \sqrt{\sigma_L} \mathcal{V}. \tag{2.34}$$

Because $\mathcal V$ is an isometry, the spectrum of ρ_A is identical to the spectrum of $\sigma=\sqrt{\sigma_L^T}\sigma_R\sqrt{\sigma_L}$, which lives in the virtual space of the tensor network. This is what is meant in the context of tensor networks by the bulk-boundary correspondance. The most immediate conclusions from this analysis, is that the entanglement entropy $S(\rho_A)$ is equivalent to $S(\sigma)$, which is simply upper bounded by $\log D$, which is the promised area law. While this derivation has been done in its most simple setting, one can provide a similar proof for higher dimensionalities, as shown in [125]. The higher dimensional setting is the one that we will attempt to reproduce in the context of another field theory ansatz, continuous TNS, in the last chapter.

Another important result from this derivation, is that the entanglement spectrum, defined as the spectrum of ρ_A is always contained in the spectrum of σ , which has big implications in the understanding of gapped phases of matter [126, 127].

In preparation for Chapter 4, let us now discuss the application of MPS to the problem of phase classification. As we have seen, for one dimensional systems at zero temperature, there is only a notion of distinct phases when considering symmetries. Let us therefore begin by considering how on-site symmetries are manifested in MPS. Suppose that our MPS transforms under the action of a physical on-site symmetry U_g as

where V_g is a unitary matrix. Any state on N sites that is defined through an MPS that fulfills Equation (2.35) is immediately $U_g^{\otimes N}$ invariant. This is clear because the operators V and V^\dagger coming from neighbouring sites will cancel in the virtual leg between them. It turns out that this is the only way to encode a global symmetry into an MPS, subject to technical conditions [128]. In other words, given a global symmetry $U_g^{\otimes N}$, one can always find a V_g such that Equation (2.35) holds.

In fact, it turns out that the matrices V_g form, in general, a projective representation of the symmetry group G, which satisfy the relation $V_gV_h=\omega(g,h)V_{gh}$ for any two elements of the group $g,h\in G$ [93]. The 2-cocycle that appears in the group multiplication corresponds to some cohomology class $[\omega]\in H^2(G,U(1))$. The virtual representation V_g therefore provides us with a transparent way of extracting such a cocycle. This is important, because one can proof that $[\omega]$ can not be changed under symmetric, gap preserving deformations of the MPS tensor, what we called symmetric LU transformations on the previous sections [15]. Therefore, states with different $[\omega]$ belong to distinct SPT phases, within the realm of MPS.

The importance of this result, is that we can extract information about the topological properties of the state, by studying the properties of the MPS tensor which is defined for a single site. In contrast to the previous section, in which the study of the topological phase involved the computation of some topological invariant as in Equation (2.10), the information about the topology of the full state is condensed on the on-site tensor.

In a future chapter, we will study this property for a different class of ansatz, field TNS, designed to exactly describe systems that host logarithmic entanglement laws exactly. There are other approaches to describing such systems with TNS that do not require field theory, most prominently an ansatz known as MERA [22]. Ultimately, our goal is to understand how much of the theory of MPS and TNS translates to our field theory scenario, which is the reason why we do not use the MERA approach.

2.2.3 Projected Entangled Pair States and Chirality

The most prominent ansatz for 2-dimensional systems is known as Projected Entangled Pair States (PEPS), which are written diagrammatically as a straightforward generalization of MPS to a square lattice as

$$|\psi\rangle =$$
 (2.36)

where we have left the boundary conditions arbitrary. The tensor at every site is a 5-legged tensor given by

$$A_{\alpha\beta\gamma\delta}^{s_i} = \alpha - \beta$$

$$\beta$$

$$(2.37)$$

PEPS automatically fulfill the area law, but computing correlation functions with them is significantly more complicated numerically than with MPS due to the appearance of closed loops in the network [52, 129]. In contrast to MPS, PEPS can describe algebraically decaying correlations, and are therefore suitable to describe gapless systems [17].

In terms of phase classification, PEPS can classify both SPT and true topological order [15]. Models that are exactly described by PEPS would be the Kitaev quantum doubles [130], simple symmetry-enriched models obtained via anyon condensation [131] or gapless systems with continuous symmetries [132]. All of these descriptions share in common that the PEPS tensor has the symmetry

$$= U_g - U_g^{\dagger}$$

$$U_g^{\dagger}$$

$$U_g^{\dagger$$

where the unitaries U_g form a representation of the relevant global symmetry. In contrast to MPS, the symmetry arises as a property of the virtual space alone. If the symmetry in the virtual space is given by a more complicated object known as a Matrix Product Operator (MPO) [133], then PEPS can capture more exotic models such as

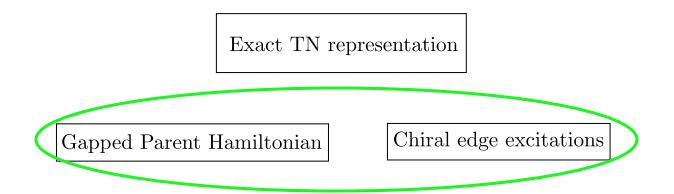


Figure 2.3: Schematic depiction of the Gapped chiral PEPS problem

the twisted quantum doubles [134] and string-net models [135]. In fact, a complete classification of the topological order that arises in terms of MPOs has been found in terms of category theory [96].

PEPS has proven itself to be an invaluable tool for providing exact representations of representative states within various very complicated phases of matter. One might even wonder whether one can find a PEPS groundstate representative for all known phases of matter. Unfortunately, there is a family states that have been eluding an exact representation in terms of PEPS for a long time, the family of quantum Hall states. It is even conjectured, that it is in fact impossible for such states to have a PEPS representation.

Historically, the argument for such a no-go result begins in the study of Wannier functions as in [136, 137]. Intuitively, the exponential localization of Wannier functions that enables an efficient TN representation, seems to be incompatible with the extended Wannier functions found in quantum Hall states. This question has also been studied within the context of TNS, such as [17, 34]. The conclusion in these papers was the PEPS can indeed showcase the correlations associated to quantum Hall states, but paying the price that the Hamiltonian of which the PEPS is a groundstate must be gapless. This is again incompatible with the gapped Hamiltonians that are associated with the topological order of the fractional quantum Hall state. Numerical studies have confirmed this intuition [138, 139], and shown that PEPS can still provide a good numerical approximation to these states, foregoing an exact analytical description.

From this set of results, we found ourselves in the situation depicted in Figure 2.3, in which one must choose two vertices of the triangle and forego the remaining one. If one chosess to describe a chiral edge with a standard PEPS, one obtains a gapless parent Hamiltonian. If one choses to guarantee a parent Hamiltonian with PEPS, one never obtains a chiral edge. Therefore, if one wishes to retain a gapped parent Hamiltonian and the chiral edge, it seems that what one must do is modify the TN representation itself, or simply restrict oneself to approximate results.

The lack of an exact representation is the second main motivation behind this thesis. By means of field theory techniques, we aim to provide one such exact analytical representation by means of field TNS. We will see in the upcoming chapter that by utilizing the connection of quantum Hall states with conformal field theory, we can provide an explicit TN representation. Very recently, there have been other studies pursuing a similar approach like [140, 141], and even a no-go result that seems to finally set in stone the incompatibility of PEPS with chiral gapped systems [142].

2.3 BACKGROUND CONCEPTS ON CONFORMAL FIELD THEORY

High energy particle physics is described by a Lorentz invariant quantum field theory and is usually concerned with the physics at the energy scales in which these symmetries are the most relevant [143]. In stark contrast, condensed matter physics wishes to describe physics at a scale in which these symmetries are not as apparent, the most obvious example being that translation invariance gets reduced to crystalline translation invariance. Whilst we could always think of a condensed matter state as a quantum field theory state with non-zero density of particles in the limit of lower energies, it is precisely the breaking of these symmetries that would demand us of the formalism of spontaneous symmetry breaking and Goldstone bosons [144]. This route is undoubtedly much harder and convoluted than what condensed matter physicists actually do, which is to simply consider theories with fewer symmetries.

As we have seen in the previous chapters, at energies that are low compared to particle physics scales, a given condensed matter state can be described starting from an effective low-energy Hamiltonian with no vestige of the high-energy symmetries. This description may take the form of a lattice model describing, for example, the interactions of mobile electrons with lattice vibrations [145]. The only remnants of spacetime symmetries in such a model will be discrete translations and rotations, therefore leading to a generically non-field theoretic description of physics.

However, a further low energy limit can be taken, which considers physics on energies well below the lattice energy scale. Very interestingly, it is found that in many important circumstances, universal continuum physics re-emerges as a faithful description of the low energy part of the spectrum as well as of the universal properties of the model [102, 146]. These phenomena occur both in gapless systems, such as in quantum critical points and Fermi liquids and in gapped systems with long-range topological interactions. These emergent universality features are the goal that low energy effective field theories aim to describe by foregoing many of the details of the lattice system.

Because low-energy effective field theories do not arise as a requirement from Lorentz symmetry, there is no a priori restriction on the class of symmetries that the theory can have. One such example are conformal field theories (CFTs), which are genuinely interacting quantum field theories that arise most naturally in the description of two-dimensional quantum critical phenomena. Conformal invariance in two dimensions can be shown to be equivalent to scale invariance, which is a well-known feature of critical points. The requirement of conformal invariance imposes that all particle-like excitations of the theory are massless, and therefore they have algebraically decaying correlation functions. This generic algebraic decay, as an underlying feature of the theory, can be used to accurately describe how correlation functions of critical models, governed by the universal critical exponents, behave. Furthermore, CFTs also shed light on the universal properties of gapped topological systems that host anyonic excitations, as CFTs provide a natural representation for the fusion mechanism that defines these exotic excitations [32, 147].

CFT is a very well-established topic of research, and there are already many fantastic reviews in the literature tailored to the different backgrounds and goals of the reader. For those with a background closer to field theory, I recommend the works of Di Francesco, Mathieu and Sénéchal [37], or the reviews by Ginsparg [148], Gawedezki [149] or Moore and Seiberg [150]. For those with a background closer to mathematical

physics, an approach based on operator algebras can be found in the review by Gaberdiel [151], which is based upon several works such as [152–157]. For those that prefer an approach closer to algebraic quantum field theory and functional spaces [158], I recommend the works by Wassermann [159], and Gabbiani and Fröhlich [160].

Of importance to this thesis are also the more recent developments in CFT that pertain both to the definition of CFT on surfaces of non-trivial genus, as well as the developments pertaining to Boundary CFT (BCFT). While these results go beyond the scope of the brief introduction based on [37] that I wish to present here. Some of the important results in the field of higher genus CFT can be found in [161–165], whilst some of the corresponding results from BCFT can be found in [166–170].

2.3.1 Basics of conformal field theory

CONFORMAL INVARIANCE IN A QUANTUM THEORY

We denote by $g_{\mu\nu}$ the metric tensor in a space-time of dimension d. A conformal transformation of the coordinates $x\to x'$ is one that leaves the metric tensor invariant up to a scale

$$g'_{\mu\nu}(x') = \Lambda(x)g_{\mu\nu}(x),$$
 (2.39)

and the name conformal comes from the fact that these preserve angles since they at most rescale the metric. The group of conformal transformations is given by SO(d+1,1), whose generators are

translations:
$$x'^{\mu} = x^{\mu} + a^{\mu}$$

dilations: $x'^{\mu} = \alpha x^{\mu}$
rotations: $x'^{\mu} = M^{\mu}_{\nu} x^{\nu}$ (2.40)
SCTs: $x'^{\mu} = \frac{x^{\mu} - b^{\mu} x^2}{1 - 2b \cdot x + b^2 x^2}$,

where we have assumed Einstein's summation convention, and SCT stands for special conformal transformation. In d=2, invariance under dilations is enough to guarantee conformal invariance [171], whilst in higher dimensions, this fact no longer holds true.

The first consequence of conformal invariance on a physical theory is that performing a variation of the action S under an infinitesimal conformal transformation $x^\mu \to x^\mu + \varepsilon^\mu$ yields

$$\delta S = \frac{1}{d} \int d^d x T^{\mu}_{\mu} \partial_{\rho} \varepsilon^{\rho}, \tag{2.41}$$

where T^μ_ν is the symmetric energy momentum tensor. Whenever the energy-momentum tensor is traceless, $T^\mu_\mu=0$, the theory will always be conformally invariant, whilst the converse is not necessarily true [37]. The fact that conformal invariance is guaranteed by the tracelessness of T^μ_ν places the energy-momentum tensor as a much more central object for CFT than the action itself, and it is indeed very common to define CFTs with no regard to an action whatsoever.

Conformal invariance at the quantum level demands that whenever we compute a correlation function such as

$$\langle \phi_1(x_1)\phi_2(x_2)\rangle = \frac{1}{Z} \int \mathcal{D}\phi \phi_1(x_1)\phi_2(x_2)e^{-S[\phi]},$$
 (2.42)

this correlation function behaves under a conformal transformation as

$$\langle \phi_1(x_1)\phi_2(x_2)\rangle = \left|\frac{\partial x'}{\partial x}\right|_{x=x_1}^{\Delta_1/d} \left|\frac{\partial x'}{\partial x}\right|_{x=x_2}^{\Delta_2/d} \langle \phi_1(x_1')\phi_2(x_2')\rangle, \tag{2.43}$$

where the Δ_i 's are a set of numbers that control how the field transforms. This transformation law completely fixes both 2 and 3- point correlators

$$\langle \phi_1(x_1)\phi_2(x_2)\rangle = \begin{cases} & \frac{C_{12}}{|x_1 - x_2|^{2\Delta_1}}, & \text{if } \Delta_1 = \Delta_2 \\ & 0, & \text{if } \Delta_1 \neq \Delta_2 \end{cases}$$
 (2.44)

where C_{12} is an arbitrary normalization constant and

$$\langle \phi_1(x_1)\phi_2(x_2)\phi_3(x_3)\rangle = \frac{C_{123}}{|x_1-x_2|^{\Delta_1+\Delta_2-\Delta_3}|x_2-x_3|^{\Delta_2+\Delta_3-\Delta_1}|x_3-x_1|^{\Delta_3+\Delta_1-\Delta_2}}, \tag{2.45}$$

where again C_{123} is a normalization constant. One can also show that further n-point functions are also heavily constrained to only depend on conformally invariant combinations of the positions, known as cross-ratios. We have so far seen that conformal invariance places heavy constraints on the possible correlation functions that can arise out of a CFT, and we are now going to see that these constraints are even stronger whenever we impose d=2.

Conformal invariance in d=2

We use the coordinates on the plane (z^0,z^1) , and under a conformal transformation $z^\mu \to w^\mu(x)$ we can see that the local condition for conformal invariance reduces to

$$\frac{\partial w^1}{\partial z^0} = \frac{\partial w^0}{\partial z_1}$$
 and $\frac{\partial w^0}{\partial z^0} = -\frac{\partial w^1}{\partial z^1}$, (2.46)

which are nothing but the Cauchy-Riemman equations that define holomorphic functions. Thus, the set of conformal transformations allowed in the plane is given by the set of holomorphic functions, which is an infinite-dimensional set! It is precisely this infinite dimensionality that which restricts correlation functions so strongly in conformally invariant field theories in d=2.

This motivates the use of a change of variables for the coordinates of the plane that is much more common to complex analysis, which is given by

$$z = z^0 + iz^1$$
, $\overline{z} = z^0 - iz^1$, (2.47)

where $\overline{z} \neq z^*$, that is, we generically understand \overline{z} as an independent coordinate of the plane, and then whenever restricting to $z^* = \overline{z}$ we say that we restrict ourselves to the physical real surface.

The condition of local conformal invariance has led to an infinite dimensional set of possible conformal transformations, which would seem to be inconsistent with the result that for a generic d, the conformal group is given by SO(d+1,1). To fix this seeming inconsistency, we need to focus on global conformal transformations on the plane, and demand that these exist and are invertible everywhere. Upon doing so, one obtains the transformations

$$f(z) = \frac{az+b}{cz+d}$$
 with $ad-bc = 1$, (2.48)

where $a,b,c,d\in\mathbb{C}$. These constitute the set of projective transformations $SL(2,\mathbb{C})$ of mappings from \mathbb{C} onto itself, which is isomorphic to SO(3,1) as expected.

With these new coordinates, we can now define a quasi-primary field as a field that, under a given conformal map $z\to w(z),\,\overline{z}\to\overline{w}(\overline{z})$ transforms as

$$\phi'(w, \overline{w}) = \left(\frac{\partial w}{\partial z}\right)^{-h} \left(\frac{\partial \overline{w}}{\partial \overline{z}}\right)^{-\overline{h}} \phi(z, \overline{z}), \tag{2.49}$$

where we call $h(\overline{h})$ the (anti)holomorphic conformal dimension. A field that transforms according to Equation (2.49) for every possible conformal transformation is a primary field, and the set of primary fields and their conformal dimensions is one of the most important aspects of any CFT.

As in higher dimensions, correlation functions are heavily constrained once more, as they must transform according to

$$\langle \phi_1(w_1,\overline{w}_1...\phi_n(w_n,\overline{w}_n))\rangle = \prod_{i=1}^n \left(\frac{\partial w}{\partial z}\right)_{w=w_i}^{-h_i} \left(\frac{\partial \overline{w}}{\partial \overline{z}}\right)_{\overline{w}=\overline{w}_i}^{-\overline{h}_i} \langle \phi_1(z_1,\overline{z}_1...\phi_n(z_n,\overline{z}_n))\rangle, \ \ \textbf{(2.50)}$$

which fixes the 2-point function to be

$$\langle \phi_1(z_1,\overline{z}_1)\phi_2(z_2,\overline{z}_2)\rangle = \frac{C_{12}}{(z_1-z_2)^{2h}(\overline{z}_1-\overline{z}_2)^{2\overline{h}}} \quad \text{with} \quad h_1=h_2=h \; , \; \overline{h}_1=\overline{h}_2=\overline{h}. \tag{2.51}$$

The 3-point function and further *n*-point function become similarly constrained. Of significant importance is the fact that the dependence on the holomorphic and anti-holomorphic variables fully factorizes, which is, in fact, a feature of CFT, as we will see later.

In order to understand how a generic correlation function $\langle X \rangle$ behaves under an infinitesimal conformal transformation, one can prove the conformal Ward identity, in which a small variation $\delta_{\varepsilon,\overline{\varepsilon}}$ yields

$$\delta_{\varepsilon,\overline{\varepsilon}}\langle X\rangle = -\frac{1}{2\pi i} \oint_C dz \varepsilon(z) \langle T(z)X\rangle + \frac{1}{2\pi i} \oint_C d\overline{z} \varepsilon(z) \langle \overline{T}(\overline{z})X\rangle, \tag{2.52}$$

where we have introduced the holomorphic and anti-holomorphic energy-momentum tensors defined as $T(z)=-2\pi T_{zz}$ and $\overline{T}(\overline{z})=-2\pi T_{\overline{z}\overline{z}}$, and the contour C encircles all divergences arising from the correlations functions within the integrals.

The most important consequence of Equation (2.52) is that the symmetry properties of any field, or combination thereof, X are encoded in the divergence structure of their correlation function with the energy-momentum tensor. In fact, for any primary field X, the holomorphic correlation functions are given by

$$\langle T(z)X\rangle = \sum_{i=1}^n \left[\frac{1}{z-w_i}\partial_{w_i}\langle X\rangle + \frac{h_i}{(z-w_i)^2}\langle X\rangle\right] + \text{reg.} \tag{2.53}$$

where reg. groups all the terms that do not diverge in the limit $z \to w_i$, and we have a similar expression for the anti-holomorphic counterpart. The idea that the divergences arising from correlation functions contain the physical information of the field is one of the most important features of CFT, as it allows us to study the properties of the theory by merely keeping track of the divergences that arise alongside any computation.

This generic behavior is what motivates us to introduce the concept of an Operator Product Expansion (OPE), which is an operation that allows us to only focus on these divergences. The OPE consists of considering the correlation function between two fields and substituting their product within the correlation functions by exclusively the divergent terms of their expansion as their positions get close. As an example, the OPE between the energy-momentum tensor T(z) and a primary field $\phi(w)$ can be read from Equation (2.53) to be

$$T(z)\phi(w) \sim \frac{h}{(z-w)^2}\phi(w) + \frac{1}{(z-w)}\partial_w\phi(w), \tag{2.54}$$

where we have only presented the holomorphic OPE, and \sim means that we are ignoring all the regular terms. It is, in fact, common to consider the OPE shown in Equation (2.54) as the better definition of a primary field, which is the approach usually followed in the algebraic approaches to CFT that are rooted in operator algebras, where the OPE enjoys a much more formal definition. Under this definition, quasi-primary or descendant fields are the ones that appear from the OPE of T(z) with a given primary.

Another very important OPE is the one of T(z) with itself, where, by conformal invariance, it can be shown that it is given by

$$T(z)T(w) \sim \frac{\frac{c}{2}}{(z-w)^4} + \frac{2T(w)}{(z-w)^2} + \frac{\partial T(w)}{(z-w)},$$
 (2.55)

where a new constant c has appeared on top of the most divergent term, which is known as the central charge. This is another one of the most important and defining numbers for a CFT, as it is an intrinsic property of the divergent structure of the energy-momentum itself. The OPE of T(z) with itself also tells us that it is a quasi-primary field with $h_T=2$.

The final important OPE is given by the OPE of two primary fields amongst themselves, which can generically be written as

$$\phi_{i}(z)\phi_{j}(w) = \sum_{k} C_{ij}^{k}(z-w)^{h_{k}-h_{i}-h_{j}}\phi_{k}(w) + \text{desc.} \tag{2.56} \label{eq:2.56}$$

where the constants C_{ijk} are a set of numbers that define the normalization of the 3-point functions and desc. stands for all the descendants that can arise from the product.

Although the dependence of higher n-point functions on cross-ratios is not fixed by conformal invariance, by repeated use of the OPE within the correlation function, every n-point function can be reduced to 2 and 3-point functions. Therefore, any correlation function of CFT is fully characterized by the numbers that appear as these OPEs are taken, which are the conformal dimensions of the primary fields h_i , the central charge c, and the 3-point function normalization constant C_{ijk} . The fact that the entire theory can be solved by repeated usage of algebraic relations between the fields is what allows for the rigorous mathematical treatment of CFTs as Operator Algebras [151].

FREE FIELD EXAMPLES

Let us begin with the simplest CFT given by the free boson action

$$S_{fb} = \frac{1}{8\pi} \int d^2x \partial_\mu \varphi \partial^\mu \varphi, \qquad (2.57)$$

whose 2-point correlators are well-known and given in two dimensions by

$$\langle \varphi(z, \overline{z})\varphi(w, \overline{w})\rangle = -\log(|z - w|^2), \qquad (2.58)$$

which indicates us that the field $\varphi(z)$ is not a primary field. However, if we take derivatives of the boson field, we obtain

$$\langle \partial_z \varphi(z,\overline{z}) \partial_w \varphi(w,\overline{w}) \rangle = -\frac{1}{(z-w)^2} \ , \ \langle \partial_{\overline{z}} \varphi(z,\overline{z}) \partial_{\overline{w}} \varphi(w,\overline{w}) \rangle = -\frac{1}{(\overline{z}-\overline{w})^2}, \quad \text{(2.59)}$$

which allows us to infer the OPE of $\partial \varphi(z)$ with itself, which contains a single divergent term. This OPE also reflects the bosonic character of the field since the positions of the fields can be swapped without affecting the correlation function. The energy-momentum tensor of the free boson is given simply by

$$T(z) = -\frac{1}{2} : \partial \varphi(z) \partial \varphi(z) :, \tag{2.60}$$

which can be obtained from the action, and normal ordering :: has been introduced since both fields are evaluated at the same point. Performing the OPE of T(z) with the field $\partial \varphi(w)$ by repeated application of Equation (2.59)

$$T(z)\partial\varphi(w) \sim \frac{\partial\varphi(w)}{(z-w)^2} + \frac{\partial_w^2\varphi(w)}{(z-w)},$$
 (2.61)

which tells us that $\partial \varphi(z)$ is indeed a primary field with conformal dimension h=1. This information also allows us to infer from Equation (2.59) the value for the 3-point constant amongst these primaries to be $C_{hh}^0=-1$ as these fields "multiplied" by the identity primary field. By using Wick's theorem, the OPE of T(z) with itself is

$$T(z)T(w) \sim \frac{1}{2(z-w)^4} + \frac{2T(w)}{(z-w)^2} + \frac{\partial T(w)}{(z-w)},$$
 (2.62)

which tells us that this CFT has c=1. It would seem that we already have all the information that we need to find any correlator of this theory, but we are missing a lot of information in fact. We have only found one primary field of this theory, $\partial \varphi(z)$, but it turns out that there are infinitely many more, all of them given in the form of vertex operators

$$\mathcal{V}_{\alpha}(z,\overline{z}) =: e^{i\alpha\varphi(z,\overline{z})}:, \tag{2.63}$$

where normal ordering is necessary to be able to perform Taylor expansions for this exponential. These fields are primary fields with conformal dimension $h(\alpha)=\frac{\alpha^2}{2}$ and their OPE is given by

$$\mathcal{V}_{\alpha}(z,\overline{z})\mathcal{V}_{\beta}(w,\overline{w}) \sim |z-w|^{2\alpha\beta}\mathcal{V}_{\alpha+\beta}(w,\overline{w}) + ..., \tag{2.64}$$

which provides us with the rest of the needed constants. Although the theory is simple enough such that we can extract all the conformal data, the challenge of this theory resides in the fact that there are infinitely many primary fields, which is a situation in strong contrast to other simple CFTs such as minimal models. In minimal models, there is only a finite amount of primary fields, but solving the algebraic relations that provide us with the conformal data is a generically hard task, which attempts to be solved by following the so called conformal bootstrap program [172].

Our next simple example is the free fermion. The action of a free Majorana Fermion is given by

$$S_{ff} = \frac{1}{2\pi} \int d^2x (\overline{\psi}\partial\overline{\psi} + \psi\overline{\partial}\psi), \qquad (2.65)$$

where the correlators amongst the fields $\psi(z,\overline{z})$ and $\overline{\psi}(z,\overline{z})$ are given by

$$\langle \psi(z, \overline{z}) \psi(w, \overline{w}) \rangle = \frac{1}{z - w},$$

$$\langle \overline{\psi}(z, \overline{z}) \overline{\psi}(w, \overline{w}) \rangle = \frac{1}{\overline{z} - \overline{w}},$$

$$\langle \psi(z, \overline{z}) \overline{\psi}(w, \overline{w}) \rangle = 0,$$
(2.66)

which allows us to read the OPEs amongst these fields. Once again, the OPE reflects the fermionic character of the field whilst also showing that the holomorphic and antiholomorphic parts of the field become decoupled. The energy-momentum tensor is given by

$$T(z) = -\frac{1}{2} : \psi(z)\partial\psi(z) :, \tag{2.67}$$

and the relevant OPEs are then given by

$$T(z)\psi(w) \sim \frac{\frac{1}{2}\psi(w)}{(z-w)^2} + \frac{\partial\psi(w)}{(z-w)},$$

$$T(z)T(w) \sim \frac{\frac{1}{4}}{(z-w)^4} + \frac{2T(w)}{(z-w)^2} + \frac{\partial T(w)}{(z-w)},$$
(2.68)

from which we obtain that $c=\frac{1}{2}$ and that the field $\psi(z)$ is a primary field with conformal dimension $h=\frac{1}{2}$.

OPERATOR FORMALISM

So far, we have shown the consequences of conformal invariance in d=2 at the level of the correlation functions obtained from path integral calculations without any reference to the underlying Hilbert space structure. Since we wish to eventually discuss the representation of symmetries on a CFT, it is important to understand the constraints that conformal invariance imposes on the space of states themselves, and not just their correlation functions.

We will concern ourselves only with the holomorphic part of the theory to ease up the notation and begin by performing a Laurent expansion of any quasi-primary field as

$$\phi(z) = \sum_{m \in \mathbb{Z}} z^{-m-h} \phi_m, \quad \phi_m = \frac{1}{2\pi i} \oint dz \ z^{m+h-1} \phi(z). \tag{2.69}$$

From this mode expansion, one can define the corresponding conjugate of the field $\phi^\dagger(z)$ via the relationship between the modes $\phi_m^\dagger=\phi_{-m}$. In order to be able to define the norm of a state, it is mandatory that the vacuum state must satisfy

$$\phi_m|0\rangle = 0 \quad \text{for} \quad m > -h. \tag{2.70}$$

With the vacuum state defined, we now define an operator as contour integrals of a holomorphic field, such as

$$A = \oint_0 a(z)dz,\tag{2.71}$$

where the contour encircles the 0 of the complex plane. With this definition, any commutation between two such operators is given by

$$[A,B] = \oint_0 dw \oint_w dz a(z)b(w). \tag{2.72}$$

This is an extremely important definition, as it allows us to relate OPEs and commutation relations. If we were to take the OPE between the fields a(z) and b(w) in Equation (2.72), only the singular terms would survive the contour integrals, and therefore this expression allows us to translate the dynamical content of the OPE into the algebraic language.

The most important object to translate to the algebraic language is the energy-momentum tensor T(z). By expanding in Laurent modes as well

$$T(z) = \sum_{n \in \mathbb{Z}} z^{-n-2} L_n \ , \ L_n = \frac{1}{2\pi i} \oint dz \ z^{n+1} t(z), \tag{2.73}$$

where the modes L_n are the generators of all conformal transformations on the Hilbert space. The generators of global conformal transformations associated with $SL(2,\mathbb{C})$ are given by L_{-1}, L_0 and L_1 , with L_0 being also identified with the Hamiltonian of the CFT [37]. Using Equation (2.72) we can now compute the commutation relations amongst the symmetry generators, and we obtain

$$\begin{split} [L_n,L_m] &= (n-m)L_{m+n} + \frac{c}{12} n \left(n^2 - 1\right) \delta_{n+m,0}, \\ \left[L_n,\overline{L}_m\right] &= 0, \end{split} \tag{2.74}$$

where \overline{L}_m are the modes arising from the anti-holomorphic component of the energy-momentum tensor. This algebra is known as the Virasoro algebra [37], which is defined as a central extension with central charge c of the previously classical Witt algebra that defined the classical conformal invariance [173]. In these commutation relations, we finally see the underlying reason for the prevalent factorization of correlation functions into a holomorphic and an anti-holomorphic part. The underlying Hilbert must organize in representation of the Virasoro algebra, and since there are two uncoupled copies, the correlations function will behave accordingly.

As with any other symmetric theory, the Hilbert space must fall into representations of the conformal algebra. Therefore, we can begin constructing this space from the conformally invariant vacuum state, which must satisfy

$$L_n|0\rangle = 0 \quad \text{for} \quad n \ge -1 \tag{2.75}$$

such that the vacuum is invariant under global conformal transformations. We can construct any state of the theory using the operator-state correspondence

$$|\phi\rangle = \lim_{z \to 0} \phi(z)|0\rangle \tag{2.76}$$

and we denote the states corresponding to primary fields by their conformal dimensions as $|h\rangle$. These states turn out to be the eigenstates of the CFT Hamiltonian

$$L_0|h\rangle = h|h|\rangle$$
, $L_n|h\rangle = 0$ if $n > 0$, (2.77)

and therefore act as the highest-weight state of the conformal representation. To generate the rest of the excited states, which are the states associated with the descendant fields of a primary, we simply act with the negative Virasoro generators as

$$L_{-k_1}L_{-k_2}...L_{-k_n}|h\rangle \ , \ k_i > 1$$
 (2.78)

which allows to reach an excited state with energy $h' = h + \sum_i k_i$, where the sum $\sum_i k_i = N$ is called the level of the descendant. The subset of the full Hilbert space generated by the primary state $|h\rangle$ and all of its descendants is closed under the action of the Virasoro operators, therefore providing us with a Verma module representation [37].

We call this representation a module because within the set of descendant states lie some special states, which are called null vectors $|\chi\rangle$. These states are special because they turn out to be descendants of a primary state and highest-weight states at the same time. Therefore, to obtain a proper representation, these states must be removed from the set of possible states, such that all the states within the representation can transform amongst themselves under any possible conformal transformation, which we will then call a conformal family $[\phi_k]$ associated to the primary field ϕ_k .

The exploration of all the possible Verma modules, and more explicitly, their reducibility or unitarity, is what led to the discovery of minimal models [37], which are defined to be irreducible unitary Verma modules. These models play very important roles as they are found, for instance, in the critical points of the Ising model in two dimensions or further families such as the critical points of the tri- or tetra-critical Ising models. Because minimal models have a finite amount of conformal families, the theory is considered to be solved as we can provide the entire spectrum and, therefore, compute any correlation function.

The structure and constraints among the states of the Verma Module can be translated back to correlation functions, where the correlation function of any combination of primary fields $X=\phi_1(w_1)...\phi_n(w_n)$ with a descendant field $\phi^{-k_1,...,-k_n}(w)$ is given by

$$\langle \phi^{-k_1,...,-k_n}(w)X\rangle = \mathcal{L}_{-k_1}...\mathcal{L}_{-k_n}\langle \phi(w)X\rangle, \tag{2.79}$$

where the \mathcal{L}_{-n} are differential operators given by

$$\mathcal{L}_{-n} = \sum_{i} \left[\frac{(n-1)h_i}{(w_i - w)^n} - \frac{\partial_{w_i}}{(w_i - w)^{n-1}} \right]. \tag{2.80}$$

Therefore, any correlation function involving descendant fields can be related to another one of the primary fields, which in turn can always be found via performing OPEs amongst the primary fields if the complete conformal data is known. Furthermore, some of the more complicated correlators can even be found directly by solving the differential equation associated with the descendant being a null field and, hence, the correlator of primaries with it vanishing.

The last piece of information that we will provide about standard CFT theory is the notion of fusion rules and fusion algebra. We have seen so far that the CFT Hilbert space organizes in families labeled by the primary fields of the theory, which we called the conformal families $[\phi_k]$. As we have seen, the OPE introduces a notion of "multiplication" in the space of primary fields, giving us a recipe with which to send two primaries to a third one. This concept is formalized as the fusion rules of the different conformal families

$$[\phi_i] \times [\phi_j] = \sum_k \mathcal{N}_{ij}^k [\phi_k], \tag{2.81}$$

where the numbers \mathcal{N}_{ij}^k are called the fusion coefficients. To each choice of fusion coefficient, one can associate the notion of a fusion algebra, which is a commutative and associative algebra with generators ϕ_j , identity $\phi_1 = \mathbb{I}$ and a product given by the OPE. These fusion rules are extremely important in the context of topological physics, as they provide us with an explicit representation of the braiding and fusing of the anyonic excitations that define long-range topological order [32].

In the upcoming sections, we will provide a very short introduction to some of the main results of the more advanced CFT topics that appear in the field of topological order, and that will be of use in the later part of this thesis.

2.3.2 MODULAR INVARIANCE

We have so far only concerned ourselves with CFTs in d=2 defined on the complex plane. However, there is no a priori restriction on the kind of manifolds on top of which we could study CFT. We know from the previous sections that one of the signifying features of topological order is that the ground state degeneracy reflects the topology of the underlying manifold. As CFT provides a natural representation of anyonic excitations due to the fusion rules, it is important to understand how the ground state of CFTs changes when placed on a different surface, like, for instance, a torus.

We present here a very short summary of the results related to studying CFTs on a torus. Firstly, the most important parameter for a torus is the ratio between the length of the two non-contractible circles ω_i , which we call the modular parameter $\tau = \frac{\omega_2}{\omega_1}$. We define a Virasoro character for a specific Verma module as

$$\mathcal{X}_{\mathcal{V}}(q) = \text{Tr}_{\mathcal{V}} q^{L_0 - \frac{c}{24}} , \quad q = e^{2i\pi\tau},$$
 (2.82)

where the trace is taken over the Verma module. The partition function on a torus is given by

$$Z(\tau) = \operatorname{Tr}\left\{q^{L_0 - \frac{c}{24}}\overline{q}^{-\overline{L}_0 - \frac{c}{24}}\right\},\tag{2.83}$$

where now the trace is taken over the entire CFT Hilbert space. As the Hilbert space is broken down into the different Verma modules associated with the primaries, the partition function becomes

$$Z(\tau) = \sum_{h,\overline{h}} \mathcal{N}_{h,\overline{h}} \mathcal{X}_h(q) \mathcal{X}_{\overline{h}}(\overline{q}), \tag{2.84}$$

where the non-negative numbers $\mathcal{N}_{h,\overline{h}}$ are called the multiplicity matrix and correspond to how many times each character \mathcal{X}_h is associated with the primary family with conformal dimension h appears.

Because the partition function is a physical quantity, it must be left invariant under any symmetry of the underlying torus coordinates, transformations known as modular transformations. These transformations are given by the modular group $PSL(2,\mathbb{Z})$ and have two generators, usually denoted by \mathcal{S} and \mathcal{T} , associated with inversions and translations of the modular parameters τ . Invariance of $Z(\tau)$ under both \mathcal{S} and \mathcal{T} introduces very stringent constraints on the possible values of the multiplicity matrix \mathcal{N} once a set of irreducible modules gets fixed. Such complete classifications have been achieved for unitary minimal models, as can be seen in [174].

The most remarkable result of modular invariance is a theorem known as the Verlinde Formula [175]. If the Virasoro characters are transformed according to the $\mathcal S$ generator, one obtains

$$\mathcal{X}_{i}(\tilde{q}) = \sum_{j} S_{ij} \mathcal{X}_{j}(q) \quad , \quad \tilde{q} = e^{-\frac{2\pi i}{\tau}}$$
 (2.85)

and the numbers S_{ij} are collected in the modular matrix S. A modular transformation is a global notion, as it involves a change of coordinates everywhere in the torus, but the Verlinde formula surprisingly links the modular matrix S to the fusion matrix \mathcal{N}_{ij}^k which arises from OPEs, which are intrinsically local operations. The Verlinde formula states

$$\mathcal{N}_{ij}^{k} = \sum_{m} \frac{S_{im} S_{jm} \overline{S}_{mk}}{S_{0m}},$$
(2.86)

where the index 0 corresponds to the vacuum representation. This is an extremely deep result that can be traced back to the underlying Fusion category theory structure of vertex operator algebras, of which CFTs are an example [176].

2.3.3 BOUNDARY CFT

In this section, we want to briefly present one of the main intuitions that will be used in Chapter 4 in order to deal with manifolds with boundaries in the context of CFT. The simplest manifold with a boundary on which we can use CFT is the Upper Half Plane (UHP) \mathbb{H} , consisting of the complex numbers with positive imaginary parts. Conformal invariance in the UHP implies that conformal transformations must keep the boundary, in this case the real line \mathbb{R} , and any boundary conditions on it invariant. This constraint reduces the set of possible global conformal transformations from $SL(2,\mathbb{C})$ down to $SL(2,\mathbb{R})$, therefore reducing in half the amount of conformal generators.

Although we have lost half of the generators of symmetry, we still possess an infinite amount of them, but the main consequence is that the holomorphic and the anti-holomorphic sectors of the CFT are no longer independent, as they have been coupled on the real line. To see this in more detail, we consider the Ward identities

$$\delta_{\varepsilon,\overline{\varepsilon}}\langle X\rangle = -\frac{1}{2\pi i} \oint_C dz \varepsilon(z) \langle T(z)X\rangle + \frac{1}{2\pi i} \oint_C d\overline{z} \varepsilon(z) \langle \overline{T}(\overline{z})X\rangle, \tag{2.87}$$

where the contour C lies entirely within the UHP. In the infinite plane, the variations $\varepsilon(z)$ and $\overline{\varepsilon}(\overline{z})$ were independent, and because of this independence, we could treat Equation (2.87) as two separate Ward identities involving only either the holomorphic or the anti-holomorphic sector, however, this is no longer the case. Now, the coordinate variation $\overline{\varepsilon}=\varepsilon^*$, and therefore in the UHP, we will regard the dependence on the anti-holomorphic variables \overline{z}_i as a dependence on the conjugated holomorphic variables z_i^* that live in the lower half plane (LHP).

We have thus essentially introduced a mirror image of the system in the LHP, which enforces that the energy-momentum tensor behaves as $T(z^*) = \overline{T}(z)$. To preserve conformal invariance, it is mandatory that $\overline{T}(z) = T(z)$ whenever $z \in \mathbb{R}$, which means that no energy or momentum can be transferred across the real axis as expected of a system with a boundary. Fortunately, we will still be able to rewrite the conformal Ward identity on the UHP as a purely holomorphic expression on the infinite plane.

The second term of Equation (2.87) becomes a mirror image of the contour on the LHP because of the complex conjugation of the variable of integration z^* . Because $\overline{T} = T$ on the real axis, both integrations can be put together once again. This results in a contour C that encircles the origin and doubles as many points as the original contours, as shown in Figure 2.4. Using this identification, which is nothing but the

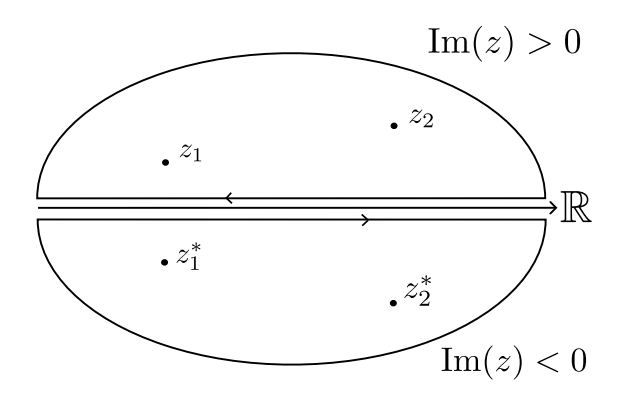


Figure 2.4: Schematic diagram showcasing how a CFT in the UHP can be dealt with using the method of images.

well-known method of images of classical electrostatics, the conformal Ward identity becomes

$$\delta_{\varepsilon,\overline{\varepsilon}}\langle X\rangle = -\frac{1}{2\pi i} \oint_C dz \varepsilon(z) \langle T(z)X'\rangle, \qquad (2.88)$$

where the contour C encircles the origin and the collection of primary fields is given by $X'=\phi_{h_1}(z_1)\overline{\phi}_{\overline{h}_1}(z_1^*)...\phi_{h_n}(z_n)\overline{\phi}_{\overline{h}_n}(z_n^*)$.

In summary, a correlator $\langle X \rangle$ in the UHP, as a function of the 2n variables $z_1, \overline{z}_1, ..., z_n, \overline{z}_n$, satisfies the same differential equations required by conformal invariance as the correlator $\langle X' \rangle$ on the entire plane regarded as a function of the 2n holomorphic variables $z_1, z_1^*, ..., z_n, z_n^*$. Effectively, we have replaced the anti-holomorphic degrees of freedom on the UHP with holomorphic degrees of freedom on the LHP. In Chapter 4, we will make use of this technique in order to properly define symmetry operators on the virtual space of fTNS.

2.3.4 WZW MODELS

So far we have only concerned ourselves with the case in which the different fields of the theory had to form representations of conformal symmetry exclusively. A very important class of CFTs are those that possess an extended symmetry, and in this case, we will briefly present those CFTs that possess a Lie-algebraic symmetry. This family of models is known as the Wess-Zumino-Witten (WZW) models [177, 178], and they are particular amongst the CFTs in the sense that they can be described by means of an action.

The defining action is given by

$$S(g) = \frac{k}{16\pi} \int_{\partial \Sigma} d^2x \operatorname{Tr}' \left[\partial^{\mu} g^{-1} \partial_{\mu} g \right] - \frac{ik}{24\pi} \int_{\Sigma} d^3y \epsilon_{\alpha\beta\gamma} \operatorname{Tr}' \left[g^{-1} \partial^{\alpha} g g^{-1} \partial^{\beta} g g^{-1} \partial^{\gamma} g \right], \tag{2.89}$$

where Σ is a 3-dimensional manifold whose boundary $\partial \Sigma$ is the 2-sphere. Tr' is a rescaled trace, $\epsilon_{\alpha\beta\gamma}$ is the Levi-Civita symbols, and the field g takes values in any Lie group G, such that $g\in G$. The second term corresponds to a topological total derivative term and the requirement that the partition function is single-valued leads to the condition that $k\in \mathbb{Z}$. This action is not only invariant under conformal transformations but also under the local action of any element $\Omega(z)\in G$ that transforms the field as

$$g(z,\overline{z}) \to \Omega(z)g(z,\overline{z})\overline{\Omega}^{-1}(\overline{z}).$$
 (2.90)

Local invariance under the action of the Lie group means that the symmetry will be characterized by the holomorphic currents

$$J(z) = -k\partial_z g g^{-1} = J^a(z) t^a = \sum_{n \in \mathbb{Z}} J_n^a z^{-n-1} t^a, \tag{2.91}$$

where t^a are elements of the Lie algebra $\mathfrak g$ corresponding to G, and similar expression equations for the anti-holomorphic sector have been ignored. The set of currents fulfills the Kác-Moody OPE [37]

$$J^{a}(z)J^{b}(w) \sim \frac{k\delta_{ab}}{(z-w)^{2}} + \sum_{c} i f_{abc} \frac{J^{c}(w)}{(z-w)},$$
 (2.92)

where f_{abc} are the structure constants of \mathfrak{g} , and this set of relations means that the set of currents forms a current algebra at level k. As was to be expected, the commutation relations between the holomorphic current algebra and its anti-holomorphic counterpart is zero, signifying the decoupling of both sectors.

The energy-momentum tensor for this theory can be constructed via the Sugawara-Sommerfeld construction to yield

$$T(z) = \frac{1}{k+h} \sum_{a=1}^{\dim(G)} : J^a J^a : (z),$$
 (2.93)

where h is the dual Coxeter number, which can be computed from the Lie Group G. The conformal currents have conformal dimension h=1 and that they are Virasoro primary fields. From this energy-momentum, one computes the Virasoro generators to obtain

$$L_n = \frac{1}{2(k+g)} \sum_{m \in \mathbb{Z}} : J_m^a J_{n-m}^a : .$$
 (2.94)

Afterwards one checks that the Virasoro generators and the modes of the currents fulfill the commutation relations

$$\begin{split} [L_n, J_m^a] &= -m J_{n+m}^a, \\ [J_n^a, J_m^b] &= i f_{abc} J_{n+m}^c + k n \delta_{ab} \delta_{n+m,0}, \end{split} \tag{2.95}$$

and the commutation relation of the Virasoro generators is that of the Virasoro algebra. From these commutation relations, we see that in the same way that the Virasoro

generators are a central extension of the Witt algebra with the central charge c, the current algebra is an affine Lie algebra, constructed as a loop-extension of the Lie algebra by the level k of the WZW theory. It is worth pointing out that the full affine Lie algebra is not a symmetry algebra since not all of its generators commute with L_0 . Only J_0^a do commute, which are the affine generators that recover the original Lie algebra, which will become relevant in Chapter 4. We will call the affine Lie algebra the spectrum-generating algebra of the theory. The central charge of the theory gets fixed in terms of the choice of G and level k to be

$$c_{WZW} = \frac{k \dim(G)}{k+h}. (2.96)$$

Primary fields are then defined by their OPEs with the currents as

$$J^{a}(z)g(w,\overline{w}) \sim \frac{-t^{a}g(w,\overline{w})}{z-w},$$
 (2.97)

where we assume that g transforms in the minimal representation of \mathfrak{g} , to which t^a refers. In the operator representation, the condition for primary becomes

$$J_0^a |\phi\rangle = -t^a |\phi\rangle,$$

$$J_n^a |\phi\rangle = 0 \text{ for } n > 0,$$
(2.98)

and then all descendant states have the form $J^a_{-n_1}...J^b_{-n_m}|\phi\rangle$ as in the case of usual CFT, with n_i being positive integers. Finally, as in the case of standard CFT, all the correlation functions involving descendant fields can be reduced to correlation functions of primary fields, and the primary fields obey certain differential equations because of the null vectors of the module. For the WZW models, this is known as the Knizhnik-Zamolodchikov equation [37], which takes the form

$$\left[\partial_{z_i} - \frac{1}{k+h} \sum_{i \neq j} \frac{t_i^a \otimes t_j^a}{z_i - z_j}\right] \langle \phi_1(z_1) ... \phi_n(z_n) \rangle = 0. \tag{2.99}$$

These models have found use as rational conformal field theories, but their most important application for our purposes is their appearance as the boundary side of the Chern-Simons/WZW duality [179]. In short, the correlation functions of WZW theories can, in general, be represented as partition functions of a specific TQFT known as the Chern-Simons theory, which is a gapped topological theory. This duality highlights the deep connection between the topological excitations of TQFTs and their CFT boundary counterparts.

3 GENERIC FTNS

In the previous chapter, we have seen a general overview of many of the different phases of matter that appear in Nature. Ranging from gapped to gapless and from short-range to long-range entangled, there is undoubtedly a myriad of phases that one can theoretically describe. We have also presented TNs as an ansatz that allows us to provide representative states within most of these phases. Because of the inherent trade-off between the amount of entanglement and the expressivity of TN states, almost all of the phases of matter mentioned above can be analytically described with TNs. Simultaneously, we have also seen the limitations of this family of ansatzs, mainly in describing gapless order with MPS or describing gapped chiral topological order in 2d.

In this chapter, we provide an approach that potentially closes this gap and provides a new family of trial wavefunctions that specifically targets the ones that were previously out of reach by standard TN methods. We call this family of states field tensor network states (fTNS). We construct this family by using the intrinsic connection that our target states have with CFT while borrowing techniques from the realm of CFT to apply them to the realm of tensor networks. Of course, no increase in the complexity of the state comes for free, and the price that we pay is that we must work with an infinite-dimensional virtual space. However, this is not any arbitrary infinite-dimensional space; otherwise, we would describe any state of the many-body Hilbert space, which we know is an arduous task. This infinite-dimensional space is constrained to fulfill the structure of the CFT and, therefore, allows us to retain analytical control over the ansatz.

We first present the generic construction of any fTNS to provide our primary example of interest, the free boson fTNS. We then study the fMPS, representing an example of a critical 1-dimensional MPS-like structure. Afterward, we present an fPEPS, which is a representative of a chiral gapped phase of matter, which is one of the main results of this thesis, as no such analytical example of a PEPS-like structure describing this topological order exactly was known before.

We then present one of the most important results of this thesis, which is the sewing condition. This condition pertains to the contraction of the virtual space of fTNS amongst any two tensors, even when this contraction involves a sum over an infinite dimensional space. Although the proof is not yet complete, we present the most recent form of the proof as well as what are the remaining steps for its completion. Afterwards, we use the developed technology to perform the closing condition of the fTNS, allowing to recover the wavefunction of the spin system.

3.1 GENERIC FTNS

3.1.1 FROM TNS TO FTNS

Our goal is to describe the quantum state of a spin system consisting of a lattice of N d-dimensional spins whose wavefunction can be written as

$$|\psi\rangle = \sum_{s_1...s_N=1}^d c_{s_1,...,s_N} |s_1...s_N\rangle. \tag{3.1}$$

As we have seen in Chapter 2, TNs are precisely an ansatz representation of such a wavefunction in terms of a set of tensors A^i , where the index i runs through all the different tensors that constitute the wavefunction. For simplicity, we will only consider a single tensor repeated on every site, setting i=1, which is the common scenario found in MPS and PEPS. Mathematically, we can generally understand the ansatz tensors as a map

$$A: \mathcal{V}_{\text{virtual}} \otimes \mathcal{H}_{\text{physical}} \longrightarrow \mathbb{C}, \tag{3.2}$$

where $\mathcal{V}_{\text{virtual}}$ is the generic vector space corresponding to the virtual legs of the tensor and $\mathcal{H}_{\text{physical}}$ is the Hilbert space corresponding to the d-dimensional spin on any site.

In almost all TNS constructions, one usually takes $\dim(\mathscr{V}_{\text{virtual}}) = \chi^{N_l}$ where χ is the bond dimension and N_l the number of legs of the tensor. The bond dimension is the main parameter that controls the expressivity of the ansatz, the amount of entanglement present in the state, and, therefore, the complexity of the state. Keeping χ finite and as small as possible is of paramount importance in all numerical tasks that use TNS [11]. Unless controlled, numerical algorithms would demand an unbounded amount of memory, rendering the task impossible.

A significant part of the fame of TNS is attributed to their success in numerical simulation. Still, in this thesis, we want to focus on providing exact analytical representations of quantum states as tensor networks. We know that TNS with finite bond dimension target precisely those states that fulfill the area-law of entanglement [10], yet we also painstakingly know that not all interesting states that one can find in Nature obey it. Firstly, states that fulfill the area law are the exception and not the rule in the Hilbert space of a local gapped Hamiltonians [79], as a generic state will almost always exhibit volume-law entanglement. Secondly, the ground state of a 1-dimensional critical system exhibits a logarithmic growth for the entanglement entropy for a subsystem [180], necessitating a different TN architecture to achieve an better representation of that state, usually in the form of a MERA [22]. Lastly, although PEPS can host algebraically decaying correlations, an exact representation of a state belonging to the FQHE family remains out of reach, and there have even been no-go theorems indicating that it may be impossible [181],[182].

It seems that before us lies a crossroad. On one path, we accept that not all states can have exact TN representations. Although we can have excellent numerical approximations, for instance via finite size scaling as in [183], we preserve our simple TN structures to describe those states approximately. On the other path, we modify the TN representation to provide an exact description of the state, at the cost of obscuring some of the previous theorems and numerical guarantees and having to study and understand a new class of ansatz. In this thesis, we follow the second path, and our main modification consists of allowing the virtual space of the TN to be ∞ -dimensional.

Let us define field Tensor Network States (fTNS) as the states constructed from a network of tensors \mathcal{A}^{s_i} , interpreted as a map

$$\mathcal{A}: \mathcal{H}_{\text{virtual}} \otimes \mathcal{H}_{\text{physical}} \longrightarrow \mathbb{C}, \tag{3.3}$$

where now $\dim(\mathscr{H}_{\text{virtual}})=\infty$. We allow the virtual Hilbert space to be an infinite dimensional space in which we can define a countably infinite basis, which is the more precise meaning of the limit $\chi \to \infty$. Note how this is different from the approach pursued in cMPS [184] or cTNS [185], where the goal is to describe a physical quantum field with TN, and thus $\mathscr{H}_{\text{physical}}$ is the space that is allowed to become infinite-dimensional. Our goal remains to describe the state of a quantum spin chain as in Equation (3.1). Therefore, the dimension of the physical Hilbert space is fixed by the spin dimension $\dim(\mathscr{H}_{\text{physical}})=d$.

The Hilbert space that we will use the most in this thesis is the space of square-integrable functions on an interval [a,b] with $a < b \in \mathbb{R}$, alongside the set of constant functions $\mathbb{L}^2([a,b]) \cup \mathbb{K}$. Note how we can also allow the interval to be infinite, \mathbb{R} or semi-infinite $[0,\pm\infty)$. We say that a function is square integrable on any given interval if and only if

$$f:[a,b]\to\mathbb{C}\in\mathbb{L}^2([a,b])\longleftrightarrow\int_a^bdx|f(x)|^2<\infty.$$
 (3.4)

Although the set of constant functions \mathbb{K} is not square integrable when the domain is unbounded, such as in the case of \mathbb{R} , we will see in the upcoming sections that they need to be accounted for in order to describe the sector of zero modes that is present in most field theories. Because the virtual space of \mathcal{A} has become a functional space, we will use the notation $\mathcal{A}[f_1, f_2, ...]$ or $\mathcal{A}_{f_1, f_2, ...}$ interchangeably to denote a functional tensor whose virtual legs have been fixed to specific functions $f_1, f_2, ... \in \mathbb{L}^2([a, b])$.

For clarity, let us establish a parallel with the much more familiar case of MPS. In the case of translationally invariant MPS, the coefficients of the wavefunction are written as

$$c_{s_1,...,s_N} = \sum_{n_1,...,n_N=1}^{D} A_{n_1,n_2}^{s_1} A_{n_2,n_3}^{s_2} ... A_{n_N,n_1}^{s_N},$$
(3.5)

where the matrices $A_{n_i,n_{i+1}}^{s_i} \in \mathbb{C}$ are the MPS tensors consisting of d complex matrices of dimension $\chi \times \chi$, $n_i = 1,...,\chi$. Similarly, the coefficients of the wavefunction obtained from a translationally invariant field Matrix Product States (fMPS) will be written as

$$c_{s_1,...,s_n} = \int \mathcal{D}f_1...\int \mathcal{D}f_n \mathcal{A}^{s_1}[f_1, f_2]...\mathcal{A}^{s_n}[f_n, f_1], \tag{3.6}$$

where the previous sum over the indices has now become an integration of all possible functions that can be given as input to the functional, commonly known as a path integral. Because we want to define our functionals parallel to what is done in standard tensor networks theory, we had to choose an infinite dimensional Hilbert space as the virtual space, as opposed to other infinitely sized spaces. Because any two finite tensors can be contracted by summing over their connecting index, we must also require that our functional tensors can. It is, therefore, mandatory that we must be able to find a basis that one can sum over in the virtual space, and Hilbert spaces provided precisely one such mathematical structure.

Without any further structure, performing this generalization would simply be an interesting mathematical experiment since sending $\chi \to \infty$ would allow us to describe

any state of the Hilbert space and, therefore, highly complicated states. Analytically, it is prohibitively hard to describe such arbitrarily entangled states without the aid of symmetries or any further properties. Numerically, it is very hard to optimize an infinite dimensional space without truncating the space and, therefore, returning to the standard formulation of TNS. We are missing one final insight: the spin wave function that we wish to describe exactly with fTNS has to be characterized by a correlator of the system's underlying low-energy effective field theory.

3.1.2 FIELD-THEORETICAL CONSTRUCTION OF THE FTNS TENSOR

From this point onwards, we will assume that our target spin system wave function corresponds to a 1- or 2-dimensional system for simplicity. The starting point of our fTNS construction is to assume that the coefficients of the spin system can be computed as

$$c_{s_1,...,s_n}(z_1, z_2, ...z_n) = \langle \phi(z_1, s_1)\phi(z_2, s_2)...\phi(z_n, s_n) \rangle, \tag{3.7}$$

where $\phi(z,s)$ is whatever field operator that is important for the correlator of the underlying low-energy effective field theory and $z_i = x_i + iy_i$ would correspond to the i^{th} -spin position in the final wavefunction. Usually, the correlator is assumed to be between the in-vacuum state and the out-vacuum state of the field theory. Different boundary states could be used to define further states of the Hilbert space, such as excited states of a 1-dimensional critical system as shown in [48].

To find the expression of the functional tensor, the first step consists in rewriting the correlator as an Euclidean path-integral

$$c_{s_1,...,s_n} = \int_{\mathcal{S}} \mathcal{D}\phi \ \phi(z_1,s_1)\phi(z_2,s_2)...\phi(z_n,s_n)e^{-S_E[\phi]}, \tag{3.8}$$

where $S_E[\phi]$ is the Euclidean action of the field theory, and $\mathcal S$ is the underlying base space of the theory, usually assumed to be the plane, an infinite cylinder, or a torus. The path integral in Equation (3.8) will sum over all possible field configurations over $\mathcal S$, and so if the underlying space can be broken down into small patches $\mathcal M_i$, we can break down the path integral into the contributions of each patch. Mainly, if $\mathcal S=\cup_i \mathcal M_i$

$$\int_{\mathcal{S}} \mathcal{D}\phi \to \int_{\mathcal{M}_1} \mathcal{D}\phi_1 \dots \int_{\mathcal{M}_n} \mathcal{D}\phi_n, \tag{3.9}$$

where now each path integral is only over the configurations within the patch \mathcal{M}_i . However, Equation (3.9) could not be complete as it stands, as now each patch has a boundary $\partial \mathcal{M}_i$ in which we need to specify boundary conditions for the field. Thus, we also need to sum over all possible boundary conditions $\phi(z)=f_i(z)$ $z\in\partial\mathcal{M}_i$, and hence the correct breakdown of the path integral is

$$\int_{\mathcal{S}} \mathcal{D}\phi = \int \mathcal{D}f_{1} \dots \int \mathcal{D}f_{n} \int_{\mathcal{M}_{1}}^{\prime} \mathcal{D}\phi_{1} \dots \int_{\mathcal{M}_{n}}^{\prime} \mathcal{D}\phi_{n}, \tag{3.10}$$

where the path integrals with a prime correspond to the sum over field configurations that obey the appropriate Dirichlet boundary conditions for that patch. Finally, we can always choose the regions \mathcal{M}_i to each enclose a single one of the operator insertions of Equation (3.7), finally reaching the expression for the functional

$$\mathcal{A}^{s_i}[f_i] = \int_{\mathcal{M}_i}^{\prime} \mathcal{D}\phi\phi(z_i, s_i) e^{-S_E[\phi]}. \tag{3.11}$$

By inputting this expression back into Equation (3.8), we find

$$c_{s_1,\dots,s_n} = \int \mathcal{D}f_1\dots \int \mathcal{D}f_n \mathcal{A}^{s_1}[f_1]\dots \mathcal{A}^{s_n}[f_n], \tag{3.12}$$

where the path integral over all possible boundary conditions is nothing but the sum over all the open indices of the functionals. Therefore, this equation is precisely the complete contraction of the tensor network, which we call the closing condition.

In order to simplify future equations, we now define a diagrammatic notation for fTNS. We will be diagrammatically representing these functionals with 2-dimensional closed manifolds \mathcal{M}_i , corresponding to the patches of Equation (3.9) as shown in Figure 3.1. The "legs" of the tensors correspond to different sections in which we choose to partition the boundary $\partial \mathcal{M}_i$, and the physical degree of freedom corresponds to the cross in the middle accompanied by its spin value.

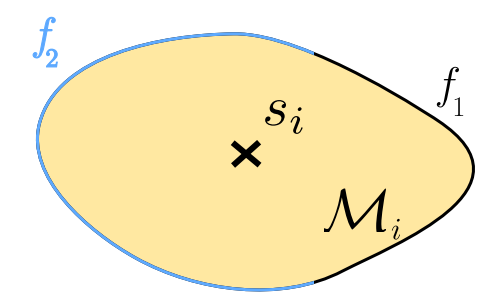


Figure 3.1: Diagrammatic notation for the functional $\mathcal{A}^{s_i}[f_1,f_2]$. Each section of the boundary $\partial\mathcal{M}$ corresponds to the different functional legs of the tensor. The physical leg corresponds to the cross in the center.

As an example, and as it was shown in [186], the two choices of \mathcal{M}_i that lead to the fMPS and fPEPS functional are depicted in Figure 3.2. An infinite strip is the only 2-dimensional surface with exactly two isomorphic boundaries, each corresponding to the functional legs of the fMPS. Similarly, four isomorphic boundaries lead to the geometry of a square, which we use for the fPEPS.

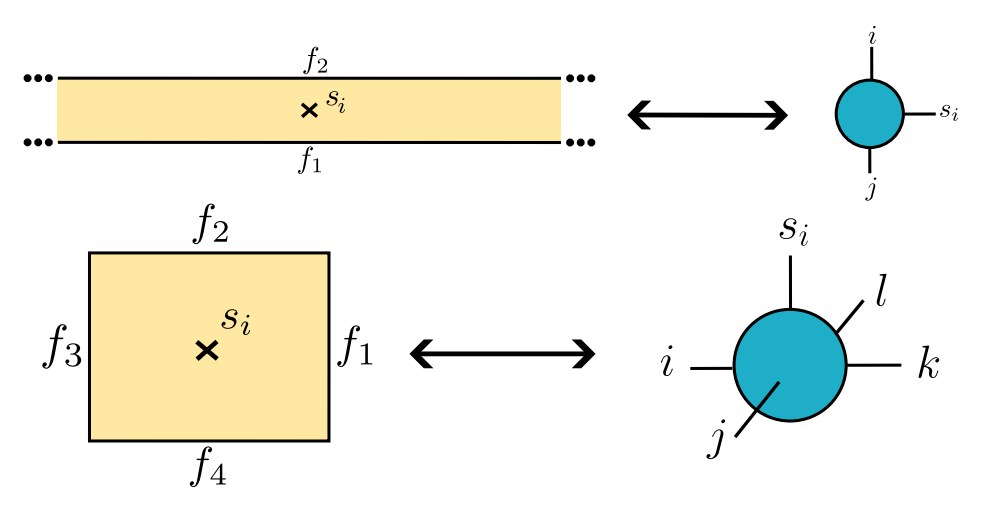


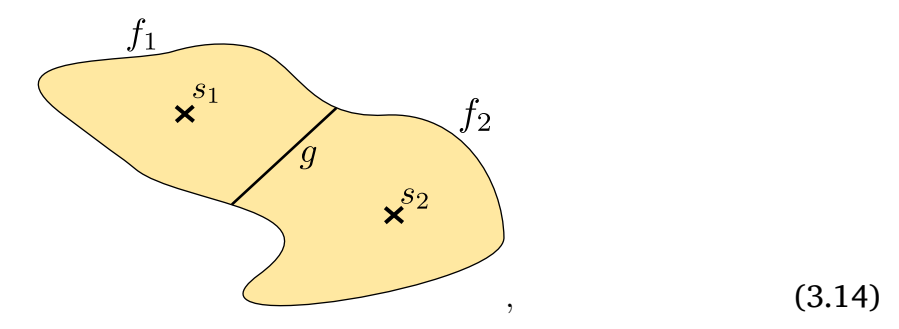
Figure 3.2: Diagrammatic notation for the MPS (top) and PEPS (bottom) functional.

With a diagrammatic notation in hand, we can now represent the most important operation of these tensors: tensor contraction. In our language, this operation corresponds to performing a path integral over all the possible functions that live in a shared

compatible boundary,

$$\int \mathcal{D}g\mathcal{A}^{s_1}[f_1, g]\mathcal{A}^{s_2}[g, f_2] = \mathcal{A}^{s_1, s_2}[f_1, f_2]$$
(3.13)

or diagrammatically,



and this operation is what we will call the sewing condition. There are several important requirements for the sewing condition to be properly defined. Firstly, the two functionals \mathcal{A}_1 and \mathcal{A}_2 must have a compatible boundary. More precisely, the submanifold of the boundary ∂M_S where the path integral takes place must be present in both \mathcal{M}_1 and \mathcal{M}_2 . Secondly, we demand that the result of sewing two functionals is again a new functional that inherits both the physical and the uncontracted functional legs of the previous ones. We will devote a future section to providing the current state of proof of the exact sewing condition for two arbitrary compatible functionals precisely.

Finally, to recover the wave function of the target state, we must keep performing sewings until there are no uncontracted functional legs left, and this last step is what we will call the closing condition. Depending on the specifics of the intermediate sewings, it is possible to emulate the geometry of the target spin system state. For instance, by sewing the MPS functionals in a ring, one ends up with a set of spins that form a periodic chain, whose closing diagrammatically is

$$c_{s_1, s_2, \dots, s_n} = \begin{pmatrix} & \times s_3 \\ & \times s_2 \\ & \times s_1 \\ & \times s_n \end{pmatrix}, \tag{3.15}$$

which can be used to recover the ground state of the critical Haldane-Shastry model [186]. Another option explored in [186] would be to generate a torus geometry with the fPEPS tensor, which we will explore in a future section with the hope of recovering the Kalmeyer-Laughlin state on a torus.

To summarize, to define an fTNS tensor, we need as an input an effective field theory, a specific operator insertion at the position of the spin, and the boundary conditions for the field that will act as the legs of the tensor for a given geometry.

3.1.3 THE FREE BOSON FTNS

DERIVATION OF THE FREE BOSON FTNS

From now on, we will focus on the case of the massless free boson, one of the simplest CFTs. As we have seen in Chapter 2, it can also be understood as the WZW $SU(2)_1$

model when its compactification radius is chosen to be $R=\sqrt{2}$ [37]. The set of target wavefunctions that we are aiming for are those that can be obtained from the vertex operator correlator

$$c_{s_1,\dots s_N} \propto \langle :e^{is_1\sqrt{\alpha}\phi(z_1)}:\dots:e^{is_N\sqrt{\alpha}\phi(z_N)}:\rangle_0, \tag{3.16}$$

where :: denotes normal ordering, $\phi(z_i)$ is the chiral real massless scalar field, z_i is the position of the spin, and the subscript 0 denotes the correlator is taken in the vacuum of the CFT. The chiral vertex operators : $e^{is_i\sqrt{\alpha}\phi(z_i)}$: with $\alpha=\frac{1}{2}$ are the spin $\frac{1}{2}$ primary fields of the WZW SU(2) $_1$ theory. This family of states is of extreme relevance to us, as it provides us with examples that are analytically out of reach for standard TN techniques. If this correlator is computed in the cylinder, the ground state of the critical point Haldane-Shastry chain is recovered [187],[188]. If solved on a plane or a torus, it yields the Kalmeyer-Laughlin state [189],[190], a paradigmatic state of 2-dimensional chiral gapped topological order.

We start by providing the fTNS tensor of the free boson on an arbitrary manifold \mathcal{M} that contains only one of the vertex operator insertions of Equation (3.16). The action of the free boson on this manifold in 2 dimensions reads

$$S_{\mathcal{M}}[\phi] = \frac{1}{8\pi} \int_{\mathcal{M}} d^2x \ \partial_i \phi(x) \partial^i \phi(x), \tag{3.17}$$

where $\phi(x)$ is the massless scalar field. The path integral that one must perform is then

$$\mathcal{A}^{s_i}[f] = \int' \mathcal{D}[\phi] e^{-S_{\mathcal{M}}[\phi]} e^{-is_i \sqrt{\alpha} \phi_i(z_i)}, \tag{3.18}$$

where the boundary condition corresponds to

$$\phi(x) = f(x) \ x \in \partial \mathcal{M}. \tag{3.19}$$

We begin by computing the path integral of the action with a source term

$$\mathcal{A}^{s_i}[f] = \int' \mathcal{D}[\phi] e^{-S_{\mathcal{M},\rho}[\phi]}, \tag{3.20}$$

where the action is now given by

$$S_{\mathcal{M},\rho}[\phi] = \frac{1}{8\pi} \int_{\mathcal{M}} d^2x \partial_i \phi(x) \partial^i \phi(x) - \frac{1}{4\pi} \int_{\mathcal{M}} d^2x \rho(x) \phi(x), \tag{3.21}$$

where the spin density is given by $\rho(x)=4\pi i\sum_{j=1}^N s_j\delta^2(x-x_j)$, where x_j are the Cartesian coordinates of the spin position, and we have absorbed the $\sqrt{\alpha}$ pre-factor as a normalization factor for the spin-values s_j .

First, we start by isolating the contribution from the constant zero mode to the path integral. If we split the field as $\phi(x) = \phi_0 + \tilde{\phi}(x)$ then Equation (3.20) becomes

$$\mathcal{A}^{s_i}[f] = \int' \mathcal{D}\phi_0 \mathcal{D}[\tilde{\phi}] e^{-S_{\mathcal{M},\rho}[\tilde{\phi}]} e^{i\phi_0 \sum_{j=1}^N s_j} = \int d\phi_0 e^{i\phi_0 \sum_{j=1}^N s_j} \int' \mathcal{D}[\tilde{\phi}] e^{-S_{\mathcal{M},\rho}[\tilde{\phi}]} \delta(\phi_0 - f_0), \tag{3.22}$$

where the zero mode path integral imposes that the constant part of the boundary condition of the classical equations of motion also splits as $f(x) = f_0 + \tilde{f}(x)$, and thus

that the zero mode of the boundary function is the same on all boundaries. Equation (3.22) then reduces to

$$\mathcal{A}^{s_i}[f] = \delta\left(\sum_{j=1}^N s_j\right) \int^{'} \mathcal{D}[\tilde{\phi}] e^{-S_{\mathcal{M},\rho}[\tilde{\phi}]} \delta(\phi_0 - f_0) \sim \delta\left(\sum_{j=1}^N s_j\right) e^{-S_{\mathcal{M},\rho}[\psi_{cl}]}, \qquad \textbf{(3.23)}$$

where in the last step, we have solved the path integral by performing a saddle point approximation around the classical solution $\psi_{cl}(x)$. This expression is obtained as the solution of the Poisson equations of motion with Dirichlet boundary conditions

$$\begin{split} \nabla^2 \psi_{cl}(x) &= -\rho(x) \\ \psi_{cl}(x) &= f(x) = \tilde{f}(x) + f_0 \ \ x \in \partial \mathcal{M}. \end{split} \tag{3.24}$$

From now on, the zero mode contribution to the boundary condition will be omitted as it will play no role in the computation of the classical solution. This equation is solved by classical Green's functions techniques [191] and yields

$$\psi_{cl}(x) = -\int_{\mathcal{M}} d^2y G_{\mathcal{M}}(x,y) \rho(y) + \int_{\partial \mathcal{M}} d\Gamma_y \tilde{f}(y) \hat{\mathcal{N}}_y G_{\mathcal{M}}(x,y), \tag{3.25}$$

where $\hat{\mathcal{N}}$ is the normal derivative operator w.r.t to the boundary $\partial \mathcal{M}$, the contour integral is taken to be counterclockwise where $d\Gamma_y$ is the parametrization of the boundary and the Green function $G_{\mathcal{M}}(x,y)$ is the solution of

$$\begin{split} &\nabla^2 G_{\mathcal{M}}(x,y) = \delta^2(x-y) \\ &G_{\mathcal{M}}(x,y) = 0 \ \ \text{if} \ \ x \ \text{or} \ y \in \partial \mathcal{M}. \end{split} \tag{3.26}$$

Now, we insert the classical solution into $S_{\mathcal{M},\rho}$, which we do after using the second Green identity to write the action in Equation (3.21) as

$$S_{\mathcal{M},\rho}[\psi_{cl}] = \frac{1}{8\pi} \int_{\partial \mathcal{M}} d\Gamma_x \tilde{f}(x) \hat{\mathcal{N}}_x \psi_{cl}(x) - \frac{1}{8\pi} \int_{\mathcal{M}} d^2x \psi_{cl}(x) \rho(x). \tag{3.27}$$

After inserting Equation (3.25) into Equation (3.27) and reorganizing the terms, one obtains

$$\begin{split} S_{\mathcal{M},\rho}[f] &= \frac{1}{8\pi} \int_{\mathcal{M}} d^2x d^2y \rho(x) \rho(y) G_{\mathcal{M}}(x,y) - \frac{1}{4\pi} \int_{\mathcal{M}} d^2x \int_{\partial \mathcal{M}} d\Gamma_y \rho(x) \tilde{f}(y) \hat{\mathcal{N}}_y G_{\mathcal{M}}(x,y) \\ &+ \frac{1}{8\pi} \int_{\partial \mathcal{M}} d\Gamma_x \int_{\partial \mathcal{M}} d\Gamma_y \tilde{f}(x) \tilde{f}(y) \hat{\mathcal{N}}_y \hat{\mathcal{N}}_x G_{\mathcal{M}}(x,y), \end{split} \tag{3.28}$$

where the variables $x, y \in \mathcal{M}$ are used as either 2-dimensional Cartesian coordinates or as a parametrization of the boundary according to their respective integration measure.

We identify the first term in the action in Equation (3.28) as a spin-spin interaction term, the second term will correspond to the spin-boundary interaction, and the last one we interpret as a propagation term amongst the different boundaries. We, therefore, have the functional tensor exclusively in terms of the Poisson Green's function on $\mathcal M$ and the spin density $\rho(x)$. Whilst $\rho(x)$ is always chosen to mimic the spatial distribution of spins, we must guarantee that we can always find such a Green's function, thus a general solution to Equation (3.26).

To obtain a generic solution, one departs from the well-known solution of the 2-dimensional Poisson Equation in \mathbb{C} , which is given by

$$G_{\mathbb{C}}(z, z') = \frac{1}{4\pi} \log|z - z'|^2,$$
 (3.29)

where z=x+iy is the position in the complex plane. Next, we use this solution to construct the solution in the Upper Half Plane (UHP) $\mathbb H$ using the method of images, which is

$$G_{\mathbb{H}}(z,z') = \frac{1}{4\pi} \log \frac{(z-z')(\overline{z}-\overline{z}')}{(z-\overline{z}')(\overline{z}-z')},\tag{3.30}$$

where now the boundary is the real line \mathbb{R} . Finally, we make use of the Riemann mapping theorem, which informally states that there always exists a conformal map g from any simply connected closed submanifold of \mathbb{C} , \mathcal{M} , to the UHP such that the boundary of \mathcal{M} is mapped to the real line. More formally, that is

$$g:\mathcal{M}\to\mathbb{H} \ \text{ s.t. } g(\partial\mathcal{M})=\mathbb{R}.$$
 (3.31)

One can use this map to find the final Green function on an arbitrary manifold $\mathcal M$

$$G_{\mathcal{M}}(x,y) = \frac{1}{4\pi} \log \left[\frac{\left(g(x) - g(y)\right) \left(\overline{g(x)} - \overline{g(y)}\right)}{\left(\overline{g(x)} - g(y)\right) \left(g(x) - \overline{g(y)}\right)} \right], \tag{3.32}$$

where x,y are now coordinates in \mathcal{M} . As we can see in Equation (3.32), we write the dependence of $G_{\mathcal{M}}(x,y)$ on the coordinates $x,y\in\mathcal{M}$ directly, although the dependence is through the conformal map g(x). We do this for ease of notation and should be remembered for all expressions that depend on the coordinates in \mathcal{M} , such as Equation (3.28).

Although the existence of such a conformal map is guaranteed, we need a specific form for it in order to compute any tensor. Whenever the geometry of interest is a polygon, we can use the Schwarz-Christoffel mapping technique [192],[193], which we shortly review. For a polygon with interior angles $\alpha, \beta, \gamma...$, the conformal map which maps $\mathbb R$ to the edges, and the UHP to the interior of the polygon, is given by

$$f(\xi) = \int^{\xi} \frac{Kd\omega}{(\omega - a)^{1 - \frac{\alpha}{\pi}} (\omega - b)^{1 - \frac{\beta}{\pi}} (\omega - c)^{1 - \frac{\gamma}{\pi}} \dots} \quad \xi \in \mathbb{H},$$
 (3.33)

where K is a constant to be fixed by boundary conditions, and a < b < c < ... are points along $\mathbb R$ that will be mapped to the vertices of the polygon. Note that this map is, in fact, the inverse of the map we described in Equation (3.31), as it maps from $\mathbb H$ to $\mathcal M$. With this technique, the two maps leading to the fMPS and the fPEPS tensors can be constructed, and they will be provided in the upcoming sections.

In summary, in this section, we have provided the generic construction of the free boson fTNS tensor on an arbitrary manifold \mathcal{M} . Furthermore, we have shown the generic construction for the Green function $G_{\mathcal{M}}$, up to an unspecified conformal map. Whenever the geometry is simpler, we can construct such a conformal map via the Schwarz-Christoffel construction.

REGULARIZATION OF THE FREE BOSON FTNS

In this section, we will explore the three different terms that appear in Equation (3.28), starting with the first one, the spin-spin interaction term. If we introduce the expression for the spin densities $\rho(x)$, the first term from Equation (3.28) becomes

$$-\frac{1}{2}\sum_{i\neq j}^{N}s_{i}s_{j}\log\left[\frac{\left(g(z_{i})-g(z_{j})\right)\left(\overline{g(z_{i})}-\overline{g(z_{j})}\right)}{\left(\overline{g(z_{i})}-g(z_{j})\right)\left(g(z_{i})-\overline{g(z_{j})}\right)}\right]\tag{3.34}$$

where the divergent terms arising from i=j, which would correspond to a spin interacting with itself, have been omitted. Their more accurate description in terms of normal ordering will be presented in a later section. This is not the only potential divergence, as this term could still diverge if the positions of two different spins were identical. Because the Green function must contain this divergent behavior to capture the correct features of the CFT, special care must be taken to evaluate all the other terms of Equation (3.28). Similar divergences will be present in all of those terms and hence a regularization procedure must be employed to guarantee that the functional tensor is finite. Furthermore, this requirement will provide insight into which boundary functions are acceptable candidates for the boundary functions of the tensor. To prevent the divergence arising from any two points being close, we will regularize these terms by evaluating the boundary integrals of Equation (3.28) in a contour that is ε close from the inside to $\partial \mathcal{M}$, which we denote by $\int_{\partial \mathcal{M}_{\varepsilon}}$.

Let us demonstrate this regularization scheme with the second term of Equation (3.28)

$$\frac{1}{4\pi} \int_{M} d^{2}x \int_{\partial \mathcal{M}_{\varepsilon}} d\Gamma_{y} \rho(x) \tilde{f}(y) \hat{\mathcal{N}}_{y} G_{\mathcal{M}}(x, y), \tag{3.35}$$

which we called the spin-boundary interaction term. After introducing the spin density, it becomes

$$i\sum_{i=1}^{N} s_{i} \int_{\partial \mathcal{M}_{\varepsilon}} d\Gamma_{y} \tilde{f}(y) \hat{\mathcal{N}}_{y} G_{\mathcal{M}}(z_{i}, y). \tag{3.36}$$

Given a parametrization of the boundary in terms of a real parameter $s \in \mathcal{D}$, where \mathcal{D} is a real domain such that $y(s) \in \partial M$, the integral reads $\int d\Gamma_x = \int_{\mathcal{D}} ds$. As a convention, we always take the orientation of the boundary integrals to be counter-clockwise. To perform the regularization, we evaluate the terms inside of the integral ε away from the boundary at $x(s) - \varepsilon n(s)$, where n(s) is the normal outwards vector at each point of the boundary. With this considerations Equation (3.36) becomes

$$i\sum_{i=1}^{N}s_{i}\int_{\mathcal{D}}ds\tilde{f}(y(s))\hat{\mathcal{N}}_{y}G_{\mathcal{M}}(z_{i},y)|_{y=y(s)-\varepsilon n(s)}, \tag{3.37}$$

where we have set $\tilde{f}(y)|_{y=y(s)-\varepsilon n(s)}=\tilde{f}(y(s))$ because we assume the boundary function to be a regular function, and thus without any divergent behavior to regularize. Then, we take the normal derivative of the Green function

$$\hat{\mathcal{N}}_y G_{\mathcal{M}}(z_i,y) = \frac{-1}{4\pi} \left[\frac{\hat{\mathcal{N}}_y g(y)}{g(z_i) - g(y)} - \frac{\hat{\mathcal{N}}_y \overline{g(y)}}{g(z_i) - \overline{g(y)}} + \frac{\hat{\mathcal{N}}_y \overline{g(y)}}{\overline{g(z_i)} - \overline{g(y)}} - \frac{\hat{\mathcal{N}}_y g(y)}{\overline{g(z_i)} - g(y)} \right], \tag{3.38}$$

where we can identify the first two terms as the chiral part and the latter ones as the anti-chiral part, as the position of the spin z_i appears either without or with complex conjugation. Because $g(y) \in \mathbb{R}$ whenever $y \in \partial \mathcal{M}$ by the construction of the conformal map, whenever $z_i \to y$, we will encounter the aforementioned divergence in all of the terms of Equation (3.38). This divergence is regularized by evaluating these terms ε -away from the boundary. Intuitively, we expect the evaluation on the regularized boundary to correspond to a small imaginary offset, as depicted in Figure 3.3.

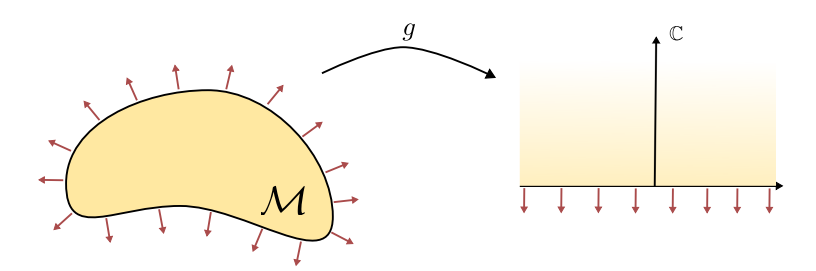


Figure 3.3: Diagram depicting the effect of the conformal map g on the normal directions of an arbitrary manifold $\mathcal M$

The proof of this intuition goes as follows. For a given parameterized boundary $y(s) \in \partial M$, then $g \circ y(s) = f(s)$ with $f(s) \in \mathbb{R}$, simply by definition of the conformal map. If we take the tangent vector along the boundary $\partial_s \left[g \circ y(s)\right] = \partial_s f(s)$, then the r.h.s will remain in \mathbb{R} . Using the chain rule on the l.h.s we get $\partial_z g(z)|_{z=y(s)}\partial_s y(s)$, where both terms are complex numbers. Writing the second one in polar coordinates, we get $\partial_z g(z)|_{z=y(s)}|\partial_s y(s)|e^{i\theta_t}$, where θ_t is the angle of the tangent direction at this point of M. This allows us to conclude that $\partial_z g(z)|_{z=y(s)}e^{i\theta_t} \in \mathbb{R}$, because the r.h.s is real.

By performing a small displacement along the normal direction like in (3.37), $g(y(s)\pm\varepsilon)$, where ε is a complex offset in the normal direction, then $g(y(s)\pm\varepsilon)\sim g(y(s))\pm\partial_z g(z)|_{z=y(s)}\varepsilon+...$ If we now use that ε is in the normal direction, a.k.a perpendicular to the tangent, then $g(y(s))\pm|\varepsilon|e^{i\theta_t+\frac{\pi}{2}}\partial_z g(z)|_{z=y(s)}+...=g(y(s))\pm i|\varepsilon|e^{i\theta_t}\partial_z g(z)|_{z=y(s)}+...$ where we now know that the second term is purely real, and thus this is a strictly imaginary offset at first order in ε . Moreover, this linear term in the expansion will always be present due to the holomorphicity of g(z). It is worth noting that it need not be a small offset, as the derivative could be arbitrarily big, but we should always be able to choose ε small enough to counter such a situation.

The previous arguments also allow us to express the normal derivative more explicitly. We immediately recognize the second term as $\pm |\varepsilon| \hat{\mathcal{N}}_y g(y)|_{y=y(s)}$, and hence as a purely imaginary quantity. The same expansion for the conjugate of the conformal map yields, $\overline{g}(y(s)\pm\varepsilon)\sim g(y(s))\mp i|\varepsilon|e^{i\theta_t}\partial_z g(z)|_{z=y(s)}$, and hence the second term is identified as $\mp |\varepsilon|\hat{\mathcal{N}}_y\overline{g}(y)|_{y=y(s)}$.

For the rest of the discussion on regularization, we will only focus on the chiral part of the expressions for simplicity. After evaluating the normal derivative according to the regularization scheme, at first order in ε , one obtains

$$\begin{split} &\hat{\mathcal{N}}_{y}^{c}G_{\mathcal{M}}(z_{i},y)|_{y=y(s)-\varepsilon\hat{n}(s)} = \\ &\frac{-1}{4\pi}\left[\frac{\hat{\mathcal{N}}_{y}g(y)|_{y=y(s)}}{g(z_{i})-g(y(s))+i|\varepsilon|e^{i\theta_{t}(s)}\partial_{z}g(z)|_{z=y(s)}} - \frac{\hat{\mathcal{N}}_{y}\overline{g(y)}|_{y=y(s)}}{g(z_{i})-g(y(s))-i|\varepsilon|e^{i\theta_{t}(s)}\partial_{z}g(z)|_{z=y(s)}}\right] \\ &= \frac{ie^{i\theta_{t}(s)}\partial_{z}g(z)|_{z=y(s)}}{4\pi} \\ &\left[\frac{1}{g(z_{i})-g(y(s))+i|\varepsilon|e^{i\theta_{t}(s)}\partial_{z}g(z)|_{z=y(s)}} + \frac{1}{g(z_{i})-g(y(s))-i|\varepsilon|e^{i\theta_{t}(s)}\partial_{z}g(z)|_{z=y(s)}}\right], \end{split} \tag{3.39}$$

where in the numerator we have again evaluated at y(s) directly, and the superscript c refers to the chiral part. To understand how to regularize these expressions, one must first see the isolated contribution of the divergence. Thus, one takes the limit alongside the tangent direction to the boundary $z_i \to y(s)$, which by a simple expansion $g(z_i) \to g(y(s)) + |z_i - y(s)||e^{i\theta_t}\partial_z g(z)|_{y=y(s)} + \dots$ leads to

$$\lim_{z_i \to y(s)} \hat{\mathcal{N}}^c_y G_{\mathcal{M}}(z_i,y)|_{y=y(s)-\varepsilon \hat{n}(s)} = \frac{i}{4\pi} \left[\frac{1}{|z_i-y(s)|+i|\varepsilon|} + \frac{1}{|z_i-y(s)|-i|\varepsilon|} \right], \quad \textbf{(3.40)}$$

which we immediately recognize as a divergence of the principal value kind. Notice how the details about the conformal map have all vanished from Equation (3.40), something to be expected as the CFT should exclusively control the divergent behavior.

We can finally define the regularized version of this kernel as

$$\begin{split} R\hat{\mathcal{N}}^c_y G_{\mathcal{M}}(z_i,y)|_{y=y(s)} &:= \hat{\mathcal{N}}^c_y G_{\mathcal{M}}(z_i,y)|_{y=y(s)} - \lim_{z_i \to y(s)} \hat{\mathcal{N}}^c_y G_{\mathcal{M}}(z_i,y)|_{y=y(s)} \\ &+ \lim_{z_i \to y(s)} \hat{\mathcal{N}}^c_y G_{M}(z_i,y)|_{y=y(s) - \varepsilon \hat{n}(s)}. \end{split} \tag{3.41}$$

To put this equation in plain words, our regularization scheme removes the divergence originating from the spin position from the original kernel and adds it again in its distributional form, in this case, a principal value with a regulator ε . If one returns now to Equation (3.39), we see that the regularized kernel can now be safely integrated against the boundary functions, as the first line of Equation (3.41) contains no divergent behavior, and the second line is a distribution integrated against a suitable well-behaved boundary function.

This is precisely the insight that allows us to choose a family of boundary functions. We have seen that the distributional divergence is of the principal value kind and thus belongs to the family of tempered distributions [194]. Therefore, the family of boundary functions that we should choose is the family of Schwartz functions $\mathcal{S}(\mathbb{R})$ on an arbitrary interval, which is the functional space dual to the space of tempered distributions. The Schwartz space is a very commonly used space in physics because :

- 1. This space is a dense subspace of square-integrable functions $\mathcal{S}(\mathbb{R}^n) \in \mathbb{L}^2(\mathbb{R}^n)$. Therefore, it remains a Hilbert space, and a contraction operation can be properly defined.
- 2. Any smooth function with compact support is in $\mathcal{S}(\mathbb{R}^n)$. Therefore, this is a good space to work with for both compact and non-compact boundaries $\partial \mathcal{M}$.

3. The Fourier transform acts as an isomorphism on the Schwartz space, providing guarantees of convergence when usable.

As we will see in the specific example of the PEPS functional in the upcoming sections, the specific details of the conformal map, such as periodicities, must be taken into account for the subtraction of all possible divergences in Equation (3.41). Thus, it is important to check for any conformal map that the following identity holds

$$\lim_{\varepsilon \to 0} (R \hat{\mathcal{N}}^c_y G_{\mathcal{M}}(z_i,y)|_{y=y(s)-\varepsilon \hat{n}(s)} - \hat{\mathcal{N}}^c_y G_{\mathcal{M}}(z_i,y)|_{y=y(s)-\varepsilon \hat{n}(s)}) = 0 \quad \forall z_i,y(s), \qquad \textbf{(3.42)}$$

where in the last equation the limit $z_i \to y(s)$ is taken before the limit $\varepsilon \to 0$. This equation guarantees that both kernels will result in the same integration when we take the limit of removing the regulators.

As with the spin-boundary term, the last term of Equation of (3.28), which we call the propagation term or the boundary-boundary term, will contain the same divergences and thus require regularization. We start by computing the double derivative

$$\begin{split} \hat{\mathcal{N}}_x \hat{\mathcal{N}}_y G_{\mathcal{M}}(x,y) &= \frac{1}{4\pi} \left[\frac{\hat{\mathcal{N}}_x g(x) \hat{\mathcal{N}}_y g(y)}{(g(x) - g(y))^2} - \frac{\hat{\mathcal{N}}_x g(x) \hat{\mathcal{N}}_y \overline{g(y)}}{\left(g(x) - \overline{g(y)}\right)^2} \right. \\ &\left. + \frac{\hat{\mathcal{N}}_x \overline{g(x)} \hat{\mathcal{N}}_y \overline{g(y)}}{\left(\overline{g(x)} - \overline{g(y)}\right)^2} - \frac{\hat{\mathcal{N}}_x \overline{g(x)} \hat{\mathcal{N}}_y g(y)}{\left(\overline{g(x)} - g(y)\right)^2} \right], \end{split} \tag{3.43}$$

where now there is no distinction between chiral and anti-chiral terms, as this term contains no information about the positions of the spins. As before, one must now evaluate this term in a regularized boundary according to the regularization scheme. However, both boundary integrals could generally have different regulators, ε and ε' . If the boundary is parameterized according to a function h(s), then

$$\begin{split} \hat{\mathcal{N}}_x \hat{\mathcal{N}}_y G_{\mathcal{M}}(x,y)|_{x=h(t)-\varepsilon \hat{n}(t)}^{y=h(s)-\varepsilon' \hat{n}(s)} &= \frac{-e^{i(\theta_t(t)+\theta_t(s))} \partial_z g(z)|_{z=h(s)} \partial_z g(z)|_{z=h(t)}}{4\pi} \\ & \left[\frac{1}{\left(g(h(t))-g(h(s))-i(e^{i\theta_t(t)} \partial_z g(z)|_{z=h(t)}|\varepsilon|-e^{i\theta_t(s)}|\varepsilon'| \partial_z g(z)|_{z=h(s)})\right)^2} \right. \\ & \left. + \frac{1}{\left(g(h(t))-g(h(s))-i(e^{i\theta_t(t)} \partial_z g(z)|_{z=h(t)}|\varepsilon|+e^{i\theta_t(s)}|\varepsilon'| \partial_z g(z)|_{z=h(s)})\right)^2} \right. \\ & \left. + \frac{1}{\left(g(h(t))-g(h(s))+i(e^{i\theta_t(t)} \partial_z g(z)|_{z=h(t)}|\varepsilon|+e^{i\theta_t(s)}|\varepsilon'| \partial_z g(z)|_{z=h(s)})\right)^2} \right. \\ & \left. + \frac{1}{\left(g(h(t))-g(h(s))+i(e^{i\theta_t(t)} \partial_z g(z)|_{z=h(t)}|\varepsilon|-e^{i\theta_t(s)}|\varepsilon'| \partial_z g(z)|_{z=h(s)})\right)^2} \right], \end{split}$$

whereas before, we kept all the regulator expansion up to the first order. As before, we isolate the divergence by taking the limit $s \to t$ for this arbitrary parametrization,

which yields

$$\begin{split} &\lim_{s \to t} \hat{\mathcal{N}}_x \hat{\mathcal{N}}_y G_{\mathcal{M}}(x,y)|_{x=h(t)-\varepsilon \hat{n}(t)}^{y=h(s)-\varepsilon' \hat{n}(s)} = \\ &\frac{-1}{4\pi} \left[\frac{1}{(|h(s)-h(t)|+i(|\varepsilon|+|\varepsilon'|))^2} + \frac{1}{(|h(s)-h(t)|-i(|\varepsilon|+|\varepsilon'|))^2} \right. \\ &\quad + \frac{1}{(|h(s)-h(t)|+i(|\varepsilon|-|\varepsilon'|))^2} + \frac{1}{(|h(s)-h(t)|-i(|\varepsilon|-|\varepsilon'|))^2} \right]. \end{split} \tag{3.45}$$

To reach a known distribution, we identify the regulators as $|\varepsilon| \pm |\varepsilon'| \to |\varepsilon|$, making the final expression be

$$\lim_{s \to t} \hat{\mathcal{N}}_x \hat{\mathcal{N}}_y G_{\mathcal{M}}(x,y)|_{x=h(t)-\varepsilon \hat{n}(t)}^{y=h(s)-\varepsilon \hat{n}(s)} = \frac{-1}{2\pi} \left[\frac{1}{(|h(s)-h(t)|+i|\varepsilon|)^2} + \frac{1}{(|h(s)-h(t)|-i|\varepsilon|)^2} \right], \tag{3.46}$$

which is precisely the derivative of the principal value distribution. With the behavior of the divergence identified, we can proceed to regularize this kernel following the same procedure as in Equation (3.41), as well as making sure that Equation (3.42) is being satisfied for the specifics of the conformal map.

In summary, we have provided a regularization scheme that guarantees that the tensor is a finite, well-behaved object for any manifold \mathcal{M} . The regularization scheme has also fixed the family of boundary functions that are compatible with the divergent structure of the free boson functional, fixing the space to be the Schwartz space. With a well-behaved tensor, we can now begin exploring the properties of this object for different geometries and tackle the question of contraction of two such tensors.

CHIRAL TRUNCATION OF THE FREE BOSON FTNS

As in [186], we will be interested in eventually performing a chiral truncation of this functional. This is because we ultimately wish to target chiral wavefunctions [190] and, therefore, wish to work exclusively with the chiral part of our tensor. The chiral truncation consists in the removal from the functional of all the terms that depend on the conjugate spin positions $\overline{z_i}$. As we have seen, these terms will always be found only in the spin-spin interaction and boundary-spin terms. For the sake of simplifying notation, we define the two following functions

$$\begin{split} B_{\mathcal{M}}(x,y) &= \hat{\mathcal{N}}_y G_{\mathcal{M}}(x,y), \\ P_{\mathcal{M}}(x,y) &= \hat{\mathcal{N}}_x \hat{\mathcal{N}}_y G_{\mathcal{M}}(x,y), \end{split} \tag{3.47}$$

which we will call the boundary and propagation kernels. With these definitions, one can then write Equation (3.38) as

$$B_{\mathcal{M}}(z_i, y) = B_{\mathcal{M}}^c(z_i, y) + \bar{B}_{\mathcal{M}}^c(z_i, y)$$
(3.48)

where

$$\begin{split} B^{c}_{\mathcal{M}}(z_{i},y) &= \frac{-1}{4\pi} \left[\frac{\hat{\mathcal{N}}_{y}g(y)}{g(z_{i}) - g(y)} - \frac{\hat{\mathcal{N}}_{y}\overline{g(y)}}{g(z_{i}) - \overline{g(y)}} \right] \\ \bar{B}^{c}_{\mathcal{M}}(z_{i},y) &= \frac{-1}{4\pi} \left[\frac{\hat{\mathcal{N}}_{y}\overline{g(y)}}{\overline{g(z_{i})} - \overline{g(y)}} - \frac{\hat{\mathcal{N}}_{y}g(y)}{\overline{g(z_{i})} - g(y)} \right] \end{split} \tag{3.49}$$

which are the previously mentioned chiral and anti-chiral terms of the boundary kernel. Therefore, the chiral truncation of the generic action in Equation (3.28) is given by

$$\begin{split} S^{c}_{\mathcal{M}}[f,\rho] &= \frac{1}{8\pi} \int_{\mathcal{M}} d^{2}x d^{2}y \rho(x) \rho(y) G^{c}_{\mathcal{M}}(x,y) - \frac{1}{4\pi} \int_{\mathcal{M}} d^{2}x \int_{\partial \mathcal{M}} d\Gamma_{y} \rho(x) \tilde{f}(y) B^{c}_{\mathcal{M}}(x,y) \\ &+ \frac{1}{8\pi} \int_{\partial \mathcal{M}} d\Gamma_{x} \int_{\partial \mathcal{M}} d\Gamma_{y} \tilde{f}(x) \tilde{f}(y) P_{\mathcal{M}}(x,y), \end{split} \tag{3.50}$$

where the chiral truncation of the Green function is given by

$$G_{\mathcal{M}}^{c}(x,y) = \frac{1}{4\pi} \log \left[(g(x) - g(y)) \right].$$
 (3.51)

MÖBIUS TRANSFORMATIONS OF THE FREE BOSON FTNS

As we have seen in Chapter 2, the free boson action is a CFT and, therefore, invariant under conformal transformations. As we have also seen, to define our tensor, we have used the method of images to map the theory to the UHP, which means that we are no longer dealing with a standard CFT but with a Boundary conformal field theory (BCFT) instead.

Cardy is one of the pioneers who developed the theory of BCFTs and their multiple applications [167]. One of his most important insights is that since a conformal transformation now needs to preserve the real line in a BCFT defined in the UHP, this restricts the set of allowed global conformal transformations to those with only real coefficients, reducing in half the amount of conformal generators. Because our theory is one such BCFT, a natural question is: How does our tensor change under the effect of one such real PSL $(2, \mathbb{R})$ transformation?

We begin by taking a look at Equation (3.28) in the UHP, where the tensor is given by

$$\begin{split} \mathcal{A}_{\mathbb{H}}\left[\tilde{f},\{z_{i},s_{i}\}_{i=1}^{N}\right] &= \exp\left(+\frac{1}{2}\sum_{i,j}s_{i}s_{j}\log\left[\frac{(z_{i}-z_{j})(\overline{z_{i}}-\overline{z_{j}})}{(z_{i}-\overline{z_{j}})(\overline{z_{i}}-z_{j})}\right] \\ &-\frac{1}{2\pi}\sum_{i}s_{i}\int_{\mathbb{R}}dy\tilde{f}(y)\left[\frac{1}{z_{i}-y}-\frac{1}{\overline{z_{i}}-y}\right] \\ &+\frac{1}{8\pi^{2}}\int_{\mathbb{R}}dx\int_{\mathbb{R}}dy\tilde{f}(x)\tilde{f}(y)\frac{1}{(x-y)^{2}}\right). \end{split} \tag{3.52}$$

We will denote a real Möbius transformations on any coordinate in the UHP by

$$z = \gamma(\omega) = \frac{\omega a_1 + a_2}{\omega a_3 + a_4} \ a_1, a_2, a_3, a_4 \in \mathbb{R}, \ z, \omega \in \mathbb{H}.$$
 (3.53)

where we demand that $a_4a_1-a_3a_2=1$, such that we restrict ourselves to the subgroup of the Möbius group that preserves the real line, $\mathrm{PSL}(2,\mathbb{R})$. We now perform a $\mathrm{PSL}(2,\mathbb{R})$ on the coordinates of the spins such that $z_i=\gamma(\omega_i)$, akin to performing a transformation only on the physical index of a standard tensor network. A fundamental property of Möbius transformations is that they leave cross-ratios invariant, and therefore the spin-spin term in the first line of Equation (3.52) will always be left invariant. On the

spin-boundary term, we can compensate the transformation on the z_i 's by changing the variables in the integral by $y=\gamma(\omega_y)$, transforming the term to

$$\begin{split} &-\frac{1}{2\pi}\sum_{i}s_{i}\int_{\mathbb{R}}dy\tilde{f}(y)\left[\frac{1}{\gamma(\omega_{i})-y}-\frac{1}{\overline{\gamma(\omega_{i})}-y}\right]=\\ &-\frac{1}{2\pi}\sum_{i}s_{i}\int_{\mathbb{R}}d\omega_{y}\tilde{f}(\gamma(\omega_{y}))\left[\frac{1}{\omega_{i}-y}\frac{a_{3}\omega_{i}+a_{4}}{a_{3}\omega_{y}+a_{4}}-\frac{1}{\overline{\omega_{i}}-y}\frac{a_{3}\overline{\omega_{i}}+a_{4}}{a_{3}\omega_{y}+a_{4}}\right]=\\ &-\frac{1}{2\pi}\int_{\mathbb{R}}d\omega_{y}\tilde{f}(\gamma(\omega_{y}))\left[\frac{1}{\omega_{i}-\omega_{y}}-\frac{1}{\overline{\omega_{i}}-\omega_{y}}\right]. \end{split} \tag{3.54}$$

Similarly, the boundary-boundary term transforms as

$$+\frac{1}{8\pi^2}\int_{\mathbb{R}}dx\int_{\mathbb{R}}dy\tilde{f}(x)\tilde{f}(y)\frac{1}{(x-y)^2}=+\frac{1}{8\pi^2}\int_{\mathbb{R}}d\omega_x\int_{\mathbb{R}}d\omega_y\tilde{f}(\gamma(\omega_x))\tilde{f}(\gamma(\omega_y))\frac{1}{(\omega_x-\omega_y)^2} \tag{3.55}$$

We can therefore reach the conclusion that under a physical $PSL(2, \mathbb{R})$ transformation, a generic tensor behaves as

$$\mathcal{A}_{\mathcal{M}}[\tilde{f}, \{\gamma(\omega_i), s_i\}_{i=1}^N] = \mathcal{A}_{\mathcal{M}}[\gamma \circ \tilde{f}, \{\omega_i, s_i\}_{i=1}^N], \tag{3.56}$$

since $\mathcal{A}_{\mathbb{H}}$ and $\mathcal{A}_{\mathcal{M}}$ are connected by the biholomorphic conformal map g(z). Equation (3.56) also implies that the wavefunctions defined by either its l.h.s or the r.h.s are identical. This is due to the fact that the composition $\hat{f} = \gamma \circ \tilde{f}$ preserves the integration measure of the path integral $\int \mathcal{D}\tilde{f} = \int \mathcal{D}\hat{f}$, because $\gamma(\mathbb{R}) = \mathbb{R}$. Therefore, the same wave function will be recovered when the virtual indices are contracted following any chosen geometry.

However, we are ultimately interested in the chiral truncation of the functional tensor, in which the Green function is no longer a cross-ratio. In this case, the chiral tensor becomes

$$\begin{split} \mathcal{A}^{c}_{\mathbb{H}}\left[\tilde{f}, \left\{\gamma(\omega_{i}), s_{i}\right\}_{i=1}^{N}\right] &= \\ \exp\left(+\frac{1}{2}\sum_{i,j}s_{i}s_{j}\left(\log\left[\left(\omega_{i}-\omega_{j}\right)\right] + \log\left[\frac{\left(a_{2}a_{4}-a_{1}a_{3}\right)}{\left(a_{4}+a_{3}\omega_{i}\right)\left(a_{4}+a_{3}\omega_{j}\right)}\right]\right) \\ &-\frac{1}{2\pi}\sum_{i}s_{i}\int_{\mathbb{R}}d\omega_{y}\tilde{f}(\gamma(\omega_{y}))\left[\frac{1}{\omega_{i}-\omega_{y}}\frac{a_{3}\omega_{i}+a_{4}}{a_{3}\omega_{y}+a_{4}}\right] \\ &+\frac{1}{8\pi^{2}}\int_{\mathbb{R}}d\omega_{x}\int_{\mathbb{R}}d\omega_{y}\tilde{f}(\gamma(\omega_{x}))\tilde{f}(\gamma(\omega_{y}))\frac{1}{\left(\omega_{x}-\omega_{y}\right)^{2}}\right). \end{split} \tag{3.57}$$

We clearly see that although all the boundary functions have become $\gamma \circ f$, a Möbius transformation induces both a pre-factor from the spin-spin term as well as a modification of the spin-boundary term, while still leaving the boundary-boundary term intact. A priori, it is not clear that a chiral tensor and its Möbius transformed version lead to the same wavefunction, but we will see in future sections that this is indeed true, at least for the basic geometry with genus 0. These chiral tensors and their Möbius transformations are very important for us, as these constitute the main pieces with which we will attempt to prove a generic sewing condition.

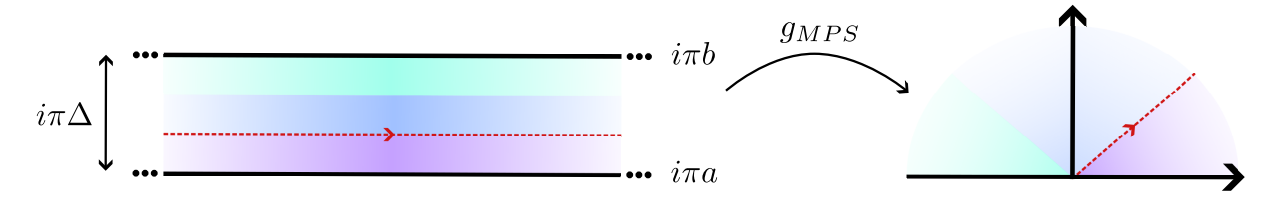


Figure 3.4: Schematic behavior of the conformal map that produces the fMPS tensor.

3.2 THE FREE BOSON FMPS

3.2.1 EXPLICIT CONSTRUCTION OF THE FMPS TENSOR

We begin this construction following [186] and will perform a summarized version of the derivation found there, as it is instructive later for us in the case of the fPEPS. We aim to map the UHP onto a polygon with only two sides, which can only be the geometry of an infinite strip of width Δ in the compactified complex plane. Therefore, the inner angles are $\alpha=\beta=0$, and we leave arbitrary where the point $z_0\in\mathbb{R}$ that gets mapped to infinity is. Then, the Schwarz-Christoffel recipe tells us

$$f(\xi) = \int^{\xi} \frac{K}{\omega - z_0} = K \log \left(\xi - z_0 \right) + C, \tag{3.58} \label{eq:3.58}$$

where K, C and z_0 are arbitrary constants. To fix them, we add the boundary conditions

$$\begin{cases} f(z_0) = -\infty \\ f(z_0 + \varepsilon) = -\infty + i\pi a \\ f(z_0 - \varepsilon) = -\infty + i\pi b \end{cases}$$
 (3.59)

where $\Delta=b-a,\ b>a$ where $\ b,a\in\mathbb{R},\ ,$ and since we left the point z_0 arbitrary, we can simply choose $z_0=0.$ Under these boundary conditions, the map from the UHP to the infinite strip becomes

$$f(\xi) = \Delta \log(\xi) + i\pi a,\tag{3.60}$$

and thus the inverse of this map is the desired conformal map that defines the fTNS tensor

$$g_{MPS}(z) = \exp\left(\frac{z - i\pi a}{\Delta}\right) \tag{3.61}$$

whose behavior is schematically shown in Figure 3.4.

One then inputs this conformal map into the action in Equation (3.28), where the boundary integrals for this geometry are given by

$$\int_{\partial\mathcal{M}} d\Gamma_y \hat{\mathcal{N}}_y(\cdot)|_{y=\partial\mathcal{M}} = \int_{\mathbb{R}} dy (-i\partial_{\mathrm{Im}(z)})(\cdot)|_{z=y+i\pi a} + \int_{\mathbb{R}} dy (i\partial_{\mathrm{Im}(z)})(\cdot)|_{z=y+i\pi b} \tag{3.62}$$

where ${\rm Im}(z)$ refers to the imaginary part of z, and thus the vertical derivative normal to the boundary. One then chooses the value of the boundary functions to be

$$\tilde{f}(g_{MPS}(z))|_{z=y+i\pi a} = f_{+}(y) , \quad \tilde{f}(g_{MPS}(z))|_{z=y+i\pi b} = f_{-}(y)$$
 (3.63)

and after computing the derivatives, introducing a generic N-spin density ρ and performing some simplifications, the action of the fMPS tensor is given by

$$\begin{split} S_{\Delta}[f_{+},f_{-},\rho] &= +\frac{1}{8\pi} \int_{MPS} d^{2}z \int_{MPS} d^{2}z' G_{MPS}(z,z') \rho(z) \rho(z') \\ &+ \frac{i}{16\pi^{2}} \int_{MPS} d^{2}z' \int_{\mathbb{R}} dx \rho(z') \left(f_{+}(x) - f_{-}(x) \right) \begin{pmatrix} v_{+,\Delta,a}(x,z') - \overline{v_{+,\Delta,a}(x,z')} \\ -v_{-,\Delta,a}(x,z') + \overline{v_{-,\Delta,a}(x,z')} \end{pmatrix} \\ &- \frac{1}{64\pi^{2}} \int_{\mathbb{R}} dx \int_{\mathbb{R}} dx' \left(f_{+}(x) - f_{-}(x) \right) \begin{pmatrix} u_{+,\Delta}(x-x') & u_{-,\Delta}(x-x') \\ u_{-,\Delta}(x-x') & u_{+,\Delta}(x-x') \end{pmatrix} \begin{pmatrix} f_{+}(x') \\ f_{-}(x') \end{pmatrix}, \end{split}$$

$$(3.64)$$

where the kernels are given by

$$\begin{split} u_{+,\Delta}(x-x') &= \frac{2}{\Delta^2} \frac{1}{\sinh\left(\frac{x-x'}{2\Delta}\right)^2} \;,\; u_{-,\Delta}(x-x') = \frac{2}{\Delta^2} \frac{1}{\cosh\left(\frac{x-x'}{2\Delta}\right)^2} \\ v_{+,\Delta,a}(x,z') &= \frac{1}{\Delta} \coth\left(\frac{x-z'+i\pi a}{2\Delta}\right) \;,\; v_{-,\Delta,a}(x,z') = \frac{1}{\Delta} \tanh\left(\frac{x-z'+i\pi a}{2\Delta}\right). \end{split} \tag{3.65}$$

Note that these are the unregulated expressions, and therefore $u_{+,\Delta}$ and $v_{\pm,\Delta}$ contain divergences. Following the regularization procedure presented in the previous section, the corresponding ε -regulated expressions are given by:

$$\begin{split} u_{+,\Delta}^{\varepsilon,\varepsilon'}(x-x') &= \frac{1}{\Delta^2} \left(\frac{1}{\sinh\left(\frac{x-x'+i(\varepsilon+\varepsilon')}{2\Delta}\right)^2} + \frac{1}{\sinh\left(\frac{x-x'-i(\varepsilon+\varepsilon')}{2\Delta}\right)^2} \right. \\ &\quad + \frac{1}{\sinh\left(\frac{x-x'+i(\varepsilon-\varepsilon')}{2\Delta}\right)^2} + \frac{1}{\sinh\left(\frac{x-x'-i(\varepsilon-\varepsilon')}{2\Delta}\right)^2} \right), \end{split} \tag{3.66}$$

$$v_{+,\Delta,a}(x,z') = \frac{1}{2\Delta} \left(\coth\left(\frac{x-z'+i\pi a+i\varepsilon}{2\Delta}\right) + \coth\left(\frac{x-z'+i\pi a-i\varepsilon}{2\Delta}\right) \right), \quad \textbf{(3.67)}$$

$$v_{-,\Delta,a}(x,z') = \frac{1}{2\Delta} \left(\tanh \left(\frac{x-z'+i\pi a+i\varepsilon}{2\Delta} \right) + \tanh \left(\frac{x-z'+i\pi a-i\varepsilon}{2\Delta} \right) \right). \tag{3.68}$$

Following the regularization procedure shown in Equation (3.41), the corresponding distributional expressions in the $\varepsilon, \varepsilon' \to 0$ limit are

$$Ru_{+,\Delta}(x-x') = \frac{2}{\Delta^2} \left(\frac{1}{\sinh\left(\frac{x-x'}{2\Delta}\right)^2} - \left(\frac{2\Delta}{x-x'}\right)^2 \right) - 8P'\left(\frac{1}{(x-x')}\right), \qquad \textbf{(3.69)}$$

$$Rv_{+,\Delta,a}(x,z') = \frac{1}{\Delta} \left(\coth\left(\frac{x-z'+i\pi a}{2\Delta}\right) - \frac{2\Delta}{x-z'} \right) + 2P\left(\frac{1}{(x-z')}\right) \tag{3.70}$$

$$Rv_{-,\Delta,a}(x,z') = \frac{1}{\Delta} \left(\tanh\left(\frac{x-z'+i\pi a}{2\Delta}\right) - \frac{2\Delta}{x-z'}\right) + 2P\left(\frac{1}{(x-z')}\right) \tag{3.71}$$

where we have introduced the principal value distribution $P\left(\frac{1}{x}\right)$ and its derivative $P'\left(\frac{1}{x}\right)$ as the limits

$$P\left(\frac{1}{x}\right) = \lim_{\varepsilon \to 0} \frac{1}{2} \left(\frac{1}{x + i\varepsilon} + \frac{1}{x - i\varepsilon}\right),\tag{3.72}$$

$$P'\left(\frac{1}{x}\right) = \lim_{\varepsilon \to 0} -\frac{1}{2} \left(\frac{1}{(x+i\varepsilon)^2} + \frac{1}{(x-i\varepsilon)^2}\right). \tag{3.73}$$

The next step is to perform the chiral truncation on the action S_{MPS} , which, after introducing the expressions for the spin densities, leads to the truncated action

$$\begin{split} S^{c}_{\Delta}[f_{+},f_{-},\{z_{i},s_{i}\}_{i=1}^{N}] &= -\sum_{i>j}^{N} s_{i} s_{j} \log \left(\mu \sinh \left(\frac{z_{i}-z_{j}}{2\Delta}\right)\right) \\ &- \frac{1}{4\pi} \sum_{i=1}^{N} s_{i} \int_{\mathbb{R}} dx \left(f_{+}(x) - f_{-}(x)\right) \begin{pmatrix} v_{+,\Delta,a}(x,z_{i}) \\ -v_{-,\Delta,a}(x,z_{i}) \end{pmatrix} \\ &- \frac{1}{64\pi^{2}} \int_{\mathbb{R}} dx \int_{\mathbb{R}} dx' \left(f_{+}(x) - f_{-}(x)\right) \begin{pmatrix} u_{+,\Delta}(x-x') & u_{-,\Delta}(x-x') \\ u_{-,\Delta}(x-x') & u_{+,\Delta}(x-x') \end{pmatrix} \begin{pmatrix} f_{+}(x') \\ f_{-}(x') \end{pmatrix}, \end{split} \tag{3.74}$$

where a constant μ has been introduced in the interaction term after the truncation that will be fixed later to yield the correct closing condition. The spin positions $z_i \in \mathcal{M}$ are such that $\pi a < \operatorname{Im}(z_i) < \pi b$, and thus are not allowed to be on the boundaries of the tensor, removing the need for regularization on the spin-boundary terms. The expression for the functional fMPS tensor is then given by

$$\mathcal{A}_{\Delta}[f_{+},f_{-},\{z_{i},s_{i}\}_{i=1}^{N}] = \exp\left(-S_{\Delta}^{c}[f_{+},f_{-},\{z_{i},s_{i}\}_{i=1}^{N}]\right) \tag{3.75}$$

or diagrammatically, the tensor corresponding to a single spin would be given by

$$\mathcal{A}_{\Delta}[f_{+}, f_{-}, \{z, s\}] = \begin{array}{c} f_{-} \\ \times \{z, s\} \end{array}$$

$$f_{+}$$

$$(3.76)$$

3.2.2 THE FMPS TENSOR IN MOMENTUM SPACE

Particular to the fMPS tensor is that we can use the Fourier transform to simplify the tensor further. If we define the Fourier transform of the boundary functions $f_{\pm}(x)$ by

$$f_{\pm}(x) = \int_{\mathbb{R}} dk e^{ikx} \hat{f}_{\pm}(k) \tag{3.77}$$

In [186], the Fourier transformations of all the integral kernels were provided, and therein, one finds the expression for the fMPS tensor in momentum space, which is given by

$$\begin{split} S^{c}_{\Delta}\left[f_{+},f_{-},\{z_{i},s_{i}\}_{i=1}^{2}\right] &= -\sum_{i>j}^{N}s_{i}s_{j}\log\left(\mu\sinh\left(\frac{z_{i}-z_{j}}{2\Delta}\right)\right) \\ &+ \frac{1}{2}\int_{0}^{\infty}\mathrm{d}k\left(\hat{f}_{+}(k)-\hat{f}_{-}(k)\right)\begin{pmatrix}\omega_{+,\Delta}(k)&\omega_{-,\Delta}(k)\\\omega_{-,\Delta}(k)&\omega_{+,\Delta}(k)\end{pmatrix}\begin{pmatrix}\hat{f}_{+}^{*}(k)\\\hat{f}_{-}^{*}(k)\end{pmatrix} \\ &- \frac{i}{2}\sum_{i=1}^{N}\int_{\mathbb{R}}\mathrm{d}k\frac{e^{ikz_{i}}s_{i}}{\sinh\left(\pi k\Delta\right)}\left(e^{\pi kb}\hat{f}_{+}(k)-e^{\pi ka}\hat{f}_{-}(k)\right), \end{split} \tag{3.78}$$

with $\omega_{+,\Delta}=k\coth{(\pi k\Delta)}$ and $\omega_{-,\Delta}=-k\operatorname{sech}(\pi k\Delta)$. After providing this tensor in momentum space, the authors performed the sewing condition for two such tensors on a fixed coordinate basis. Here, we generalize their result to an arbitrary coordinate basis, as the computation follows identically as in their study. The computation relies precisely on the Fourier Transform of the tensor, which allows the diagonalization of the Gaussian integral, which is the bottleneck of the computation. As we hope to provide a more general version of the sewing condition in the upcoming sections, we do not reproduce their computation explicitly here. Derived originally in [186] and generalized in this work, the sewing condition for two fMPS tensors with a single spin reads

$$\int \mathcal{D}g\mathcal{A}_{\Delta_{1}}\left[f_{0}, f_{+}, g, \{z_{1}, s_{1}\}\right] \mathcal{A}_{\Delta_{2}}\left[f_{0}, g, f_{-}, \{z_{2}, s_{2}\}\right]
= \mathcal{A}_{\Delta_{1} + \Delta_{2}}\left[f_{0}, f_{+}, f_{-}, \{z_{i}, s_{i}\}_{i=1}^{2}\right],$$
(3.79)

where now the exponent of the sewn strips is given by:

$$\begin{split} S_{\Delta_{1}\cup\Delta_{2}}^{c}\left[f_{+},f_{-},\{z_{i},s_{i}\}_{i=1,2}\right] &= \frac{s_{1}^{2}}{2}\log\Delta_{f} + \frac{s_{2}^{2}}{2}\log\Delta_{f} \\ &+ \frac{1}{2}\int_{0}^{\infty}\mathrm{d}k\left(\hat{f}_{+}(k) - \hat{f}_{-}(k)\right)\begin{pmatrix}\omega_{+,\Delta_{f}}(k) & \omega_{-,\Delta_{f}}(k) \\ \omega_{-,\Delta_{f}}(k) & \omega_{+,\Delta_{f}}(k)\end{pmatrix}\begin{pmatrix}\hat{f}_{+}^{*}(k) \\ \hat{f}_{-}^{*}(k)\end{pmatrix} \\ &- \frac{i}{2}\int_{\mathbb{R}}\mathrm{d}k\frac{\sum_{i=1,2}e^{ikz_{i}}s_{i}}{\sinh\left(\pi k\Delta_{f}\right)}\left(e^{\pi kb_{2}}\hat{f}_{+}(k) - e^{\pi ka_{1}}\hat{f}_{-}(k)\right) \\ &- s_{1}s_{2}\log\left(\mu\sinh\left(\frac{z_{2}-z_{1}}{2\Delta_{f}}\right)\right), \end{split} \tag{3.80}$$

where $\Delta_f = \Delta_1 + \Delta_2$ and $\mu = -2i$. Diagrammatically, Equation (3.79) is given by

$$\int \mathcal{D}g \xrightarrow{\mathbf{x}\{z_2,s_2\}} \begin{array}{c} f_{-} \\ \mathbf{x}\{z_2,s_2\} \\ \mathbf{x}\{z_1,s_1\} \\ f_{+} \end{array} = \begin{array}{c} f_{-} \\ \mathbf{x}\{z_2,s_2\} \\ \mathbf{x}\{z_1,s_1\} \\ f_{+} \end{array}$$

$$(3.81)$$

Notice how in the first line of Equation (3.80) the terms $\frac{s_i^2}{2}\log\Delta_f$ have appeared, which are there to ensure that this tensor has the correct scaling dimension under a scaling transformation. This means that we must modify all previous tensors to include them as a constant within the action so that the sewing condition is now exact. The way to find this constant before performing the sewing condition is to explore the divergence arising in the $z_i \to z_j$ limit of the Green function in the spin-spin term in Equation (3.74). If one demands normal ordering, and thus the removal of the divergence, the sub-leading 0^{th} -order term that appears is precisely this factor.

The main difference concerning the derivation in [186] is that now the sewing of these tensors can be performed with arbitrary lengths Δ_i as well as at any height b_i, a_i , a feature that is needed in Chapter 4 to study the properties of these tensors in regards to its symmetries. The generalization to more spins is straightforward and follows from repeated application of Equation (3.80).

Furthermore, the closing condition for the fMPS was also provided by using again the result of the sewing integral. Diagrammatically shown in Equation (3.15), the result is given by

$$\int \mathcal{D}f_0 \int \mathcal{D}f \mathcal{A}_{\Delta}[f_0,f,f,\{z_i,s_i\}_{i=1}^N] = 2\pi\delta\left(\sum_{i=1}^N s_i\right) \prod_{j>i} \left(\Delta \sin\left(\frac{y_j-y_i}{\Delta}\right)\right)^{s_j s_i} \ \ \textbf{(3.82)}$$

which is precisely the conformal correlator

$$2\pi\delta\left(\sum_{i=1}^{N} s_i\right) \langle \prod_{j>i}^{N} : e^{is_j\varphi(z_j)} :: e^{is_j\varphi(z_i)} : \rangle_{\text{cyl}}$$
 (3.83)

evaluated in the geometry of a cylinder, which is almost the desired Haldane-Shastry wavefunction and the exact ground state of the critical point of the Majumdar-Ghosh model. Interestingly, the connection with Haldane-Shastry appears when the z's are uniformly distributed, while the connection with Majumdar-Ghosh is in the limit where the coordinates approach one another pairwise. To recover it exactly, one should have added in the definition of the tensors a phase that depends on the spin value found within the tensor. In this particular case, this is the Marshall factor χ_{s_n} for each site, which is given for the even sites by

$$\chi_{s_m} = e^{im\pi(s_m - 1)/2} \tag{3.84}$$

which globally counts the number of "down"-spins on odd sites and gives a phase accordingly. With this, the final wavefunction is given by

$$c_{s_1,\dots s_N} \propto \delta_{\sum_n s_n,0} \prod_n \chi_{s_n} \prod_{n>m} \left(\sin \left[\frac{\pi(n-m)}{N} \right] \right)^{\frac{s_n s_m}{2}}, \tag{3.85}$$

which is now precisely the exact desired ground state.

There are two main takeaways from these last two computations:

- 1. **Sewing is key:** The sewing condition allows both to contract tensors and close them entirely, exactly and in the $\chi \to \infty$ limit. Therefore, and unlike in numerical approaches, performing a single contraction is as hard as performing exponentially many of them, as the hardness comes from solving the Gaussian integral found in the most simple sewing. It is thus of utmost importance to provide any fTNS with its corresponding sewing condition if one wishes to provide an analytical tool with which one can provide new exact TNS representations of states.
- 2. The conformal map encodes the geometry: Interestingly, the conformal correlator of Equation (3.61) is the one corresponding to a compactified boson on a cylinder of perimeter Δ , and yet we constructed our function from the uncompactified free boson. This means that the field's geometry information is encoded in the conformal map $g_{MPS}(z)$, where we can identify the cylindrical geometry. It would be interesting to perform the closing condition in this case with a slightly different boundary condition, such that the geometry of a Möbius strip would be recovered, as that is the only other possible geometry that this map allows for.

This result suggests many possible open directions. Firstly and most obviously, provide the fMPS tensor corresponding to other simple Gaussian CFTs for which a local action exists, such as the free Majorana/Dirac fermion or the ghost system. Other generic options would be other WZW theories via the Wakimoto free field representation or simple minimal models for which a Couloumb-gas representation exists [37]. Ultimately, a more generic BCFT approach should be possible and needed for non-Gaussian CFTs by representing these tensors as conformal correlators between Ishibasi or Cardy states with a fixed boundary condition. Still, we leave this exciting approach for future projects.

3.3 THE FREE BOSON FPEPS

3.3.1 EXPLICIT CONSTRUCTION OF THE PEPS FUNCTIONAL

In this section, we provide a derivation analogous to the one for the fMPS tensor but for the geometry corresponding to a PEPS tensor. This is then the formal derivation of the fPEPS tensor. We start by constructing the conformal map according to the Schwarz-Christoffel recipe that diagrammatically achieves Figure 3.5. To this end, we choose 4 points of the real line, -b, -a, a, b with $a < b \in \mathbb{R}^+$ and set all the interior angles to be $\alpha = \beta = \gamma = \delta = \frac{\pi}{2}$. Then Equation (3.33), becomes

$$f(\xi) = \int^{\xi} \frac{Kd\omega}{\sqrt{(\omega^2 - a^2)(\omega^2 - b^2)}},$$
 (3.86)

which, after manipulating it, one obtains

$$f(\xi) = \frac{K}{b} \int_{a}^{\frac{\xi}{a}} \frac{d\omega}{\sqrt{(1-\omega^2)(1-\kappa^2\omega^2)}},$$
 (3.87)

where $\kappa = \frac{a}{b}$ is the elliptic modulus, and because a < b, then $0 < \kappa < 1$. Now, taking the following change of variables $\phi = \arcsin{(\omega)}$ yields

$$f(\xi) = \frac{K}{b} \int_{-\infty}^{\arcsin\frac{\xi}{a}} \frac{d\phi}{\sqrt{1 - \kappa^2 \sin^2 \phi}} = \frac{K}{b} F(\arcsin\frac{\xi}{a}, \kappa) + C, \tag{3.88}$$

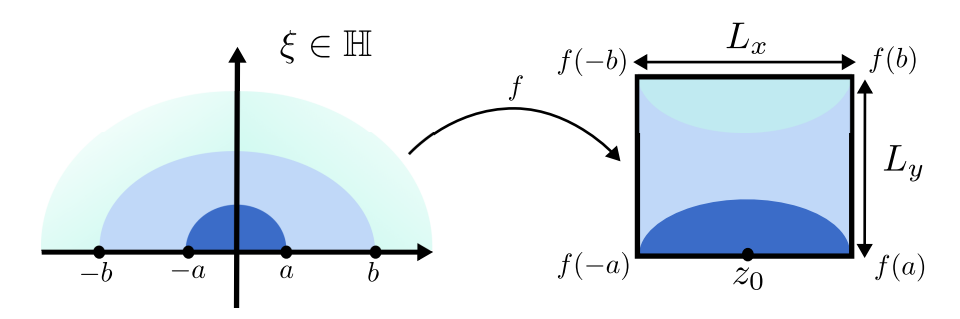


Figure 3.5: Diagrammatic representation of the PEPS Schwarz-Christoffel map.

| $n,m\in\mathbb{Z}$ | $sn(R(z),\kappa)$ | $cn(R(z),\kappa)$ | $dn(R(z),\kappa)$ |
|--------------------|---------------------|--|-----------------------------------|
| Periods | $2mL_x + 2niL_y$ | $2mL_x + 2n(\frac{L_x}{2} + iL_y)$ | $mL_x + 4niL_y$ |
| Zeroes | $mL_x + 2niL_y$ | $(m+\frac{1}{2})L_x+2niL_y$ | $(m+\frac{1}{2})L_x + (2n+1)iL_y$ |
| Poles | $mL_x + (2n+1)iL_y$ | $mL_x \stackrel{\text{\tiny 2}}{+} (2n+1)iL_y$ | $mL_x^2 + (2n+1)iL_y$ |
| Residues | | $ \begin{array}{c} mL_x + (2n+1)iL_y \\ i(-1)^{m-1}\kappa^{-1} \end{array} $ | $(-1)^{n-1}i$ |

Table 3.1: Positions of zeroes, poles, periodicities, and residues in our coordinate system for all the relevant Jacobi elliptic functions.

where $F(\cdot, \kappa)$ is the incomplete elliptic integral of the first kind and C an arbitrary constant. To fix all the free parameters, we now employ the boundary conditions

$$\begin{cases} f(-a) = z_0 - \frac{L_x}{2} \\ f(a) = z_0 + \frac{L_x}{2} \\ f(b) = z_0 + \frac{L_x}{2} + iL_y \\ f(-b) = z_0 - \frac{L_x}{2} + iL_y \end{cases} \tag{3.89}$$

where z_0 is an arbitrary reference point of the complex plane and L_x, L_y , are the width and height of the rectangle in Figure 3.5. Upon solving the system of equations, one arrives at

$$f(\xi) = \frac{L_x}{2K(\kappa)} F(\arcsin\frac{\xi}{a}, \kappa) + z_0, \tag{3.90} \label{eq:3.90}$$

where $K(\kappa)$ is the complete elliptic integral of the first kind, and $\frac{L_x}{L_y}=\frac{2K(\kappa)}{\widetilde{K}(\kappa)}$ with $\widetilde{K}(\kappa)=K(\widetilde{\kappa})$ and $\widetilde{\kappa}=\sqrt{1-\kappa^2}$. Finally, one inverts this equation to obtain the desired conformal map, which is given by

$$g_{PEPS}(z) = a \; sn \left(\frac{2K(\kappa)}{L_x} \left(z - z_0 \right), \kappa \right), \tag{3.91} \label{eq:3.91}$$

where $f(\xi)=z$ and the function $sn(\cdot,\kappa)$ is known as the Jacobi elliptic sine, and the a parameter can be freely chosen to be one. The Jacobi elliptic functions [195] are a family of 12 functions that form a lattice of simple poles and zeros in the complex plane, spanned by the quarter periods $K(\kappa)$ and $\widetilde{K}(\kappa)$. To ease notation, we define the following function

$$R(z) = \frac{2K(\kappa)}{L_x}(z-z_0) = \frac{2K(\kappa)}{L_x}(x-x_0) + i\frac{\widetilde{K}(\kappa)}{L_y}(y-y_0) = Rh(x) + iRv(y), \quad \textbf{(3.92)}$$

where $\mathrm{Re}(z_0)=x_0$ and $\mathrm{Im}(z_0)=y_0$. In Table 3.1, we have translated all the relevant properties of the most important Jacobi functions according to our coordinate system, the most relevant one being the double periodicity as it plays a role in the regularization procedure.

The next step is to introduce the expression of the conformal map into the action in Equation (3.28), take derivatives and obtain specific forms for all the terms. To do so in an orderly manner, we assign different boundary functions to each of the sides

according to Figure 3.6, such that after taking derivatives, the final expression for the action is

$$\begin{split} S_{\mathcal{M}}[\tilde{h}_{+},\tilde{h}_{-},\tilde{v}_{+},\tilde{v}_{+},\rho] &= \frac{1}{8\pi} \int_{\mathcal{M}} d\vec{x} \int_{\mathcal{M}} d\vec{x}' G_{\mathcal{M}}(\vec{x},\vec{x}') \rho(\vec{x}) \rho(\vec{x}') \\ &- \frac{1}{64\pi^{2}} \int_{x_{0} - \frac{L_{x}}{2}}^{x_{0} + \frac{L_{x}}{2}} dx \int_{x_{0} - \frac{L_{x}}{2}}^{x_{0} + \frac{L_{x}}{2}} dx' \left(\tilde{h}_{+}(x) \;, \; \tilde{h}_{-}(x)\right) \begin{pmatrix} U_{h_{+},h_{+}}(x,x') \;, \; U_{h_{+},h_{-}}(x,x') \\ U_{h_{-},h_{+}}(x,x') \;, \; U_{h_{-},h_{-}}(x,x') \end{pmatrix} \begin{pmatrix} \tilde{h}_{+}(x') \\ \tilde{h}_{-}(x') \end{pmatrix} \\ &- \frac{1}{64\pi^{2}} \int_{y_{0}}^{y_{0} + L_{y}} dy \int_{y_{0}}^{y_{0} + L_{y}} dy' \left(\tilde{v}_{+}(y) \;, \; \tilde{v}_{-}(y)\right) \begin{pmatrix} U_{v_{+},v_{+}}(y,y') \;, \; U_{v_{+},v_{-}}(y,y') \\ U_{v_{-},v_{+}}(y,y') \;, \; U_{v_{-},v_{-}}(y,y') \end{pmatrix} \begin{pmatrix} \tilde{v}_{+}(y') \\ \tilde{v}_{-}(y') \end{pmatrix} \\ &- \frac{1}{64\pi^{2}} \int_{x_{0} - \frac{L_{x}}{2}}^{x_{0} + \frac{L_{x}}{2}} dx \int_{y_{0}}^{y_{0} + L_{y}} dy' \left(\tilde{h}_{+}(x) \;, \; \tilde{h}_{-}(x)\right) \begin{pmatrix} U_{h_{+},v_{+}}(x,y') \;, \; U_{h_{+},v_{-}}(x,y') \\ U_{h_{-},v_{+}}(x,y') \;, \; U_{h_{-},v_{-}}(x,y') \end{pmatrix} \begin{pmatrix} \tilde{v}_{+}(y') \\ \tilde{v}_{-}(y') \end{pmatrix} \\ &- \frac{1}{64\pi^{2}} \int_{y_{0}}^{y_{0} + L_{y}} dy \int_{x_{0} - \frac{L_{x}}{2}}^{x_{0} + \frac{L_{x}}{2}} dx' \left(\tilde{v}_{+}(y) \;, \; \tilde{v}_{-}(y)\right) \begin{pmatrix} U_{v_{+},h_{+}}(y,x') \;, \; U_{v_{+},h_{-}}(y,x') \\ U_{v_{-},h_{+}}(y,x') \;, \; U_{v_{-},h_{-}}(y,x') \end{pmatrix} \begin{pmatrix} \tilde{h}_{+}(x') \\ \tilde{h}_{-}(x') \end{pmatrix} \\ &+ \frac{i}{16\pi^{2}} \int_{x_{0} - \frac{L_{x}}{2}}^{x_{0} + \frac{L_{x}}{2}} dx \int_{M} d\vec{x}' \rho(\vec{x}') \left(\tilde{h}_{+}(x) \;, \; \tilde{h}_{-}(x)\right) \begin{pmatrix} V_{h_{+}}(x,x') - \overline{V}_{h_{+}}(x,x') \\ -V_{h_{-}}(x,x') - \overline{V}_{h_{-}}(x,x') \end{pmatrix} \\ &+ \frac{i}{16\pi^{2}} \int_{y_{0}}^{y_{0} + L_{y}} dy \int_{M} d\vec{x}' \rho(\vec{x}') \left(\tilde{h}_{+}(x) \;, \; \tilde{v}_{-}(y)\right) \begin{pmatrix} -V_{v_{+}}(y,x') + \overline{V}_{v_{-}}(y,x') \\ -V_{h_{-}}(x,x') - \overline{V}_{v_{-}}(y,x') \end{pmatrix} , \\ &+ \frac{i}{16\pi^{2}} \int_{y_{0}}^{y_{0} + L_{y}} dy \int_{M} d\vec{x}' \rho(\vec{x}') \left(\tilde{v}_{+}(y) \;, \; \tilde{v}_{-}(y)\right) \begin{pmatrix} -V_{v_{+}}(y,x') + \overline{V}_{v_{-}}(y,x') \\ -V_{v_{-}}(y,x') - \overline{V}_{v_{-}}(y,x') \end{pmatrix} , \\ &+ \frac{i}{16\pi^{2}} \int_{y_{0}}^{y_{0} + L_{y}} dy \int_{M} d\vec{x}' \rho(\vec{x}') \left(\tilde{v}_{+}(y) \;, \; \tilde{v}_{-}(y)\right) \begin{pmatrix} -V_{v_{+}}(y,x') + \overline{V}_{v_{-}}(y,x') \\ -V_{v_{-}}(y,x') - \overline{V}_{v_{-}}(y,x') \end{pmatrix} \right), \\ &+ \frac{i}{16\pi^{2}} \int_{y_{0}}^{y_{0} + L_{y}} dy \int_{M} d\vec{x}' \rho(\vec{x}') \left(\tilde{v}_{$$

where \tilde{h}_{\pm} and \tilde{v}_{\pm} are the horizontal and vertical boundary conditions without the zero modes, the integral kernels $V_{h_{\pm}}$ and $V_{v_{\pm}}$ correspond to the spin-boundary terms, and the $U_{h_{\pm}h_{\pm}}$ and the rest of its variants are the boundary-boundary terms. We use interchangeably the notation $G_{\mathcal{M}}(\vec{x},\vec{x}')$ and $G_{\mathcal{M}}(z,z')$ with z=x+iy, both notations are used to denote the same object and the different notation is merely to adapt better to the context in which it is found, in this case to mimic the coordinates of the integral over \mathcal{M} .

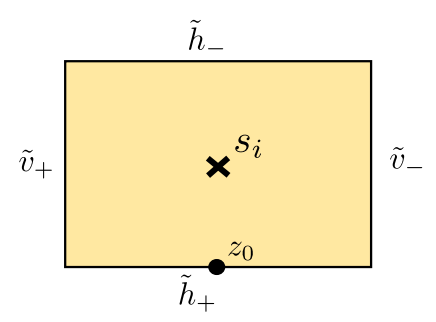


Figure 3.6: Schematic representation of the PEPS functional, with all the different boundary conditions, the spin position, and the reference point of the conformal map.

Let us explore each term separately, starting with the spin-spin term. The Green function of the first line, denoting $sn(\cdot,\kappa)=sn(\cdot)$ is given by

$$G_{M}(\vec{x},\vec{x}') = \frac{1}{4\pi} \log \left[\frac{\left(sn\left(\frac{2K}{L_{x}}\left(z-z_{0}\right)\right) - sn\left(\frac{2K}{L_{x}}\left(z'-z_{0}\right)\right)\right)\left(sn\left(\frac{2K}{L_{x}}\left(\overline{z}-\overline{z_{0}}\right)\right) - sn\left(\frac{2K}{L_{x}}\left(\overline{z}'-\overline{z_{0}}\right)\right)\right)}{\left(sn\left(\frac{2K}{L_{x}}\left(z-z_{0}\right)\right) - sn\left(\frac{2K}{L_{x}}\left(\overline{z}'-\overline{z_{0}}\right)\right)\right)\left(sn\left(\frac{2K}{L_{x}}\left(\overline{z}-\overline{z_{0}}\right)\right) - sn\left(\frac{2K}{L_{x}}\left(z'-z_{0}\right)\right)\right)}\right]$$

We simplify notation by re-defining:

$$\begin{split} G_M(z,z') &= \frac{1}{4\pi} \log \left[\frac{J(R(z),R(z'))J(\overline{R(z)},\overline{R(z')})}{J(R(z),\overline{R(z')})J(\overline{R(z)},R(z'))} \right], \\ J(f_1,f_2) &= sn(f_1) - sn(f_2). \end{split} \tag{3.95}$$

For later purposes, we must explicitly find when $J(f_1,f_2)$ becomes either 0 or infinite, as this will be the origin of the regularizable divergences. The most straightforward way in which this can happen is whenever $f_1=f_2$, or because of the periodicity of sn, whenever

$$f_1 = f_2 + 4mK(\kappa) + i2n\tilde{K}(\kappa) \quad n, m \in \mathbb{Z}.$$
(3.96)

Translating to the more intuitive coordinates of the rectangle using Table 3.1, that translates to

$$z_1 = z_2 + 2mL_x + 2niL_y \ n, m \in \mathbb{Z}.$$
 (3.97)

However, it could also happen that both terms of $J(f_1,f_2)$ vanish simultaneously, corresponding to the zeroes of $sn(\cdot)$ located at

If both f_1 and f_2 are at a zero of sn, they must either be at the same zero or differ by a lattice vector mL_x+2niL_y . However, the values that the spin positions z_i can take are restricted to be within the rectangle $\frac{1}{2}[x_0-L_x,x_0+L_x]\times i[y_0,y_0+L_y]$, and hence only the zero corresponding to (n,m)=(0,0) is possible. Thus, this divergence corresponds to the previous case.

The boundary-spin terms correspond to the first normal derivative of the Green function, which, because of the geometry, is either $\pm \partial_x$ for the vertical boundaries or $\pm \partial_y$ for the horizontal ones. Compactly, as in Equation (3.38), these read

$$\partial_i G_M(z,z') = \frac{1}{4\pi} \left[\frac{\partial_i J(R(z),R(z'))}{J(R(z),R(z'))} + \frac{\partial_i J(\overline{R(z)},\overline{R(z')})}{J(\overline{R(z)},\overline{R(z')})} - \frac{\partial_i J(R(z),\overline{R(z')})}{J(R(z),\overline{R(z')})} - \frac{\partial_i J(\overline{R(z)},R(z'))}{J(\overline{R(z)},R(z'))} - \frac{\partial_i J(\overline{R(z)},R(z'))}{J(\overline{R(z)},R(z'))} \right]. \tag{3.99}$$

Evaluating these derivatives at the respective non-regularized boundaries yields the kernels

$$\begin{split} V_{h_+}(x,z') &= \frac{4K(\kappa)}{L_x} \frac{cn(Rh(x))dn(Rh(x))}{(sn(Rh(x)) - sn(R(z')))} \\ V_{h_-}(z,z') &= \frac{4K(\kappa)}{L_x} \frac{cn(Rh(x))dn(Rh(x))}{sn(Rh(x))(1 - \kappa sn(Rh(x))sn(R(z')))} \\ V_{v_+}(y,z') &= \frac{2\tilde{\kappa}^2 \widetilde{K}(\kappa)}{L_y} \frac{\widetilde{sn}(Rv(y))\widetilde{cn}(Rv(y))}{\widetilde{dn}(Rv(y))(1 + \widetilde{dn}(Rv(y))sn(R(z')))} \\ V_{v_-}(y,z') &= \frac{2\tilde{\kappa}^2 \widetilde{K}(\kappa)}{L_y} \frac{\widetilde{sn}(Rv(y))\widetilde{cn}(Rv(y))}{\widetilde{dn}(Rv(y))(1 - \widetilde{dn}(Rv(y))sn(R(z')))}, \end{split} \tag{3.100}$$

where any Jacobi elliptic function with a tilde corresponds to $\widetilde{sn}(\cdot,\kappa)=sn(\cdot,\widetilde{\kappa})$, $x\in[x_0-\frac{L_x}{2},x_0+\frac{L_x}{2}]$, $y\in[y_0,y_0+L_y]$ and z' will correspond to the spin position

variable after the integral with $\rho(\vec{x}')$ in Equation (3.93). One can find the regularized counterparts of all these kernels by performing the following substitution

$$V_{h_+}^\varepsilon(x,z') = \frac{1}{2} \left(V_{h_+}(x+i\varepsilon,z') + V_{h_+}(x-i\varepsilon,z') \right) \tag{3.101}$$

and safely removing the ε from all the well-behaved terms, which corresponds exactly to the evaluation on the regularized boundary described in Equation (3.36). In Equation (3.101), V_{h_+} was picked as means of an example, as the prescription works for all the kernels. As we have discussed in previous sections, we expect a divergence on all of these kernels whenever $z' \in \partial \mathcal{M}$, which one can confirm by finding the zeroes of all the denominators of Equation (3.100). We also confirm that the potential divergences coming from the poles of the Jacobi elliptic functions in the numerator are unreachable because the variables x,y are confined within the rectangle. While the distributional counterpart of the divergence is again a principal value as in Equation (3.71) or (3.70), we have already seen in the case of fMPS that there is no need to provide their regularized distributional counterparts. This divergence can never be triggered as long as we demand that all the spin positions z_i are never exactly at the boundary $\partial \mathcal{M}$.

The boundary-boundary terms correspond to the second normal derivative of the Green function w.r.t the second variable,

$$\begin{split} \partial_j' \partial_i G_M(z,z') &= \frac{1}{4\pi} \left[\frac{\partial_i J(R(z),\overline{R(z')}) \partial_j' J(R(z),\overline{R(z')})}{J(R(z),\overline{R(z')})^2} + \frac{\partial_i J(\overline{R(z)},R(z')) \partial_j' J(\overline{R(z)},R(z'))}{J(\overline{R(z)},R(z'))^2} \right. \\ & \left. - \frac{\partial_i J(\overline{R(z)},\overline{R(z')}) \partial_j' J(\overline{R(z)},\overline{R(z')})}{J(\overline{R(z)},\overline{R(z')})^2} - \frac{\partial_i J(R(z),R(z')) \partial_j' J(R(z),R(z'))}{J(R(z),R(z'))^2} \right]. \end{split}$$

Once again, evaluating all these terms yields the sixteen boundary-boundary kernels of Equation (3.28). Let us start with the terms connecting two of the horizontal boundary terms

$$\begin{split} U_{h_-h_-}(x,x') &= U_{h_+h_+}(x,x') = \frac{8(4K(\kappa)^2)}{L_x^2} \frac{cn(Rh(x))dn(Rh(x))cn(Rh(x'))dn(Rh(x'))}{(sn(Rh(x)) - sn(Rh(x')))^2}, \\ U_{h_-h_+}(x,x') &= U_{h_+h_-}(x,x') = \frac{8\kappa(4K(\kappa)^2)}{L_x^2} \frac{cn(Rh(x))dn(Rh(x))cn(Rh(x'))dn(Rh(x'))}{(1 - \kappa sn(Rh(x))sn(Rh(x')))^2}, \end{split}$$

where $x,x'\in\left[x_0-\frac{L_x}{2},x_0+\frac{L_x}{2}\right]$ and the ones connecting the two vertical boundaries are

$$\begin{split} U_{v_-v_-}(y,y') &= U_{v_+v_+}(y,y') = \frac{8\widetilde{\kappa}^4 \widetilde{K}(\kappa)^2}{L_y^2} \frac{\widetilde{sn}(Rv(y))\widetilde{cn}(Rv(y))\widetilde{sn}(Rv(y'))\widetilde{cn}(Rv(y'))}{(\widetilde{dn}(Rv(y)) - \widetilde{dn}(Rv(y')))^2}, \\ U_{v_-v_+}(y,y') &= U_{v_+v_-}(y,y') = \frac{8\widetilde{\kappa}^4 \widetilde{K}(\kappa)^2}{L_y^2} \frac{\widetilde{sn}(Rv(y))\widetilde{cn}(Rv(y))\widetilde{sn}(Rv(y'))\widetilde{cn}(Rv(y'))}{(\widetilde{dn}(Rv(y)) + \widetilde{dn}(Rv(y')))^2}, \end{split}$$

where $y,y'\in [y_0,y_0+L_y]$. Before moving on to the crossed boundary propagation terms, we can find all the regularized versions of these kernels using the following

prescription

$$\begin{split} U_{h_{+}h_{+}}^{\varepsilon,\varepsilon'}(x,x') &= \frac{1}{4} \left(U_{h_{+}h_{+}}(x+i\varepsilon,x'+i\varepsilon') + U_{h_{+}h_{+}}(x-i\varepsilon,x'-i\varepsilon') \right. \\ &\left. + U_{h_{+}h_{+}}(x+i\varepsilon,x'-i\varepsilon') + U_{h_{+}h_{+}}(x-i\varepsilon,x'+i\varepsilon') \right), \end{split} \tag{3.105}$$

where as before, ${\cal U}_{h_+h_+}$ was simply picked as an example. The horizontal to vertical propagation terms are given by

$$\begin{split} U_{h_+v_+}(x,y') &= \frac{8\tilde{\kappa}^2\tilde{K}(\kappa)^2}{L_y^2} \frac{cn(Rh(x))dn(Rh(x))\tilde{sn}(Rv(y'))\tilde{cn}(Rv(y'))}{(sn(Rh(x))\tilde{dn}(Rv(y'))+1)^2}, \\ U_{h_+v_-}(x,y') &= \frac{8\tilde{\kappa}^2\tilde{K}(\kappa)^2}{L_y^2} \frac{cn(Rh(x))dn(Rh(x))\tilde{sn}(Rv(y'))\tilde{cn}(Rv(y'))}{(sn(Rh(x))\tilde{dn}(Rv(y'))-1)^2}, \\ U_{h_-v_+}(x,y') &= \frac{8\kappa\tilde{\kappa}^24K(\kappa)^2}{L_x^2} \frac{cn(Rh(x))dn(Rh(x))\tilde{sn}(Rv(y'))\tilde{cn}(Rv(y'))}{(\kappa sn(Rh(x))+\tilde{dn}(Rv(y')))^2}, \\ U_{h_-v_-}(x,y') &= \frac{8\kappa\tilde{\kappa}^24K(\kappa)^2}{L_x^2} \frac{cn(Rh(x))dn(Rh(x))\tilde{sn}(Rv(y'))\tilde{cn}(Rv(y'))}{(\kappa sn(Rh(x))-\tilde{dn}(Rv(y')))^2}, \end{split} \label{eq:Uh_v} \end{split}$$

and the terms corresponding to vertical to horizontal propagation are identical to the ones in Equation (3.106) with the role of the variables exchanged, that is $U_{vh}(x',y)=U_{hv}(x',y)$. As both the horizontal-vertical and the vertical-horizontal kernels are identical, one may wonder why we did not add both terms in Equation (3.93). The reasoning is that doing so involves an exchange in the order of integration, which can only be done if the integrals are finite. As seen in previous sections, all these kernels contain divergences, which could make said integrals problematic unless they are properly regularized. Hence, we now provide a second, more complicated example of the regularization scheme shown in Equation (3.41) for the PEPS functional, due to the periodicities of the Jacobi functions.

3.3.2 REGULARIZATION OF THE PEPS FUNCTIONAL

We begin with the regularization of $U_{h_+h_+}(x,x')$ as a representative of the horizontal to horizontal terms. By solving for the zeroes of the denominator in Equation (3.103), we find

$$\begin{split} sn(Rh(x)) - sn(Rh(x')) &= 0 \to x - x' = 2mL_x + 2niL_y \\ sn(Rh(x)) + sn(Rh(x') + 2K(\kappa)) &= 0 \to (x - x_0) + (x' - x_0) = (2m - 1)L_x + 2niL_y. \end{split}$$

Since $x, x', x_0 \in \mathbb{R}$ and $x, x' \in \left[x_0 - \frac{L_x}{2}, x_0 + \frac{L_x}{2}\right]$, then n = 0 in the previous equation. Expanding the kernel around these lines, one obtains

$$\begin{split} &\lim_{x\to x'+2mL_x} U_{h_+h_+} = \frac{8}{(x-x'-2mL_x)^2} + \mathcal{O}\left((x-x'-2mL_x)^0\right) \\ &\lim_{x\to -x'+2x_0+2mL_x} U_{h_+h_+} = \frac{-8}{(x+x'-2x_0-(2m-1)L_x)^2} + \mathcal{O}\left((x+x'-2x_0-(2m-1)L_x)^0\right), \end{split} \tag{3.108}$$

from which we see that the divergences form an alternating fishnet-like structure. Finally, according to Equation (3.41), we subtract the divergences while adding their regularized counterparts

$$RU_{h_{+}h_{+}}^{\varepsilon}(x,x') = \left[U_{h_{+}h_{+}}(x,x') - \sum_{m=-\infty}^{\infty} \frac{8}{(x-x'-2mL_{x})^{2}} + \sum_{m=-\infty}^{\infty} \frac{8}{(x+x'-2x_{0}-(2m-1)L_{x})^{2}} \right] + \sum_{m=-\infty}^{\infty} 4 \left[\frac{1}{(x-x'-2mL_{x}+i\varepsilon)^{2}} + \frac{1}{(x-x'-2mL_{x}-i\varepsilon)^{2}} \right] - \sum_{m=-\infty}^{\infty} 4 \left[\frac{1}{(x+x'-2x_{0}-(2m-1)L_{x}+i\varepsilon)^{2}} + \frac{1}{(x+x'-2x_{0}-(2m-1)L_{x}-i\varepsilon)^{2}} \right], \tag{3.109}$$

which in the limit of $\varepsilon \to 0$ allows us to identify the distributional divergence as the derivative of the principal value once again shown in Equation (3.73).

One can then confirm that Equation (3.42) is indeed satisfied $\forall x, x'$, but most importantly, is to check that the integral against the boundary function is indeed finite, as we have added and subtracted an infinite amount of divergences in Equation (3.109). Mainly, one must show that

$$\int_{x_0 - \frac{L_x}{2}}^{x_0 + \frac{L_x}{2}} \mathrm{d}x \int_{x_0 - \frac{L_x}{2}}^{x_0 + \frac{L_x}{2}} \mathrm{d}x' h_+(x) h_+(x') R U_{h_+, h_+}(x, x') < \infty \tag{3.110}$$

Let us first start with the first line of Equation (3.109), which when integrating it in the domain $x,x'\in\left[x_0-\frac{L_x}{2},x_0+\frac{L_x}{2}\right]$, the divergence coming from $U_{h_+h_+}(x,x')$ is mitigated exclusively by the counter terms with m=0. As we assume all boundary functions $h_+(x)$ to be well-behaved, the integral of the first line with m=0 will be finite. The integrals of the second and third lines for the terms that can diverge in this interval are reduced to

$$\begin{split} 8 \int_{x_{0} - \frac{L_{x}}{2}}^{x_{0} + \frac{L_{x}}{2}} \mathrm{d}x \int_{x_{0} - \frac{L_{x}}{2}}^{x_{0} + \frac{L_{x}}{2}} \mathrm{d}x' h_{+}(x) h_{+}(x') \frac{1}{2} \left[\frac{1}{(x - x' + i\varepsilon)^{2}} + \frac{1}{(x - x' - i\varepsilon)^{2}} \right] \\ & - \frac{1}{2} \left[\frac{1}{(x + x' - 2x_{0} + L_{x} + i\varepsilon)^{2}} + \frac{1}{(x + x' - 2x_{0} + L_{x} - i\varepsilon)^{2}} \right] \\ & - \frac{1}{2} \left[\frac{1}{(x + x' - 2x_{0} - L_{x} + i\varepsilon)^{2}} + \frac{1}{(x + x' - 2x_{0} - L_{x} - i\varepsilon)^{2}} \right]. \end{split}$$

By sending $x \to x - x_0$ and $x' \to x' - x_0$, and in the limit of $\varepsilon \to 0$

$$8\int_{-\frac{L_x}{2}}^{+\frac{L_x}{2}}\mathrm{d}x\int_{-\frac{L_x}{2}}^{+\frac{L_x}{2}}\mathrm{d}x'h_+(x+x_0)h_+(x'+x_0)\left[P'(\frac{1}{x-x'})-P'(\frac{1}{x+x'+L_x})-P'(\frac{1}{x+x'-L_x})\right]. \tag{3.112}$$

From this expression, we can see why this integral is finite. In the inside of the domain of integration, the only term that can diverge is $P'(\frac{1}{x-x'})$, but because this is a principal value, the divergence gets removed from the support symmetrically from both sides. This is, however, not possible strictly at two points, the two edges of the integral

 $x=x'=\pm \frac{L_x}{2}$. But it is precisely at these two points where the two other principal values participate to exactly diverge as well but with opposite signs, hence making the whole expression finite. For $m\neq 0$, $U_{h_+h_+}$ has no divergence inside of the domain of integration, and thus the limit $\varepsilon\to 0$ can be safely taken in Equation (3.109), removing all the counter terms. The reason for subtracting all the divergences, as opposed to only the one inside of the domain of integration, will be made apparent when exploring the $\kappa\to 1$ limit of the functional.

Following the same procedure, an example of the regularized version of a vertical-to-vertical propagation kernel is

$$RU_{v_{+}v_{+}}^{\varepsilon}(y,y') = \left[U_{v_{+}v_{+}}(y,y') - \sum_{m=-\infty}^{\infty} \frac{8}{(y-y'-2mL_{y})^{2}} + \sum_{m=-\infty}^{\infty} \frac{8}{(y+y'-2y_{0}-2mL_{y})^{2}} \right] + \sum_{m=-\infty}^{\infty} 4 \left[\frac{1}{(y-y'-2mL_{y}+i\varepsilon)^{2}} + \frac{1}{(y-y'-2mL_{y}-i\varepsilon)^{2}} \right] - \sum_{m=-\infty}^{\infty} 4 \left[\frac{1}{(y+y'-2y_{0}-2mL_{y}+i\varepsilon)^{2}} + \frac{1}{(y+y'-2y_{0}-2mL_{y}-i\varepsilon)^{2}} \right],$$
(3.113)

where we again subtract all the divergences, even those beyond the domain of integration. As in the previous case, this regularization scheme leads to a finite integral when integrated against the vertical boundary functions for the same reasons.

For the regularization of the horizontal to vertical terms, we encounter a different divergence, as both boundaries meet only at a single point. Therefore, whereas in the previous examples, the divergence would correspond to a line, for these kernels, it is localized at a single point and leads to the following regularization

$$\begin{split} RU_{h_{+}v_{-}}^{\varepsilon}(x,y') &= \left[U_{h_{+}v_{-}}(x,y') + \sum_{m,n=-\infty}^{\infty} \frac{8(x-x_{0}-(2m+\frac{1}{2})L_{x})(y-y_{0}-2nL_{y})}{((x-x_{0}-(2m+\frac{1}{2})L_{x})^{2}+(y-y_{0}-2nL_{y})^{2})^{2}} \right] \\ &- \sum_{m,n=-\infty}^{\infty} \frac{1}{4} \frac{8(x-x_{0}-(2m+\frac{1}{2})L_{x})(y-y_{0}-2nL_{y})}{((x-x_{0}-(2m+\frac{1}{2})L_{x}+i\varepsilon)^{2}+(y-y_{0}-2nL_{y}+i\varepsilon)^{2})^{2}} \\ &- \sum_{m,n=-\infty}^{\infty} \frac{1}{4} \frac{8(x-x_{0}-(2m+\frac{1}{2})L_{x})(y-y_{0}-2nL_{y}+i\varepsilon)^{2})^{2}}{((x-x_{0}-(2m+\frac{1}{2})L_{x}-i\varepsilon)^{2}+(y-y_{0}-2nL_{y}+i\varepsilon)^{2})^{2}} \\ &- \sum_{m,n=-\infty}^{\infty} \frac{1}{4} \frac{8(x-x_{0}-(2m+\frac{1}{2})L_{x})(y-y_{0}-2nL_{y}-i\varepsilon)^{2})^{2}}{((x-x_{0}-(2m+\frac{1}{2})L_{x}+i\varepsilon)^{2}+(y-y_{0}-2nL_{y}-i\varepsilon)^{2})^{2}} \\ &- \sum_{m,n=-\infty}^{\infty} \frac{1}{4} \frac{8(x-x_{0}-(2m+\frac{1}{2})L_{x})(y-y_{0}-2nL_{y}-i\varepsilon)^{2})^{2}}{((x-x_{0}-(2m+\frac{1}{2})L_{x}-i\varepsilon)^{2}+(y-y_{0}-2nL_{y}-i\varepsilon)^{2})^{2}}, \end{split}$$

where for these kernels the precise location of the divergence will depend on which of the different kernels is being regularized. As with the previous regularizations, the only divergence present in the integration domain is the one corresponding to m, n = 0. Similarly, as in the previous case, the first line of Equation (3.114) is finite

when integrated, and the remaining terms that previously led to the derivatives of the principal value are

$$-\frac{2(x-x_{0}-\frac{1}{2}L_{x})(y-y_{0})}{((x-x_{0}-\frac{1}{2}L_{x}+i\varepsilon)^{2}+(y-y_{0}+i\varepsilon)^{2})^{2}}-\frac{2(x-x_{0}-\frac{1}{2}L_{x})(y-y_{0})}{((x-x_{0}-\frac{1}{2}L_{x}+i\varepsilon)^{2}+(y-y_{0}+i\varepsilon)^{2})^{2}}-\frac{2(x-x_{0}-\frac{1}{2}L_{x}-i\varepsilon)^{2}+(y-y_{0}+i\varepsilon)^{2})^{2}}{((x-x_{0}-\frac{1}{2}L_{x}+i\varepsilon)^{2}+(y-y_{0}-i\varepsilon)^{2})^{2}}-\frac{2(x-x_{0}-\frac{1}{2}L_{x})(y-y_{0})}{((x-x_{0}-\frac{1}{2}L_{x}-i\varepsilon)^{2}+(y-y_{0}-i\varepsilon)^{2})^{2}}.$$

$$(3.115)$$

In the limit of $\varepsilon \to 0$, these terms correspond to the kernel associated with the Riesz transform [196], primarily used in harmonic analysis. This transformation can be considered a generalization of the Hilbert transform [197], the latter being the transformation usually associated with the principal value distribution in \mathbb{R} . Similarly, the Riesz transform defines a linear bounded operator from $L^2(\mathbb{R}^2)$ to itself, and hence its kernel is also a tempered distribution. Therefore, the expression in Equation (3.115) is nothing but an ϵ -limit of this tempered distribution, and thus, when integrated against the boundary function, it yields a finite result.

3.3.3 THE MPS FUNCTIONAL AS A LIMIT OF THE PEPS FUNCTIONAL

It was conjectured at the end of the Supplementary Material of [186] that by taking the $\kappa \to 1$ limit in the PEPS conformal map (3.91), one should recover a functional that would be either the fMPS functional exactly or rather a Möbius transformation thereof. Performing the calculation of this limit explicitly serves a double purpose. Firstly, it allows us to check the integrity of the fPEPS functional by contrasting this limit with the much more well-known fMPS functional. Secondly, it allows us to understand the effect of Möbius transformations on our functionals and constraints the possible classes of functions that can serve as boundary functions. In this limit, the first elliptic integrals behave as $K(1) = \infty$, $\tilde{K}(1) = \frac{\pi}{2}$, which means that the defining ratio of the conformal map

$$\frac{L_y}{L_x} = \frac{\tilde{K}(\kappa)}{2K(\kappa)} \to 0. \tag{3.116}$$

Therefore, in this limit, $L_x>>L_y$, and because we want to recover an infinitely long strip with a finite width, we demand that L_y remains a finite quantity and, therefore, that $L_x\to\infty$ in this limit. As it was shown in [186], if one defines a Möbius transformation by

$$f(z) = \frac{a_1z + a_2}{a_3z + a_4}, \quad a_1a_4 - a_2a_3 = 1, \quad a_1, a_2, a_3, a_4 \in \mathbb{C} \tag{3.117}$$

then the $\kappa \to 1$ limit of Equation (3.91) is

$$\lim_{\kappa \to 1} sn(R(z)) = \tanh(R(z)) = \frac{\sinh(R(z))}{\cosh(R(z))} = \frac{e^{2R(z)} - 1}{e^{2R(z)} + 1} = \frac{e^{\frac{\pi}{L_y}(z - z_0)} - 1}{e^{\frac{\pi}{L_y}(z - z_0)} + 1} \qquad \textbf{(3.118)}$$

which is a Möbius transformation of the MPS conformal map $g_{MPS}(z)=\exp\left(\frac{z-i\pi a}{\Delta}\right)$ with $\Delta=\frac{L_y}{\pi}$, $i\pi a=z_0$ and $(a_1,a_2,a_3,a_4)=(1,-1,1,1)$, where $a\in\mathbb{R}$. Using the expressions shown in Equations (3.57) both $G^c_{\mathcal{M}}(z,z')$ as well as $V_{h_\pm}(x,z')$ correctly reduce to the expected Möbius transformations of the MPS functional, whilst $V_{v_\pm}(y,z)\to 0 \ \forall y,z$.

More interestingly, this limit also provides information on what the behavior of the boundary functions must be, since the domain of integration of the horizontal boundary functions goes from a finite domain $\frac{1}{2}[x_0-L_x,x_0+L_x]$ to $\mathbb R$. This is precisely the origin of the restriction of the boundary functions to the space of Schwarz functions, even in the case of fPEPS, as they must be able to become the ones of the fMPS tensor.

The most interesting aspects of this limit appear in the propagation terms. We expect both the horizontal-vertical propagation terms and the vertical-vertical ones to vanish in this limit, while the horizontal-horizontal ones become the ones of the MPS functional. Let us start with $U_{h_{\perp}v_{\perp}}(x,y')$

$$\lim_{\kappa \to 1} U_{h_+ v_+}(x, y') = \frac{2\tilde{\kappa}^2}{\Delta^2} e^{-\frac{x}{\Delta}} \sin\left(\frac{y' - \pi a}{2\Delta}\right) \cos\left(\frac{y' - \pi a}{2\Delta}\right) \to 0 \tag{3.119}$$

as it is expected. However, it is not just the kernel that must vanish, but the integral as well, and the exponential term obstructs that. The integral that must vanish in this limit is then

$$\left(\int_{-\infty}^{\infty} dx h_{+}(x) e^{\frac{-x}{\Delta}} \int_{0}^{\pi\Delta} dy v_{+}(y+\pi a) \sin\left(\frac{y}{\Delta}\right)\right) \frac{2\tilde{\kappa}^{2}}{\Delta^{2}}, \tag{3.120}$$

which implies that $h_+(x)$ must decay faster than an exponential in the $x\to -\infty$ limit. From the rest of the horizontal to vertical kernels $U_{h_+v_-}(x,y'), U_{h_-v_+}(x,y'), U_{h_-v_-}(x,y')$ one extracts similar conditions, leading to the restriction of the horizontal boundary functions $h_\pm(x)$ to belong to the space of Schwartz functions [191]. This restriction is not only necessitated for a solid convergence of this limit but also for a proper guarantee of convergence of the integrals presented in the regularization procedure, such as those found in Equations (3.112), (3.113) and (3.114).

For the horizontal to horizontal terms, we recover the correct regularized limit

$$\lim_{\kappa \to 1} R U_{h_+ h_+}^{\varepsilon \to 0}(x, x') = U_{h_+ h_+}(x, x') - \frac{8}{(x - x')^2} + 8P'(\frac{1}{x - x'})$$
(3.121)

because the $L_x \to \infty$ limit removes all the terms of the sum in Equation (3.109) except for the ones where L_x is not present on the denominator.

Finally, we reach the vertical to vertical terms, and while $U_{v_+v_-}(y,y')$ correctly reduces to zero in this limit, $U_{v_+v_-}(y,y')$ does not

$$\lim_{\kappa \to 1} U_{v_+v_+}(y,y') = \frac{2}{\Delta^2} \left(\frac{1}{\sin\left(\frac{(y-y')}{2\Delta}\right)^2} - \frac{1}{\sin\left(\frac{(y+y'-2\pi a)}{2\Delta}\right)^2} \right), \tag{3.122}$$

and furthermore, it is clearly a divergent kernel. This is precisely the reason that all the possible divergences were subtracted in the regularization procedure, as one can then use the following identity

$$\frac{1}{\sin{(\pi x)^2}} = \frac{1}{\pi^2} \sum_{k=-\infty}^{\infty} \frac{1}{(x-k)^2} \to \sum_{m=-\infty}^{\infty} \frac{1}{(y-y'-2m\pi\Delta)^2} = \frac{1}{4\Delta^2} \frac{1}{\sin{\left(\frac{(y-y')}{2\Delta}\right)^2}}, \tag{3.123}$$

to write the first line of Equation (3.113) as

$$U_{v_{+}v_{+}}(y,y') - \frac{2}{\Delta^{2}} \frac{1}{\sin\left(\frac{y-y'}{2\Delta}\right)^{2}} + \frac{2}{\Delta^{2}} \frac{1}{\sin\left(\frac{y+y'-2\pi a}{2\Delta}\right)^{2}},$$
 (3.124)

which completely subtracts the divergent leftovers of the $\kappa \to 1$ limit. All that is left are the remaining terms in the second and third lines of Equation (3.113), which by the choice of the boundary function $v_\pm(y)$ to be a Schwartz function, it contributes a finite amount to the functional. Furthermore, these pieces are the only dependence on $v_\pm(y)$ in the $\kappa \to 1$ limit. Because they contribute quadratically to the action, they can be integrated out into a constant that can be absorbed into the normalization of the overall state.

A pictorial way in which this constant can also be understood is that the $\kappa \to 1$ limit indeed must send $L_x \to \infty$ but not necessarily $L_y \to 0$, therefore leaving a leftover that was never there in the fMPS case and that is absorbed as a constant due to this term being uncoupled from the rest of the action.

3.3.4 CHIRAL TRUNCATION OF THE GENERIC AND PEPS FUNCTIONAL.

As we already know, we are ultimately interested in a chiral tensor. Following the procedure described in the previous sections, the fPEPS functional from Equation (3.93) reduces to

$$\begin{split} S_{\mathcal{M}}^{c}[\tilde{h}_{+},\tilde{h}_{-},\tilde{v}_{+},\tilde{v}_{+},\rho] &= \frac{1}{8\pi} \int_{\mathcal{M}} d\vec{x} \int_{\mathcal{M}} d\vec{x}' G_{\mathcal{M}}^{c}(\vec{x},\vec{x}') \rho(\vec{x}) \rho(\vec{x}') \\ &- \frac{1}{64\pi^{2}} \int_{x_{0} - \frac{L_{x}}{2}}^{x_{0} + \frac{L_{x}}{2}} dx \int_{x_{0} - \frac{L_{x}}{2}}^{x_{0} + \frac{L_{x}}{2}} dx' \left(\tilde{h}_{+}(x) \; , \; \; \tilde{h}_{-}(x) \right) \begin{pmatrix} U_{h_{+},h_{+}}(x,x') \; , \; U_{h_{+},h_{-}}(x,x') \\ U_{h_{-},h_{+}}(x,x') \; , \; U_{h_{-},h_{-}}(x,x') \end{pmatrix} \begin{pmatrix} \tilde{h}_{+}(x') \\ \tilde{h}_{-}(x') \end{pmatrix} \\ &- \frac{1}{64\pi^{2}} \int_{y_{0}}^{y_{0} + L_{y}} dy \int_{y_{0}}^{y_{0} + L_{y}} dy' \left(\tilde{v}_{+}(y) \; , \; \; \tilde{v}_{-}(y) \right) \begin{pmatrix} U_{v_{+},v_{+}}(y,y') \; , \; U_{v_{+},v_{-}}(y,y') \\ U_{v_{-},v_{+}}(y,y') \; , \; U_{v_{-},v_{-}}(y,y') \end{pmatrix} \begin{pmatrix} \tilde{v}_{+}(y') \\ \tilde{v}_{-}(y') \end{pmatrix} \\ &- \frac{1}{32\pi^{2}} \int_{x_{0} - \frac{L_{x}}{2}}^{x_{0} + \frac{L_{x}}{2}} dx \int_{y_{0}}^{y_{0} + L_{y}} dy' \left(\tilde{h}_{+}(x) \; , \; \; \tilde{h}_{-}(x) \right) \begin{pmatrix} U_{h_{+},v_{+}}(x,y') \; , \; U_{h_{+},v_{-}}(x,y') \\ U_{h_{-},v_{+}}(x,y') \; , \; U_{h_{-},v_{-}}(x,y') \end{pmatrix} \begin{pmatrix} \tilde{v}_{+}(y') \\ \tilde{v}_{-}(y') \end{pmatrix} \\ &+ \frac{i}{16\pi^{2}} \int_{x_{0} - \frac{L_{x}}{2}}^{y_{0} + L_{y}} dx \int_{\mathcal{M}} d\vec{x}' \rho(\vec{x}') \left(\tilde{h}_{+}(x) \; , \; \; \tilde{h}_{-}(x) \right) \begin{pmatrix} V_{h_{+}}(x,\vec{x}') \\ -V_{h_{-}}(x,\vec{x}') \end{pmatrix} \\ &+ \frac{i}{16\pi^{2}} \int_{y_{0}}^{y_{0} + L_{y}} dy \int_{\mathcal{M}} d\vec{x}' \rho(\vec{x}') \left(\tilde{v}_{+}(y) \; , \; \; \tilde{v}_{-}(y) \right) \begin{pmatrix} -V_{v_{+}}(y,\vec{x}') \\ V_{v_{-}}(y,\vec{x}') \end{pmatrix}, \end{cases} \\ &+ \frac{i}{16\pi^{2}} \int_{y_{0}}^{y_{0} + L_{y}} dy \int_{\mathcal{M}} d\vec{x}' \rho(\vec{x}') \left(\tilde{v}_{+}(y) \; , \; \; \tilde{v}_{-}(y) \right) \begin{pmatrix} -V_{v_{+}}(y,\vec{x}') \\ V_{v_{-}}(y,\vec{x}') \end{pmatrix}, \end{cases}$$

where we have now collected the cross-propagation term under the same integral, and thanks to the regularization scheme, we have been able to exchange the order of integration. With the truncated action, we can also introduce the spin densities to extract the conformal dimension factor, akin to the fMPS case shown in Equation (3.80). To extract it, one simply takes the regularized limit

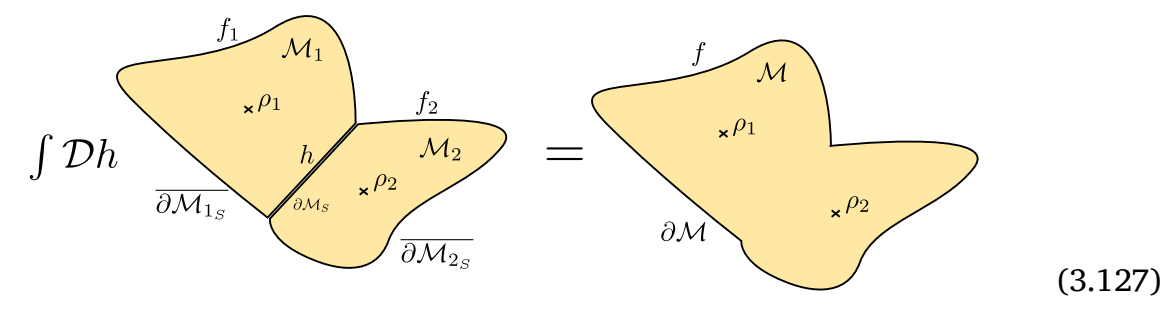
$$: \lim_{z \to \omega} G_{\mathcal{M}}(z,\omega) := s^2 \log \left(\frac{2K(\kappa)}{L_x} \right) \tag{3.126}$$

where we have subtracted the divergent term to extract the 0^{th} -order term of the expansion. This term correctly reduces to the corresponding conformal dimension term of the fMPS functional in the $\kappa \to 1$ limit.

3.4 The sewing condition for the free boson

SET UP AND SPLIT OF THE FUNCTIONALS

In this section, we will present the most general proof of the sewing condition for any two chiral tensors $\mathcal{A}_{\mathcal{M}_1}^c$ and $\mathcal{A}_{\mathcal{M}_2}^c$. Our starting point is two functionals defined in two distinct manifolds \mathcal{M}_1 and \mathcal{M}_2 employing the conformal maps g_1 and g_2 . Each tensor hosts their own set of spins denoted by ρ_1 and ρ_2 , and we will demand that they have a compatible boundary. To be more precise, one begins splitting the boundary into two sections, the section in which the sewing takes place $\partial \mathcal{M}_S$ and the rest of the boundary in which it does not $\overline{\partial \mathcal{M}_S}$, such that $\partial \mathcal{M} = \partial \mathcal{M}_S \cup \overline{\partial \mathcal{M}_S}$, a.k.a the two manifolds can be glued together. Diagrammatically, we are aiming to prove the following identity



where the path integral sums only over the functions present in the shared compatible boundary h. Exploring the sewing condition for generic functionals $\mathcal{A}_{\mathcal{M}}$ is a very complicated task. Still, we will use conformal invariance to treat this problem with the respective representations of both tensors in the UHP, where all the expressions become much simpler. In the coordinates shown in Equation (3.127), we would split the boundary functions as

$$\tilde{f}_i(g_i(x)) = f_i(g_i(x))\chi(x \in \overline{\partial \mathcal{M}_{i_S}}) + h(g_i(x))\chi(x \in \partial \mathcal{M}_S) \tag{3.128}$$

where $\chi(x)$ is the indicator distribution, and we have explicitly included the conformal map's dependence on the functions. If one wishes to split the original function $\tilde{f}(x)$ in a continuous fashion, then one should choose the endpoints of the indicators to be $\chi(\partial\partial\mathcal{M}_S)=\frac{1}{2}.$ However, that is not strictly necessary for the function to remain within the Schwartz space.

If we wish to perform the sewing of the common boundary in the coordinates of the UHP, then we need to undo the change of variables from the conformal maps g_i , therefore leading to the following split in the UHP

$$\tilde{f}_i(x) = f_i(x)\chi(x \in g_i\left(\overline{\partial\mathcal{M}_{i_S}}\right)) + h(x)\chi(x \in g_i\left(\partial\mathcal{M}_S\right)) \tag{3.129}$$

where $g_i\left(\partial\mathcal{M}_{i_S}\right)\cup g_i\left(\partial\mathcal{M}_S\right)=\mathbb{R}$ by definition of the conformal map. Therefore, in the UHP, the sewing boundary $\partial\mathcal{M}_S$ gets in general sent to different subdomains of the real line $D_i=g_i\left(\partial\mathcal{M}_S\right)$, while the remaining of the boundary of each functional gets sent to the remainder of \mathbb{R} , $\overline{D_i}=g_i\left(\overline{\partial\mathcal{M}_{i_S}}\right)$. This is schematically shown in Figure 3.7 for two arbitrary domains and randomly chosen domains in the UHP to showcase that generically $D_1\neq D_2$, and that these can be either compact or non-compact. Moving to the UHP allows to forego the potentially complicated geometry of $\partial\mathcal{M}_S$, while simply backloading that information on the specific forms of the subdomains D_i and $\overline{D_i}$.

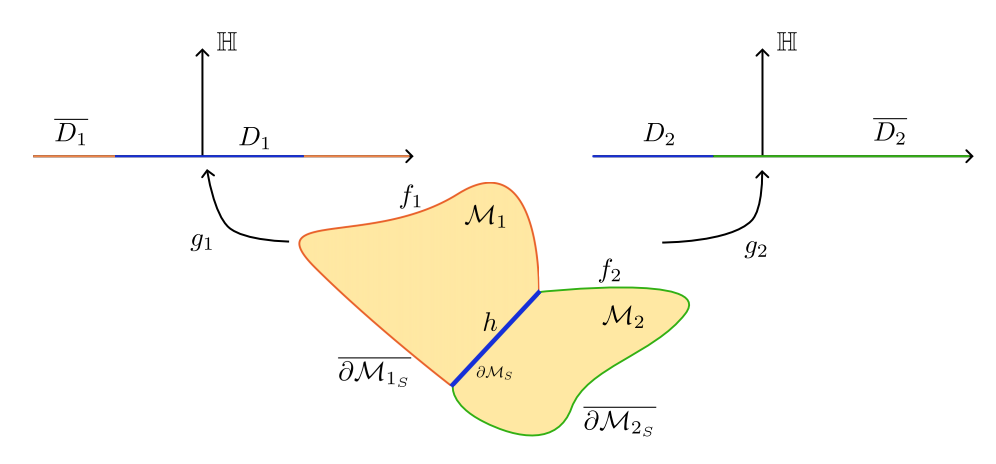


Figure 3.7: Schematic depiction of the pre-image of $\partial \mathcal{M}_S$ in the UHP for generic conformal maps g_i .

Therefore, the minimal tensor in the UHP that captures any potential sewing scenario is that of an UHP tensor whose boundary function is split between a generic sub-domain of \mathbb{R} , D and its complement \overline{D} .

Our starting point is then the chiral UHP functional tensor derived from Equation (3.52) using the chiral truncation, given by

$$\begin{split} \mathcal{A}^c_{\mathbb{H}}\left[\tilde{f},\{z_i,s_i\}_{i=1}^N\right] &= \exp\left(+\frac{1}{2}\sum_{i,j}s_is_j\left(\log\left[(z_i-z_j)\right]\right) - \frac{1}{2\pi}\sum_is_i\int_{\mathbb{R}}dy\tilde{f}(y)\frac{1}{z_i-y} \right. \\ &\left. + \frac{1}{8\pi^2}\int_{\mathbb{R}}dx\int_{\mathbb{R}}dy\tilde{f}(x)\tilde{f}(y)\frac{1}{(x-y)^2}\right). \end{split} \tag{3.130}$$

where we split the boundary integral as

$$\int_{\mathbb{R}} dx \tilde{f}(x) = \int_{D} dx h(x) + \int_{\overline{D}} dx f(x), \qquad (3.131)$$

such that then the tensor becomes

$$\begin{split} \mathcal{A}^{c}_{\,\, \mathbb{H}} \left[f, h, \{ z_{i}, s_{i} \}_{i=1}^{N} \right] &= \exp \left(+ \frac{1}{2} \sum_{i,j} s_{i} s_{j} \left(\log \left[(z_{i} - z_{j}) \right] \right) \right. \\ &\left. - \frac{1}{2\pi} \sum_{i} s_{i} \left(\int_{D} dy h(y) \frac{1}{z_{i} - y} + \int_{\overline{D}} dy f(y) \frac{1}{z_{i} - y} \right) \right. \\ &\left. + \frac{1}{8\pi^{2}} \int_{\overline{D}} dx \int_{\overline{D}} dy f(x) f(y) \frac{1}{(x - y)^{2}} + \frac{1}{4\pi^{2}} \int_{\overline{D}} dx \int_{D} dy f(x) h(y) \frac{1}{(x - y)^{2}} \right. \\ &\left. + \frac{1}{8\pi^{2}} \int_{D} dx \int_{D} dy h(x) h(y) \frac{1}{(x - y)^{2}} \right), \end{split} \tag{3.132}$$

which we can re-organize as

$$\begin{split} \mathcal{A}^{c}_{\ \mathbb{H}}\left[f,h,\{z_{i},s_{i}\}_{i=1}^{N}\right] &= \mathcal{B}^{c}_{\mathbb{H},\overline{D}}\left[f,\{z_{i},s_{i}\}_{i=1}^{N}\right] \exp\left(-\frac{1}{2\pi}\sum_{i}s_{i}\int_{D}dyh(y)\frac{1}{z_{i}-y}\right. \\ &\left. + \frac{1}{4\pi^{2}}\int_{\overline{D}}dx\int_{D}dyf(x)h(y)\frac{1}{(x-y)^{2}} + \frac{1}{8\pi^{2}}\int_{D}dx\int_{D}dyh(x)h(y)\frac{1}{(x-y)^{2}}\right), \end{split} \tag{3.133}$$

where in $\mathcal{B}^c_{\mathbb{H},\overline{D}}$ we have accumulated all the terms that will not take part in the sewing path integral over the function h, which are

$$\begin{split} \mathcal{B}^{c}_{\mathbb{H},\overline{D}}\left[f,\{z_{i},s_{i}\}_{i=1}^{N}\right] &= \exp\left(+\frac{1}{2}\sum_{i,j}s_{i}s_{j}\left(\log\left[(z_{i}-z_{j})\right]\right) - \frac{1}{2\pi}\sum_{i}s_{i}\left(\int_{\overline{D}}dy f(y)\frac{1}{z_{i}-y}\right) \right. \\ &\left. + \frac{1}{8\pi^{2}}\int_{\overline{D}}dx\int_{\overline{D}}dy f(x)f(y)\frac{1}{(x-y)^{2}}\right). \end{split} \tag{3.134}$$

With the expressions for a generic split of the boundary, we can now move forward toward the sewing equation, given in the UHP by

$$\int \mathcal{D}h \mathcal{A}_{\mathbb{H}_{1}}^{c} \left[f_{1}, h, \left\{ z_{i,1}, s_{i,1} \right\}_{i=1}^{N} \right] \mathcal{A}_{\mathbb{H}_{2}}^{c} \left[f_{2}, h, \left\{ z_{i,2}, s_{i,2} \right\}_{i=1}^{N} \right]$$
 (3.135)

which after introducing Equation (3.133) becomes

$$\begin{split} &\mathcal{B}^{c}_{\mathbb{H},\overline{D}_{1}}\left[f_{1},\left\{z_{i,1},s_{i,1}\right\}_{i=1}^{N}\right]\mathcal{B}^{c}_{\mathbb{H},\overline{D}_{2}}\left[f_{2},\left\{z_{i,2},s_{i,2}\right\}_{i=1}^{N}\right]\times\\ &\int\mathcal{D}h\exp\left(-\frac{1}{2\pi}\sum_{i}s_{i,1}\int_{D_{1}}dyh(y)\frac{1}{z_{i,1}-y}-\frac{1}{2\pi}\sum_{i}s_{i,2}\int_{D_{2}}dyh(y)\frac{1}{z_{i,2}-y}\right.\\ &\left.+\frac{1}{4\pi^{2}}\int_{\overline{D}_{1}}dx\int_{D_{1}}dyf_{1}(x)h(y)\frac{1}{(x-y)^{2}}+\frac{1}{4\pi^{2}}\int_{\overline{D}_{2}}dx\int_{D_{2}}dyf_{2}(x)h(y)\frac{1}{(x-y)^{2}}\right.\\ &\left.+\frac{1}{8\pi^{2}}\int_{D_{1}}dx\int_{D_{1}}dyh(x)h(y)\frac{1}{(x-y)^{2}}+\frac{1}{8\pi^{2}}\int_{D_{2}}dx\int_{D_{2}}dyh(x)h(y)\frac{1}{(x-y)^{2}}\right), \end{split} \tag{3.136}$$

where the range of the spin sums goes from 1 to either N_1 or N_2 as indicated by the spin subindex. From now on, we will focus exclusively on the terms under the functional integral. To express the integral of Equation (3.136) as a Gaussian integral over the function h, we first need the domains of the integrals under which the function h appears to be the same. Here, we can use Möbius transformations to change the domains D_1 and D_2 to a common one that we will name D. A very natural choice would be for $D = \mathbb{R}^+$, which would then make $\overline{D} = \mathbb{R}^-$. If $D_1 = \gamma_1(D)$ and $D_2 = \gamma_2(D)$, then obviously $\overline{D_1} = \gamma_1(\overline{D})$ and $\overline{D_2} = \gamma_2(\overline{D})$, due to the biholomorphicity of the Möbius transformation. We parametrize these transformations by

$$y = \gamma_i(\omega_y) = \frac{a_i \omega_y + b_i}{c_i \omega_y + d_i} \quad , \quad a_i, b_i, c_i, d_i \in \mathbb{R}$$
 (3.137)

Changing variables employing these transformations, both for the boundary integrals

and the spin positions as $z_{i,j}=\gamma_j(\omega_{i,j})$, one writes Equation (3.136) as

$$\begin{split} &\int \mathcal{D}h \exp\left(-\frac{1}{2\pi}\sum_{i}s_{i,1}\int_{D}d\omega_{y}h(\gamma_{1}(\omega_{y}))\frac{1}{\omega_{i,1}-\omega_{y}}\frac{c_{1}\omega_{i,1}+d_{1}}{c_{1}\omega_{y}+d_{1}}\right.\\ &\left.-\frac{1}{2\pi}\sum_{i}s_{i,2}\int_{D}d\omega_{y}h(\gamma_{2}(\omega_{y}))\frac{1}{\omega_{i,2}-\omega_{y}}\frac{c_{2}\omega_{i,2}+d_{2}}{c_{2}\omega_{y}+d_{2}}\right.\\ &\left.+\frac{1}{4\pi^{2}}\int_{D}d\omega_{x}\int_{D}d\omega_{y}f_{1}(\gamma_{1}(\omega_{x}))h(\gamma_{1}(\omega_{y}))\frac{1}{(\omega_{x}-\omega_{y})^{2}}\right.\\ &\left.+\frac{1}{4\pi^{2}}\int_{D}d\omega_{x}\int_{D}d\omega_{y}f_{2}(\gamma_{2}(\omega_{x}))h(\gamma_{2}(\omega_{y}))\frac{1}{(\omega_{x}-\omega_{y})^{2}}\right.\\ &\left.+\frac{1}{8\pi^{2}}\int_{D}d\omega_{x}\int_{D}d\omega_{y}h(\gamma_{1}(\omega_{x}))h(\gamma_{1}(\omega_{y}))\frac{1}{(\omega_{x}-\omega_{y})^{2}}\right.\\ &\left.+\frac{1}{8\pi^{2}}\int_{D}d\omega_{x}\int_{D}d\omega_{y}h(\gamma_{2}(\omega_{x}))h(\gamma_{2}(\omega_{y}))\frac{1}{(\omega_{x}-\omega_{y})^{2}}\right), \end{split} \label{eq:final_poly}$$

where one can now finally put together all the previously different integrals to obtain

$$\begin{split} &\int \mathcal{D}h \exp\left(-\frac{1}{2\pi} \int_{D} d\omega_{y} \left[\sum_{i} s_{i,1} \frac{h(\gamma_{1}(\omega_{y}))}{\omega_{i,1} - \omega_{y}} \frac{c_{1}\omega_{i,1} + d_{1}}{c_{1}\omega_{y} + d_{1}} + \sum_{j} s_{j,2} \frac{h(\gamma_{2}(\omega_{y}))}{\omega_{j,2} - \omega_{y}} \frac{c_{2}\omega_{j,2} + d_{2}}{c_{2}\omega_{y} + d_{2}} \right] \\ &\quad + \frac{1}{4\pi^{2}} \int_{D} d\omega_{x} \int_{D} d\omega_{y} \frac{1}{(\omega_{x} - \omega_{y})^{2}} \left[f_{1}(\gamma_{1}(\omega_{x}))h(\gamma_{1}(\omega_{y})) + f_{2}(\gamma_{2}(\omega_{x}))h(\gamma_{2}(\omega_{y})) \right] \\ &\quad + \frac{1}{8\pi^{2}} \int_{D} d\omega_{x} \int_{D} d\omega_{y} \frac{1}{(\omega_{x} - \omega_{y})^{2}} \left[h(\gamma_{1}(\omega_{x}))h(\gamma_{1}(\omega_{y})) + h(\gamma_{2}(\omega_{x}))h(\gamma_{2}(\omega_{y})) \right] \right). \end{split} \tag{3.139}$$

At this point, we can already start to see the structure of the Gaussian integral emerge, as we have both a quadratic and a linear term in h, albeit their arguments are different due to the different Möbius transformations required to make both domains be the same. In order to move forward, we will now assume that there exists an integral transform and an inverse of the form

$$h(x) = \int_C dx' K(x, x') \hat{h}(x') , \hat{h}(x) = \int_{C^{-1}} dx' K^{-1}(x, x') h(x')$$
 (3.140)

for unspecified domains of integration C and C^{-1} such that $\int_C dy K(x,y) K^{-1}(y,z) = \delta(x-z)$. Assuming such a transformation exists, we will further assume that it preserves the measure of the functional integration, which means $\int \mathcal{D}h = \int \mathcal{D}\hat{h}$, and therefore that this transformation preserves the Schwartz space. An example of such a transformation would be the well-known Fourier transform or the Hilbert transform.

Inserting the expressions for h in the transformed basis, one obtains

$$\begin{split} &\int \mathcal{D}\hat{h} \exp\big(\\ &-\frac{1}{2\pi} \int_{C} d\omega_{y}' \hat{h}(\omega_{y}') \int_{D} d\omega_{y} \left[\sum_{i} s_{i,1} \frac{K(\omega_{y}', \gamma_{1}(\omega_{y}))}{\omega_{i,1} - \omega_{y}} \frac{c_{1}\omega_{i,1} + d_{1}}{c_{1}\omega_{y} + d_{1}} + \sum_{j} s_{j,2} \frac{K(\omega_{y}', \gamma_{2}(\omega_{y}))}{\omega_{j,2} - \omega_{y}} \frac{c_{2}\omega_{j,2} + d_{2}}{c_{2}\omega_{y} + d_{2}} \right] \\ &+ \frac{1}{4\pi^{2}} \int_{C} d\omega_{y}' \hat{h}(\omega_{y}') \int_{D} d\omega_{x} \int_{D} d\omega_{y} \frac{1}{(\omega_{x} - \omega_{y})^{2}} \left[f_{1}(\gamma_{1}(\omega_{x})) K(\omega_{y}', \gamma_{1}(\omega_{y})) + f_{2}(\gamma_{2}(\omega_{x})) K(\omega_{y}', \gamma_{2}(\omega_{y})) \right] \\ &+ \frac{1}{8\pi^{2}} \int_{C} d\omega_{x}' d\omega_{y}' \hat{h}(\omega_{x}') \hat{h}(\omega_{y}') \int_{D} d\omega_{x} d\omega_{y} \frac{K(\omega_{x}', \gamma_{1}(\omega_{x})) K(\omega_{y}', \gamma_{1}(\omega_{y})) + K(\omega_{x}', \gamma_{2}(\omega_{x})) K(\omega_{y}', \gamma_{2}(\omega_{y}))}{(\omega_{x} - \omega_{y})^{2}} \\ \end{pmatrix} \end{split}$$

THE GAUSSIAN INTEGRAL

To reach the final Gaussian integral form, one collects the terms linear on \hat{h} and those quadratic in separate terms as

$$\begin{split} J(\omega_y',f_1,f_2) &= -\frac{1}{2\pi} \left[\int_D \omega_y \sum_i s_{i,1} \frac{K(\omega_y',\gamma_1(\omega_y))}{\omega_{i,1} - \omega_y} \frac{c_1 \omega_{i,1} + d_1}{c_1 \omega_y + d_1} + \sum_j s_{j,2} \frac{K(\omega_y',\gamma_2(\omega_y))}{\omega_{j,2} - \omega_y} \frac{c_2 \omega_{j,2} + d_2}{c_2 \omega_y + d_2} \right] \\ &+ \frac{1}{4\pi^2} \int_D d\omega_x \int_D d\omega_y \frac{1}{(\omega_x - \omega_y)^2} \left[f_1(\gamma_1(\omega_x)) K(\omega_y',\gamma_1(\omega_y)) + f_2(\gamma_2(\omega_x)) K(\omega_y',\gamma_2(\omega_y)) \right], \end{split} \tag{3.142}$$

and

$$W(\omega_x',\omega_y',\gamma_1,\gamma_2) = -\frac{1}{4\pi^2} \int_D d\omega_x d\omega_y \frac{K(\omega_x',\gamma_1(\omega_x))K(\omega_y',\gamma_1(\omega_y)) + K(\omega_x',\gamma_2(\omega_x))K(\omega_y',\gamma_2(\omega_y))}{(\omega_x - \omega_y)^2}, \tag{3.143}$$

where we have made explicit the dependance of W on the Möbius transformations involved in the specific sewing scenario. With these definitions, Equation (3.141) becomes

$$\int \mathcal{D}\hat{h} \exp\left(+\int_{C} d\omega_{y}' \hat{h}(\omega_{y}') J(\omega_{y}', f_{1}, f_{2}) - \frac{1}{2} \int_{C} d\omega_{x}' d\omega_{y}' \hat{h}(\omega_{x}') \hat{h}(\omega_{y}') W(\omega_{x}', \omega_{y}', \gamma_{1}, \gamma_{2})\right). \tag{3.144}$$

This Gaussian functional integral is very well known, and ignoring a potentially infinite pre-factor constant, its solution is given by

$$\propto \exp\left(\frac{1}{2}\int_C d\omega_x' d\omega_y' J(\omega_x', f_1, f_2) W^{-1}(\omega_x', \omega_y', \gamma_1, \gamma_2) J(\omega_y', f_1, f_2)\right), \tag{3.145}$$

where $W^{-1}(\omega_x',\omega_y',\gamma_1,\gamma_2)$ is another function that fulfills

$$\int_{C} d\omega_{z} W(\omega_{x}, \omega_{z}, \gamma_{1}, \gamma_{2}) W^{-1}(\omega_{z}, \omega_{y}, \gamma_{1}, \gamma_{2}) = \delta(\omega_{x} - \omega_{y}), \tag{3.146}$$

and therefore acts as the functional inverse of the Gaussian Kernel. Finding this inverse kernel is, in general, very hard. However, some solutions for this family of kernels can be explicitly found in the theory of Hilbert Transforms [197], and more specifically in the realm of finite Hilbert Transforms [198].

In order to aid with intuition, we present here two examples of kernels and their respective inverses. The Hilbert transform of a function f is denoted $H[f] = \tilde{f}$, with $f \in \mathbb{L}^p(\mathbb{R}), \ 1 \leq p < \infty$ and it is usually defined as an integral over \mathbb{R}

$$H[f](t) = \frac{1}{\pi}(\text{p.v.}) \int_{\mathbb{R}} \frac{\mathrm{d}x f(x)}{x - t}, \tag{3.147} \label{eq:3.147}$$

where $t \in \mathbb{R}$ and hence as a convolution with the principal value distribution. The main result from which we depart, is the convolution of the principal value with itself,

$$H\left[p.v.\left(\frac{1}{x}\right)\right] = -\pi\delta(t),\tag{3.148}$$

which is precisely the kind of expression we wish to achieve for the Gaussian kernel W(x,y). The first step in constructing such an inverse, is to derive a similar expression as Equation (3.148) but for a function that behaves as $\sim \frac{1}{(x-t)^2}$. We start by introducing the regularized distributions of the principal value and the Dirac distribution

$$P\left(\frac{1}{x},\varepsilon\right) = \frac{1}{2}\left(\frac{1}{x+i\varepsilon} + \frac{1}{x-i\varepsilon}\right),$$

$$\delta(x,\varepsilon) = \frac{1}{2\pi i}\left(\frac{1}{x+i\varepsilon} - \frac{1}{x-i\varepsilon}\right),$$
(3.149)

where $x \in \mathbb{R}, \ \varepsilon \in \mathbb{R}, \ \varepsilon > 0$. Then, if one integrates by parts in the l.h.s of

$$\int_{\mathbb{R}} \mathrm{d}x P\left(\frac{1}{x-s}, \varepsilon_1\right) P\left(\frac{1}{x-u}, \varepsilon_1\right) = -\frac{1}{\pi^2} \delta(s-u, \varepsilon_1 + \varepsilon_2), \tag{3.150}$$

one obtains

$$\int_{\mathbb{R}} \mathrm{d}x P'\left(\frac{1}{x-s},\varepsilon_1\right) \frac{1}{2} \log\left[(x-u)^2 + \varepsilon_2^2\right] = \frac{1}{\pi^2} \delta(s-u,\varepsilon_1+\varepsilon_2), \tag{3.151}$$

which is much closer to the functional form of W(x,y). However,the logarithm in Equation (3.151) is far from being our desired inverse, as the domain integration is \mathbb{R} , whilst the domain of integration found in the Gaussian integral can in general be finite. We thus turn our attention to the theory of finite Hilbert transforms, defined by

$$H[f](t) = \frac{1}{\pi}(\text{p.v.}) \int_{a}^{b} \frac{dx f(x)}{x - t},$$
 (3.152)

where f is supported on the domain [a,b] and $t \in [a,b]$. In [199], an explicit inversion formula for this transform was found, given by

$$f(t) = \frac{1}{\pi\sqrt{(t-a)(b-t)}} \left(\int_{a}^{b} \frac{\mathrm{d}x H[f](x)}{(x-t)} \sqrt{(x-a)(b-x)} + \int_{a}^{b} f(x) \mathrm{d}x \right), \quad (3.153)$$

with $f \in \mathbb{L}^p(\mathbb{R})$. The simplest case is to consider a semi-infinite line with a=0 and $b\to\infty$, and if one demands that $H[f](x)=\delta(x-u), u\geq 0$ then

$$f(t) = \sqrt{\frac{u}{t}} \frac{1}{u - t} \tag{3.154}$$

which one can then use to derive a similar expression to Equation (3.151). By basic integration techniques, one finds

$$\delta(t-u) = \int_0^\infty \frac{\mathrm{d}s}{s-t} \sqrt{\frac{u}{s}} \frac{1}{u-s} = \int_0^\infty \frac{\mathrm{d}s}{(s-t)^2} 2 \operatorname{Arctanh}\left(\sqrt{\frac{s}{u}}\right) \tag{3.155}$$

which is then our desired inverse. As a general rule of thumb, we see that these inverses have branch cuts when studied as complex functions, which will become relevant later on.

For the time being, we will proceed forward by leaving it as an arbitrary unknown function. We will see that we can derive it by comparing the expressions found in this functional via sewing with the corresponding functions that correspond to a functional directly defined with the characteristics of the sown functional.

THE FINAL SOWN FUNCTIONAL

The next step is to insert the currents from Equation (3.142) into Equation (3.145), which leads to

$$\exp\left(\frac{1}{2}\int_{C}d\omega_{x}'d\omega_{y}'W^{-1}(\omega_{x}',\omega_{y}',\gamma_{1},\gamma_{2})\left[SS(\omega_{x}',\omega_{y}')+SB(\omega_{x}',\omega_{y}')+BB(\omega_{x}',\omega_{y}')\right]\right),\tag{3.156}$$

where we have already grouped up all the terms that will become spin-spin terms in $SS(\omega_x',\omega_y')$, the ones that will become spin-boundary ones in $SB(\omega_x',\omega_y')$ and the ones regarding boundary-boundary terms in $BB(\omega_x',\omega_y')$. The explicit expressions of these kernels are

$$SS(\omega_{x}', \omega_{y}') = \frac{1}{4\pi^{2}} \int_{D} d\omega_{y} \int_{D} d\omega_{y}''$$

$$\left(\sum_{i} s_{i,1} \frac{K(\omega_{y}', \gamma_{1}(\omega_{y}))}{\omega_{i,1} - \omega_{y}} \frac{c_{1}\omega_{i,1} + d_{1}}{c_{1}\omega_{y} + d_{1}} + \sum_{j} s_{j,2} \frac{K(\omega_{y}', \gamma_{2}(\omega_{y}))}{\omega_{j,2} - \omega_{y}} \frac{c_{2}\omega_{j,2} + d_{2}}{c_{2}\omega_{y} + d_{2}} \right)$$

$$\left(\sum_{k} s_{k,1} \frac{K(\omega_{x}', \gamma_{1}(\omega_{y}''))}{\omega_{k,1} - \omega_{y}''} \frac{c_{1}\omega_{k,1} + d_{1}}{c_{1}\omega_{y}'' + d_{1}} + \sum_{l} s_{l,2} \frac{K(\omega_{x}', \gamma_{2}(\omega_{y}''))}{\omega_{l,2} - \omega_{y}''} \frac{c_{2}\omega_{l,2} + d_{2}}{c_{2}\omega_{y}'' + d_{2}} \right),$$
(3.157)

$$SB(\omega_{x}', \omega_{y}') = -\frac{1}{8\pi^{3}} \int_{\overline{D}} d\omega_{x}'' \int_{D} d\omega_{y}$$

$$\left(\sum_{i} s_{i,1} \frac{K(\omega_{y}', \gamma_{1}(\omega_{y}))}{\omega_{i,1} - \omega_{y}} \frac{c_{1}\omega_{i,1} + d_{1}}{c_{1}\omega_{y} + d_{1}} + \sum_{j} s_{j,2} \frac{K(\omega_{y}', \gamma_{2}(\omega_{y}))}{\omega_{j,2} - \omega_{y}} \frac{c_{2}\omega_{j,2} + d_{2}}{c_{2}\omega_{y} + d_{2}} \right)$$

$$\left(\frac{\left(f_{1}(\gamma_{1}(\omega_{x}''))K(\omega_{x}', \gamma_{1}(\omega_{y}'')) + f_{2}(\gamma_{2}(\omega_{x}''))K(\omega_{x}', \gamma_{2}(\omega_{y}''))) \right)}{(\omega_{x}'' - \omega_{y}'')^{2}} \right)$$

$$- \frac{1}{8\pi^{3}} \int_{\overline{D}} d\omega_{x} \int_{D} d\omega_{y} \int_{D} d\omega_{y}''$$

$$\left(\sum_{k} s_{k,1} \frac{K(\omega_{x}', \gamma_{1}(\omega_{y}''))}{\omega_{k,1} - \omega_{y}''} \frac{c_{1}\omega_{k,1} + d_{1}}{c_{1}\omega_{y}'' + d_{1}} + \sum_{l} s_{l,2} \frac{K(\omega_{x}', \gamma_{2}(\omega_{y}''))}{\omega_{l,2} - \omega_{y}''} \frac{c_{2}\omega_{l,2} + d_{2}}{c_{2}\omega_{y}'' + d_{2}} \right)$$

$$\left(\frac{\left(f_{1}(\gamma_{1}(\omega_{x}))K(\omega_{y}', \gamma_{1}(\omega_{y})) + f_{2}(\gamma_{2}(\omega_{x}))K(\omega_{y}', \gamma_{2}(\omega_{y})) \right)}{(\omega_{x} - \omega_{y})^{2}} \right),$$

$$(3.158)$$

$$BB(\omega_{x}', \omega_{y}') = \frac{1}{16\pi^{4}} \int_{\overline{D}} d\omega_{x} \int_{D} d\omega_{y} \int_{\overline{D}} d\omega_{x}'' \int_{D} d\omega_{y}'' \\ \left(\frac{\left(f_{1}(\gamma_{1}(\omega_{x}''))K(\omega_{x}', \gamma_{1}(\omega_{y}'')) + f_{2}(\gamma_{2}(\omega_{x}''))K(\omega_{x}', \gamma_{2}(\omega_{y}'')) \right)}{(\omega_{x}'' - \omega_{y}'')^{2}} \right)$$

$$\left(\frac{\left(f_{1}(\gamma_{1}(\omega_{x}))K(\omega_{y}', \gamma_{1}(\omega_{y})) + f_{2}(\gamma_{2}(\omega_{x}))K(\omega_{y}', \gamma_{2}(\omega_{y})) \right)}{(\omega_{x} - \omega_{y})^{2}} \right).$$
(3.159)

To start simplifying all these terms, we will first get rid of the integral transform by defining the transformed inverse kernel \hat{W}^{-1} to be

$$\hat{W}^{-1}(\gamma_j(\omega_y''),\gamma_i(\omega_y)) = \int_C d\omega_y' d\omega_x' K(\omega_y',\gamma_i(\omega_y)) W^{-1}(\omega_x',\omega_y',\gamma_1,\gamma_2) K(\omega_x',\gamma_j(\omega_y'')), \tag{3.160}$$

such that now all the previous integrals can make use of this definition to get rid of the integrals over the domain C and where we have omitted the dependence of \hat{W}^{-1} on the original Möbius transformations for the sake of easing notation. With this definition, the spin-spin terms are simplified to

$$\frac{1}{2} \int_{C} d\omega'_{x} d\omega'_{y} W^{-1}(\omega'_{x}, \omega'_{y}, \gamma_{1}, \gamma_{2}) SS(\omega'_{x}, \omega'_{y}) =$$

$$\frac{1}{8\pi^{2}} \int_{D} d\omega_{y} \int_{D} d\omega''_{y} \left[\sum_{i,k} s_{i,1} s_{k,1} \frac{(c_{1}\omega_{i,1} + d_{1})}{(c_{1}\omega_{y} + d_{1})} \frac{(c_{1}\omega_{k,1} + d_{1})}{(c_{1}\omega''_{y} + d_{1})} \frac{\hat{W}^{-1}(\gamma_{1}(\omega''_{y}), \gamma_{1}(\omega_{y}))}{(\omega_{i,1} - \omega_{y})(\omega_{k,1} - \omega''_{y})} \right]$$

$$+ \sum_{i,l} s_{i,1} s_{l,2} \frac{(c_{1}\omega_{i,1} + d_{1})}{(c_{1}\omega_{y} + d_{1})} \frac{(c_{2}\omega_{l,2} + d_{2})}{(c_{2}\omega''_{y} + d_{2})} \frac{\hat{W}^{-1}(\gamma_{2}(\omega''_{y}), \gamma_{1}(\omega_{y}))}{(\omega_{i,1} - \omega_{y})(\omega_{l,2} - \omega''_{y})}$$

$$+ \sum_{j,k} s_{j,2} s_{k,1} \frac{(c_{2}\omega_{j,2} + d_{2})}{(c_{2}\omega_{y} + d_{2})} \frac{(c_{1}\omega_{k,1} + d_{1})}{(c_{1}\omega''_{y} + d_{1})} \frac{\hat{W}^{-1}(\gamma_{1}(\omega''_{y}), \gamma_{2}(\omega_{y}))}{(\omega_{j,2} - \omega_{y})(\omega_{k,1} - \omega''_{y})}$$

$$+ \sum_{j,l} s_{j,2} s_{l,2} \frac{(c_{2}\omega_{j,2} + d_{2})}{(c_{2}\omega_{y} + d_{2})} \frac{(c_{2}\omega_{l,2} + d_{2})}{(c_{2}\omega''_{y} + d_{2})} \frac{\hat{W}^{-1}(\gamma_{2}(\omega''_{y}), \gamma_{2}(\omega_{y}))}{(\omega_{j,2} - \omega_{y})(\omega_{l,2} - \omega''_{y})}$$

$$+ \sum_{j,l} s_{j,2} s_{l,2} \frac{(c_{2}\omega_{j,2} + d_{2})}{(c_{2}\omega_{y} + d_{2})} \frac{(c_{2}\omega_{l,2} + d_{2})}{(c_{2}\omega''_{y} + d_{2})} \frac{\hat{W}^{-1}(\gamma_{2}(\omega''_{y}), \gamma_{2}(\omega_{y}))}{(\omega_{j,2} - \omega_{y})(\omega_{l,2} - \omega''_{y})}$$

$$+ \sum_{j,l} s_{j,2} s_{l,2} \frac{(c_{2}\omega_{j,2} + d_{2})}{(c_{2}\omega_{y} + d_{2})} \frac{(c_{2}\omega_{l,2} + d_{2})}{(c_{2}\omega''_{y} + d_{2})} \frac{\hat{W}^{-1}(\gamma_{2}(\omega''_{y}), \gamma_{2}(\omega_{y}))}{(\omega_{j,2} - \omega_{y})(\omega_{l,2} - \omega''_{y})}$$

$$+ \sum_{j,l} s_{j,2} s_{l,2} \frac{(c_{2}\omega_{j,2} + d_{2})}{(c_{2}\omega_{y} + d_{2})} \frac{(c_{2}\omega_{l,2} + d_{2})}{(c_{2}\omega''_{y} + d_{2})} \frac{\hat{W}^{-1}(\gamma_{2}(\omega''_{y}), \gamma_{2}(\omega_{y}))}{(\omega_{j,2} - \omega_{y})(\omega_{l,2} - \omega''_{y})}$$

$$+ \sum_{j,l} s_{j,2} s_{l,2} \frac{(c_{2}\omega_{j,2} + d_{2})}{(c_{2}\omega''_{y} + d_{2})} \frac{(c_{2}\omega''_{y} + d_{2})}{(c_{2}\omega''_{y} + d_{2})} \frac{(c_{2}\omega$$

and if we now undo the Möbius transformations we obtain

$$\begin{split} SS(\left\{z_{i,1},s_{i,1},z_{j,2},s_{j,2}\right\}_{i,j=1}^{N_{1},N_{2}}) = & + \frac{1}{8\pi^{2}}\sum_{i,k}s_{i,1}s_{k,1}\int_{D_{1}}dy\int_{D_{1}}dy''\frac{\hat{W}^{-1}(y'',y)}{(z_{i,1}-y)(z_{k,1}-y'')} \\ & + \frac{1}{8\pi^{2}}\sum_{i,l}s_{i,1}s_{l,2}\int_{D_{1}}dy\int_{D_{2}}dy''\frac{\hat{W}^{-1}(y'',y)}{(z_{i,1}-y)(z_{l,2}-y'')} \\ & + \frac{1}{8\pi^{2}}\sum_{j,k}s_{j,2}s_{k,1}\int_{D_{2}}dy\int_{D_{1}}dy''\frac{\hat{W}^{-1}(y'',y)}{(z_{j,2}-y)(z_{k,1}-y'')} \\ & + \frac{1}{8\pi^{2}}\sum_{j,2}s_{j,2}s_{l,2}\int_{D_{2}}dy\int_{D_{2}}dy''\frac{\hat{W}^{-1}(y'',y)}{(z_{j,2}-y)(z_{l,2}-y'')}. \end{split}$$

In Equation (3.162), we see how sewing has generated all the necessary spin-spin terms. The first line corresponds to the interaction of one of the spins from \mathcal{M}_1 with the sewing boundary $\partial \mathcal{M}_S$ and with one of the \mathcal{M}_1 spins again. The fourth line corresponds to the same situation for the spins in \mathcal{M}_2 , and the second and third lines are the interactions between a spin from \mathcal{M}_1 and another one from \mathcal{M}_2 , which arises as a new interaction from the sewing procedure. To further derive the form of \hat{W}^{-1} we will compare this result with the corresponding functional constructed directly as $\mathcal{M}=\mathcal{M}_1\cup\mathcal{M}_2$, but before doing so let us also bring the rest of the terms to a form suitable for this comparison.

After using Equation (3.160) on Equation (3.158) the spin-boundary term arising from sewing simplifies down to

$$\begin{split} &\frac{1}{2} \int_{C} d\omega_{x}' d\omega_{y}' W^{-1}(\omega_{x}', \omega_{y}', \gamma_{1}, \gamma_{2}) SB(\omega_{x}', \omega_{y}') = \\ &- \frac{1}{16\pi^{3}} \int_{D} d\omega_{x}'' \int_{D} d\omega_{y}' \int_{D} d\omega_{y} \\ &\left[+ \sum_{i} s_{i,1} \frac{(c_{1}\omega_{i,1} + d_{1})}{(c_{1}\omega_{y} + d_{1})} \frac{f_{1}(\gamma_{1}(\omega_{x}''))}{(\omega_{i,1} - \omega_{y})} \frac{(\hat{W}^{-1}(\gamma_{1}(\omega_{y}''), \gamma_{1}(\omega_{y})) + \hat{W}^{-1}(\gamma_{1}(\omega_{y}), \gamma_{1}(\omega_{y}')))}{(\omega_{x}'' - \omega_{y}'')^{2}} \right. \\ &+ \sum_{i} s_{i,1} \frac{(c_{1}\omega_{i,1} + d_{1})}{(c_{1}\omega_{y} + d_{1})} \frac{f_{2}(\gamma_{2}(\omega_{x}''))}{(\omega_{i,1} - \omega_{y})} \frac{(\hat{W}^{-1}(\gamma_{2}(\omega_{y}''), \gamma_{1}(\omega_{y})) + \hat{W}^{-1}(\gamma_{1}(\omega_{y}), \gamma_{2}(\omega_{y}')))}{(\omega_{x}'' - \omega_{y}'')^{2}} \\ &+ \sum_{j} s_{j,2} \frac{(c_{2}\omega_{j,2} + d_{2})}{(c_{2}\omega_{y} + d_{2})} \frac{f_{1}(\gamma_{1}(\omega_{x}''))}{(\omega_{j,2} - \omega_{y})} \frac{(\hat{W}^{-1}(\gamma_{1}(\omega_{y}''), \gamma_{2}(\omega_{y})) + \hat{W}^{-1}(\gamma_{2}(\omega_{y}), \gamma_{1}(\omega_{y}'')))}{(\omega_{x}'' - \omega_{y}'')^{2}} \\ &+ \sum_{j} s_{j,2} \frac{(c_{2}\omega_{j,2} + d_{2})}{(c_{2}\omega_{y} + d_{2})} \frac{f_{2}(\gamma_{2}(\omega_{x}''))}{(\omega_{j,2} - \omega_{y})} \frac{(\hat{W}^{-1}(\gamma_{2}(\omega_{y}''), \gamma_{2}(\omega_{y})) + \hat{W}^{-1}(\gamma_{2}(\omega_{y}), \gamma_{2}(\omega_{y}')))}{(\omega_{x}'' - \omega_{y}'')^{2}} \right]. \end{aligned} \tag{3.163}$$

which after undoing the corresponding Möbius transformations the result is

$$\begin{split} SB[\left\{z_{i,1},s_{i,1},z_{j,2},s_{j,2}\right\}_{i,j=1}^{N_{1},N_{2}},f_{1},f_{2}] = \\ &-\frac{1}{16\pi^{3}}\sum_{i}s_{i,1}\int_{\overline{D}_{1}}dx''\int_{D_{1}}dy''\int_{D_{1}}dy\frac{f_{1}(x'')}{z_{i,1}-y}\frac{(\hat{W}^{-1}(y'',y)+\hat{W}^{-1}(y,y''))}{(x''-y'')^{2}} \\ &-\frac{1}{16\pi^{3}}\sum_{i}s_{i,1}\int_{\overline{D}_{2}}dx''\int_{D_{2}}dy''\int_{D_{1}}dy\frac{f_{2}(x'')}{z_{i,1}-y}\frac{(\hat{W}^{-1}(y'',y)+\hat{W}^{-1}(y,y''))}{(x''-y'')^{2}} \\ &-\frac{1}{16\pi^{3}}\sum_{j}s_{j,2}\int_{\overline{D}_{1}}dx''\int_{D_{1}}dy''\int_{D_{2}}dy\frac{f_{1}(x'')}{z_{j,2}-y}\frac{(\hat{W}^{-1}(y'',y)+\hat{W}^{-1}(y,y''))}{(x''-y'')^{2}} \\ &-\frac{1}{16\pi^{3}}\sum_{j}s_{j,2}\int_{\overline{D}_{2}}dx''\int_{D_{2}}dy''\int_{D_{2}}dy\frac{f_{2}(x'')}{z_{j,2}-y}\frac{(\hat{W}^{-1}(y'',y)+\hat{W}^{-1}(y,y''))}{(x''-y'')^{2}} \end{split}$$

As before, we can interpret both first(last) lines as the interactions between the spins in $\mathcal{M}_{1(2)}$ with the final boundary function index $f_{1(2)}$ that originally came from the same functional. Therefore, the second and third lines correspond to the interaction between the spins on $\mathcal{M}_{1(2)}$ with the leftover boundary function of $\mathcal{M}_{2(1)}$. Lastly, the

boundary-boundary term becomes

$$\begin{split} &\frac{1}{2} \int_{C} d\omega_{x}' d\omega_{y}' W^{-1}(\omega_{x}', \omega_{y}', \gamma_{1}, \gamma_{2}) BB(\omega_{x}', \omega_{y}') = \\ &+ \frac{1}{32\pi^{4}} \int_{\overline{D}} d\omega_{x} \int_{D} d\omega_{y} \int_{\overline{D}} d\omega_{x}'' \int_{\overline{D}} d\omega_{y}'' \frac{1}{(\omega_{x}'' - \omega_{y}'')^{2}} \frac{1}{(\omega_{x} - \omega_{y})^{2}} \\ & \left(f_{1}(\gamma_{1}(\omega_{x}'')) f_{1}(\gamma_{1}(\omega_{x})) \hat{W}^{-1}(\gamma_{1}(\omega_{y}''), \gamma_{1}(\omega_{y})) + f_{1}(\gamma_{1}(\omega_{x}'')) f_{2}(\gamma_{2}(\omega_{x})) \hat{W}^{-1}(\gamma_{1}(\omega_{y}''), \gamma_{2}(\omega_{y})) \\ & f_{2}(\gamma_{2}(\omega_{x}'')) f_{1}(\gamma_{1}(\omega_{x})) \hat{W}^{-1}(\gamma_{2}(\omega_{y}''), \gamma_{1}(\omega_{y})) + f_{2}(\gamma_{2}(\omega_{x}'')) f_{2}(\gamma_{2}(\omega_{x})) \hat{W}^{-1}(\gamma_{2}(\omega_{y}''), \gamma_{2}(\omega_{y})) \right). \end{split} \tag{3.165}$$

and as before, undoing the Möbius transformations yields

$$BB[f_{1}, f_{2}] = +\frac{1}{32\pi^{4}} \int_{\overline{D}_{1}} dx \int_{D_{1}} dy \int_{\overline{D}_{1}} dx'' \int_{D_{1}} dy'' \frac{f_{1}(x'')\hat{W}^{-1}(y'', y)f_{1}(x)}{(x'' - y'')^{2}(x - y)^{2}}$$

$$+\frac{1}{32\pi^{4}} \int_{\overline{D}_{2}} dx \int_{D_{2}} dy \int_{\overline{D}_{1}} dx'' \int_{D_{1}} dy'' \frac{f_{1}(x'')\hat{W}^{-1}(y'', y)f_{2}(x)}{(x'' - y'')^{2}(x - y)^{2}}$$

$$+\frac{1}{32\pi^{4}} \int_{\overline{D}_{1}} dx \int_{D_{1}} dy \int_{\overline{D}_{2}} dx'' \int_{D_{2}} dy'' \frac{f_{2}(x'')\hat{W}^{-1}(y'', y)f_{1}(x)}{(x'' - y'')^{2}(x - y)^{2}}$$

$$+\frac{1}{32\pi^{4}} \int_{\overline{D}_{2}} dx \int_{D_{2}} dy \int_{\overline{D}_{2}} dx'' \int_{D_{2}} dy'' \frac{f_{2}(x'')\hat{W}^{-1}(y'', y)f_{2}(x)}{(x'' - y'')^{2}(x - y)^{2}}$$

$$(3.166)$$

As in the previous terms, the first and last term corresponds to the self-interaction of the leftover boundary functions $f_{1(2)}$ from $\mathcal{M}_{1(2)}$ through the one that was sowed in $\partial \mathcal{M}_S$. The second and third correspond then to the new interaction between the leftover indices of each of the original manifolds, such that the final manifold $\mathcal{M} = \mathcal{M}_1 \cup \mathcal{M}_2$ contains interactions between the functions on its entire boundary $\partial \mathcal{M}$.

We have finally collected and simplified all the terms that have arisen from the sewing integral, and we can, therefore, bring back the non-sewing participating terms that we grouped in the constants $\mathcal{B}^c_{\mathbb{H},\overline{D}_1}$ and $\mathcal{B}^c_{\mathbb{H},\overline{D}_2}$ at the very beginning of the computation to obtain the final result of the chiral sown amplitude

$$\begin{split} \mathcal{A}^{c}_{\mathbb{H}_{\text{sw}}}[f_{1},f_{2},\left\{z_{i,1},s_{i,1},z_{j,2},s_{j,2}\right\}_{i,j=1}^{N_{1},N_{2}}] &= \exp\left(SS_{\text{sw}}[\left\{z_{i,1},s_{i,1},z_{j,2},s_{j,2}\right\}_{i,j=1}^{N_{1},N_{2}}]\right. \\ &\left. + SB_{\text{sw}}[\left\{\omega_{i,1},s_{i,1},\omega_{j,2},s_{j,2}\right\}_{i,j=1}^{N_{1},N_{2}},f_{1},f_{2}]\right. \\ &\left. + BB_{\text{sw}}[f_{1},f_{2}]\right) \end{split} \tag{3.167}$$

where each of the terms is given by

$$\begin{split} SS_{\text{sw}}[\left\{z_{i,1}, s_{i,1}, z_{j,2}, s_{j,2}\right\}_{i,j=1}^{N_1,N_2}] = \\ &+ \frac{1}{2} \sum_{i,k} s_{i,1} s_{k,1} \left(\log\left[z_{i,1} - z_{k,1}\right] + \frac{1}{4\pi^2} \int_{D_1} dy \int_{D_1} dy'' \frac{\hat{W}^{-1}(y'',y)}{(z_{i,1} - y)(z_{k,1} - y'')}\right) \\ &+ \frac{1}{2} \sum_{i,l} s_{i,1} s_{l,2} \frac{1}{4\pi^2} \int_{D_1} dy \int_{D_2} dy'' \frac{(\hat{W}^{-1}(y'',y) + \hat{W}^{-1}(y,y''))}{(z_{i,1} - y)(z_{l,2} - y'')} \\ &+ \frac{1}{2} \sum_{j,2} s_{j,2} s_{l,2} \left(\log\left[z_{j,2} - z_{l,2}\right] + \frac{1}{4\pi^2} \int_{D_2} dy \int_{D_2} dy'' \frac{\hat{W}^{-1}(y'',y)}{(z_{j,2} - y)(z_{l,2} - y'')}\right), \end{split}$$

$$\begin{split} SB_{\text{sw}}[\left\{z_{i,1},s_{i,1},z_{j,2},s_{j,2}\right\}_{i,j=1}^{N_{1},N_{2}},f_{1},f_{2}] = \\ &-\frac{1}{2\pi}\sum_{i}s_{i,1}\int_{D_{1}}dx''f_{1}(x'')\left[\frac{1}{z_{i,1}-x''}+\frac{1}{8\pi^{2}}\int_{D_{1}}dy''\int_{D_{1}}dy\frac{1}{z_{i,1}-y}\frac{(\hat{W}^{-1}(y'',y)+\hat{W}^{-1}(y,y''))}{(x''-y'')^{2}}\right] \\ &-\frac{1}{16\pi^{3}}\sum_{i}s_{i,1}\int_{D_{2}}dx''\int_{D_{2}}dy''\int_{D_{1}}dy\frac{f_{2}(x'')}{z_{i,1}-y}\frac{(\hat{W}^{-1}(y'',y)+\hat{W}^{-1}(y,y''))}{(x''-y'')^{2}} \\ &-\frac{1}{16\pi^{3}}\sum_{j}s_{j,2}\int_{D_{1}}dx''\int_{D_{1}}dy''\int_{D_{2}}dy\frac{f_{1}(x'')}{z_{j,2}-y}\frac{(\hat{W}^{-1}(y'',y)+\hat{W}^{-1}(y,y''))}{(x''-y'')^{2}} \\ &-\frac{1}{2\pi}\sum_{j}s_{j,2}\int_{D_{2}}dx''f_{2}(x'')\left[\frac{1}{z_{j,2}-x''}+\frac{1}{8\pi^{2}}\int_{D_{2}}dy''\int_{D_{2}}dy\frac{1}{z_{j,2}-y}\frac{(\hat{W}^{-1}(y'',y)+\hat{W}^{-1}(y,y''))}{(x''-y'')^{2}}\right], \end{split}$$

and

$$\begin{split} &BB_{\text{sw}}[f_{1},f_{2}] = \\ &+ \frac{1}{8\pi^{2}} \int_{\overline{D}_{1}} dx \int_{\overline{D}_{1}} dx'' f_{1}(x'') f_{1}(x) \left[\frac{1}{(x''-x)^{2}} + \frac{1}{4\pi^{2}} \int_{D_{1}} dy'' \int_{D_{1}} dy \frac{\hat{W}^{-1}(y'',y)}{(x''-y'')^{2}(x-y)^{2}} \right] \\ &+ \frac{1}{32\pi^{4}} \int_{\overline{D}_{2}} dx \int_{D_{2}} dy \int_{\overline{D}_{1}} dx'' \int_{D_{1}} dy'' \frac{f_{1}(x'')(\hat{W}^{-1}(y'',y) + \hat{W}^{-1}(y,y'')) f_{2}(x)}{(x''-y'')^{2}(x-y)^{2}} \\ &+ \frac{1}{8\pi^{2}} \int_{\overline{D}_{2}} dx \int_{\overline{D}_{2}} dx'' f_{2}(x'') f_{2}(x) \left[\frac{1}{(x''-x)^{2}} + \frac{1}{4\pi^{2}} \int_{D_{2}} dy \int_{D_{2}} dy'' \frac{\hat{W}^{-1}(y'',y)}{(x''-y'')^{2}(x-y)^{2}} \right]. \end{split} \tag{3.170}$$

Equation (3.167) alongside Equations (3.168)-(3.170) is the resulting new tensor that arises from an arbitrary exact contraction.

COMPARISON AGAINST AN EQUIVALENT UNSOWN FUNCTIONAL

Within these expressions, we have assumed the existence of the kernel \hat{W}^{-1} , which we will now attempt to find. As we have mentioned before, we will do so by comparing the result of the tensor arising from sewing against a tensor defined directly in the final manifold $\mathcal{M}=\mathcal{M}_1\cup\mathcal{M}_2$ with spin density corresponding to $\rho=\rho_1+\rho_2$, which fixes both their values s_i and positions z_i to be the ones of the original manifolds.

Because we choose the spin positions to be the same in the coordinate system of the original manifolds, their image in the UHP under the respective conformal maps will be different because $g_1(z_{i,1}) \neq g(z_{i,1})$. We will denote the spin positions in the UHP obtained via the conformal map that defines the final tensor g(z), by $g(z_{i,j}) = \mu_{i,j}$, and the ones obtained via the conformal maps of the pre-sewing manifolds by $g_j(z_{i,j}) = \beta_{i,j}$. A similar situation is found for the notation of the unsown boundary functions f_1, f_2 of the original manifolds, where they will be compared against the functions of the final tensor h_1, h_2 that are defined in the same parts of the boundary as the originals, but whose image in the UHP will be different. Figure 3.8 showcases these identifications and notations.

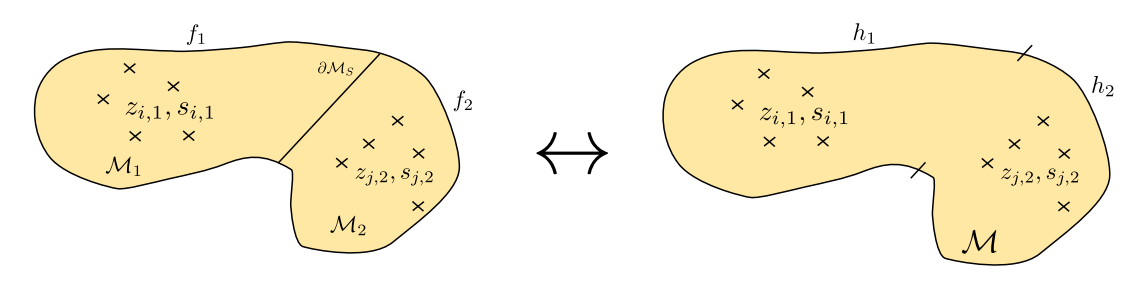


Figure 3.8: Diagrammatic showcase of the notation used for the comparison between the result of sewing two tensors and the final tensor.

We begin by first writing the UHP tensor of the final amplitude in this notation as

$$\begin{split} \mathcal{A}^{c}_{\mathbb{H}_{\text{final}}} \left[h_{1}, h_{2}, \{\mu_{i}, s_{i}\}_{i=1}^{N} \right] &= \exp\left(+ \frac{1}{2} \sum_{i,j} s_{i} s_{j} \left(\log\left[(\mu_{i} - \mu_{j}) \right] \right) \right. \\ &\left. - \frac{1}{2\pi} \sum_{i} s_{i} \left(\int_{D_{f}} dy h_{1}(y) \frac{1}{\mu_{i} - y} + \int_{\overline{D_{f}}} dy h_{2}(y) \frac{1}{\mu_{i} - y} \right) \right. \\ &\left. + \frac{1}{8\pi^{2}} \int_{\overline{D_{f}}} dx \int_{\overline{D_{f}}} dy h_{2}(x) h_{2}(y) \frac{1}{(x - y)^{2}} + \frac{1}{4\pi^{2}} \int_{\overline{D_{f}}} dx \int_{D_{f}} dy h_{2}(x) h_{1}(y) \frac{1}{(x - y)^{2}} \right. \\ &\left. + \frac{1}{8\pi^{2}} \int_{D_{f}} dx \int_{D_{f}} dy h_{1}(x) h_{1}(y) \frac{1}{(x - y)^{2}} \right), \end{split} \tag{3.171}$$

where $D_f=g(\partial\mathcal{M}_1)$ and $\overline{D_f}=g(\partial\mathcal{M}_2)$. We can further split the sum over the spin indices as $\sum_{i=1}^N s_i = \sum_{i=1}^{N_1} s_{i,1} + \sum_{k=1}^{N_2} s_{k,2}$, such that each sum corresponds to the spins originating from \mathcal{M}_1 or \mathcal{M}_2 . After this split, we demand that

$$\mathcal{A}^{c}_{\mathbb{H}_{\text{sw}}}[f_{1}, f_{2}, \left\{\beta_{i,1}, s_{i,1}, \beta_{j,2}, s_{j,2}\right\}_{i,j=1}^{N_{1},N_{2}}] = \mathcal{A}^{c}_{\mathbb{H}_{\text{final}}}\left[h_{1}, h_{2}, \left\{\mu_{i}, s_{i}\right\}_{i=1}^{N}\right], \tag{3.172}$$

which will provide the necessary constraints to extract the unknown kernel \hat{W}^{-1} . We will begin identifying terms by first comparing the spin-spin terms of both sides.

The spin-spin term coming from the final amplitude is given by

$$\begin{split} &+\frac{1}{2}\sum_{i,j=1}^{N}s_{i}s_{j}\log\left[(\mu_{i}-\mu_{j})\right] = +\frac{1}{2}\sum_{i,j=1}^{N_{1}}s_{i,1}s_{j,1}\log\left[(\mu_{i,1}-\mu_{j,1})\right] \\ &+\frac{1}{2}\sum_{i,j=1}^{N_{2}}s_{i,2}s_{j,2}\log\left[(\mu_{i,2}-\mu_{j,2})\right] + \sum_{i,j=1}^{N_{1},N_{2}}s_{i,1}s_{j,2}\log\left[(\mu_{i,1}-\mu_{j,2})\right] + \frac{1}{2}\sum_{i,j=1}^{N_{1},N_{2}}s_{i,1}s_{j,2}(i\pi) \end{split} \tag{3.173}$$

where the last term is a spin-dependent phase factor that factorizes to the front of the exponential. The spin-spin terms from the resulting sewing tensor are given in Equation (3.168). We then start by equating the terms that multiply the sum that includes the spins from \mathcal{M}_1 , which yields

$$\log \left[\frac{\mu_{i,1} - \mu_{j,1}}{\beta_{i,1} - \beta_{j,1}} \right] = \frac{1}{4\pi^2} \int_{D_1} dy \int_{D_1} dy'' \frac{\hat{W}^{-1}(y'',y)}{(\beta_{i,1} - y)(\beta_{j,1} - y'')}, \tag{3.174}$$

where if we restore the dependence on the original spin coordinates via the conformal transformations g_1 and g, we obtain

$$\log \left[\frac{g(z_{i,1}) - g(z_{j,1})}{g_1(z_{i,1}) - g_1(z_{j,1})} \right] = \frac{1}{4\pi^2} \int_{D_1} dy \int_{D_1} dy'' \frac{\hat{W}^{-1}(y'', y)}{(g_1(z_{i,1}) - y)(g_1(z_{j,1}) - y'')}. \tag{3.175}$$

This is the first equation that provides us with information for obtaining \hat{W}^{-1} , and by equating the terms that arise from the products of spins from \mathcal{M}_2 on both sides of Equation (3.172) we obtain a similar condition

$$\log \left[\frac{g(z_{i,2}) - g(z_{j,2})}{g_2(z_{i,2}) - g_2(z_{j,2})} \right] = \frac{1}{4\pi^2} \int_{D_2} dy \int_{D_2} dy'' \frac{\hat{W}^{-1}(y'', y)}{(g_2(z_{i,2}) - y)(g_2(z_{j,2}) - y'')}. \tag{3.176}$$

When comparing the terms that correspond to the spin-spin interaction between \mathcal{M}_1 and \mathcal{M}_2 , we obtain the condition

$$\log\left[g(z_{i,1})-g(z_{j,2})\right] = \frac{1}{8\pi^2} \int_{D_1} dy \int_{D_2} dy'' \frac{\hat{W}^{-1}(y'',y)+\hat{W}^{-1}(y,y'')}{(g_1(z_{i,1})-y)(g_2(z_{j,2})-y'')}. \tag{3.177}$$

These three equations already provide us with means for obtaining \hat{W}^{-1} , but let us first find the rest of the equalities by exploring the spin-boundary and boundary-boundary terms.

Let us begin with the boundary-boundary terms, where the terms coming from the final tensor on the r.h.s of Equation (3.172) are given in the UHP by

$$\begin{split} &+\frac{1}{8\pi^2}\int_{D_f}dx\int_{D_f}dy h_2(x)h_2(y)\frac{1}{(x-y)^2}+\frac{1}{4\pi^2}\int_{D_f}dx\int_{D_f}dy h_2(x)h_1(y)\frac{1}{(x-y)^2}\\ &+\frac{1}{8\pi^2}\int_{D_f}dx\int_{D_f}dy h_1(x)h_1(y)\frac{1}{(x-y)^2}, \end{split} \tag{3.178}$$

and this expression should be equated term-by-term against Equation (3.170). However, the integrals on both sides pertain to different subdomains of $\mathbb R$, and therefore, these expressions need to be sent to the same "gauge" through more Möbius transformations. If we denote by $\gamma_1(D_f) = \overline{D}_1, \gamma_1(\overline{D}_f) = D_1$ and $\gamma_2(\overline{D}_f) = \overline{D}_2, \gamma_2(D_f) = D_2$

such that $x(y) = \gamma_i(\omega_{x(y)})$, then Equation (3.170) becomes

$$\begin{split} BB_{\text{sw}}[f_{1},f_{2}] &= \\ &+ \frac{1}{8\pi^{2}} \int_{D_{f}} d\omega_{x} \int_{D_{f}} d\omega_{x}'' f_{1}(\gamma_{1}(\omega_{x}'')) f_{1}(\gamma_{1}(\omega_{x})) \left[\frac{1}{(\omega_{x}'' - \omega_{x})^{2}} \right. \\ &+ \frac{1}{4\pi^{2}} \int_{D_{f}} d\omega_{y}'' \int_{D_{f}} d\omega_{y} \frac{\hat{W}^{-1}(\gamma_{1}(\omega_{y}''), \gamma_{1}(\omega_{y}))}{(\omega_{x}'' - \omega_{y}'')^{2}(\omega_{x} - \omega_{y})^{2}} \right] \\ &+ \frac{1}{32\pi^{4}} \int_{D_{f}} d\omega_{x} \int_{D_{f}} d\omega_{x}'' f_{1}(\gamma_{1}(\omega_{x}'')) f_{2}(\gamma_{2}(\omega_{x})) \\ &\int_{D_{f}} d\omega_{y}'' \int_{D_{f}} d\omega_{y} \frac{(\hat{W}^{-1}(\gamma_{1}(\omega_{y}''), \gamma_{2}(\omega_{y})) + \hat{W}^{-1}(\gamma_{2}(\omega_{y}), \gamma_{1}(\omega_{y}'')))}{(\omega_{x}'' - \omega_{y}'')^{2}(\omega_{x} - \omega_{y})^{2}} \\ &+ \frac{1}{8\pi^{2}} \int_{D_{f}} d\omega_{x} \int_{D_{f}} d\omega_{x}'' \frac{\hat{W}^{-1}(\gamma_{2}(\omega_{x}'')) f_{2}(\gamma_{2}(\omega_{x}))}{(\omega_{x}'' - \omega_{y}'')^{2}(\omega_{x} - \omega_{y})^{2}} \\ &+ \frac{1}{4\pi^{2}} \int_{D_{f}} d\omega_{y} \int_{D_{f}} d\omega_{y}'' \frac{\hat{W}^{-1}(\gamma_{2}(\omega_{y}''), \gamma_{2}(\omega_{y}))}{(\omega_{x}'' - \omega_{y}'')^{2}(\omega_{x} - \omega_{y})^{2}} \right]. \end{split}$$

Now, we can start comparing the terms within the integrals individually. Comparing first the terms with integrals over D_f , we obtain

$$h_1(x)h_1(y) = f_1(\gamma_1(x))f_1(\gamma_1(y)) \left[1 + \frac{1}{4\pi^2} \int_{\overline{D}_f} d\omega_y'' \int_{\overline{D}_f} d\omega_y \frac{(x-y)^2 \hat{W}^{-1}(\gamma_1(\omega_y''), \gamma_1(\omega_y))}{(x-\omega_y'')^2 (y-\omega_y)^2} \right] \tag{3.180}$$

which allows us to infer the behavior of the integral found within the brackets in Equation (3.180). Because the product of Schwarz functions is again Schwarz and the l.h.s is one such product, the r.h.s must be Schwarz again. Therefore, whatever function arises from the integral in the bracket must result in a function that does not spoil the product f_1f_1 from being Schwarz. Thus, it must be a bounded smooth function with bounded derivatives.

Analyzing the terms that go with the integrals over \overline{D}_f , we obtain a similar expression

$$h_2(x)h_2(y) = f_2(\gamma_2(x))f_1(\gamma_2(y)) \left[1 + \frac{1}{4\pi^2} \int_{D_f} d\omega_y'' \int_{D_f} d\omega_y \frac{(x-y)^2 \hat{W}^{-1}(\gamma_2(\omega_y''), \gamma_2(\omega_y))}{(x-\omega_y'')^2 (y-\omega_y)^2} \right] \tag{3.181}$$

and comparing the crossed-terms we obtain

$$\begin{split} h_1(x)h_2(y) = & \frac{f_1(\gamma_1(x))f_2(\gamma_2(y))}{8\pi^2} \\ & \int_{\overline{D}_f} d\omega_y'' \int_{D_f} d\omega_y \frac{(x-y)^2(\hat{W}^{-1}(\gamma_1(\omega_y''),\gamma_2(\omega_y)) + \hat{W}^{-1}(\gamma_2(\omega_y),\gamma_1(\omega_y'')))}{(x-\omega_y'')^2(y-\omega_y)^2}, \end{split} \tag{3.182}$$

which concludes the comparisons on the boundary-boundary terms.

All that is left are the spin-boundary terms, which are the most complicated as they are not gauge-invariant due to the chiral truncation. The terms arising from the r.h.s

of Equation (3.172) are given by

$$\begin{split} &-\frac{1}{2\pi}\sum_{i=1}^{N_1}s_{i,1}\left(\int_{D_f}dy h_1(y)\frac{1}{\mu_{i,1}-y}+\int_{\overline{D_f}}dy h_2(y)\frac{1}{\mu_{i,1}-y}\right)\\ &-\frac{1}{2\pi}\sum_{i=1}^{N_2}s_{i,2}\left(\int_{D_f}dy h_1(y)\frac{1}{\mu_{i,2}-y}+\int_{\overline{D_f}}dy h_2(y)\frac{1}{\mu_{i,2}-y}\right), \end{split} \tag{3.183}$$

and the corresponding terms from the l.h.s of Equation (3.172) are the ones found in Equation (3.169). As with the boundary-boundary terms, we can not start equating terms because all the integrals are defined over different subdomains of \mathbb{R} due to the different conformal maps. Using the same conformal maps as before, we can rewrite Equation (3.169) in the gauge of Equation (3.183) as

$$\begin{split} SB_{\text{SW}}[\left\{\omega_{i,1}, s_{i,1}, \omega_{j,2}, s_{j,2}\right\}_{i,j=1}^{N_{1},N_{2}}, f_{1}, f_{2}] = \\ &-\frac{1}{2\pi}\sum_{i} s_{i,1} \int_{D_{f}} d\omega_{x}'' f_{1}(\gamma_{1}(\omega_{x}'')) \left[\frac{(c_{1}\omega_{i,1} + d_{1})}{(\omega_{i,1} - \omega_{x}'')(c_{1}\omega_{x}'' + d_{1})} + \right. \\ &\frac{1}{8\pi^{2}} \int_{\overline{D}_{f}} d\omega_{y}'' \int_{\overline{D}_{f}} d\omega_{y} \frac{(c_{1}\omega_{i,1} + d_{1})(\hat{W}^{-1}(\gamma_{1}(\omega_{y}''), \gamma_{1}(\omega_{y})) + \hat{W}^{-1}(\gamma_{1}(\omega_{y}), \gamma_{1}(\omega_{y}')))}{(\omega_{i,1} - \omega_{y})(c_{1}\omega_{y} + d_{1})(\omega_{x}'' - \omega_{y}'')^{2}} \right] \\ &- \frac{1}{16\pi^{3}} \sum_{i} s_{i,1} \int_{\overline{D}_{f}} d\omega_{x}'' f_{2}(\gamma_{2}(\omega_{x}'')) \\ &\int_{D_{f}} d\omega_{y}'' \int_{\overline{D}_{f}} d\omega_{y} \frac{(c_{1}\omega_{i,1} + d_{1})(\hat{W}^{-1}(\gamma_{2}(\omega_{y}''), \gamma_{1}(\omega_{y})) + \hat{W}^{-1}(\gamma_{1}(\omega_{y}), \gamma_{2}(\omega_{y}'')))}{(\omega_{i,1} - \omega_{y})(c_{1}\omega_{y} + d_{1})(\omega_{x}'' - \omega_{y}'')^{2}} \\ &- \frac{1}{16\pi^{3}} \sum_{j} s_{j,2} \int_{D_{f}} d\omega_{x}'' f_{1}(\gamma_{1}(\omega_{x}'')) \\ &\int_{\overline{D}_{f}} d\omega_{y}'' \int_{D_{f}} d\omega_{y} \frac{(c_{2}\omega_{j,2} + d_{2})(\hat{W}^{-1}(\gamma_{1}(\omega_{y}''), \gamma_{2}(\omega_{y})) + \hat{W}^{-1}(\gamma_{2}(\omega_{y}), \gamma_{1}(\omega_{y}'')))}{(\omega_{j,2} - \omega_{y})(c_{2}\omega_{y} + d_{2})(\omega_{x}'' - \omega_{y}'')^{2}} \\ &- \frac{1}{2\pi} \sum_{j} s_{j,2} \int_{\overline{D}_{f}} d\omega_{x}'' f_{2}(\gamma_{2}(\omega_{x}'')) \left[\frac{(c_{2}\omega_{j,2} + d_{2})}{(\omega_{j,2} - \omega_{x}'')(c_{2}\omega_{x}'' + d_{2})} + \\ \frac{1}{8\pi^{2}} \int_{D_{f}} d\omega_{y}'' \int_{D_{f}} d\omega_{y} \frac{(c_{2}\omega_{j,2} + d_{2})(\hat{W}^{-1}(\gamma_{2}(\omega_{y}''), \gamma_{2}(\omega_{y})) + \hat{W}^{-1}(\gamma_{2}(\omega_{y}), \gamma_{2}(\omega_{y}')))}{(z\omega_{j,2} - \omega_{y})(c_{2}\omega_{y} + d_{2})(\omega_{x}'' - \omega_{y}'')^{2}} \right], \tag{3.184} \end{split}$$

which is an expression ready for comparison. Comparing first the terms multiplying the $s_{i,1}$ and running along D_f one obtains

$$\begin{split} h_1(y) &= f_1(\gamma_1(y)) \left[\frac{(\mu_{i,1} - y)(c_1\omega_{i,1} + d_1)}{(\omega_{i,1} - y)(c_1y + d_1)} + \right. \\ &\left. \frac{1}{8\pi^2} \int_{D_f} d\omega_y'' \int_{D_f} d\omega_y \frac{(c_1\omega_{i,1} + d_1)(\mu_{i,1} - y)}{(\omega_{i,1} - \omega_y)(c_1\omega_y + d_1)} \frac{(\hat{W}^{-1}(\gamma_1(\omega_y''), \gamma_1(\omega_y)) + \hat{W}^{-1}(\gamma_1(\omega_y), \gamma_1(\omega_y'')))}{(y - \omega_y'')^2} \right] \end{split}$$

which is a priori a surprising expression. The surprise stems from the fact that the resulting boundary function seems to depend on the spin positions through the gauge

transformations. This is, however, a consequence of the chiral truncation, as this phenomenon can already be seen in the gauge transformations shown in Equation (3.54). Equating now the terms that go with $s_{i,1}$ and \overline{D}_f one gets

$$h_{2}(y) = \frac{1}{8\pi^{2}} f_{2}(\gamma_{2}(y))$$

$$\int_{D_{f}} d\omega_{y}'' \int_{\overline{D}_{f}} d\omega_{y} \frac{(\mu_{i,1} - y)(c_{1}\omega_{i,1} + d_{1})(\hat{W}^{-1}(\gamma_{2}(\omega_{y}''), \gamma_{1}(\omega_{y})) + \hat{W}^{-1}(\gamma_{1}(\omega_{y}), \gamma_{2}(\omega_{y}'')))}{(\omega_{i,1} - \omega_{y})(c_{1}\omega_{y} + d_{1})(y - \omega_{y}'')^{2}},$$
(3.186)

which again has a phenomenology similar to the last term. The final two comparisons yield

$$h_{1}(y) = \frac{1}{8\pi^{2}} f_{1}(\gamma_{1}(y))$$

$$\int_{\overline{D}_{f}} d\omega_{y}'' \int_{D_{f}} d\omega_{y} \frac{(\mu_{i,2} - y)(c_{2}\omega_{j,2} + d_{2})(\hat{W}^{-1}(\gamma_{1}(\omega_{y}''), \gamma_{2}(\omega_{y})) + \hat{W}^{-1}(\gamma_{2}(\omega_{y}), \gamma_{1}(\omega_{y}'')))}{(\omega_{j,2} - \omega_{y})(c_{2}\omega_{y} + d_{2})(y - \omega_{y}'')^{2}},$$
(3.187)

and

$$\begin{split} h_2(y) &= f_2(\gamma_2(y)) \left[\frac{(\mu_{j,2} - y)(c_2\omega_{j,2} + d_2)}{(\omega_{j,2} - y)(c_2y + d_2)} + \right. \\ &\left. \frac{1}{8\pi^2} \int_{D_f} d\omega_y'' \int_{D_f} d\omega_y \frac{(c_2\omega_{j,2} + d_2)(\mu_{j,2} - y)}{(\omega_{j,2} - \omega_y)(c_2\omega_y + d_2)} \frac{(\hat{W}^{-1}(\gamma_2(\omega_y''), \gamma_2(\omega_y)) + \hat{W}^{-1}(\gamma_2(\omega_y'), \gamma_2(\omega_y'')))}{(y - \omega_y'')^2} \right]. \end{split} \tag{3.188}$$

Because all of these equations must be valid simultaneously we can equate either Equations (3.185) and (3.187) or (3.186) and (3.188) to extract more constraints on \hat{W}^{-1} . These constraints can then be supplemented with even more constraints arising from the comparisons from the boundary-boundary terms from Equations (3.180),(3.181) and (3.182). This is the final step missing for the completion of the proof of the arbitrary sewing condition, which will lead to the completion of the upcoming paper.

As a final note, it is possible to isolate \hat{W}^{-1} from the spin-spin comparisons, albeit with some assumptions on its behavior. Assuming that \hat{W}^{-1} contains no branch cuts that can spoil the forthcoming contour integrals, then from Equation (3.175), one can invert the equation by

$$\begin{split} \oint_{D_1} dg_1(z_{i,1}) \oint_{D_2} dg_1(z_{j,1}) \log \left[\frac{g(z_{i,1}) - g(z_{j,1})}{g_1(z_{i,1}) - g_1(z_{j,1})} \right] = \\ \frac{1}{4\pi^2} \int_{D_1} dy \int_{D_1} dy'' \hat{W}^{-1}(y'',y) \oint_{D_1} dg_1(z_{i,1}) \oint_{D_1} dg_1(z_{j,1}) \frac{1}{(g_1(z_{i,1}) - y)(g_1(z_{j,1}) - y'')} \\ = -|D_1|^2 \hat{W}^{-1}(g_1(z_{j,1}), g_1(z_{i,1})), \end{split} \tag{3.189}$$

where $|D_1|$ stands for the length of the real interval D_1 , and \oint_{D_1} means a counterclockwise contour integral that encircles the interval D_1 entirely. Similar equations can be obtained from Equations (3.177) and (3.176) following the same logic, but it remains to be checked whether this solution complies with all the constraints derived from the sewing condition.

3.5 The closing condition for the free boson

In the previous section, we presented the most advanced proof of the arbitrary sewing condition. Although not fully complete yet, its current form already provides enough information to start tackling the computation of the full contraction of the fTNs, which is the closing condition. The closing condition is nothing but the sewing condition in the scenario in which no functions are left un-integrated according to some chosen pattern that defines the underlying topology of the state. In the simplest case, we sew two open boundaries together to reach the topology of a sphere, which is also a plane or an infinite cylinder due to conformal invariance, which corresponds to the translational invariant scenarios. One can think of these closing conditions as equivalent to the

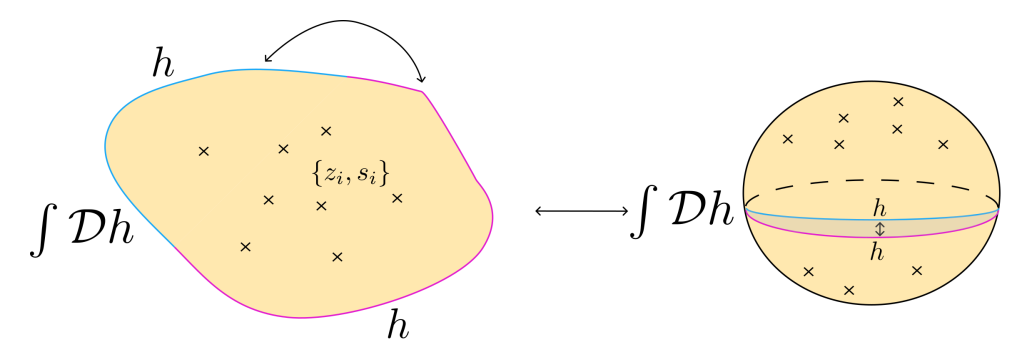


Figure 3.9: Diagrammatic representation of the closing condition leading to a wavefunction with the underlying topology of a sphere.

contraction of a TN with periodic boundary conditions. Alternatively, one can also choose to integrate these open functional indices against another functional to simulate the open boundary condition scenario, whose simplest form is to fix the functions such that a number is obtained. We can diagrammatically represent the periodic boundary condition scenarios as shown in Figures 3.9 and 3.10.

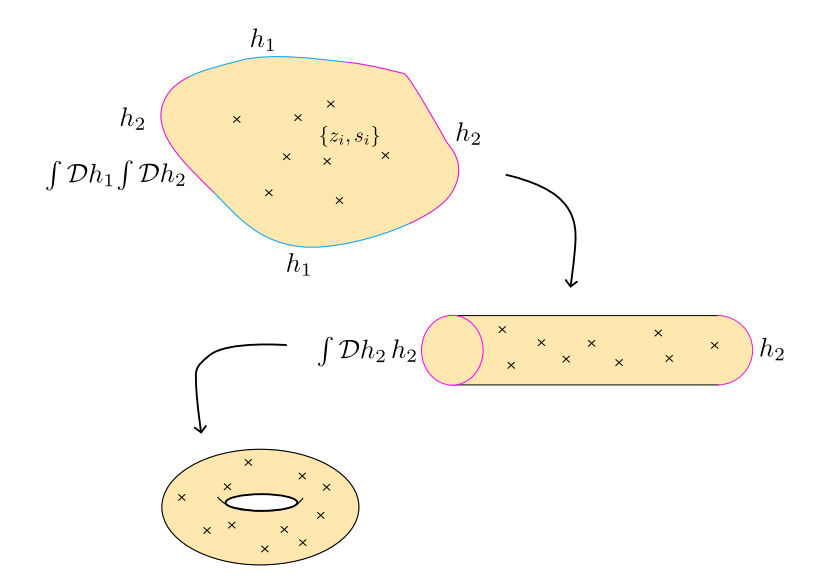


Figure 3.10: Diagrammatic representation of the closing condition leading to a wavefunction with the underlying topology of a torus.

In the section in which we presented the Möbius transformations of fTNS, we also stated that for these transformations to be "gauge" transformations of the chiral tensor,

it was important that the resulting wavefunction remained invariant. We will now prove the closing condition to the topology of a ball, which was already proven for the fMPS case in [186]. However, we will perform this computation with the machinery developed in the UHP and in an arbitrary gauge, such that we can show that Möbius transformations are indeed a gauge transformation of the tensor.

CLOSING CONDITION FOR A SPHERE TOPOLOGY

Our starting point is then a chiral tensor in an arbitrary gauge in the UHP given by

$$\begin{split} \mathcal{A}^{c}_{\mathbb{H}}\left[\tilde{f}, \left\{\gamma(\omega_{i}), s_{i}\right\}_{i=1}^{N}\right] &= \exp\left(+\frac{1}{2}\sum_{i,j}s_{i}s_{j}\left(\log\left[(\omega_{i}-\omega_{j})\right] + \log\left[\frac{(a_{2}a_{4}-a_{1}a_{3})}{(a_{4}+a_{3}\omega_{i})(a_{4}+a_{3}\omega_{j})}\right]\right) \\ &-\frac{1}{2\pi}\sum_{i}s_{i}\int_{\mathbb{R}}d\omega_{y}\tilde{f}(\gamma(\omega_{y}))\left[\frac{1}{\omega_{i}-\omega_{y}}\frac{a_{3}\omega_{i}+a_{4}}{a_{3}\omega_{y}+a_{4}}\right] \\ &+\frac{1}{8\pi^{2}}\int_{\mathbb{R}}d\omega_{x}\int_{\mathbb{R}}d\omega_{y}\tilde{f}(\gamma(\omega_{x}))\tilde{f}(\gamma(\omega_{y}))\frac{1}{(\omega_{x}-\omega_{y})^{2}}\right). \end{split} \tag{3.190}$$

The first thing one notices is that the second term of the first line can go out of the exponential to become

$$\begin{split} (a_2 a_4 - a_1 a_3)^{\sum_{i,j} \frac{s_i s_j}{2}} \exp\left(-\frac{1}{2} \sum_j s_j \sum_i s_i \log\left[(a_4 + a_3 \omega_i)\right] \\ -\frac{1}{2} \sum_i s_i \sum_j s_j \log\left[(a_4 + a_3 \omega_j)\right]\right) = 1 \end{split} \tag{3.191}$$

due to the charge neutrality condition $\sum_i s_i = 0$. With this simplification, we can now proceed to execute the closing condition by splitting the function as

$$\tilde{f}(\gamma(\omega)) = h(\gamma(\omega))\Theta(\omega \in D) + h(\gamma(\omega))\Theta(\omega \in \overline{D})$$
(3.192)

where the manifold D is fixed because of the conformal map g by whatever split of the original boundary $\partial \mathcal{M}$ was chosen, as depicted in Figure (3.9). However since we added the arbitrary gauge, we can choose without loss of generality that $D=(0,\infty]$. As part of the sewing condition, we identify the points $h(\gamma(\omega))=h(-\gamma(\omega))$. With this split, one then performs the closing condition

$$\int \mathcal{D}h\mathcal{A}^{c}_{\mathbb{H}}\left[\gamma\circ h,\gamma\circ h,\{\gamma(\omega_{i}),s_{i}\}_{i=1}^{N}\right] = \int \mathcal{D}h\mathcal{A}^{c}_{\mathbb{H}}\left[h,h,\{\gamma(\omega_{i}),s_{i}\}_{i=1}^{N}\right] \tag{3.193}$$

as we assume that the measure of the path integral is invariant under such Möbius transformations, and therefore it does not matter whether we integrate over all h or

 $\gamma \circ h$. Inserting Equation (3.190) into Equation (3.193) we obtain

$$\begin{split} \prod_{i,j} (\omega_i - \omega_j)^{\frac{s_i s_j}{2}} & \int \mathcal{D}h \exp\left(-\frac{1}{2\pi} \sum_i s_i \int_D d\omega_y h(\omega_y) \left[\frac{1}{\omega_i - \omega_y} \frac{a_3 \omega_i + a_4}{a_3 \omega_y + a_4}\right] \right. \\ & \left. - \frac{1}{2\pi} \sum_i s_i \int_{\overline{D}} d\omega_y h(\omega_y) \left[\frac{1}{\omega_i - \omega_y} \frac{a_3 \omega_i + a_4}{a_3 \omega_y + a_4}\right] \right. \\ & \left. + \frac{1}{8\pi^2} \int_D d\omega_x \int_D d\omega_y h(\omega_x) h(\omega_y) \frac{1}{(\omega_x - \omega_y)^2} \right. \\ & \left. + \frac{1}{4\pi^2} \int_D d\omega_x \int_{\overline{D}} d\omega_y h(\omega_x) h(\omega_y) \frac{1}{(\omega_x - \omega_y)^2} \right. \\ & \left. + \frac{1}{8\pi^2} \int_{\overline{D}} d\omega_x \int_{\overline{D}} d\omega_y h(\omega_x) h(\omega_y) \frac{1}{(\omega_x - \omega_y)^2} \right. \end{split}$$

which can be readily simplified by performing changes of variables on the different integrals and the sewing identification $h(\omega_x)=h(-\omega_x)$ to

$$\begin{split} \prod_{i,j} (\omega_i - \omega_j)^{\frac{s_i s_j}{2}} & \int \mathcal{D}h \exp\left(-\frac{1}{2\pi} \sum_i s_i \int_0^\infty d\omega_y h(\omega_y) \left[\frac{1}{\omega_i - \omega_y} \frac{a_3 \omega_i + a_4}{a_3 \omega_y + a_4} + \frac{1}{\omega_i + \omega_y} \frac{a_3 \omega_i + a_4}{a_4 - a_3 \omega_y}\right] \\ & + \frac{1}{4\pi^2} \int_0^\infty d\omega_x \int_0^\infty d\omega_y h(\omega_x) h(\omega_y) \left[\frac{1}{(\omega_x - \omega_y)^2} + \frac{1}{(\omega_x + \omega_y)^2}\right]\right), \end{split} \tag{3.195}$$

which is not very surprising given Equation (3.192). This equation is already in the form of a Gaussian integral, with the current given by

$$J(\omega_{i}, s_{i}, \omega_{y}) = -\frac{1}{2\pi} \sum_{i} s_{i} \left[\frac{1}{\omega_{i} - \omega_{y}} \frac{a_{3}\omega_{i} + a_{4}}{a_{3}\omega_{y} + a_{4}} + \frac{1}{\omega_{i} + \omega_{y}} \frac{a_{3}\omega_{i} + a_{4}}{a_{4} - a_{3}\omega_{y}} \right], \quad (3.196)$$

and the kernel is given by

$$W(\omega_{x}, \omega_{y}) = -\frac{1}{2\pi^{2}} \left[\frac{1}{(\omega_{x} - \omega_{y})^{2}} + \frac{1}{(\omega_{x} + \omega_{y})^{2}} \right]. \tag{3.197}$$

because the domain of integration is the entire real line \mathbb{R} on all the terms. This is the perfect setting to use the Fourier transform to find the inverse kernel, but in order to be consistent with the sewing condition, we will finish this computation entirely in real space. The inverse of this kernel on the positive real line is known from the theory of Hilbert transforms [197], and it is given by

$$W^{-1}(x,y) = \frac{1}{2} \log \left((x^2 - y^2)^2 \right). \tag{3.198}$$

After performing the gaussian integral in Equation (3.195) we obtain

$$\prod_{i,j} (\omega_i - \omega_j)^{\frac{s_i s_j}{2}} \exp \left(\frac{1}{2} \int_0^\infty d\omega_x \int_0^\infty d\omega_y J(\omega_i, s_i, \omega_x) W^{-1}(\omega_x, \omega_y) J(\omega_j, s_j, \omega_y) \right). \tag{3.199}$$

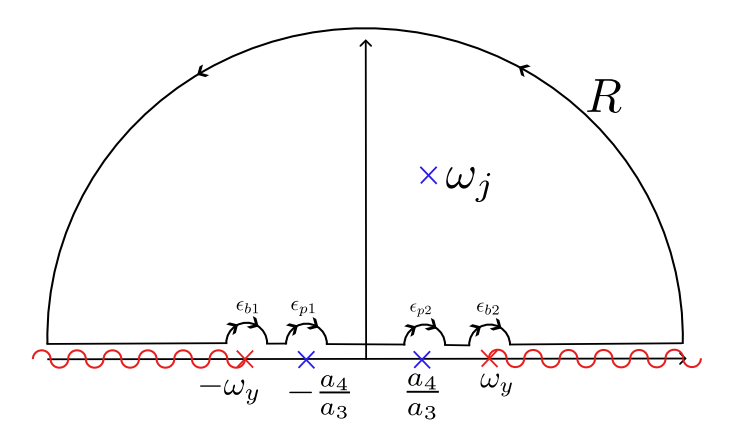


Figure 3.11: Schematic representation of the pole and branch cut structure of Equation (??)

After inserting the expressions for the currents, one obtains

$$\begin{split} \prod_{i,j} (\omega_i - \omega_j)^{\frac{s_i s_j}{2}} \exp\left(\frac{1}{8\pi^2} \sum_{i,j} s_i s_j \int_0^\infty d\omega_x \int_0^\infty d\omega_y \left[\frac{1}{\omega_i - \omega_x} \frac{a_3 \omega_i + a_4}{a_3 \omega_x + a_4} + \frac{1}{\omega_i + \omega_x} \frac{a_3 \omega_i + a_4}{a_4 - a_3 \omega_x}\right] \\ W^{-1}(\omega_x, \omega_y) \left[\frac{1}{\omega_j - \omega_y} \frac{a_3 \omega_j + a_4}{a_3 \omega_y + a_4} + \frac{1}{\omega_j + \omega_y} \frac{a_3 \omega_j + a_4}{a_4 - a_3 \omega_y}\right]\right). \end{split} \tag{3.200}$$

To perform these integrals, we need to provide more details on the branch cuts of $W^{-1}(\omega_x,\omega_y)$ to extend these integrals to complex contour integrals safely. Given that the integrals are over \mathbb{R}^+ , the most natural contours would be semicircle contours that either close through the UHP or the LHP, given that the integrand is invariant under $\omega_x \to -\omega_x$.

Let us focus now on the first integral over ω_x

$$\int_{0}^{\infty} d\omega_{x} W^{-1}(\omega_{x}, \omega_{y}) \left[\frac{1}{\omega_{i} - \omega_{x}} \frac{a_{3}\omega_{i} + a_{4}}{a_{3}\omega_{x} + a_{4}} + \frac{1}{\omega_{i} + \omega_{x}} \frac{a_{3}\omega_{i} + a_{4}}{a_{4} - a_{3}\omega_{x}} \right], \tag{3.201}$$

where we will choose the branchcuts of $W^{-1}(\omega_x,\omega_y)$ to go to infinity along the real axis and thus close the contour through the UHP to encircle the pole at ω_i . As depicted in Figure 3.11, there are another two poles located on top of the path of integration at $\omega_x=\pm\frac{a_4}{a_3}$. As is usual in these kind of calculations, the integral over the big semicircle of radius R vanishes in the limit of $R\to\infty$, while the contribution from the small semicircles of radius $\epsilon_{b1},\epsilon_{b2}$ around the branch cut points vanishes in the limit of $\epsilon_{b1},\epsilon_{b2}\to0$. By residue techniques, the contribution from the pole at ω_j as well as from the semicircles that dodge the poles on the real axis yield

$$\pi i W^{-1}(\omega_i,\omega_y) + i \pi a_3 W^{-1}(\frac{a_4}{a_3},\omega_y), \tag{3.202} \label{eq:3.202}$$

where we have used that $W^{-1}(-\omega_x,\omega_y)=W^{-1}(\omega_x,\omega_y)$. The next integral to perform is then given by

$$\int_{\mathbb{R}} d\omega_y (\pi i W^{-1}(\omega_i, \omega_y) + i \pi a_3 W^{-1}(-\frac{a_4}{a_3}, \omega_y)) \left[\frac{1}{\omega_j - \omega_y} \frac{a_3 \omega_j + a_4}{a_3 \omega_y + a_4} + \frac{1}{\omega_j + \omega_y} \frac{a_3 \omega_j + a_4}{a_4 - a_3 \omega_y} \right]. \tag{3.203}$$

By using the exact same contour, this integral becomes

$$\begin{split} &-\pi^2 W^{-1}(\omega_i,\omega_j) - \pi^2 a_3 W^{-1}(-\frac{a_4}{a_3},\omega_j) \\ &-\pi^2 a_3 W^{-1}(\omega_i,\frac{a_4}{a_3}) - \pi^2 a_3^2 W^{-1}(\frac{a_4}{a_3},\frac{a_4}{a_3}) \end{split} \tag{3.204}$$

Because of the charge neutrality condition, only the term that involves both ω_i and ω_j will survive, which removes all the information about the gauge of the UHP as promised in previous sections. This means that Möbius transformations are a genuine gauge transformation of the tensor. Finally one inserts the form of W^{-1} such that the final result of the closing condition is given by

$$\prod_{i,j} (\omega_i - \omega_j)^{\frac{s_i s_j}{2}} \exp\left(-\frac{1}{16} \sum_{i,j} s_i s_j \log\left((\omega_i^2 - \omega_j^2)^2\right)\right). \tag{3.205}$$

After bringing the terms from the exponent down one obtains

$$\psi_{s_1,...,s_n}(\omega_1,...,\omega_n) = \prod_{i,j} (\omega_i - \omega_j)^{\frac{s_i s_j}{2}} \left(\omega_i^2 - \omega_j^2\right)^{-\frac{s_i s_j}{8}}, \tag{3.206}$$

which has to be the the wavefunction obtained from a CFT computation in which there has been a conformal transformation from the UHP to another surface of genus zero. At this point in time, this transformation is not quite fully understood yet, but this computation serves both to illustrate how the gauge transformation of the tensor does not affect the wavefunction as well as to provide an explicit example of a closing condition. The final details of this conformal map will be finalized in the upcoming work [1].

CLOSING CONDITION FOR A TORUS TOPOLOGY

The closing condition to obtain the topology of a torus is the next more natural step, yet it involves a significant step up in difficulty, as the inverse kernel of the Gaussian is more challenging to find, and we will have to perform a transformation other than a Möbius transformations to bring the tensors into a form in which the Gaussian integral can be performed on a connected interval. Because this is an unfinished computation, we cannot write down the final wave function entirely in this thesis. What follows is merely a showcase of the main structure of the calculation so that the main roadblocks can be readily identified.

As with any closing, we depart from a tensor in the UHP, this time without any gauge transformation given by

$$\begin{split} \mathcal{A}^c_{\mathbb{H}}\left[\tilde{f},\{z_i,s_i\}_{i=1}^N\right] &= \exp\left(+\frac{1}{2}\sum_{i,j}s_is_j\log\left[(z_i-z_j)\right] \\ &-\frac{1}{2\pi}\sum_is_i\int_{\mathbb{R}}dy\tilde{f}(y)\left[\frac{1}{z_i-y}\right] \\ &+\frac{1}{8\pi^2}\int_{\mathbb{R}}dx\int_{\mathbb{R}}dy\tilde{f}(x)\tilde{f}(y)\frac{1}{(x-y)^2}\right). \end{split} \tag{3.207}$$

and because we wish to obtain the topology of a torus, we cut the boundary function as

$$\tilde{f}(x) = h_1(x)\Theta(x \in D_1) + h_2(x)\Theta(x \in D_2) + h_1(x)\Theta(x \in D_3) + h_2(x)\Theta(x \in D_4)$$
 (3.208)

such that $\bigcup_{i=1}^4 D_i = \mathbb{R}$ and the specific split in the subsections D_i corresponds to the one determined by the conformal map g from Figure 3.10. Inserting Equation (3.208) into Equation (3.207) we obtain

$$\begin{split} \mathcal{A}_{\mathbb{H}}^{c} \left[h_{1}, h_{2}, h_{1}, h_{2}, \{z_{i}, s_{i}\}_{i=1}^{N} \right] &= \exp\left(+ \frac{1}{2} \sum_{i,j} s_{i} s_{j} \log\left[(z_{i} - z_{j}) \right] \right. \\ &- \frac{1}{2\pi} \sum_{i} s_{i} \left(\int_{D_{1}} dy + \int_{D_{3}} dy \right) h_{1}(y) \left[\frac{1}{z_{i} - y} \right] - \frac{1}{2\pi} \sum_{i} s_{i} \left(\int_{D_{2}} dy + \int_{D_{4}} dy \right) h_{2}(y) \left[\frac{1}{z_{i} - y} \right] \\ &+ \frac{1}{8\pi^{2}} \left(\int_{D_{1}} dx \int_{D_{1}} dy + 2 \int_{D_{1}} dx \int_{D_{3}} dy + \int_{D_{3}} dx \int_{D_{3}} dy \right) \frac{h_{1}(x)h_{1}(y)}{(x - y)^{2}} \\ &+ \frac{1}{8\pi^{2}} \left(\int_{D_{1}} dx + \int_{D_{3}} dx \right) h_{1}(x) \left(2 \int_{D_{2}} \frac{h_{2}(y)}{(x - y^{2})} + 2 \int_{D_{4}} dy \frac{h_{2}(y)}{(x - y)^{2}} \right) \\ &+ \frac{1}{8\pi^{2}} \left(\int_{D_{2}} dx \int_{D_{2}} dy + 2 \int_{D_{2}} dx \int_{D_{4}} dy + \int_{D_{4}} dx \int_{D_{4}} dy \right) \frac{h_{2}(x)h_{2}(y)}{(x - y)^{2}} \right). \end{split} \tag{3.209}$$

In Equation (3.209), we see that we will have to perform a similar computation as the one we did in the sewing condition, as all the integrals are over different intervals. Following Figure 3.10, we will first integrate over h_1 . By collecting all the participating terms in this integral from Equation (3.209), one obtains

$$\int \mathcal{D}h_{1} \exp\left(-\frac{1}{2\pi} \sum_{i} s_{i} \left(\int_{D_{1}} dy + \int_{D_{3}} dy\right) h_{1}(y) \left[\frac{1}{z_{i} - y}\right] + \frac{1}{8\pi^{2}} \left(\int_{D_{1}} dx \int_{D_{1}} dy + 2 \int_{D_{1}} dx \int_{D_{3}} dy + \int_{D_{3}} dx \int_{D_{3}} dy\right) \frac{h_{1}(x)h_{1}(y)}{(x - y)^{2}} + \frac{1}{8\pi^{2}} \left(\int_{D_{1}} dx + \int_{D_{3}} dx\right) h_{1}(x) \left(2 \int_{D_{2}} \frac{h_{2}(y)}{(x - y)^{2}} + 2 \int_{D_{4}} dy \frac{h_{2}(y)}{(x - y)^{2}}\right)\right). \tag{3.210}$$

If we denote by $\tilde{D}=D_1\cup D_3$ a disjoint interval of \mathbb{R} , and its complement $\overline{\tilde{D}}=D_2\cup D_4$, then we simplify Equation (3.210) down to

$$\begin{split} \int \mathcal{D}h_1 \exp\left(-\frac{1}{2\pi} \sum_i s_i \int_{\tilde{D}} dy \frac{h_1(y)}{z_i - y} + \frac{1}{8\pi^2} \int_{\tilde{D}} dx dy \frac{h_1(x)h_1(y)}{(x - y)^2} \right. \\ \left. + \frac{1}{4\pi^2} \int_{\tilde{D}} dx \left(\int_{\tilde{D}} \frac{h_2(y)h_1(x)}{(x - y^2)} \right) \right). \end{split} \tag{3.211}$$

We can, therefore, write down a Gaussian integral as

$$\begin{split} &\int \mathcal{D}h_1 \exp \left(-\frac{1}{2} \int_{\tilde{D}} dx \int_{\tilde{D}} dy h_1(x) W_1(x,y) h_1(y) + \int_{\tilde{D}} dy J_1(s_i,z_i,y) h_1(y) \right) \\ &W_1(x,y) = -\frac{1}{2\pi^2} \frac{1}{(x-y)^2} \\ &J_1(s_i,z_i,y) = -\frac{1}{2\pi} \sum_i s_i \frac{1}{z_i-y} + \frac{1}{4\pi^2} \int_{\tilde{D}} dx \frac{h_2(x)}{(x-y)^2}. \end{split} \tag{3.212}$$

Whilst we could again keep going by assuming the inverse of W_1 on the disjoint interval \tilde{D} , we can no longer use Möbius transformations to bring any interval to the half-line \mathbb{R}^+ where we have more knowledge about the inverse of W_1 . This is because there is no way to bijectively map two intervals into a continuous one using $\mathrm{PSL}(2,\mathbb{R})$ alone. This is the missing piece of this computation needed to complete the closing condition on a torus, and more work is needed to understand this problem.

To showcase the rest of the computation, we will assume that an inverse W_1^{-1} can be found on \tilde{D} , therefore obtaining as a result of the integral

$$\begin{split} &\exp\left(\frac{1}{2}\int_{\tilde{D}}dx\int_{\tilde{D}}dyJ_{1}(s_{i},z_{i},x)W_{1}^{-1}(x,y)J_{1}(s_{j},z_{j},y)\right) = \\ &\exp\left(\frac{1}{8\pi^{2}}\int_{\tilde{D}}dx\int_{\tilde{D}}dyW_{1}^{-1}(x,y)\left[\sum_{i,j}\frac{s_{i}s_{j}}{(z_{i}-x)(z_{j}-y)}-\frac{1}{2}\sum_{i}s_{i}\int_{\tilde{D}}dx'\frac{h_{2}(x')}{(z_{i}-x)(x'-y)^{2}}\right. \\ &\left.-\frac{1}{2}\sum_{j}s_{j}\int_{\tilde{D}}dx'\frac{h_{2}(x')}{(x'-x)^{2}(z_{j}-y)}+\frac{1}{4}\int_{\tilde{D}}dx'\int_{\tilde{D}}dy'\frac{h_{2}(x')h_{2}(y')}{(x'-y)^{2}(y'-x)^{2}}\right]\right). \end{split} \tag{3.213}$$

Now we can bring back the rest of the terms from Equation (3.209) to obtain

$$\begin{split} &\exp\left(+\frac{1}{2}\sum_{i,j}s_{i}s_{j}\log\left[(z_{i}-z_{j})\right]-\frac{1}{2\pi}\sum_{i}s_{i}\int_{\tilde{D}}dy\left[\frac{h_{2}(y)}{z_{i}-y}\right]+\frac{1}{8\pi^{2}}\int_{\tilde{D}}dxdy\frac{h_{2}(x)h_{2}(y)}{(x-y)^{2}}\right.\\ &\left.\frac{1}{8\pi^{2}}\int_{\tilde{D}}dx\int_{\tilde{D}}dyW_{1}^{-1}(x,y)\left[\sum_{i,j}\frac{s_{i}s_{j}}{(z_{i}-x)(z_{j}-y)}-\frac{1}{2}\sum_{i}s_{i}\int_{\tilde{D}}dx'\frac{h_{2}(x')}{(z_{i}-x)(x'-y)^{2}}\right.\right.\\ &\left.-\frac{1}{2}\sum_{j}s_{j}\int_{\tilde{D}}dx'\frac{h_{2}(x')}{(x'-x)^{2}(z_{j}-y)}+\frac{1}{4}\int_{\tilde{D}}dx'\int_{\tilde{D}}dy'\frac{h_{2}(x')h_{2}(y')}{(x'-y)^{2}(y'-x)^{2}}\right]\right), \end{split} \tag{3.214}$$

where we can again identify the terms that will become the currents and the kernel for the integral over h_2 . We can then write

$$\begin{split} \exp\left(+ \frac{1}{2} \sum_{i,j} s_i s_j \log\left[(z_i - z_j) \right] + \frac{1}{8\pi^2} \int_{\tilde{D}} dx \int_{\tilde{D}} dy W_1^{-1}(x,y) \sum_{i,j} \frac{s_i s_j}{(z_i - x)(z_j - y)} \right) \\ \int \mathcal{D}h_2 \exp\left(-\frac{1}{2} \int_{\tilde{D}} dx \int_{\tilde{D}} dy h_2(x) W_2(x,y) h_2(y) + \int_{\tilde{D}} dy J_2(s_i,z_i,y) h_2(y) \right) \end{split} \tag{3.215}$$

where the kernel and current are given by

$$W_2(x,y) = -\frac{1}{4\pi^2} \frac{1}{(x-y)^2} - \frac{1}{16\pi^2} \int_{\tilde{D}} dx' \int_{\tilde{D}} dy' \frac{W_1^{-1}(x',y')}{(x-y')^2(y-x')^2}$$
(3.216)

and

$$J_2(s_i,z_i,y) = -\frac{1}{2\pi} \sum_i \frac{s_i}{z_i-y} - \frac{1}{16\pi^2} \sum_i s_i \int_{\tilde{D}} dx' \int_{\tilde{D}} dy' \frac{W_1^{-1}(x',y') + W_1^{-1}(y',x')}{(x-y')^2(z_i-x')} \tag{3.217}$$

We would then assume again the existence of an inverse kernel W_2^{-1} so that we can obtain the result of this final Gaussian integral. This leads to a function that no longer depends on any boundary function and, therefore, corresponds to the contraction of the fTNS. As this is only a showcase of this computation, we will not proceed further than this point, as there are too many assumptions on the inverse kernels to extract any meaningful conclusion about the final resulting state. As a final note, it is possible to significantly constrain these inverse kernels in the case of the torus because the order in which the sewings were performed, either with h_1 first and h_2 or vice versa, should not matter. Therefore, comparing the closing conditions following both routes should give us meaningful constraints about the inverse kernels. As there are still many lessons to be learned about the inverse kernels from the sewing and closing conditions, we will leave the rest of this computation for the upcoming paper.

3.6 OUTLOOK

In this chapter, we have presented a new ansatz for many-body states, which we name fTNS. It is an ansatz that targets states whose wave function can be written as a correlator of an a priori given QFT. Although it preserves the local structure of a TN in terms of its theoretical construction, the virtual space must become infinite dimensional such that correlations beyond area law can be obtained. We have focused uniquely on the first known example of fTNS, the free boson fTNS.

We began by deriving the free boson fTNS from the first principles so that this procedure can be repeated for other free theories. We showcased how to understand and remove all potential divergences within the tensor, most of them arising from the need to normal order the underlying field theory correlator. As we always wish to target chiral states, we showed how to perform a chiral truncation of the tensor and then showed how Möbius transformations act as a notion of gauge freedom for the tensor.

We then briefly showcased the corresponding free boson fMPS as the tensor that allows us to provide an exact MPS reproducing log-like area law correlations, a scenario out of reach for MPS. We briefly showed its momentum space representation, a feature of this tensor not commonly found in other fTNS, and generalized its sewing condition to an arbitrary coordinate frame.

Our next step was to provide an extensive study of the free boson fPEPS, a candidate for an exact description of gapped chiral topological order believed to be out of reach for PEPS. We studied its regularization structure, as well as its connection to the fMPS tensor and its chiral truncation.

The most important part of this chapter was the proof of the arbitrary sewing condition, which deals with exact contraction between any two compatible free boson fTNS.

Although the proof is incomplete, we have readily identified and highly constrained the remaining pieces such that they can be soon found. We hope to provide the final solution in our upcoming work, showing that fTNS can be contracted exactly even though they possess an infinite dimensional virtual space.

As an application of the sewing condition, one can fully contract an fTNS to obtain back a wave function. The underlying topology of the field theory that defines this wavefunction can be constructed from the sewing recipe of the closing condition. In this thesis, we have wholly shown how to obtain the topology of a sphere and only showcased the structure of the computation that would lead to the topology of the torus, as the missing piece from the sewing condition is also needed to finish this computation.

In summary, we have presented the first examples of fTNS and their use cases. From this point onwards, several open directions would be fascinating to pursue. In no particular order, we want to highlight:

- 1. **Fermions and Ghosts:** The Majorana fermion and the ghost system [37] are the subsequent simplest free CFT actions whose fTNS could be explored. Obtaining fTNS arising for different systems is an exciting avenue as then the relationship between different symmetry groups can be explored as in Chapter 4, or new states can be found by examining the closing conditions with different topologies.
- 2. Non-orientable topologies: We have explored the closing condition so that orientable manifolds with either no holes or one hole are recovered. Already, in the simplest case of fMPS, one could wonder how to recover a non-orientable surface such as a Möbius strip by performing a modification of the sewing condition in which the different boundaries get identified with a twist. This would allow us to obtain more families of states out of known ansatz without deriving any new sewing or tensor.
- 3. Numerical breakdown: A very appealing direction would be to consider a truncation of the infinite-dimensional virtual space such that the tensor can be explored via numerics. Of particular interest would be understanding how the properties believed to be unique to the infinite-dimensional virtual space break down once this is truncated. For fMPS, this would entail computing the entanglement entropy and finding that it no longer behaves with a logarithm. In contrast, for fPEPS, this would entail that the corresponding chiral correlations should break and reproduce results closer to [138].
- 4. *G***-WZW theory:** The ultimate goal for constructing a model in the functional space representation of fTNS would be to provide a tensor whose symmetry structure can be given by an arbitrary group *G*. This is possible because this theory remains Gaussian thanks to the Wakimoto free field representation, which provides us with the hope that such a tensor can be understood and dealt with in this language.
- 5. **Topological order in fPEPS:** As we will see in Chapter (4), we can understand the SPT classification theorem of MPS in the context of fMPS. Therefore, the most natural question, once we have obtained the fPEPS, is whether the classification and signatures of topological order of standard PEPS theory still hold in the context of fPEPS. This is a very natural next project after the results of this

- thesis, as it would hopefully cement our intuition that fTNS are a great natural generalization of TNS.
- 6. **Algebratization of fTNS:** While the language in terms of functional spaces is the most intuitive, we have seen already that it is very hard in general to perform any computation, and the few we can do are highly constrained due to the Gaussianity of the theory. The breakdown of the QFT correlator in smaller pieces can also be done within the language of CFT, leading to a definition of the fTNS tensor as a bracket between Cardy states [167]. This would correspond to a more algebraic approach that would serve CFTs beyond Gaussian free field theories and hopefully provide a cleaner description for the sewing description. Ideally, this would also allow us to explore other symmetry structures, such as the categorical descriptions of TQFTs. This direction is, without a doubt, the most exciting and potentially powerful one.

4 FMPS AND SYMMETRIES

As we have seen in Chapter 3, we can define an ∞ -dimensional object that we call an fMPS tensor, which can be contracted as if it were a finite MPS to provide the ground state of critical or chiral models. Although MERA is already an ansatz that targets the correlations of a 1-dimensional critical ground state, fMPS retains the same local geometry of an MPS. It is then natural to ask, what are the properties and results from standard TNs theory, specifically MPS, that carry over to fMPS? More specifically, as seen in Chapter 2, MPSs fully classifies SPT order in 1D. Can we provide a similar result for fMPS? We will explore this question for the case of the WZW SU(2) $_1$ free boson CFT presented in the previous chapter.

4.1 SYMMETRIES AS FTNS

In Chapter 2, we presented several important analytical properties of TNS states, amongst which the theorem that they constitute the exact groundstates of gapped frustration-free Hamiltonians [200]. As such, it is important to understand and find representatives of all possible phases of matter generated by such Hamiltonians. This is a problem known as the phase classification problem, which in the context of TNSs has been positively answered for a wide variety of phases, including both the ones with non-topological order but degenerate groundstates as well as proper topological phases as shown in [15]. We will particularly focus on the results in 1-dimensional systems, where our TN ansatz of choice are MPSs.

Phase classification for MPSs was positively and completely solved in several works such as [201],[202] and reviewed, for example, in [10]. We briefly showcase the main result we wish to understand in the context of fMPS. When a state is symmetric under a representation U_g of a symmetry group $g \in G$ and can be represented by an injective MPS in its canonical form [10], then the following relation holds

where the representation on the virtual space V_g can in general be a projective representation [203]. In equation form for an MPS tensor denoted $A_{j,k}^{s_i}$,

$$\sum_{s_i} (U_g)_{s_i, s_j} A_{n,m}^{s_j} = \sum_{k, l} (V_g)_{n, k} A_{k, l}^{s_i} (V_g^{\dagger})_{l, m}, \tag{4.2}$$

which holds, for instance, when G is a Lie group, and we can use the exponential map to write $U_g(\theta)=e^{i\theta a}$, where $a\in\mathfrak{g}$ is an element of the corresponding Lie algebra.

Projective representations differ from linear ones in that they fulfill the more general composition rule

$$V_q V_h = e^{i\omega(g,h)} V_{qh}, \tag{4.3}$$

where the extra phase factor is known as the cocycle $\omega(g,h) \in \mathcal{H}^2(G,\mathsf{U}(1))$ which is known to classify SPT order in 1-dimensional gapped systems fully [10, 201, 204].

The current known classifications are well established for gapped 1-dimensional systems, with classifications for gapless systems already studied, for instance, in [205–207]. Most of these results rely upon the computation of topological obstructions computed from the underlying CFT of the corresponding spin model. We wish to ask a similar yet methodologically different question. Is it possible to translate in a one-to-one fashion the phase classification result of standard MPS to fMPS? In other words, Equation (4.3) is the main relation we wish to establish for fTNS. To answer this question, we first need to identify the relevant symmetries for the free boson fMPS and how they are represented on the discrete physical index and the continuous functional space.

4.1.1 Symmetries of the free boson FMPS

First, let us understand the physical index of fMPS. As we have seen already, the family of states defined by the correlator in Equation 3.16 are the groundstates of a family of long-range Hamiltonians as shown in [208]. One of the most simple examples is the critical point of the Haldane-Shastry chain, defined by the Hamiltonian

$$\mathcal{H}_{HS} = -\sum_{i \neq j} \frac{z_i z_j}{\left(z_i - z_j\right)^2} \left(\mathcal{P}_{ij} - 1\right),\tag{4.4}$$

where z_i are the positions of the spins in real space and \mathcal{P}_{ij} is the spin permutation operator. This is a paradigmatic model of criticality, and its ground state can be obtained from the state defined in equation (3.16) by choosing $s_i=\pm 1,~\alpha=\frac{1}{2},~\chi_{s_m}=e^{im\pi(s_m-1)/2}$ and defining the CFT to be on a cylinder of circumference πN [37]. Since the spin-permutation operator for $\frac{1}{2}$ -spins is given by

$$\mathcal{P}_{ij} = \frac{1}{2} (\mathbb{I} + 2\vec{\sigma}_i \cdot \vec{\sigma}_j), \tag{4.5}$$

it is clear that $[\mathcal{H}_{HS}, \sigma_i] = 0$ i = 1, 2, 3. Therefore, since there is no spontaneous symmetry breaking, the ground state of this Hamiltonian must be invariant under the action of the symmetry group SU(2), whose action on the physical index is generated by the usual Pauli matrices.

We use the Hilbert space of the free boson's boundary functions on the virtual space, which is also a symmetry-extended CFT, the WZW $SU(2)_1$ theory. As we have seen in Chapter 2, WZW theories have as a fundamental property that their conserved currents $J^a(z)$ form a current algebra, which is defined through the OPE

$$J^{a}(z)J^{b}(w) \sim \frac{k\delta_{ab}}{(z-w)^{2}} + \sum_{c} if_{abc} \frac{J^{c}(w)}{(z-w)},$$
 (4.6)

where k is the level of the theory and f_{abc} the structure constants of the Lie algebra $\mathfrak g$ associated to the G-WZW. The conformal dimension of all the WZW currents is $h_J=1$.

While these theories have two independent current algebras, one for the holomorphic sector and another for the anti-holomorphic one, we will focus exclusively on the holomorphic one. The SU(2) $_1$ WZW theory has k=1 and G=SU(2), and therefore $f_{abc}=2i\varepsilon_{abc}$. At the same time there are only two primary fields, denoted by $\phi_0,\phi_{\frac{1}{2}}$, to establish a connection with the more familiar spin representations. While the field ϕ_0 acts as the identity, the field $\phi_{\frac{1}{2}}$ should be thought of as a spin-" $\frac{1}{2}$ -spin" field, and therefore we can understand the field components $\phi_{\pm\frac{1}{2}}$ as the corresponding spin projections along a chosen direction. The Virasoro central charge and the fusion rules of this theory are given by

$$c = \frac{3k}{k+2} = 1 , \quad \phi_{\frac{1}{2}} \times \phi_{\frac{1}{2}} = \phi_0 , \quad \phi_0 \times \phi_{\frac{1}{2}} = \phi_{\frac{1}{2}} , \quad \phi_0 \times \phi_0 = \phi_0,$$
 (4.7)

and the conformal dimensions of these fields are $h_0=0$ and $h_{\frac{1}{2}}=\frac{1}{4}$. For this specific theory, we can represent all of these primary fields and their currents in terms of the compactified free boson field with radius $R=\sqrt{2}$. Firstly, in terms of the chiral field $\varphi(z)$, the currents are given by

$$\begin{split} \mathbf{H}(z) &=: i \partial \varphi(z):, \\ \mathbf{E}^{\pm}(z) &=: e^{\pm i \sqrt{2} \varphi(z)}:, \end{split} \tag{4.8}$$

where :: denotes normal ordering, and we want to identify these operators with the usual spin operators $J^0\leftrightarrow {\rm H}(z)$, $J^\pm\leftrightarrow {\rm E}^\pm(z)$. Then, the corresponding states that act as the highest-weight states for the representations are generated by the primary fields

$$\phi_{\pm \frac{1}{2}}(z) =: e^{\frac{i}{\sqrt{2}}\varphi(z)}:, \tag{4.9}$$

which have the correct conformal dimension. As we already know from Chapter 2, performing OPEs amongst all these fields provides us with information about their commutation relations. Among the currents, these are

$$E^{+}(z)E^{-}(w) \sim \frac{1}{(z-w)^{2}} + \frac{\sqrt{2}H(w)}{(z-w)},$$

$$H(z)E^{\pm}(w) \sim \frac{\pm\sqrt{2}E^{\pm}(w)}{(z-w)},$$

$$H(z)H(w) \sim \frac{1}{(z-w)^{2}},$$
(4.10)

which is nothing but an explicit version of Equation (4.6) for the $SU(2)_1$ WZW. The OPEs between primary fields and the currents are given by

$$\begin{split} E^{\pm}(z)\phi_{\pm\frac{1}{2}}(w) &\sim 0, \\ E^{\pm}(z)\phi_{\mp\frac{1}{2}}(w) &\sim \frac{\phi_{\pm\frac{1}{2}}(w)}{(z-w)}, \end{split} \tag{4.11}$$

which we can interpret as the effect of raising and lowering operators on spin eigenstates. If one attempts to act with the raising (lowering) operator $E^{+(-)}(z)$ on the

highest (lowest) state of the ladder $\phi_{+(-)\frac{1}{2}}$ then the resulting OPE provides no contribution, and therefore destroys the state. Similarly, raising (lowering) with $E^{+(-)}(z)$ the lowest (highest) state $\phi_{-(+)\frac{1}{2}}$ provides us with the corresponding primary field $\phi_{+(-)\frac{1}{2}}$. Similarly, the remaining OPE is given by

$$H(z)\phi_{\pm\frac{1}{2}}(w) \sim \frac{\pm\frac{1}{2}\phi_{\pm\frac{1}{2}}}{(z-w)},$$
 (4.12)

akin to how σ_z would provide the value of the spin projection in standard spin theory.

We have identified the set of extended symmetries present in the free boson's virtual space beyond the conformal symmetries. We wish now to establish an analogous relation to Equation (4.1) for the free boson fMPS. Immediately, we are faced with a significant problem: the symmetry algebra of the physical index is given by the $\mathfrak{su}(2)$ algebra and, therefore, is finite; this object plays the role of defining U_g in Equation (4.1). However, the symmetry of the virtual space is a current algebra, a Kâc-Moody algebra, and therefore infinite dimensional algebra since it is an affine extension of $\mathfrak{su}(2)$, as shown for example in [37].

To understand which object plays the role of V_g in a possible generalization of Equation (4.1), we begin by writing the Laurent expansion of the currents as

$$J^{a}(z) = \sum_{n \in \mathbb{Z}} z^{-n-1} J_{n}^{a}, \tag{4.13}$$

from which one can derive the equivalent expression to Equation (4.6) in terms of the modes to be the Kâc-Moody algebra relation given by

$$[J_n^a, J_m^b] = \sum_c i f_{abc} J_{n+m}^c + kn \delta_{a,b} \delta_{n+m,0}.$$
 (4.14)

From this equation, we immediately notice that one can recover the standard Lie algebra relations for the generators if one sticks to the zeroth term of the mode expansions. Indeed,

$$[J_0^a, J_0^b] = \sum_c i f_{abc} J_0^c, \tag{4.15}$$

which is precisely the standard finite Lie algebra relation upon which the affine extension is constructed. To obtain the zero modes from the currents in standard CFT, one computes the corresponding Noether charges in radial quantization by

$$Q^{a} = \frac{1}{2\pi i} \oint_{0} dz J^{a}(z) = J_{0}^{a}, \tag{4.16}$$

where the integral encircles the origin. Because we now have again a finite algebra, in fact, the same as the one in the physical index, we can use these Noether charges as the field theory objects in the virtual space that will play the role of the V_g 's of Equation (4.1).

As a final technical detail, we must remember that our fTNS tensors are defined in the UHP, and therefore one should use the definitions of BCFTs as opposed to the usual CFT ones like in Equation (4.16). Using the method of images, one should define the correct Noether charges in BCFT as

$$Q = \frac{1}{2\pi i} \oint dz J(z) = \frac{1}{2\pi i} \int_{\square} dz \left(J(z) - J(\bar{z})\right). \tag{4.17}$$

where now the contour is a semi-circle that only visits the UHP. We will use these charges in the future, as failing to do so and using the ones from Equation (4.16) leads to diverging results.

4.1.2 VIRTUAL SYMMETRIES AS FMPSS

Our goal was to provide the equivalent of the V_g 's from Equation (4.1), and these must be precisely the BCFT charges arising from the integration of the algebra currents of the $\mathrm{SU}(2)_1$ WZW theory. By construction, the free boson fMPS from Equations (3.76) and (3.78) is the corresponding fTNS of the vertex operator : $e^{is\varphi(z)}$:, and therefore we know how to represent any vertex operator as an fMPS. This entails that we readily have the two primary fields from Equation (4.9) as fMPSs since these are simply vertex operators and hence given by

$$\phi_{\pm \frac{1}{2}}(z_i) = \mathcal{A}_{\Delta} \left[f_+, f_-, \{ z_i, \pm \frac{1}{\sqrt{2}} \} \right], \tag{4.18}$$

and we will think of these tensors as the corresponding "up" and "down" spin fMPSs. Similarly, we can easily find the tensors corresponding to the raising and lowering currents, which are given by

$$E^{\pm}(z) \longleftrightarrow -\frac{\mu}{2} \mathcal{A}_{\Delta} \left[f_{+}, f_{-}, \left\{ z, \pm \sqrt{2} \right\} \right], \tag{4.19}$$

where the constant $\mu=-2i$ is a requirement for the correct normalization of the algebra arising from the fMPS sewing condition, as seen in [186]. To obtain the H(z) current, one simply realizes that the derivative of the field can be found by differentiating the field's exponential and then only retaining the first order of the expansion. In equation form $\partial_z:e^{i\alpha q\varphi(z)}:=i\alpha q\partial_z\varphi(z):e^{i\alpha q\varphi(z)}:=\alpha qH(z):e^{i\alpha q\varphi(z)}:$. Therefore, the fMPS representation of the U(1) term of the algebra is

$$H(z) \longleftrightarrow \sqrt{2} \lim_{q \to 0} \frac{1}{q} \partial_z \mathcal{A}_{\Delta} \left[f_+, f_-, \left\{ z, \frac{q}{\sqrt{2}} \right\} \right], \tag{4.20}$$

where we have introduced the parameter q to take the limit and isolate the derivative of the field, and the $\sqrt{2}$ factors arise from the radius of compactification of the free boson.

To check that these fMPSs indeed represent the current algebra, we can start by checking the OPEs from Equation (4.10). To take these OPEs, one first performs the sewing of both fMPS and then takes the $z \to w$ limit. These can, therefore, be easily checked from Equation (3.80) to ensure that we have found the correct fMPS representation of these operators.

Let us start, for example, with the OPE of the raising and lowering currents, the first

line of (4.10),

$$E^{+}(z)E^{-}(w) \longleftrightarrow \lim_{z \to w} \frac{\mu^{2}}{4} \int \mathcal{D}g\mathcal{A}_{\Delta_{1}} \left[f_{+}, g, \left\{ z, +\sqrt{2} \right\} \right] \mathcal{A}_{\Delta_{2}} \left[g, f_{-}, \left\{ w, -\sqrt{2} \right\} \right] =$$

$$= -\lim_{z \to w} \frac{f_{-}}{\int_{-\infty}^{\infty} \left\{ w, -\sqrt{2} \right\}} \int_{\Delta_{1}}^{\Delta_{2}} \int_{\Delta_{1}}^{\Delta_{2}} \left[\int_{-\infty}^{\infty} dk f(k) \Omega(k, \Delta_{f}) f(k)^{\dagger} \right] + \dots,$$

$$= \frac{\mu^{2}}{4} \frac{1}{\Delta_{f}^{2}} \frac{4\Delta_{f}^{2}}{\mu^{2} (z - w)^{2}} \exp\left(-\frac{1}{2} \int_{0}^{\infty} dk f(k) \Omega(k, \Delta_{f}) f(k)^{\dagger} \right) + \dots,$$

$$(4.21)$$

with $\Delta_f = \Delta_1 + \Delta_2$, the momentum integral is a shortcut notation for the propagation term of Equation (3.78), and the expression correctly reproduces the first term of the desired OPE. The fractions in the pre-factor have been left unsimplified to explain where each of them is coming from. The first one, $\frac{\mu^2}{4}$ arises from the normalization of the currents as functionals, $\frac{1}{\Delta_f}$ arises from the conformal dimension factors of the

amplitude, and $\frac{4\Delta_f^2}{\mu^2(z-w)^2}$ comes from the expansion of the interaction term in the limit of $z\to w$. Because the expansion of the interaction term can only contain even terms in (z-w), the second term of the OPE in Equation (4.10) must arise from the spin-boundary term, the only other term of the fMPS that contains information about the spin position. Taking the limit $z\to w$ of that term alone yields

$$\begin{split} &\lim_{z\to w} \exp\left(+\frac{i}{2}\int_{\mathbb{R}} \mathrm{d}k \frac{e^{ikz}\sqrt{2}-\sqrt{2}e^{ikw}}{\sinh\left(\pi k\Delta_f\right)} \left(e^{\pi kb_f}\hat{f}_+(k)-e^{\pi ka_f}\hat{f}_-(k)\right)\right) \\ &=1+\frac{i}{2}\int_{\mathbb{R}} \mathrm{d}k \frac{ike^{ikw}(z-w)\sqrt{2}}{\sinh\left(\pi k\Delta_f\right)} \left(e^{\pi kb_f}\hat{f}_+(k)-e^{\pi ka_f}\hat{f}_-(k)\right)+O\left((z-w)^2\right), \end{split} \tag{4.22}$$

which is the promised linear term that arises from the first position derivative of the expansion. Hence the OPE between the fMPSs of $E^+(z)$ and $E^-(w)$ is

$$\begin{split} &=\frac{1}{(z-w)^2}\exp\left(-\frac{1}{2}\int_0^\infty dk f(\vec{k})\Omega(k,\Delta_f)f(\vec{k})^\dagger\right)\\ &+\frac{i}{\sqrt{2}\left(z-w\right)}\int_{\mathbb{R}} dk \frac{ike^{ikw}}{\sinh\left(\pi k\Delta_f\right)}\left(e^{\pi kb_f}\hat{f}_+(k)-e^{\pi ka_f}\hat{f}_-(k)\right)\exp\left(-\frac{1}{2}\int_0^\infty dk f(\vec{k})\Omega(k,\Delta_f)f(\vec{k})^\dagger\right)\\ &+O\left((z-w)^0\right), \end{split} \tag{4.23}$$

and one can readily see that the complicated prefactor that has appeared exactly corresponds to the H(z) current as shown in Equation (4.20), as it is nothing but a position derivative. The final result is then

$$\frac{1}{(z-w)^{2}} \exp \left\{ \left(-\frac{1}{2} \int_{0}^{\infty} dk f(\vec{k}) \Omega(k, \Delta_{f}) f(\vec{k})^{\dagger} \right) \right\} + \frac{\sqrt{2} \sqrt{2} \lim_{q \to 0} \frac{1}{q} \partial_{z} \mathcal{A}_{\Delta_{f}} \left[f_{+}, f_{-}, \left\{ z, \frac{q}{\sqrt{2}} \right\} \right]}{(z-w)}, \tag{4.24}$$

which perfectly reproduces the OPE and, therefore, allows us to identify the identity operator in the functional space with

$$\phi_0 = \mathbb{I} \longleftrightarrow \mathcal{A}_{\Delta_f} \left[f_+, f_-, \{z, 0\} \right] = \exp \left\{ \left(-\frac{1}{2} \int_0^\infty dk f(\vec{k}) \Omega(k, \Delta_f) f(\vec{k})^\dagger \right) \right\}. \tag{4.25}$$

Let us now perform the OPE of H(z) with itself. This corresponds to

$$H(z)H(w) \longleftrightarrow 2\lim_{z \to w} \lim_{q_1, q_2 \to 0} \frac{1}{q_1 q_2} \partial_w \partial_z \int \mathcal{D}g \mathcal{A}_{\Delta_1} \left[f_+, g, \left\{ z, \frac{q_1}{\sqrt{2}} \right\} \right] \mathcal{A}_{\Delta_2} \left[g, f_-, \left\{ w, \frac{q_2}{\sqrt{2}} \right\} \right]$$

$$= 2\lim_{z \to w} \lim_{q_1, q_2 \to 0} \frac{1}{q_1 q_2} \partial_z \partial_w$$

$$\downarrow \{z, \frac{q_1}{\sqrt{2}}\}$$

$$\downarrow f_+$$

$$\downarrow f$$

$$=2\exp\left\{\left(-\frac{1}{2}\int_{0}^{\infty}dkf(\vec{k})\Omega(k,\Delta_{f})f(\vec{k})^{\dagger}\right)\right\}\lim_{z\to w}\lim_{q_{1},q_{2}\to 0}\frac{1}{q_{1}q_{2}}\partial_{w}\partial_{z}\left(\mu\sinh\left(\frac{z-w}{2\Delta_{f}}\right)\right)^{\frac{q_{1}q_{2}}{2}}$$

$$=\frac{1}{(w-z)^{2}}\mathcal{A}_{\Delta_{f}}\left[f_{+},f_{-},\{z,0\}\right],$$

$$(4.26)$$

where in the step between the second and third line we have dropped all the terms of the expansion that are regular in the OPE limit.

Finally, the OPE of H(z) with either of $E^{\pm}(w)$ will be given by

$$H(z)E^{\pm}(w) \longleftrightarrow -\sqrt{2}\frac{\mu}{2}\lim_{z\to w}\lim_{q\to 0}\frac{1}{q}\partial_{z}\int \mathcal{D}g\mathcal{A}_{\Delta_{1}}\left[f_{+},g,\left\{z,\frac{q}{\sqrt{2}}\right\}\right]\mathcal{A}_{\Delta_{2}}\left[g,f_{-},\left\{w,\pm\sqrt{2}\right\}\right]$$

$$= -\frac{\mu}{\sqrt{2}}\lim_{z\to w}\lim_{q\to 0}\frac{1}{q}\partial_{z}\underbrace{\left\{u,\pm\sqrt{2}\right\}}_{f_{+}}$$

$$= -\frac{\mu}{\sqrt{2}}\lim_{z\to w}\lim_{q\to 0}\frac{1}{q}\partial_{z}\left(\mu\sinh\left(\frac{w-z}{2\Delta_{f}}\right)\right)^{\pm q}\mathcal{A}_{\Delta_{f}}\left[f_{+},f_{-},\left\{w,\pm\sqrt{2}\right\}\right]$$

$$= \frac{\pm\sqrt{2}}{(z-w)}\left(-\frac{\mu}{2}\mathcal{A}_{\Delta_{f}}\left[f_{+},f_{-},\left\{w,\pm\sqrt{2}\right\}\right]\right),$$

$$(4.27)$$

which is again the desired OPE.

Up until now, we have been using the symbol \longleftrightarrow to establish the identification between the corresponding current and its fMPS representation; the reason for this will now be made clear with the study of the OPE between the current and the primary field fMPS representation. Let us begin with the simplest ones, the OPEs in Equation (4.11), where the first line reads

$$\begin{split} E^{\pm}(z)\phi_{\pm\frac{1}{2}}(w) &\longleftrightarrow -\frac{\mu}{2}\lim_{z\to w}\int \mathcal{D}g\mathcal{A}_{\Delta_{1}}\left[f_{+},g,\left\{z,\pm\sqrt{2}\right\}\right]\mathcal{A}_{\Delta_{2}}\left[g,f_{-},\left\{w,\frac{\pm1}{\sqrt{2}}\right\}\right]\\ &= -\frac{\mu}{2}\lim_{z\to w}\mathcal{A}_{\Delta_{f}}\left[f_{+},f_{-},\left\{z,\pm\sqrt{2},w,\frac{\pm1}{\sqrt{2}}\right\}\right]\to 0, \end{split} \tag{4.28}$$

which is true because both charges have the same sign, and therefore, the expansion of the interaction term in the $z\to w$ has no divergent terms whatsoever. On the other hand, the OPE $E^\mp(z)\phi_{\pm\frac12}(w)$ reads

$$\begin{split} E^{\mp}(z)\phi_{\pm\frac{1}{2}}(w) &\longleftrightarrow -\frac{\mu}{2}\lim_{z \to w} \int \mathcal{D}g\mathcal{A}_{\Delta_{1}}\left[f_{+},g,\left\{z,\mp\sqrt{2}\right\}\right]\mathcal{A}_{\Delta_{2}}\left[g,f_{-},\left\{w,\frac{\pm1}{\sqrt{2}}\right\}\right] \\ &= -\frac{\mu}{2}\lim_{z \to w} \mathcal{A}_{\Delta_{f}}\left[f_{+},f_{-},\left\{z,\mp\sqrt{2},w,\frac{\pm1}{\sqrt{2}}\right\}\right] \\ &= -\frac{\mu}{2}\frac{1}{\Delta_{f}}\lim_{z \to w} \left(\mu\sinh\left(\frac{w-z}{2\Delta_{f}}\right)\right)^{-1}\mathcal{A}_{\Delta_{f}}\left[f_{+},f_{-},\left\{w,\frac{\mp1}{\sqrt{2}}\right\}\right] \\ &= \frac{1}{(z-w)}\mathcal{A}_{\Delta_{f}}\left[f_{+},f_{-},\left\{w,\frac{\mp1}{\sqrt{2}}\right\}\right] \end{split} \tag{4.29}$$

which is almost the OPE we wanted to recover up to a significant detail. The new tensor representing the primary field is defined on a strip of width $\Delta_f = \Delta_1 + \Delta_2$, while the original primary field tensor was defined on a strip of width Δ_2 !

The fact that the sewing property enlarges the resulting fMPS tensor with the width Δ of the newly sown strip is precisely the obstruction to establishing a strict equality in Equations (4.18),(4.20),(4.19) and (4.25). To understand why this is a problem, let us go back to the field theory definition of our fMPS state, that is, as a correlator of primaries

$$\langle \phi_{s_1}(z_1)\phi_{s_2}(z_2)...\phi_{s_N}(z_N)\rangle = \langle \phi_{s_1}(z_1)\phi_0\phi_{s_2}(z_2)...\phi_{s_N}(z_N)\rangle, \tag{4.30}$$

where the equality holds because the fusion rules of the identity field in Equation (4.7) with any other field are trivial, and therefore one can insert as many identity field primaries as desired. Therefore, the correlator on the r.h.s of Equation (4.30) would be computed as the closing condition of N+1 strips, where the one corresponding to ϕ_0 would host no spin and width $\Delta_{\mathbb{I}}$. But because this correlator is equal to that of N spins on a system of total length $\Delta_T = \sum_i \Delta_i$, it is not sensible that it is also equal to the one of a system of length $\Delta_T + \Delta_{\mathbb{I}}$. Therefore, the only correct way in which one can insert a current operator, or the identity, on a correlator defined through the closing condition of Equation (3.82), is if one then also takes the limit of $\Delta_{\mathbb{I}}, \Delta_J \to 0$.

This limit, mandatory to recover the correct OPEs and correlation functions, has important implications. If one naively attempts to take the limit $\Delta \to 0$ in the expression of the fMPS tensor as in Equation (3.78) one will encounter divergences in the propagation, the spin-boundary term as well as the interaction term, essentially leading to a completely useless tensor. However, we have already seen that we have encountered no such issues in either of the OPEs in Equation (4.28) or (4.29). This means that this limit can only make sense after sewing has already occurred, akin to how a regularized distribution is only well-defined in the limit of the regulator going to 0 when integrated against suitable test functions.

Therefore, we finally define the current operators as fMPS with

$$\begin{split} E^{\pm}(z) &= -\frac{\mu}{2} \lim_{\Delta \to 0} \mathcal{A}_{\Delta} \left[f_+, f_-, \left\{ z, \pm \sqrt{2} \right\} \right], \\ H(z) &= \sqrt{2} \lim_{\Delta \to 0} \lim_{q \to 0} \frac{1}{q} \partial_z \mathcal{A}_{\Delta} \left[f_+, f_-, \left\{ z, \frac{q}{\sqrt{2}} \right\} \right], \\ \phi_0 &= \delta(f_+ - f_-) = \lim_{\Delta \to 0} \mathcal{A}_{\Delta_f} \left[f_+, f_-, \left\{ z, 0 \right\} \right] = \exp \left(-\frac{1}{2} \int_0^{\infty} dk f(\vec{k}) \Omega(k, \Delta_f) f(\vec{k})^{\dagger} \right), \end{split} \tag{4.31}$$

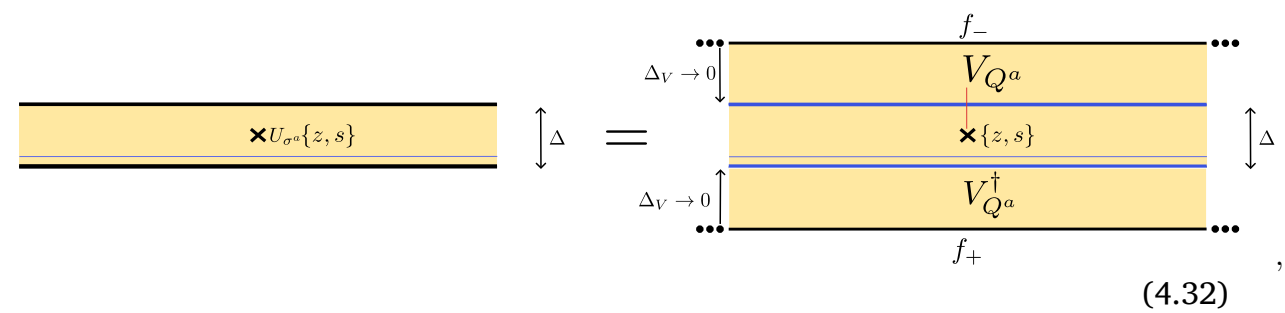
where all of these limits have to be understood in the distributional sense, in which the corresponding integral is the sewing operation, and the corresponding test functions are any other fMPS tensors that represent a vertex operator in a correlator. The last line constitutes the identity in functional space and, thus, the free boson fMPS representation of a functional Dirac distribution.

4.2 THE PUSH-THROUGH RELATION OF THE FREE BOSON FMPS

We now tackle the original question of this chapter:

Can we translate the pushing-through condition for symmetries of injective MPSs, shown in Equation (4.1), to the setting of fMPS?

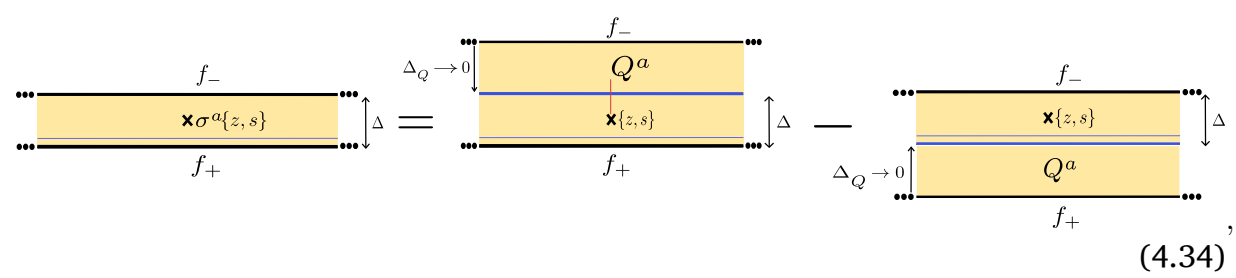
We wish to reproduce that equation exactly, and thus, diagrammatically, we are aiming at an equation of the form



where the blue lines correspond to sewing operations, U_{σ^a} corresponds to the exponentiated matrix group representation of SU(2), with σ^a the usual Pauli matrices, and V_{J^a} the corresponding exponentiated group representation of the charge algebra $\mathfrak{su}(2)$, originating from the current algebra $\mathfrak{su}(2)_1$. As we have already seen, we have an fMPS representation of the charges Q^a and not their exponentials. Assuming that $V_{Q^a} \propto \exp\{\alpha Q^a\}$, one can then use the usual Lie algebra derivation in which one expands

$$U_{\sigma^a} = \exp(\alpha \sigma^a) \to \lim_{\alpha \to 0} \frac{1}{\alpha} \partial_\alpha U_{\sigma^a} = \sigma^a. \tag{4.33}$$

Performing this limit on Equation (4.32), yields



where Δ_Q is the width associated with the fMPS charge andthe limit of $\Delta_Q \to 0$ is taken after the sewing. It is important to emphasize that the symmetry on the l.h.s is acting on a spin state and is represented by a 2×2 matrix, which gets translated to the r.h.s employing the commutation of a Noether charge with the tensor. Our next goal is to prove this relation for all currents, which we call the "algebra-level" pushthrough relation, to afterward prove the complete group-level relation via the usual exponentiation techniques.

PROOF OF THE ALGEBRA-LEVEL PUSH-THROUGH EQUATION

In this section, we derive the rules of the action for the fMPS conformal charges on a single primary fMPS, which correspond to either of the two terms of 4.34, where we are we will be using that the spin value of the primary fields fMPS has the normalization $q=\frac{s}{\sqrt{2}}$. We start with the action of the H(z) current, whose charge is denoted by Q^0 . First and foremost, we need to choose a convention for the order in which we sew strips in situations where we have more than two. In this thesis we choose to always sew from the lower boundary first and then move upwards. In strip form, what we need to compute is

$$\begin{array}{c|c}
f_{-} \\
\hline
Q^{0} \\
\hline
\mathbf{x}_{\{z,q\}} \\
\hline
f_{+}
\end{array} = (a). \tag{4.35}$$

In equation form, equation (4.35) is written as

$$(a) = \int \mathcal{D}g \frac{1}{2\pi i} \int_{\mathbb{R}} dz_1 \mathcal{A}_{\Delta} \left[f_+, g, \{z, q\} \right] \lim_{q_1 \rightarrow 0} \frac{\sqrt{2}}{q_1} \left(\partial_{z_1} \mathcal{A}_{\Delta_1} \left[g, f_-, \{z_1, q_1\} \right] - (z_1 \leftrightarrow \bar{z}_1) \right), \tag{4.36}$$

where $\int_{\mathbb{R}} dz_1$ means the integration over \mathbb{R} of the real part of z_1 and corresponds to the contour integral of the charge construction in the UHP, as shown in Equation (4.17). After performing the sewing integral, one finds

$$(a) = \frac{1}{2\pi i} \int_{\mathbb{R}} dz_1 \lim_{q_1 \to 0} \frac{\sqrt{2}}{q_1} \left[\partial_{z_1} \mathcal{A}_{\Delta_f} \left[f_+, f_-, \{z, q, z_1, q_1\} \right] - (z_1 \leftrightarrow \bar{z}_1) \right], \tag{4.37}$$

where $\Delta_f = \Delta + \Delta_1$. Performing the derivative with respect to z_1 , one obtains:

$$\begin{split} (a) &= \frac{1}{2\pi i} \int_{\mathbb{R}} dz_1 \lim_{q_1 \to 0} \frac{\sqrt{2}}{q_1} \left[\frac{i}{2} \int_{\mathbb{R}} dk \frac{ikq_1 e^{ikz_1}}{\sinh\left(\pi k \Delta_f\right)} \left(e^{\pi k b_f} f_+(k) - e^{\pi k a_f} f_-(k) \right) \right. \\ &\left. - \frac{qq_1}{2\Delta_f} \coth\left(\frac{z_1 - z}{2\Delta_f}\right) \left(\mu \sinh\left(\frac{z_1 - z}{2\Delta_f}\right) \right)^{qq_1} \right] \mathcal{A}_{\Delta_f} \left[f_+, f_-, \{z, q, z_1, q_1\} \right] \\ &\left. - (z_1 \leftrightarrow \bar{z}_1), \end{split} \tag{4.38}$$

and in what follows, we treat both terms separately. Let us start with the first line, that is the integral

$$\frac{1}{2\pi i} \int_{\mathbb{R}} dz_1 \frac{i}{\sqrt{2}} \int_{\mathbb{R}} dk \frac{ike^{ikz_1}}{\sinh\left(\pi k\Delta_f\right)} \left(e^{\pi kb_f} f_+(k) - e^{\pi ka_f} f_-(k)\right). \tag{4.39}$$

We first swap the order of integration, that is we first perform the z_1 -integral and then the k-integral. To be able to perform this change for this specific Riemmann, it is enough to guarantee that the k-integral is convergent. We start by analyzing the behavior of the integrand in the $k \to \pm \infty$ limits

$$\begin{cases} k \to +\infty & \propto k e^{ikz_1 - \pi k(\Delta_f - b_f)} f_+(k) - e^{ikz_1 - \pi k(\Delta_f - a_f)} f_-(k) \to 0 \\ k \to -\infty & \propto k e^{ikz_1 + \pi k(\Delta_f + b_f)} f_+(k) - e^{ikz_1 + \pi k(\Delta_f + a_f)} f_-(k) \to 0, \end{cases}$$
 (4.40)

where the decay to 0 in the limit is guaranteed because ${\rm Im}(z_1)<\Delta_f=b_f-a_f$ and $f_\pm(k)$ are quickly decaying functions. The other potentially problematic point is k=0, but the divergence is tamed by the power of k in the numerator. We can thus exchange the order of integrals and use the Dirac delta distribution to obtain :

$$\frac{i}{\sqrt{2}} \int_{\mathbb{R}} dk \frac{k\delta(k) e^{-\pi k \operatorname{Im}(z_1)}}{\sinh\left(\pi k \Delta_f\right)} \left(e^{\pi k b_f} f_+(k) - e^{\pi k a_f} f_-(k) \right). \tag{4.41}$$

All that is left is the evaluation of the k-integral by means of the Dirac distribution. In this case, we must evaluate the limit $k \to 0$

$$\lim_{k\to 0} \frac{ke^{-\pi k \text{Im}(z_1)}}{\sinh{(\pi k \Delta_f)}} \left(e^{\pi k b_f} f_+(k) - e^{\pi k a_f} f_-(k)\right) = \frac{1}{\pi \Delta_f} (f_+(0) - f_-(0)) = 0, \tag{4.42}$$

where the last equality follows from the fact that the zero-mode is chosen to be the same amongst all the different sewing points on a state, as explained in Chapter 3. Thus, we have simplified Equation (4.38) down to

$$\begin{split} (a) &= \frac{1}{2\pi i} \int_{\mathbb{R}} dz_1 \lim_{q_1 \to 0} \frac{\sqrt{2}}{q_1} \\ &\left[\frac{qq_1}{2\Delta_f} \coth\left(\frac{z_1 - z}{2\Delta_f}\right) \left(\mu \sinh\left(\frac{z_1 - z}{2\Delta_f}\right)\right)^{qq_1} \right] \mathcal{A}_{\Delta_f} \left[f_+, f_-, \{z, q, z_1, q_1\}\right] - (z_1 \leftrightarrow \bar{z}_1). \end{split} \tag{4.43}$$

We are now in a position to take the limit $q_1 \to 0$, obtaining

$$(a) = \mathcal{A}_{\Delta_f} \left[f_+, f_-, \{z, q\} \right] \frac{q}{\sqrt{2} \Delta_f} \frac{1}{2\pi i} \int_{\mathbb{R}} dz_1 \left[\coth \left(\frac{z_1 - z}{2\Delta_f} \right) - \coth \left(\frac{\bar{z}_1 - z}{2\Delta_f} \right) \right], \tag{4.44}$$

where the limit removed the z_1 contribution to the functional \mathcal{A}_{Δ_f} and thus allows us to take it out of the integral. The remaining integral can be computed by residue calculus, and it yields

$$(a) = \frac{\sqrt{2}q \text{Im}(z_1)}{\pi \Delta_f} \mathcal{A}_{\Delta_f} \left[f_+, f_-, \{z, q\} \right]. \tag{4.45}$$

Finally, we can take the limit $\Delta_1 \to 0$ without any danger of any part diverging, which in turn forces $\mathrm{Im}(z_1)$ to be at the edge of the original strip, in this case, the upper edge $\mathrm{Im}(z_1)=\pi b$. This concludes this computation yielding

$$(a) = \frac{\sqrt{2qb}}{\Delta} \mathcal{A}_{\Delta} [f_{+}, f_{-}, \{z, q\}].$$
 (4.46)

To conclude the computation of the commutator (4.34), we now need to compute the second term of its l.h.s

$$\begin{array}{c}
f_{-} \\
 & \times \{z,q\} \\
 & Q^{0}
\end{array}$$

$$\begin{array}{c}
 & \downarrow \Delta \\
 & Q^{0}
\end{array}$$

$$\begin{array}{c}
 & \downarrow \Delta \\
 & \downarrow \Delta
\end{array}$$

$$\begin{array}{c}
 & \downarrow \Delta \\
 & \downarrow \Delta
\end{array}$$

$$\begin{array}{c}
 & \downarrow \Delta \\
 & \downarrow \Delta
\end{array}$$

$$\begin{array}{c}
 & \downarrow \Delta \\
 & \downarrow \Delta
\end{array}$$

$$\begin{array}{c}
 & \downarrow \Delta \\
 & \downarrow \Delta
\end{array}$$

$$\begin{array}{c}
 & \downarrow \Delta \\
 & \downarrow \Delta
\end{array}$$

$$\begin{array}{c}
 & \downarrow \Delta \\
 & \downarrow \Delta
\end{array}$$

$$\begin{array}{c}
 & \downarrow \Delta \\
 & \downarrow \Delta
\end{array}$$

$$\begin{array}{c}
 & \downarrow \Delta \\
 & \downarrow \Delta
\end{array}$$

$$\begin{array}{c}
 & \downarrow \Delta \\
 & \downarrow \Delta
\end{array}$$

$$\begin{array}{c}
 & \downarrow \Delta \\
 & \downarrow \Delta
\end{array}$$

$$\begin{array}{c}
 & \downarrow \Delta \\
 & \downarrow \Delta
\end{array}$$

$$\begin{array}{c}
 & \downarrow \Delta \\
 & \downarrow \Delta
\end{array}$$

$$\begin{array}{c}
 & \downarrow \Delta \\
 & \downarrow \Delta
\end{array}$$

$$\begin{array}{c}
 & \downarrow \Delta \\
 & \downarrow \Delta
\end{array}$$

$$\begin{array}{c}
 & \downarrow \Delta \\
 & \downarrow \Delta
\end{array}$$

$$\begin{array}{c}
 & \downarrow \Delta \\
 & \downarrow \Delta
\end{array}$$

$$\begin{array}{c}
 & \downarrow \Delta \\
 & \downarrow \Delta
\end{array}$$

$$\begin{array}{c}
 & \downarrow \Delta \\
 & \downarrow \Delta
\end{array}$$

$$\begin{array}{c}
 & \downarrow \Delta \\
 & \downarrow \Delta
\end{array}$$

$$\begin{array}{c}
 & \downarrow \Delta \\
 & \downarrow \Delta
\end{array}$$

$$\begin{array}{c}
 & \downarrow \Delta \\
 & \downarrow \Delta
\end{array}$$

$$\begin{array}{c}
 & \downarrow \Delta \\
 & \downarrow \Delta
\end{array}$$

$$\begin{array}{c}
 & \downarrow \Delta \\
 & \downarrow \Delta
\end{array}$$

$$\begin{array}{c}
 & \downarrow \Delta \\
 & \downarrow \Delta
\end{array}$$

$$\begin{array}{c}
 & \downarrow \Delta \\
 & \downarrow \Delta
\end{array}$$

$$\begin{array}{c}
 & \downarrow \Delta \\
 & \downarrow \Delta
\end{array}$$

$$\begin{array}{c}
 & \downarrow \Delta$$

$$\begin{array}{c}
 & \downarrow \Delta
\end{array}$$

$$\begin{array}{c}
 & \downarrow \Delta
\end{array}$$

$$\begin{array}{c}
 & \downarrow \Delta
\end{array}$$

$$\begin{array}{c}
 & \downarrow \Delta$$

$$\begin{array}{c}
 & \downarrow \Delta
\end{array}$$

$$\begin{array}{c}
 & \downarrow \Delta
\end{array}$$

$$\begin{array}{c}
 & \downarrow \Delta$$

$$\begin{array}{c}
 & \downarrow \Delta
\end{array}$$

$$\begin{array}{c}
 & \downarrow \Delta$$

$$\begin{array}{c}
 & \downarrow \Delta
\end{array}$$

$$\begin{array}{c}
 & \downarrow \Delta$$

$$\begin{array}{c}
 & \downarrow \Delta$$

$$\begin{array}{c}
 & \downarrow \Delta
\end{array}$$

$$\begin{array}{c}
 & \downarrow \Delta$$

$$\begin{array}{c}
 & \downarrow \Delta$$

$$\begin{array}{c}
 & \downarrow \Delta
\end{array}$$

$$\begin{array}{c}
 & \downarrow \Delta$$

$$\begin{array}{c}
 & \downarrow \Delta
\end{array}$$

$$\begin{array}{c}
 & \downarrow \Delta$$

$$\begin{array}{c}
 & \downarrow \Delta$$

$$\begin{array}{c}
 & \downarrow \Delta
\end{array}$$

$$\begin{array}{c}
 & \downarrow \Delta$$

$$\begin{array}{c}
 & \downarrow \Delta$$

$$\begin{array}{c}
 & \downarrow \Delta
\end{array}$$

$$\begin{array}{c}
 & \downarrow \Delta$$

$$\begin{array}{c}
 & \downarrow \Delta$$

$$\begin{array}{c}
 & \downarrow \Delta
\end{array}$$

$$\begin{array}{c}
 & \downarrow \Delta$$

$$\begin{array}{c}
 & \downarrow \Delta
\end{array}$$

$$\begin{array}{c}
 & \downarrow \Delta$$

$$\begin{array}{c}
 & \downarrow \Delta
\end{array}$$

$$\begin{array}{c}
 & \downarrow \Delta$$

$$\begin{array}{c}
 & \downarrow \Delta
\end{array}$$

$$\begin{array}{c}
 & \downarrow \Delta$$

$$\begin{array}{c}
 & \downarrow \Delta$$

$$\begin{array}{c}
 & \downarrow \Delta$$

$$\begin{array}{c}
 & \downarrow \Delta
\end{array}$$

$$\begin{array}{c}
 & \downarrow \Delta$$

$$\begin{array}{c}
 & \downarrow \Delta$$

$$\begin{array}{c}
 & \downarrow \Delta
\end{array}$$

$$\begin{array}{c}
 & \downarrow \Delta$$

$$\begin{array}{c}
 & \downarrow \Delta
\end{array}$$

$$\begin{array}{c}
 & \downarrow \Delta$$

$$\begin{array}{c}
 & \downarrow \Delta
\end{array}$$

$$\begin{array}{c}
 & \downarrow \Delta$$

$$\begin{array}{c}
 & \downarrow \Delta
\end{array}$$

$$\begin{array}{c}
 & \downarrow$$

which is a computation that follows along the same lines as the one we have just done. To see this, we can look at (4.38) to see the effect of sewing from the lower boundary. The main difference is that all the terms that depend on z_1-z will now go as $z-z_1$ and the sign in front will change because of the derivative. Since the cotangent is an odd function, we recover (4.44) at the end of the computation. With this result, the commutator with Q^0 becomes

$$(a)-(b)=\frac{\sqrt{2}qb}{\Delta}\mathcal{A}_{\Delta}\left[f_{+},f_{-},\left\{z,q\right\}\right]-\frac{\sqrt{2}qa}{\Delta}\mathcal{A}_{\Delta}\left[f_{+},f_{-},\left\{z,q\right\}\right]=\sqrt{2}q\mathcal{A}_{\Delta}\left[f_{+},f_{-},\left\{z,q\right\}\right],$$

since $\Delta=b-a$. This is the expected action on a single spin with the usual σ_z operator, given that the charge is chosen to be $q=\frac{s}{\sqrt{2}}$. In equation form, we have deduced that

$$\sigma_{ss'}^{z} \mathcal{A}_{\Delta} \left[z, \frac{s'}{\sqrt{2}} \right] = s \mathcal{A}_{\Delta} \left[f_{+}, f_{-}, \left\{ z, \frac{s}{\sqrt{2}} \right\} \right], \tag{4.49}$$

which is nothing but the expected action of the σ^z operator on a spin eigenstate but computed through its action on the virtual space.

We now turn our attention to the action of the lowering and raising currents $J^{\pm}(z)$, whose charges we will denote Q^{\pm} . As before, we start with the action on the upper

edge of a strip, which in strip form reads

$$\begin{array}{c|c}
f_{-} \\
\hline
\Delta_{1} \rightarrow 0 \\
\hline
Q^{\pm} \\
\hline
\chi_{\{z,q\}} \\
\hline
f_{+}
\end{array} = (c), \tag{4.50}$$

or in equation form

$$(c) = \int \mathcal{D}g \frac{1}{2\pi i} \left(-\frac{\mu}{2} \right) \int_{\mathbb{R}} dz_1 \mathcal{A}_{\Delta} \left[f_+, g, \{z, q\} \right] \mathcal{A}_{\Delta_1} \left[g, f_-, \{z_1, \pm \sqrt{2}\} \right] - (z_1 \leftrightarrow \bar{z}_1), \tag{4.51}$$

where $-\frac{\mu}{2}$ ensures proper normalization. We then perform the sewing and factorize what does not depend on z_1 outside of the integral to obtain

$$\begin{split} (c) &= \mathcal{A}_{\Delta} \left[f_{+}, f_{-}, \{z, q\} \right] \Delta^{-\frac{q_{1}^{2}}{2}} \frac{1}{2\pi i} \left(-\frac{\mu}{2} \right) \int_{\mathbb{R}} dz_{1} \left(\mu \sinh \left(\frac{z_{1} - z}{2\Delta_{f}} \right) \right)^{\pm \sqrt{2}q} \\ &= \exp \left\{ \left(\frac{i}{2} \int_{\mathbb{R}} dk \frac{\pm \sqrt{2} e^{ikz_{1}}}{\sinh \left(\pi k \Delta_{f} \right)} \mathcal{C}(k) \right) \right\} - (z_{1} \leftrightarrow \bar{z}_{1}), \end{split} \tag{4.52}$$

where $\mathcal{C}(k) = \left(e^{\pi k b_f} \hat{f}_+(k) - e^{\pi k a_f} \hat{f}_-(k)\right)$ is a shorthand notation for the functional part of the boundary term. To tackle this integral, we start by Taylor-expanding the second exponential as

$$\begin{split} \exp &\left\{ \left(\frac{i}{2} \int_{\mathbb{R}} dk \frac{\pm \sqrt{2} e^{ikz_1}}{\sinh \left(\pi k \Delta_f \right)} \mathcal{C}(k) \right) \right\} = \\ &\sum_{n=0}^{\infty} \int_{\mathbb{R}} dk_1 ... dk_n \left(\frac{i}{2} \right)^n \left(\pm \sqrt{2} \right)^n \prod_{m=1}^n \frac{\mathcal{C}(k_m)}{\sinh \left(\pi k_m \Delta_f \right)} e^{i\omega z_1}, \end{split} \tag{4.53}$$

where $\omega = \sum_{l=1}^{m} k_l$. We can then again exchange the order of integration as both integrals are finite, as was shown in the previous computation for the charge Q^0 . Then,

$$\begin{split} (c) &= \mathcal{A}_{\Delta} \left[f_{+}, f_{-}, \{z, q\} \right] \Delta^{-\frac{q_{1}^{2}}{2}} \frac{1}{2\pi i} \left(-\frac{\mu}{2} \right) \sum_{n=0}^{\infty} \int_{\mathbb{R}} dk_{1} ... dk_{n} \\ \left(\frac{i}{2} \right)^{n} \left(\pm \sqrt{2} \right)^{n} \prod_{m=1}^{n} \frac{\mathcal{C}(k_{m})}{\sinh \left(\pi k_{m} \Delta_{f} \right)} \int_{\mathbb{R}} dz_{1} \left(\mu \sinh \left(\frac{z_{1} - z}{2\Delta_{f}} \right) \right)^{\pm \sqrt{2}q} e^{i\omega z_{1}} - (z_{1} \leftrightarrow \bar{z}_{1}), \end{split} \tag{4.54}$$

and we can apply residue calculus to the integral

$$\int_{\mathbb{R}} dz_1 \left(\mu \sinh \left(\frac{z_1 - z}{2\Delta_f} \right) \right)^{\pm \sqrt{2}q} e^{i\omega z_1} - \left(\mu \sinh \left(\frac{\bar{z}_1 - z}{2\Delta_f} \right) \right)^{\pm \sqrt{2}q} e^{i\omega \bar{z}_1}. \tag{4.55}$$

To evaluate these integrals, we need to choose both $q = \frac{s}{\sqrt{2}}$ as well as the sign of the current $J^{\pm}(z)$. We can start by first considering the case when we choose $J^{\pm}(z)$ and

 $q=\pm \frac{1}{\sqrt{2}}$, which corresponds to the case of annihilating the state by acting with the raising (lowering) operator on a state that is already the highest (lowest) element of the spin multiplet. In both of these cases, the integral reads

$$\mu \int_{\mathbb{R}} dz_1 \sinh\left(\frac{z_1 - z}{2\Delta_f}\right) e^{i\omega z_1} - \sinh\left(\frac{\bar{z}_1 - z}{2\Delta_f}\right) e^{i\omega \bar{z}_1},\tag{4.56}$$

and we can compute it by turning this integral into a contour integral. We start by more explicitly writing $z_1 = x + iy$ and expanding the hyperbolic sines into exponentials as

$$\frac{\mu}{2} \int_{\mathbb{R}} dx e^{\frac{x(i\omega+1)+y(i-\omega)-z}{2\Delta f}} - e^{\frac{x(i\omega-1)-y(i+\omega)+z}{2\Delta f}} - e^{\frac{x(i\omega-1)-y(i-\omega)-z}{2\Delta f}} + e^{\frac{x(i\omega-1)+y(i+\omega)+z}{2\Delta f}}, \tag{4.57}$$

which, after manipulating a bit, yields

$$\mu \int_{\mathbb{R}} dx \sinh\left(\frac{y(i-\omega)}{2\Delta_f}\right) e^{\frac{x(i\omega+1)-z}{2\Delta_f}} + \sinh\left(\frac{y(i+\omega)}{2\Delta_f}\right) e^{\frac{x(i\omega-1)+z}{2\Delta_f}}. \tag{4.58}$$

To ensure the convergence of these integrals, for $\omega > 0$, we must extend the contour with a semicircle above the real axis, while for $\omega < 0$, we must do so below the real axis. Special attention is required for the case $\omega = 0$, where the integral reads

$$\mu \sinh\left(\frac{iy}{2\Delta_f}\right) \int_{\mathbb{R}} dx \cosh\left(\frac{x-z}{2\Delta_f}\right), \tag{4.59}$$

which is clearly divergent. However, this divergence will get canceled once the commutator's second term is subtracted, as we are only dealing with the first term right now. We can thus write

$$\begin{split} \Theta(\omega)\mu \oint_{\text{UHP}} dx \sinh\left(\frac{y(i-\omega)}{2\Delta_f}\right) e^{\frac{x(i\omega+1)-z}{2\Delta_f}} + \sinh\left(\frac{y(i+\omega)}{2\Delta_f}\right) e^{\frac{x(i\omega-1)+z}{2\Delta_f}} + \\ \Theta(-\omega)\mu \oint_{\text{LHP}} dx \sinh\left(\frac{y(i-\omega)}{2\Delta_f}\right) e^{\frac{x(i\omega+1)-z}{2\Delta_f}} + \sinh\left(\frac{y(i+\omega)}{2\Delta_f}\right) e^{\frac{x(i\omega-1)+z}{2\Delta_f}} = 0, \end{split} \tag{4.60}$$

where UHP/LHP stands for the sunrise contour going along the upper/lower half plane and $\Theta(\omega)$ is the step function. However, since these contours encircle no poles whatsoever, as the integrand has none, the result of this integral is simply zero. We thus find that acting with the raising (lowering) current on the highest (lowest) states of a multiplet correctly sends them to zero. Of course, sewing from below yields the same result while subtracting the aforementioned divergence because the hyperbolic cosine is even.

We can now go back to (4.55) and consider the case of $J^{\mp}(z)$ and $s=\pm 1$, which is the case in which we go from the higher to the lower state of the multiplet or vice-versa. In this case (4.55) reads

$$\frac{1}{\mu} \int_{\mathbb{R}} dz_1 \mathrm{csch}\left(\frac{z_1-z}{2\Delta_f}\right) e^{i\omega z_1} - \mathrm{csch}\left(\frac{\bar{z}_1-z}{2\Delta_f}\right) e^{i\omega \bar{z}_1}, \tag{4.61}$$

and performing a similar analysis as the previous one, we can end up writing it as the contours integrals

$$\begin{split} \Theta(\omega) \frac{1}{\mu} \oint_{\text{UHP}} dz_1 \text{csch}\left(\frac{z_1 - z}{2\Delta_f}\right) e^{i\omega z_1} - \text{csch}\left(\frac{\bar{z}_1 - z}{2\Delta_f}\right) e^{i\omega \bar{z}_1} + \\ \Theta(-\omega) \frac{1}{\mu} \oint_{\text{LHP}} dz_1 \text{csch}\left(\frac{z_1 - z}{2\Delta_f}\right) e^{i\omega z_1} - \text{csch}\left(\frac{\bar{z}_1 - z}{2\Delta_f}\right) e^{i\omega \bar{z}_1}. \end{split} \tag{4.62}$$

Let us focus first on the first line of (4.62). If we write $z_1 = x + iy$ as previously, then the poles of the first term are located at $x = z - iy + 2\pi i n \Delta_f$ and the ones of the second term at $x = z + iy + 2\pi i n \Delta_f$ for $n \in \mathbb{Z}$. These are infinite towers of poles sitting in the imaginary axis, and the UHP contour encircles the poles corresponding to $n \in [1, \infty)$ for the first term and $n \in [0, \infty)$ for the second term since z < iy as we are sewing from the upper edge. We thus evaluate this integral using the residue theorem as

$$\begin{split} \Theta(\omega) \frac{1}{\mu} \oint_{\text{UHP}} dz_1 \left[\text{csch} \left(\frac{z_1 - z}{2\Delta_f} \right) e^{i\omega z_1} - \text{csch} \left(\frac{\bar{z}_1 - z}{2\Delta_f} \right) e^{i\omega \bar{z}_1} \right] = \\ \Theta(\omega) \frac{1}{\mu} 2\pi i \left[\sum_{n=1}^{\infty} 2\Delta_f (-1)^n e^{i\omega z + 2\Delta_f \pi \omega n} - \sum_{n=0}^{\infty} 2\Delta_f (-1)^n e^{i\omega z + 2\Delta_f \pi \omega n} \right] = \\ - \Theta(\omega) \frac{1}{\mu} 2\pi i 2\Delta_f e^{i\omega z}. \end{split} \tag{4.63}$$

Similarly, for the second line of (4.62), the LHP contour encircles the poles corresponding to $n \in [0, -\infty)$ for the first term and to $n \in [-1, -\infty)$ for the second term for $n \in \mathbb{Z}$. Similarly, but with the contour now being counterclockwise, the integral reads

$$\begin{split} \Theta(-\omega)\frac{1}{\mu}\oint_{\text{LHP}}dz_1 \text{csch}\left(\frac{z_1-z}{2\Delta_f}\right) e^{i\omega z_1} - \text{csch}\left(\frac{\bar{z}_1-z}{2\Delta_f}\right) e^{i\omega\bar{z}_1} = \\ \Theta(-\omega)\frac{1}{\mu}(-2\pi i)\left[\sum_{n=0}^{-\infty}2\Delta_f(-1)^n e^{i\omega z + 2\Delta_f\pi\omega n} - \sum_{n=1}^{-\infty}2\Delta_f(-1)^n e^{i\omega z + 2\Delta_f\pi\omega n}\right] = \\ -\Theta(-\omega)\frac{1}{\mu}2\pi i 2\Delta_f e^{i\omega z}. \end{split} \tag{4.64}$$

Collecting all the results, we conclude

$$\frac{1}{\mu} \int_{\mathbb{R}} dz_1 \operatorname{csch}\left(\frac{z_1 - z}{2\Delta_f}\right) e^{i\omega z_1} - \operatorname{csch}\left(\frac{\bar{z}_1 - z}{2\Delta_f}\right) e^{i\omega \bar{z}_1} = -\frac{2\pi i}{\mu} 2\Delta_f e^{i\omega z}. \tag{4.65}$$

Inserting this result back into (4.54) yields

$$(c) = \mathcal{A}_{\Delta} \left[f_{+}, f_{-}, \{z, q\} \right] \frac{1}{\Delta_{f}} \frac{1}{2\pi i} \left(-\frac{\mu}{2} \right) \sum_{n=0}^{\infty} \int_{\mathbb{R}} \mathrm{d}k_{1} ... \mathrm{d}k_{n} \left(\pm \frac{i}{2} \sqrt{2} \right)^{n}$$

$$\prod_{m=1}^{n} \frac{\mathcal{C}(k_{m})}{\sinh \left(\pi k_{m} \Delta_{f} \right)} \left(-\frac{2\pi i}{\mu} \right) 2\Delta_{f} e^{i\omega z},$$

$$(4.66)$$

which allows us to collect the sum back into an exponential to finally write, after taking the $\Delta_1 \to 0$ limit,

$$(c) = \frac{1}{2} \mathcal{A}_{\Delta} \left[f_{+}, f_{-}, \{ z, q \pm \sqrt{2} \} \right] \delta_{q, \mp \frac{1}{\sqrt{2}}}$$
 (4.67)

As before, sewing from the lower edge of the strip would again change the sign of the terms depending on z_1-z , and thus only change an overall minus sign. Therefore, in equation form, we have derived that

$$\sigma_{ss'}^{\pm}\mathcal{A}_{\Delta}\left[z,\frac{s'}{\sqrt{2}}\right] = \left\{ \begin{array}{c} 0, \ (s=\pm 1) \\ \mathcal{A}_{\Delta}\left[z,\frac{s}{\sqrt{2}} \pm \sqrt{2}\right], \ (s=\mp 1), \end{array} \right.$$

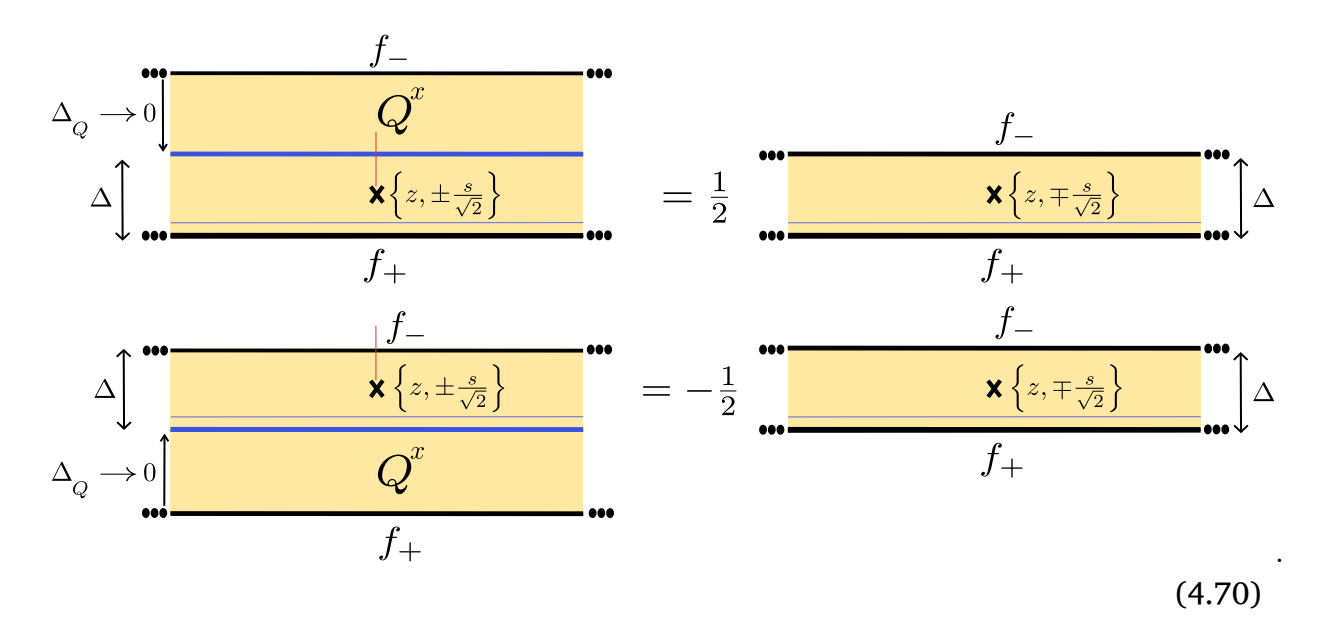
which is again the expected action of the raising and lowering operators σ^{\pm} on the corresponding states of the spin multiplet, but computed through the virtual space.

With these two computations we have confirmed the action of the algebra on the physical space via its representation on the virtual one. From these computations, we can also summarize the following rules for the action of single fMPS charges Q^a on a primary and in the usual spin basis, as these will be useful in the next section. Using that $\sigma^x = \frac{1}{2} \left(\sigma^+ + \sigma^-\right)$ and $\sigma^y = \frac{1}{2i} \left(\sigma^+ - \sigma^-\right)$, one can write for Q^x , first in equation form

$$\lim_{\Delta_Q \to 0} \int \mathcal{D}g Q_{\Delta_Q}^x[f_+,g] \mathcal{A}_{\Delta} \left[g,f_-,\left\{z,\pm\frac{s}{\sqrt{2}}\right\}\right] = \frac{1}{2} \mathcal{A}_{\Delta} \left[f_+,f_-,\left\{z,\mp\frac{s}{\sqrt{2}}\right\}\right], \qquad \textbf{(4.68)}$$

$$\lim_{\Delta_Q \to 0} \int \mathcal{D}g \mathcal{A}_{\Delta} \left[f_+, g, \left\{ z, \pm \frac{s}{\sqrt{2}} \right\} \right] Q_{\Delta_Q}^x[g, f_-] = -\frac{1}{2} \mathcal{A}_{\Delta} \left[f_+, f_-, \left\{ z, \mp \frac{s}{\sqrt{2}} \right\} \right], \quad \text{(4.69)}$$

or in diagrammatic notation

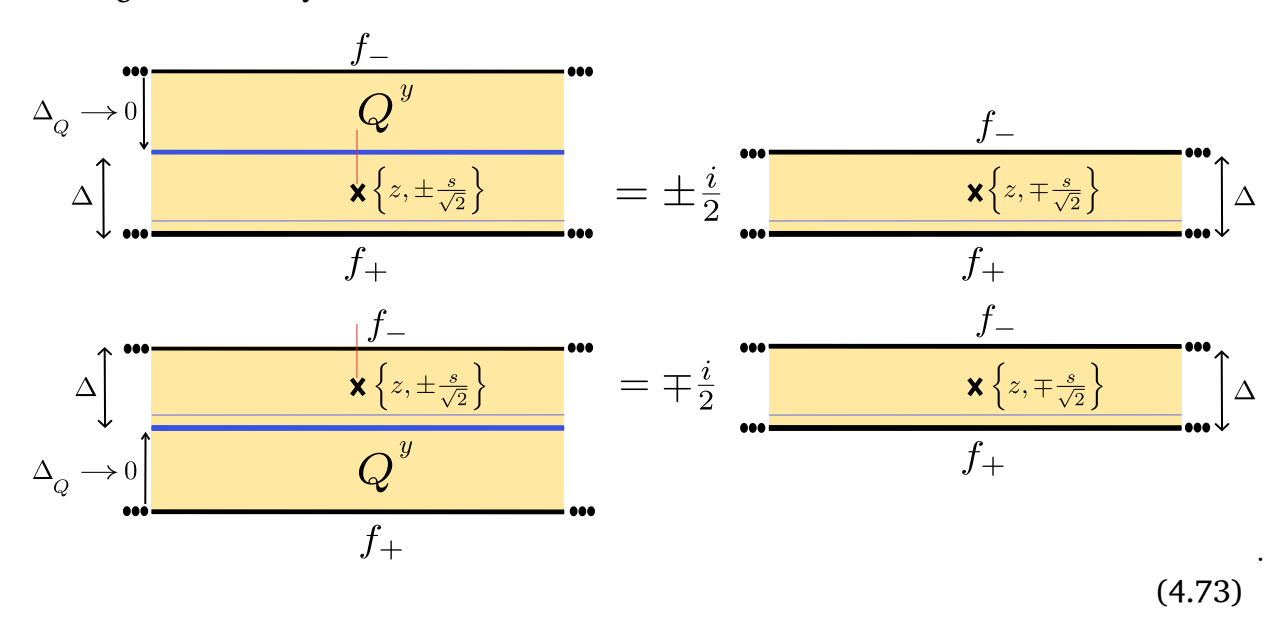


Analogously for Q^y , in equation form

$$\lim_{\Delta_Q \to 0} \int \mathcal{D}g Q_{\Delta_Q}^y[f_+, g] \mathcal{A}_{\Delta} \left[g, f_-, \left\{ z, \pm \frac{s}{\sqrt{2}} \right\} \right] = \pm \frac{i}{2} \mathcal{A}_{\Delta} \left[f_+, f_-, \left\{ z, \mp \frac{s}{\sqrt{2}} \right\} \right], \quad (4.71)$$

$$\lim_{\Delta_Q \to 0} \int \mathcal{D}g \mathcal{A}_{\Delta} \left[f_+, g, \left\{ z, \pm \frac{s}{\sqrt{2}} \right\} \right] Q_{\Delta_Q}^y[g, f_-] = \mp \frac{i}{2} \mathcal{A}_{\Delta} \left[f_+, f_-, \left\{ z, \mp \frac{s}{\sqrt{2}} \right\} \right], \ \ \textbf{(4.72)}$$

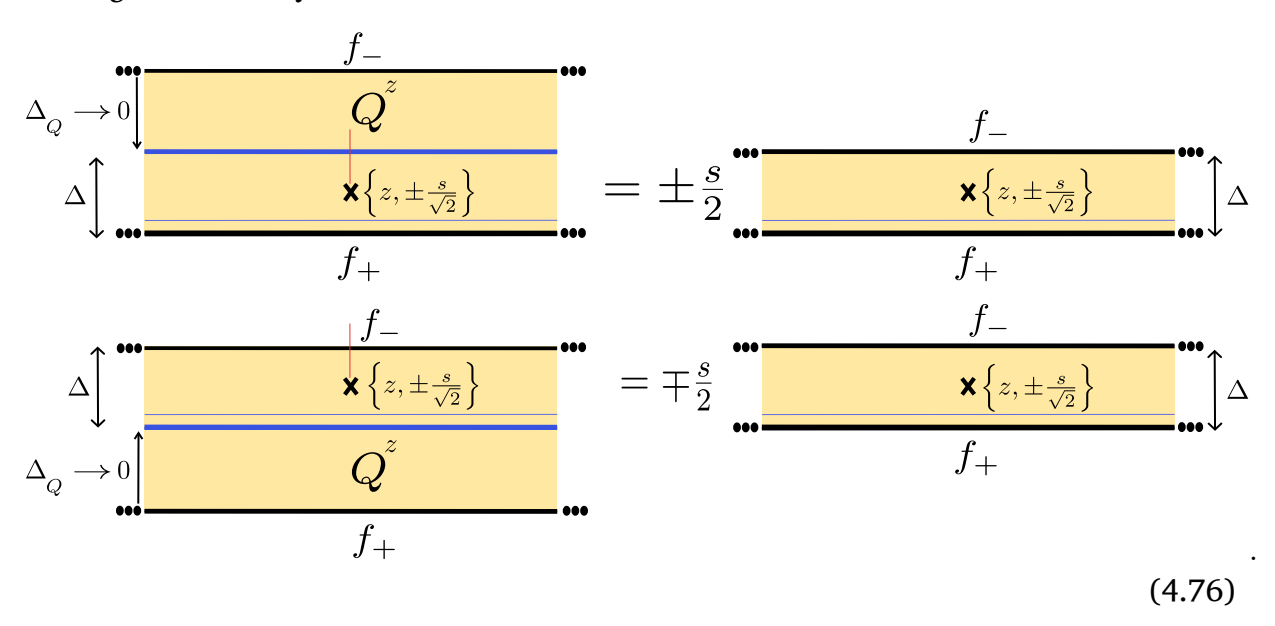
or diagrammatically



And finally for $Q^z=Q^0$, in equation form

$$\begin{split} &\lim_{\Delta_Q \to 0} \int \mathcal{D}g Q_{\Delta_Q}^z[f_+,g] \mathcal{A}_\Delta \left[g,f_-,\left\{z,\pm\frac{s}{\sqrt{2}}\right\}\right] = \pm\frac{s}{2} \mathcal{A}_\Delta \left[f_+,f_-,\left\{z,\pm\frac{s}{\sqrt{2}}\right\}\right], \quad \text{(4.74)} \\ &\lim_{\Delta_Q \to 0} \int \mathcal{D}g \mathcal{A}_\Delta \left[f_+,g,\left\{z,\pm\frac{s}{\sqrt{2}}\right\}\right] Q_{\Delta_Q}^z[g,f_-] = \mp\frac{s}{2} \mathcal{A}_\Delta \left[f_+,f_-,\left\{z,\pm\frac{s}{\sqrt{2}}\right\}\right], \quad \text{(4.75)} \end{split}$$

or diagrammatically



where if we compare this last equation with Equation (4.46), we see that we choose the limits of the strip to be $a=-\frac{\Delta}{2}$ and $b=\frac{\Delta}{2}$.

PROOF OF STATE INVARIANCE WITH THE GROUP-LEVEL PUSH-THROUGH RELATION

In this section, we prove that a state described by an fMPS is invariant under the group action corresponding to the infinitesimal algebra-level relations derived in the previous

section. Suppose we draw intuition from the usual SU(2) Lie group theory. In that case, the goal is to show that the state is invariant under a full rotation with angle θ and not only invariant with respect to the generators of said rotation. To prove this statement, the main formula of use is the following version of the renowned BCH formula

$$e^{-i\theta X}Ye^{i\theta X} = Y + i\theta[Y, X] + \frac{(i\theta)^2}{2}[X, [X, Y]] + \dots$$
 (4.77)

Since we have computed all the commutators in the previous section, it is easy to see the action of the whole exponential on a single strip, and they perfectly mirror the well-known results for SU(2). If we write a state described by a fMPS as

$$|\psi\rangle = \sum_{s_1...s_N = \pm 1} \int \mathcal{D}f_1...\mathcal{D}f_N \mathcal{A}_{f_1,f_2}^{s_1}...\mathcal{A}_{f_N,f_1}^{s_N} |s_1...s_N\rangle,$$
 (4.78)

where we use $\mathcal{A}_{f_i,f_{i+1}}$ for the functionals to simplify notation with the boundary indices and we act with the unitary matrix corresponding to a rotation around any of the axes $\alpha=x,y,z$, $U_i^\alpha(\theta)=\exp\{(i\theta\sigma_i^\alpha)\}$ on the i^{th} -spin, we can translate the action of this unitary onto the strip with the previously derived rules and the BCH formula. By moving the action to the virtual space, we have

$$\begin{split} U_{i}^{\alpha}(\theta)|\psi\rangle &= \sum_{s_{1}...s_{N}=1}^{d} \int \mathcal{D}f_{1}...\mathcal{D}f_{N}\mathcal{A}_{f_{1},f_{2}}^{s_{1}}...\mathcal{A}_{f_{N},f_{1}}^{s_{N}}U_{i}^{\alpha}(\theta)|s_{1}...s_{N}\rangle \\ &= \sum_{s_{1}...s_{N}=1}^{d} \int \mathcal{D}f_{1}...\mathcal{D}f_{N}\mathcal{A}_{f_{1},f_{2}}^{s_{1}}.\mathcal{A}_{f_{i},f_{i+1}}^{U_{i}^{\alpha}(\theta)s_{i}}.\mathcal{A}_{f_{N},f_{1}}^{s_{N}}|s_{1}...s_{N}\rangle, \end{split} \tag{4.79}$$

where what is meant by $\mathcal{A}_{f_i,f_{i+1}}^{U_i^{\alpha}(\theta)s_i}$ is that the unitary acts on the physical space of the i^{th} -strip, and thus it can be moved onto the virtual space by means of Equation (4.32). Mathematically, what we mean is

$$\mathcal{A}_{f_i,f_{i+1}}^{U_i^\alpha(\theta)s_i} = \int \mathcal{D}g\mathcal{D}f \exp\{(i\theta Q^\alpha[f_i,f])\} \\ \mathcal{A}_{f,g}^{s_i} \exp\{(-i\theta Q^\alpha[g,f_{i+1}])\}, \tag{4.80}$$

which is the same as Equation (4.32). Now, the BCH formula can be used to rewrite this in terms of commutators as

$$\mathcal{A}_{f_{i},f_{i+1}}^{U_{i}^{\alpha}(\theta)s_{i}} = \mathcal{A}_{f_{i},f_{i+1}}^{s_{i}} + i\theta \left[Q^{\alpha},\mathcal{A}^{s_{i}}\right]_{f_{i},f_{i+1}} + \dots \,. \tag{4.81}$$

Before we proceed any further, it is important to recall that the common zero mode enforces the charge neutrality condition upon the closing of the fTNS, which means that any term of the superposition (4.78) fulfills $\sum_{i=1}^N s_i = 0$. We start by considering the charge Q^z associated to the current H(z), whose commutator acts as $[Q^z, \mathcal{A}^{s_i}] = s_i \mathcal{A}_{f_i, f_{i+1}}^{s_i}$. Accordingly, the charges associated to the other generators act as $[Q^x, \mathcal{A}^{\pm s_i}] = \mathcal{A}_{f_i, f_{i+1}}^{\mp s_i}$ and $[Q^y, \mathcal{A}^{\pm s_i}] = \pm i \mathcal{A}_{f_i, f_{i+1}}^{\mp s_i}$, where all of these relations have been derived by repeated usage of the rules proved in the last section. We can then re-sum the commutator expansion, similar to how one does it for Pauli matrices, and obtain

$$\begin{split} \mathcal{A}_{f_{i},f_{i+1}}^{U_{i}^{z}(\theta)s_{i}} &= e^{i\theta s_{i}} \mathcal{A}_{f_{i},f_{i+1}}^{s_{i}} \\ \mathcal{A}_{f_{i},f_{i+1}}^{U_{i}^{x}(\theta)(\pm s_{i})} &= \cos\left(\frac{\theta}{2}\right) \mathcal{A}_{f_{i},f_{i+1}}^{\pm s_{i}} + i \sin\left(\frac{\theta}{2}\right) \mathcal{A}_{f_{i},f_{i+1}}^{\mp s_{i}} \\ \mathcal{A}_{f_{i},f_{i+1}}^{U_{i}^{y}(\theta)(\pm s_{i})} &= \cos\left(\frac{\theta}{2}\right) \mathcal{A}_{f_{i},f_{i+1}}^{\pm s_{i}} \mp \sin\left(\frac{\theta}{2}\right) \mathcal{A}_{f_{i},f_{i+1}}^{\mp s_{i}}. \end{split} \tag{4.82}$$

Once we know the action of a full rotation on a strip, we can tackle the question of whether the full state is invariant under this operation. Clearly, (4.78) is not invariant under the action of a single unitary on a site but only invariant under a unitary that acts on all spins simultaneously. We can easily see the invariance under rotations around the z-axis since

$$\begin{split} &U_{1}^{z}(\theta)\otimes...\otimes U_{N}^{z}(\theta)|\psi\rangle = \sum_{s_{1}...s_{N}=\pm1}\int\mathcal{D}f_{1}...\mathcal{D}f_{N}\mathcal{A}_{f_{1},f_{2}}^{U_{1}^{z}(\theta)s_{1}}...\mathcal{A}_{f_{N},f_{1}}^{U_{N}^{z}(\theta)s_{N}}|s_{1}...s_{N}\rangle\\ &=\sum_{s_{1}...s_{N}=\pm1}e^{i\theta\sum_{i}s_{i}}\int\mathcal{D}f_{1}...\mathcal{D}f_{N}\mathcal{A}_{f_{1},f_{2}}^{s_{1}}...\mathcal{A}_{f_{N},f_{1}}^{s_{N}}|s_{1}...s_{N}\rangle = |\psi\rangle, \end{split} \tag{4.83}$$

where the last equality follows from charge neutrality. For our concrete example of fMPS, the phase factors χ_{s_i} present in (3.85) are known collectively as the Marshall sign, which counts the number of "down"-spins on odd sites and gives a phase accordingly. This sign is the key to showing invariance under rotations under any of the other two axes, and we show it for the x-axis by means of induction. Let us assume that $U_1^x(\theta) \otimes ... \otimes U_{2n}^x(\theta) |\psi\rangle = |\psi\rangle$ for a state consisting of n pairs of spins. Then, for a state consisting of n+1 pairs

$$\begin{split} &U_{1}^{x}(\theta)\otimes\ldots\otimes U_{2n}^{x}(\theta)\otimes U_{2n+1}^{x}(\theta)\otimes U_{2n+2}^{x}(\theta)|\psi\rangle = U_{1}^{x}(\theta)\otimes\ldots\otimes U_{2n}^{x}(\theta)\\ &\sum_{s_{1}\dots s_{2n}=\pm1}\sum_{s_{2n+1},s_{2n+2}=\pm1}\int\mathcal{D}[f_{1}]\dots\mathcal{D}[f_{2n+2}]\mathcal{A}_{f_{1},f_{2}}^{s_{1}}\dots\mathcal{A}_{f_{2n},f_{1}}^{s_{2n}}\mathcal{A}_{f_{2n+1},f_{2n+2}}^{U_{2n+1}^{x}(\theta)s_{2n+2}}\mathcal{A}_{f_{2n+2},f_{1}}^{U_{2n+2}^{x}(\theta)s_{2n+2}}|s_{1}\dots s_{2n+2}\rangle, \end{split}$$

where we acted with the unitaries corresponding to the last pair. The action of these two unitaries yields

$$\mathcal{A}_{f_{2n+1},f_{2n+2}}^{U_{2n+1}^{x}(\theta)s_{2n+1}} \mathcal{A}_{f_{2n+2},f_{1}}^{U_{2n+2}^{x}(\theta)s_{2n+2}} = \left(\cos\left(\frac{\theta}{2}\right) \mathcal{A}_{f_{2n+1},f_{2n+2}}^{\pm s_{2n+1}} + i\sin\left(\frac{\theta}{2}\right) \mathcal{A}_{f_{2n+1},f_{2n+2}}^{\mp s_{2n+1}}\right) \cdot \\ \left(\cos\left(\frac{\theta}{2}\right) \mathcal{A}_{f_{2n+2},f_{1}}^{\pm s_{2n+2}} + i\sin\left(\frac{\theta}{2}\right) \mathcal{A}_{f_{2n+2},f_{1}}^{\mp s_{2n+2}}\right), \tag{4.85}$$

on the two functionals alone. Since the charge neutrality condition must be obeyed by all the terms of the superposition of spins, only configurations that preserve it can contribute to the sum. That means that for every term of the sum with fixed spin values $s_1, ..., s_{2n}$, the two remaining spins can only be able to either flip their value or remain the same together. That means that we can then simplify (4.85) to

$$\cos\left(\frac{\theta}{2}\right)^{2}\mathcal{A}_{f_{2n+1},f_{2n+2}}^{\pm s_{2n+1}}\mathcal{A}_{f_{2n+2},f_{1}}^{\pm s_{2n+2}} - \sin\left(\frac{\theta}{2}\right)^{2}\mathcal{A}_{f_{2n+1},f_{2n+2}}^{\mp s_{2n+1}}\mathcal{A}_{f_{2n+2},f_{1}}^{\mp s_{2n+2}} = \mathcal{A}_{f_{2n+1},f_{2n+2}}^{\pm s_{2n+1}}\mathcal{A}_{f_{2n+2},f_{1}}^{\pm s_{2n+2}},$$

$$(4.86)$$

where the last equality follows from the fact that the first and second terms are related by the Marshall sign. The Marshall sign always changes when two neighboring spins swap values together, as that operation can only change the number of "down" spins that are sitting at odd sites. This shows that we recover back the same state when we add an extra pair and it also shows the invariance of a single pair, thus concluding the proof.

4.3 APPLICATION TO THE MAJUMDAR-GOSH MODEL AND SPT PHASES

Our original question for this chapter was: Can we understand the SPT classification of standard MPS in the context of fMPS? So far, we have seen that we can define a consistent notion of symmetries for the physical and virtual space of fMPS while also establishing a push-through relation between both representations. We know from Chapter 2 that the representation found in the virtual space of an MPS can be, in general, projective, such that non-trivial cocycle can help us distinguish different SPT phases. Therefore, we must check whether the representation defined by the fMPSs of Q^x , Q^y , and Q^z is projective.

For the standard representation theory of SU(2), it is common knowledge that the representations with half-integer spin are projective representations of SO(3), while the ones with integer spin are linear representations [209]. One way that one can check this is by computing any of the group commutators to extract the cocycle. For the case of the spin $-\frac{1}{2}$ representations of SU(2) one such group commutator reads $\sigma^x \sigma^z \sigma^x \sigma^z$. Indeed, if one computes this product of matrices, one obtains $-\mathbb{I}$, as opposed to the expected \mathbb{I} for a linear representation. The minus sign is the characteristic cocycle of projective representations, and therefore it will be enough for us to show that such a sign appears for fMPS.

Our first approach would be to compute

$$\sigma^x \sigma^z \sigma^x \sigma^z \mathcal{A}_{\Lambda} [f_1, f_2, \{z, s\}], \tag{4.87}$$

through its action in the virtual space. By recursive usage of Equation (4.34), one can push these four algebra operators down to the virtual space to obtain a combination of 16 different sewing setups. Slowly working through them, after consistent application of the rules found in Equations (4.70),(4.73) and (4.76), one obtains that

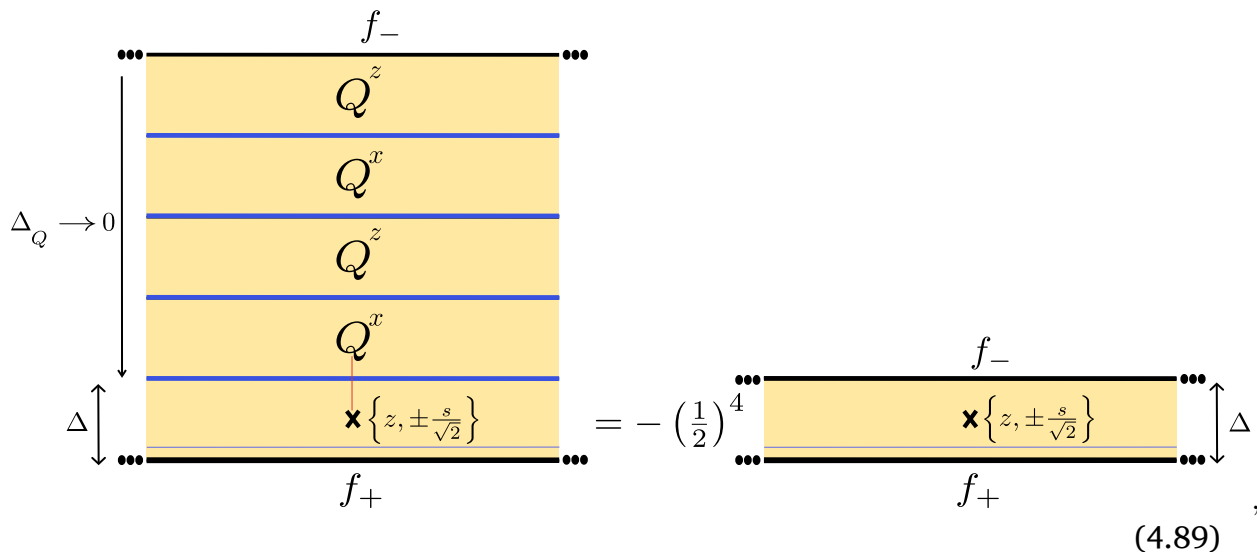
$$\sigma^{x}\sigma^{z}\sigma^{x}\sigma^{z}\mathcal{A}_{\Lambda}[f_{1}, f_{2}, \{z, s\}] = -\mathcal{A}_{\Lambda}[f_{1}, f_{2}, \{z, s\}], \tag{4.88}$$

which is consistent with the fact that the representation on the physical space was projective from the very beginning. After confirming that the virtual space reproduces the correct representation of the physical space, we can now turn to the question of whether the operators Q^x , Q^y , Q^z themselves form a projective representation of SO(3).

We can extract some conclusions even before computing anything by using some knowledge borrowed from representation theory. For instance, we already know that the Kâc-Moody algebra will always yield projective representations, as it is an affine extension of a standard Lie algebra. This is a consequence of a very deep theorem of representation theory known as Bargmann's theorem [210]. Informally, this theorem states that if the second cohomology group for a continuous Lie group $H^2(\mathfrak{g},\mathbb{R})$ is trivial, any projective representation G can be lifted to a linear one by means of its double cover. In other words, as long as a non-trivial central extension exists, an infinite dimensional representation of a Lie group will always be projective. Therefore, this guarantees that any Kâc-Moody algebra will yield a projective representation. However, we are dealing just with the Noether charges that originate from this current algebra, and we wish to understand them as if they were a "matrix" representation.

Thus, we compute the group commutator as the product $Q^xQ^zQ^xQ^z$. Because of the distributional character of these fMPS due to the $\Delta_Q \to 0$ limit, we must act with this

product on a primary fMPS so that we can have a well-defined operation. Thus, the task is to compute diagrammatically



which yields the negative sign in front of the normalization factor $\frac{1}{2^4}$, indicating that the charges Q^a form a projective representation.

This result opens the door to exploring tasks such as classifying different states described by this fMPS according to the usual criterion of SPT classification that one finds in MPS [201]. As we have shown already in Chapter 3, specifically Equation 3.85, among the states within the family defined by the free boson, fMPS are the ground-states of the critical point of the Haldane-Shastry model. In [44], a similar ansatz based on vertex operators named infinite MPS (iMPS), the original prototype behind fTNS, was used to study different models whose critical points were described by a c=1 CFT. In their study, the positions of the vertex operator insertions were treated as the variational parameters to maximize the overlap with the real ground state numerically. Because both the iMPS and the fMPS descriptions describe the same states, the following question arises:

Can we use the physical position of the spin in fMPS to change the properties of the whole state? If so, can we predict this change in the properties of the entire state from one or a few tensors, similarly to how one does it in MPS?

We explore this question by analyzing how the representation of the extended SU(2) symmetry in the virtual space depends on the spin positions of two tensors.

First, we consider the limit in which two spins are placed very close together, as shown on the left Figure 4.1, which in CFT literature is the limit that one must consider when computing an OPE [37]. As was shown in Equation (4.7) for the WZW SU(2)₁ model, the fusion rules for the two primary fields $\phi_{\frac{1}{2}}$ are $\phi_{\frac{1}{2}} \times \phi_{\frac{1}{2}} = \phi_0$. This means that whenever two spins are very close, CFT tells us that the dominant term in the expansion should be the identity. By taking the limit $z_2 \to z_1$ in equation (3.80), similar to the one taken when performing an OPE, the expression for a strip with two spins in this

limit becomes

$$\begin{split} \lim_{z_1 \to z_2} \mathcal{A}_{\Delta} \left[f_+, f_-, \{ z_1, s_1, z_2, s_2 \} \right] &\sim \frac{\mu^{\frac{s_1 s_2}{2}} \delta_{s1, -s2} \sqrt{2\Delta}}{\sqrt{z_1 - z_2}} \mathcal{A}_{\Delta} \left[f_+, f_-, \{ z_1, 0 \} \right] = \\ \frac{\sqrt{2} \delta_{s1, -s2}}{\mu \sqrt{z_1 - z_2}} \mathbb{I}_{\Delta} [f_+, f_-], \end{split}$$

where $\delta_{s1,-s2}$ ensures the spins have opposite value and \sim means that we have omitted sub-leading terms in z_1-z_2 . Remarkably, whenever two insertions get close to each other, the functional greatly simplifies and becomes an identity in the virtual space. The decoupling of the virtual space from the physical space is a phenomenon one encounters when considering dimerized states in MPS theory [93]. To mimic the results of MPS, we are interested in seeing how the symmetry is represented in this limit. We can see by applying the rules (4.70), (4.73) and (4.76) on the identity, that since it corresponds to a strip with s=0, the outcome is always 0. This is akin to how the monomial representation of $\mathfrak{su}(2)$ acts on the j=0 element. The main point to take away is that this limit forces the virtual space to be on the trivial representation j=0 of SU(2), making all the symmetry operators simply the identity.

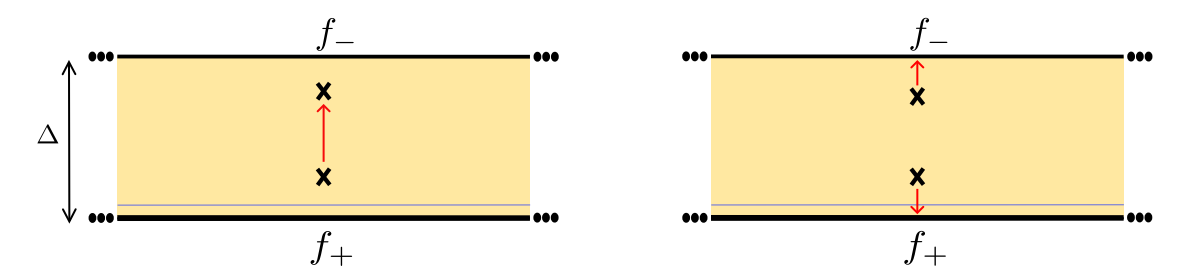


Figure 4.1: This figure shows the two limits of interest for a pair of spin insertions. The left strip corresponds to the trivial representation, while the right strip belongs to the non-trivial one.

To obtain the $j=\frac{1}{2}$ representation, we consider the opposite limit, in which two spins are placed as far apart from one another as possible, as shown on the right Figure of 4.1. Because of the inherent long-range interaction of the strips, we can only clearly understand the virtual space representation of any of the two boundaries when we take the limit $\Delta \to \infty$, such that only the dominant representation remains. Let us first study this limit for a single spin, in which we can approach the limit in different ways. We could send the strip's upper (lower) boundary to the $(-)\infty$ limit or both of them simultaneously. In either case, whenever the spin is not located exactly at the boundary, the functional simplifies to

$$\lim_{\Delta \to \infty} \mathcal{A}_{\Delta} \left[f_+, f_-, \{z, s\} \right] = \frac{1}{\Lambda^{\frac{s^2}{4}}} \mathbb{I}_{\infty} [f_+, f_-], \tag{4.90}$$

where $\mathbb{I}_{\infty}[f_+,f_-]$ stands for the corresponding identity on virtual space for an infinitely wide strip. However, whenever the spin is sitting exactly at one of the boundaries being taken to infinity, the virtual space does not fully trivialize and instead remains within the corresponding spin representation, and we denote this limit by

$$\lim_{\Delta \to \infty} \mathcal{A}_{\Delta} \left[f_{+}, f_{-}, \{ z_{b}, s \} \right] = \frac{1}{\Delta^{\frac{s^{2}}{4}}} \mathcal{A}_{\infty} \left[f_{+}, f_{-}, \{ z_{b}, s \} \right], \tag{4.91}$$

where z_b is $i\pi b$ $(i\pi a)$ for the upper (lower) boundary. The explicit expression corresponding to equation (4.90) is

$$\begin{split} \mathbb{I}_{\infty} \left[f_{+}, f_{-} \right] &= e^{-R_{\infty} \left[f_{+}, f_{-} \right]}, \\ R_{\infty} \left[f_{+}, f_{-} \right] &= + \frac{1}{2} \int_{0}^{\infty} \mathrm{d}k \left(\hat{f}_{+}(k) \quad \hat{f}_{-}(k) \right) \begin{pmatrix} k & 0 \\ 0 & k \end{pmatrix} \begin{pmatrix} \hat{f}_{+}^{*}(k) \\ \hat{f}_{-}^{*}(k) \end{pmatrix}, \end{split} \tag{4.92}$$

and the one for equation (4.91) is

$$\begin{split} \mathcal{A}_{\infty} \left[f_{+}, f_{-}, \{ z_{b}, s \} \right] &= e^{-R_{\infty} \left[f_{+}, f_{-}, \{ z_{b}, s \} \right]}, \\ R_{\infty} \left[f_{+}, f_{-}, \{ z_{b}, s \} \right] &= + \frac{1}{2} \int_{0}^{\infty} \mathrm{d}k \left(\hat{f}_{+}(k) - \hat{f}_{-}(k) \right) \begin{pmatrix} k & 0 \\ 0 & k \end{pmatrix} \begin{pmatrix} \hat{f}_{+}^{*}(k) \\ \hat{f}_{-}^{*}(k) \end{pmatrix} \\ &- \frac{i}{2\sqrt{2}} s \int_{\mathbb{R}} \mathrm{d}k \hat{f}_{b}(k), \end{split} \tag{4.93}$$

where the contribution of the zero mode has been omitted and $\hat{f}_b(k)$ is the corresponding boundary function of whichever boundary the spin is located at. We can then apply the rules (4.70), (4.73) and (4.76), which were derived in a Δ -independent fashion, to conclude that the boundary of the strip at which the spin sits remains in the $s=\frac{1}{2}$ representation. Similar expressions are obtained whenever we have several spins within the strip, the only contributions surviving the infinite width limit being the boundary ones. We can hence see that in this limit, the virtual space representation is completely dominated by whichever spin is located exactly at the boundary. It is, hence, non-trivial and carries the representation label of the spin itself.

When considering the case of finite Δ , we can only detect when one representation is favored by parameterizing the spin insertions by their distance away from the translation symmetric configuration. Let us take the case of two insertions, whose positions are parameterized by $z_1=i\pi a-\frac{i\pi\Delta}{4}\mp i\pi\delta$ and $z_2=i\pi a+\frac{i\pi\Delta}{4}\pm i\pi\delta$, where the term $i\pi a$ is there to ensure our choice of coordinate axis for the insertions do not matter. With these explicit positions, the 2-spin functional reads

$$\left(\frac{i\mu}{\sqrt{2}}\right)^{\frac{s_1s_2}{2}} \left(\cos\left(\frac{\delta\pi}{\Delta}\right) \pm \sin\left(\frac{\delta\pi}{\Delta}\right)\right)^{\frac{s_1s_2}{2}} \mathcal{A}_{\Delta}^*,\tag{4.94}$$

where \mathcal{A}_{Δ}^* we mean the two-strip functional without the interaction term between the spins, that is, without the last line of equation (3.80). We can then check which values of δ maximize this expression and how these relate to the different phases. We can see that whenever the spins have opposite value $\frac{s_1s_2}{2}=-1$, the Equation (4.94) diverges for $\delta=\pm\frac{\Delta}{4}$, which exactly corresponds to the configuration presented in Equation (??). These positions correspond to the spins meeting at the center of the system, and as we have seen, this situation corresponds to the virtual space trivializing. Once we close the strip, the charge-neutrality condition prevents the strip with $\frac{s_1s_2}{2}=+1$ from contributing. However, we can still see which representations are favored in this case. We find that the maximum happens as well for $\delta=\pm\frac{\Delta}{4}$, in which case the functional simply inherits the representation of the spin closest to each boundary, as that is the dominant term as we take the $\Delta \to \infty$ limit. Thus, we see that as soon as the insertions depart from the perfect spacing, one of the two representations immediately becomes favored, depending on which pairing is encouraged.

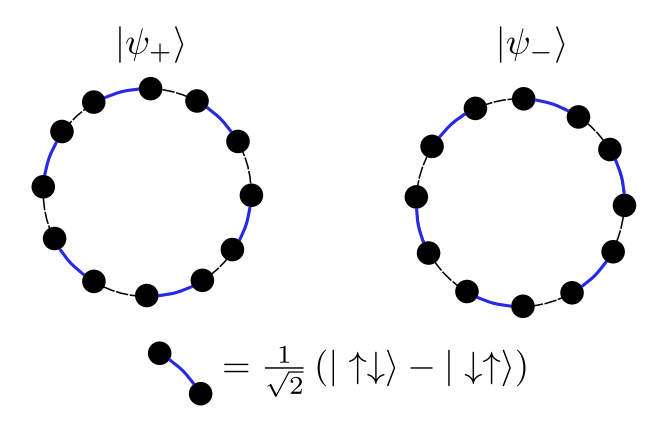


Figure 4.2: Schematic representation of the two possible configurations of dimer states

We can now take the spin configuration on the left of Figure 4.1 a step further for the case in which we have more than two spins. Let us start with four spins and consider the limit $z_1 \to z_2$ and $z_3 \to z_4$, which corresponds to a situation like in equation (??). If the distance between any two spins is denoted by $z_i - z_j = z_{ij}$, in the limit where $z_{12}, z_{34} \to 0$ the four-spin functional becomes

$$\frac{2\delta_{s_1,-s_2}\delta_{s_3,-s_4}}{\mu\sqrt{z_{12}}\sqrt{z_{34}}}\mathbb{I}_{\Delta}[f_+,f_-] + \frac{\delta_{s_1,s_2}\delta_{s_3,s_4}\delta_{s_1,-s_3}\mu\sqrt{z_{12}}\sqrt{z_{34}}}{2}\mathcal{A}_{\Delta}\left[f_+,f_-,\{z_i^*,2s_i^*\}_{i=1}^2\right],$$

where z_i^* are the positions at which the different pair of spins meet, and s_i^* is the value of any of the two original spins of the pair. The dominant term is the expected identity in the virtual space as it arises from the charge neutrality condition. However, having two pairs allows for the individual pairs not to have opposite spin values but for the different pairs to compensate for each other's sign, and thus, a new sub-leading term can arise. This sub-leading term corresponds exactly to a strip containing two spins of higher value, and thus, a state constructed out of this term falls into a higher SU(2) spin representation from the original one.

The different limits explored in this section are useful as they also correspond to the two distinct topological ground states of the Majumdar-Ghosh [211] point of the $J_1 - J_2$ Heisenberg model on an even number of sites N, defined by

$$\mathcal{H}_{J_1,J_2} = \sum_{i=1}^{N} \left(J_1 \vec{S}_i \cdot \vec{S}_{i+1} + J_2 \vec{S}_i \cdot \vec{S}_{i+2} \right), \tag{4.95}$$

where \vec{S}_i is the spin operator on the i^{th} -site and periodic boundary conditions are assumed. This model hosts an exactly solvable point at $\frac{J_2}{J_1}=0.5$ in which it is known that the exact ground states are the two dimerized states, also known as an RVB configuration [212]. These states can be schematically represented on a 1-dimensional chain as in Figure 4.2. In the left figure, we see a potential dimerization configuration, in which all spins maximally entangle themselves with either of its two neighbors, whilst the other configuration is concerned with the other possible choice. We wish to establish a parallel to these two configurations with the limits found in Figure 4.1.

In [44], the connection between fTNS and this model was established. With our results, we can now tell apart the two dimerized ground states based only on symmetry considerations, analogous to the treatment of the AKLT model with MPS [213, 214]. Indeed, the first dimerized configuration corresponds to the left of Figure 4.1 but for N

pairs of spins, in which we have seen that the dominant contribution carries the trivial representation on its virtual space. On the other hand, the opposite dimerized configuration, corresponding to the opposite pairing, will host a pair of spins on the edges that will carry a non-trivial representation, which we identify with the topologically inequivalent ground state. Therefore, it seems like we can understand SPT order in the context of a gapless model with fMPS while utilizing the same logic of MPS techniques.

Before concluding, we should elaborate on what we mean by two fTNS corresponding to distinct critical SPT phases. While we can check which SU(2)-representation lies on the virtual space, a priori, it could be possible that by redefining the parameters of the fTNS, such as the boundary functions $f_+(k), f_-(k)$ or its width Δ , we could map to a different representation. We can easily see that a redefinition of the boundary functions alone is not enough to change the representation since the new functions $\tilde{f}_+(k), \tilde{f}_-(k)$ must still be square-integrable by definition. If we take a look at the last term of Equation (3.78), we note that the spin representation is determined by the term $s_i e^{ikz_i}$. In order to change the representation, the new function would need to change this term, and since it is exponential, it would be impossible for it to remain in $\mathbb{L}^2(\mathbb{R})$.

The only way in which this term could be absorbed would be if the width of the strip after the map $\tilde{\Delta}$ were to be such that the function remained integrable or if it simply changed the s_i directly. However, there is no way to redefine the functions in a way that simultaneously keeps the boundary functions in $\mathbb{L}^2(\mathbb{R})$ and keeps the sewing condition of Equation (3.80) intact. Thus, the only way in which a fTNS can change its representation is with the value and position of the spin that it represents. Consequently, we can call inequivalent two fTNSs which describe different spin representations as they can not be mapped into one another by a redefinition of the parameters of the virtual space.

4.4 OUTLOOK

In this Chapter, we have provided evidence that the theory of MPS can be translated to fMPS, allowing us to preserve our intuition from TNS in a realm in which it was previously impossible to do so analytically. To establish a parallel with the standard theory of SPT phase classification of MPS, we have derived the relation between the finite representation of SU(2) on the physical index of a fTNS and its corresponding representation as functional conformal charges on the virtual space. We have used this construction to identify the different topological properties of the two distinct ground states of the Majumdar-Ghosh point of the J_1-J_2 model. The way in which we understand these different groundstates draws intuition and mimics the theory of standard MPS, which was our departing goal for this project. Ultimately, we wish to further understand fTNS as a generalization of TNS in any dimension, but such that we can still retain most of the knowledge and structure of the theory of TNS. Therefore, understanding the simplest case of a 1-dimensional system was the first successful stepping stone in this direction.

As possible, new open directions and interesting computations in the context of symmetric models that can be suitably represented by 1-dimensional fMPS we propose :

1. Computing the fMPS corresponding to one of the simplest fermionic actions, the $c=\frac{1}{2}$ CFT, commonly known as the Majorana fermion. This theory also has a

simple description in terms of a linear action, and therefore, the techniques developed for the free boson fMPS should apply as well. In fact, a theory of N real fermions constitutes an example of the $\mathfrak{so}(N)_1$ WZW model, and therefore, another model in which one could also ask questions about the extended symmetry of the CFT and its connection to the physical symmetry of the spin.

- 2. When it comes to the study of symmetries, another potentially interesting and simple model would be the ghost model [37]. Although its connection to real physical systems is much more limited and serves more as an academic example, it is known from the Wakimoto free field representation of WZW models that any Lie algebra g can be constructed out of a number of free bosons and pairs of ghost systems [37]. Therefore, the study of the ghost system alone would represent a stepping stone in order to develop the free field fMPS representation of a generic WZW theory and, therefore, of any generic virtual extended symmetry.
- 3. In chapter 3 we have also seen the construction of fPEPS and therefore a natural question would be whether we can also translate the theory of PEPS to fPEPS. As we have seen in Chapter 2, the study of topological order with PEPS involves only virtual symmetries of the tensor. Therefore, in the context of fPEPS we would first need to find an operator in the context of the CFT that leaves the vertex operators within the correlators invariant. From there, one can start constructing the analogous symmetry operators of PEPS by breaking down and representing the CFT operator as fTNSs as well. This and other questions related to fPEPS are already being explored in one of the upcoming works mentioned at the beginning of this thesis.
- 4. Finally, a description of fTNS in the basis of Cardy states [167] would also constitute a valuable upgrade in the context of the study of symmetries. Such a representation would allow to describe symmetries of CFTs without the need to translate them into a functional tensor, removing, for instance, the need to consider them as distributional objects. As we mentioned in the Outlook of Chapter 3, such a representation would also allow for the study of, even if not exactly, non-Gaussian and more complicated CFTs, as was done in [140].

5 CTNS RESULTS

Throughout this thesis, we have focused on providing new TN ansatzes for spin systems, such that these can exactly describe systems previously out of reach for TN techniques. To do so, we have focused on describing the virtual space by means of a field theory, therefore studying an infinite-dimensional virtual space and, thus, a possible notion of a continuum theory. A very natural question would be the following: how would a TN ansatz look if the target physical system of study was not a discrete spin system or generically a system with a local finite Hilbert space? Could one provide an ansatz targeting already continuous theories, such as QFTs?

Naturally, this question has already been answered in 1-dimensional non-relativistic systems, leading to the ansatz known as continuous MPS (cMPS) [184],[215]. This ansatz constitutes the first example of a TN approach to the analytical description of a QFT using an optimization over a virtual space. Particular of cMPS is that the variational space remains finite-dimensional, allowing for variational optimization of the groundstates of interacting theories in external potentials [216] or even the time evolution of an interacting Bose gas as shown in [217]. Another possible extension of 1-dimensional TNS is found in continuous MERA (cMERA) [218], in which a similar theoretical generalization as in cMPS was carried out for the MERA architecture [219]. cMERA has also been successfully used in several scenarios, such as in the description of Chern insulators [220] or for conformal field theories with boundaries and defects [221].

Despite the success of 1-dimensional systems, attempts to extend TNS theory to the continuum in higher dimensions have proven to be challenging. A naive extension faces the issue of a preferred temporal direction and, therefore, the breaking of Euclidean invariance, a symmetry paramount for non-relativistic QFTs. Although the most prominent extension that solved this problem is the one found in [222], one can show that this extension is no longer the limit to the continuum of a finite TNs [223].

The lack of a satisfactory extension to higher dimensional systems that followed a TN approach motivated the authors of [185] to provide the first continuous TN ansatz in higher dimensions, which was named a continuous Tensor Network state (cTNS). cTNS are shown to be a genuine continuum limit of a finite TNs that retain Euclidean invariance, and they can be shown to reduce to cMPS for 1-dimensional systems. Despite a very elegant theoretical construction, there have not been as many numerical results that explore their applications for physical systems. The main result so far has been a variational optimization over Gaussian bosonic states [224].

Although cTNS is a very recent theoretical development, its applicability to physical systems remains largely unexplored numerically or analytically. This lack of exploration is precisely the starting point that motivates our question for this Chapter:

Is it possible to analytically find a suitable use-case scenario to show that cTNS has a theoretical advantage over other ansatzes? Can we use the theory of TNS, mainly the bulk-boundary correspondence, to obtain new analytical insights into the correlation functions of interacting QFTs?

5.1 DEFINITION OF CONTINUOUS TNS

Continuous TNS (cTNS) are intuitively defined as an ansatz that couples a virtual QFT to the target physical QFT, such that one can compute correlations of the latter via the correlations of the former. To define such a state, one must first define all the parameters of both QFTs. Let the pair (\mathcal{M},g) denote a d-dimensional orientable Riemannian manifold with a boundary $\partial \mathcal{M}$ and metric tensor g. Let D be a positive integer to which we will refer as the bond field dimension, whose purpose is to quantify the number of virtual fields present in the virtual QFT. Let V and α_i , for $i=1,\ldots,N$ be complex-valued functions on \mathbb{R}^D , and let B be a complex-valued functional on $L^2(\partial \mathfrak{M})$ that specifies the boundary conditions. These three functions, V,α_i,B , serve as the variational parameters that act as the "optimization" parameters for the virtual QFT.

A cTNS with a bosonic virtual QFT is then defined, slightly more generally than in [185], by a path integral of a D-component virtual bosonic field ϕ :

$$\begin{split} |V,B,\{\alpha_i\}\rangle &= \int_{\mathcal{M}} \mathcal{D}\phi B\left(\phi|_{\partial\mathcal{M}}\right) \exp\left\{-\int_{\mathcal{M}} d^dx \sqrt{g} \left(\frac{1}{2}\sum_{k=1}^D g^{\mu\nu}\partial_{\mu}\phi_k\partial_{\nu}\phi_k + V[x,\phi(x),\nabla\phi(x)]\right) - \sum_{i=1}^N \alpha_i \left[x,\phi(x),\nabla\phi(x)\right]\psi_i^{\dagger}(x)\right)\right\} |0\rangle, \end{split} \tag{5.1}$$

where $|0\rangle$ is the Fock vacuum state of the physical theory, and $[\psi_i(x),\psi_j^\dagger(y)]=\delta_{ij}\delta^d(x-y)$, so that $\psi_i(x)$ are the N usual bosonic field operators of the physical theory. The virtual field ϕ over which the path integral sums should be interpreted as the bond dimension degree of freedom that is known from usual TNs. If both V and the α_i 's do not depend explicitly on $x\in\mathcal{M}$, then the cTNS is translationally invariant. As seen in Equation (5.1) The function $V[x,\phi(x),\nabla\phi(x)]$ acts as the "potential" term of the action of the virtual QFT, while the $\alpha_i[x,\phi(x),\nabla\phi(x)]$ serve as the coupling between the physical and the virtual QFTs. Each of the terms α_i couples the virtual QFT to each physical field ψ_i . Finally, the functional B serves as the boundary condition for the virtual QFT, meaning that if $\partial\mathcal{M}=\emptyset$, then it can be simply set to $B(\phi|_{\partial\mathcal{M}})=1$, making the virtual QFT live in a compact space such as a surface with genus χ . If the space \mathcal{M} is compact, then one needs to specify Dirichlet, Neumann, or more arbitrary boundary conditions as shown in [185].

In the simplest case, \mathcal{M} is taken to be just a simple subset of Euclidean space (i.e., a

non-empty connected open set) $\Omega \subseteq \mathbb{R}^d$. In this case

$$\begin{split} |V,B,\{\alpha_i\}\rangle &= \int \!\! \mathcal{D}\phi B\left(\phi|_{\partial\Omega}\right) \exp\left\{-\int_{\Omega} d^dx \left(\frac{1}{2}\sum_{k=1}^D \left[\nabla\phi_k(x)\right]^2 + V[x,\phi(x),\nabla\phi(x)]\right. \right. \\ &\left. -\sum_{i=1}^N \alpha_i \left[x,\phi(x),\nabla\phi(x)\right]\psi_i^\dagger(x)\right)\right\} |0\rangle, \end{split} \tag{5.2}$$

The above state can be written equivalently in the form

$$|V, B, \{\alpha_i\}\rangle = \int d\mu(\phi) \mathcal{A}_V(\phi) |\alpha(\phi)\rangle, \tag{5.3}$$

with $d\mu(\phi)$ being the massless free probability measure for ϕ

$$d\mu(\phi) = \mathcal{D}\phi \exp\left(-\frac{1}{2} \int_{\Omega} d^dx \sum_{k=1}^{D} \left[\nabla \phi_k(x)\right]^2\right), \tag{5.4}$$

the operator within the path integral is given by

$$\mathcal{A}_{V}\!(\phi) = B\left(\phi|_{\partial\Omega}\right) \exp\left\{-\int_{\Omega} d^{d}x V[x,\phi(x),\nabla\phi(x)]\right\}, \tag{5.5}$$

and

$$|\alpha(\phi)\rangle = \exp\left\{\int_{\Omega} d^dx \, \sum_{i=1}^N \alpha_i \left[x,\phi(x),\nabla\phi(x)\right] \psi_i^\dagger(x)\right\} |0\rangle, \tag{5.6}$$

which is nothing but a coherent state of the physical theory. One can, therefore, interpret a cTNS in terms of a path integration over all possible coherent state configurations of the physical QFT weighted by the dynamics and coupling of the virtual QFT. If one wished to now describe a generic state $|\psi\rangle$ of the bosonic Fock space $\mathcal{F}[L^2(\mathbb{R}^2,\mathbb{C})]^D$, then one begins by expanding it into the basis of n-particle wavefunctions

$$|\psi\rangle = \sum_{n=0}^{+\infty} \int_{\Omega^n} dx_1 ... dx_n \frac{\varphi_n(x_1, ..., x_n)}{n!} \psi_i^{\dagger}(x_1) ... \psi_j^{\dagger}(x_n) |0\rangle, \tag{5.7}$$

where the state of the Fock space could involve the different physical bosonic species ψ_i . Each of the n-particle wavefunctions can be computed by expanding the exponential in Equation (5.3) to obtain

$$\varphi_n(x_1, ..., x_n) = \int d\mu(\phi) \mathcal{A}_V(\phi) \alpha_i[\phi(x_1)] ... \alpha_j[\phi(x_n)], \tag{5.8}$$

where we interpret the wave function of the physical theory as a correlator of the coupling operators of the virtual theory. As shown in [185], one can see that the computation of correlation functions involves the product of α_i with itself inside of the exponential, and thus, any dependence above linear dependence on the field will introduce non-Gaussianities into the theory.

While the state presented in Equation (5.1) is more intuitively understood from the field theory perspective, we wish to establish a closer parallel to the language found in

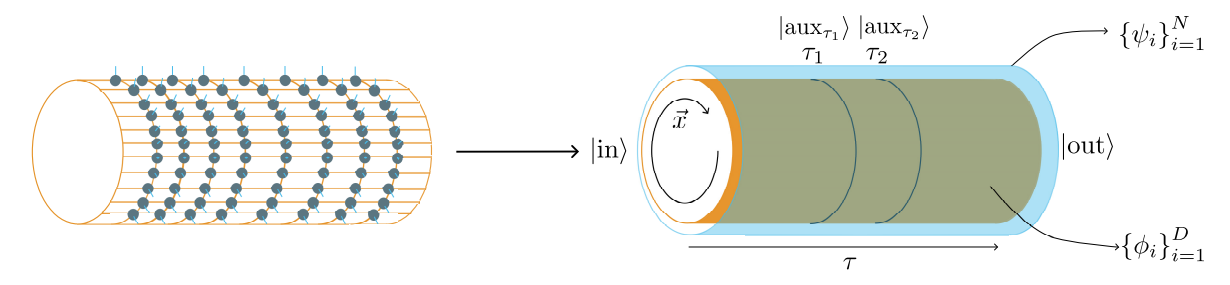


Figure 5.1: Diagram of the operator representation of the cTNS ansatz. In the left we can identify a standard tensor network, where the virtual space is colored orange and the physical space light blue. After taking the continuum limit, they become two coupled QFTs on the right figure. The presented cTNS on the right has open boundary conditions denoted by the $|\text{in}\rangle$ and $|\text{out}\rangle$.

TN theory. Such a representation was already provided in [185], where they showed that an equivalent operator representation exists for any given cTNS defined on the previous domains. As in any Hamiltonian representation of a theory, a specific direction needs to be chosen as the "time" direction so that we can define the Hamiltonian operator in charge of evolving the theory. To this end, we will suppose that the domain is of the form $\Omega = \left[-\frac{T}{2}, \frac{T}{2}\right] \times S$ with $\partial S = \emptyset$. It is helpful to build intuition from one of the more intuitive examples of such an Ω , which would be a finite cylinder, where S would be the compact direction and T would be the total length/height of the cylinder.

Then, the operator representation of cTNS is given by

$$\begin{split} |V,B,\{\alpha_i\}\rangle = \\ \operatorname{tr}\left\{\widehat{B}\mathcal{T}\exp\left[-\int_{-\frac{T}{2}}^{\frac{T}{2}}d\tau\int_{S}d\vec{x}\left(\mathcal{H}(\tau,\vec{x})-\sum_{i=1}^{N}\alpha_i[\tau,\vec{x},\hat{\phi}(\vec{x}),\hat{\pi}(\vec{x})]\psi_i^{\dagger}(\tau,\vec{x})\right)\right]\right\}|0\rangle, \end{split} \tag{5.9}$$

with

$$\mathcal{H}(\tau, \vec{x}) = \underbrace{\sum_{k=1}^{D} \left(\frac{[\hat{\pi}_{k}(\vec{x})]^{2}}{2} + \frac{[\nabla \hat{\phi}_{k}(\vec{x})]^{2}}{2} \right)}_{\mathcal{H}_{0}(\vec{x})} + V[\tau, \vec{x}, \hat{\phi}(\vec{x}), \hat{\pi}(\vec{x})], \tag{5.10}$$

where $\mathcal T$ is the τ -ordering operator, and $\hat \pi_k$ are the conjugate momentum of $\hat \phi_k$ acting on D copies of the virtual d-1 dimensional bosonic Fock space, $\mathcal F[L^2(S,\mathbb C)]^D$, over which the above trace is taken, i.e.

$$[\hat{\phi}_k(\vec{x}), \hat{\pi}_l(\vec{y})] = i\delta_{kl}\delta^{d-1}(\vec{x} - \vec{y}).$$
 (5.11)

It is important to stress that both variational functions V and α_i 's may depend on both \vec{x} and τ in the most general setting. Restricting them not explicitly to depend on either of these parameters would make the cTNS translationally invariant and as in the previous representation, the operator \hat{B} implements boundary conditions on the virtual theory. The natural condition for a τ -invariant theory would be $\hat{B} = \mathbb{I}$, but a condition that is also very interesting would be $\hat{B} = |\mathrm{in}\rangle\langle\mathrm{out}|$. The latter boundary condition turns the trace operator into the correlator between a $|\mathrm{in}\rangle$ and $|\mathrm{out}\rangle$ state of the virtual theory. Diagrammatically, we can see this representation as in the right of Figure 5.1, where both virtual and physical QFTs are depicted with a solid color on top of the geometry of Ω . As in the coherent state representation, the n-particle

wavefunction is now computed as

$$\varphi_{n} = \operatorname{tr}\left[\hat{B}\hat{G}_{\tau_{n},\frac{T}{2}}\hat{\alpha}_{j}(\tau_{n},\vec{x_{n}})\hat{G}_{\tau_{n-1},\tau_{n}}...\hat{G}_{\tau_{1},\tau_{2}}\hat{\alpha}_{i}(\tau_{1},\vec{x}_{1})\hat{G}_{-\frac{T}{2},\tau_{1}}\right],\tag{5.12}$$

where $\hat{\alpha}_i(t_k,\vec{x_k}) = \alpha \left[\tau_k,\vec{x_k},\hat{\phi}(\vec{x_k},\hat{\pi}(\vec{x_k})) \right]$ and $\hat{G}_{u,v} = \mathcal{T} \exp\left(-\int_u^v d\tau \int_S d\vec{x} \mathcal{H}(\vec{x})\right)$. The interpretation of Equation (5.12) is as follows. To compute the n-particle wavefunction of physical fields $\psi_i(x_i)$, one computes the trace over the coupling operators of the virtual space, where the virtual space is first initialized in some initial state $|\text{in}\rangle$. Then, the virtual space is evolved with the virtual evolution operator $\hat{G}_{-\frac{T}{2},\tau_1}$ from its initial time $-\frac{T}{2}$ to the time of the physical field insertion τ_1 . At that time, the corresponding coupling operator $\hat{\alpha}_i$ is evaluated, and the procedure is repeated until we reach the final boundary condition of the virtual space $|\text{out}\rangle$. To compute correlation functions, field theory tells us to evaluate the generating functionals with currents given by

$$\mathcal{Z}_{j',j} = \frac{\langle V, B, \{\alpha_i\} | \exp\left(\int_S d\vec{x} \sum_{i=1}^N j_i'(\vec{x}) \psi_i^\dagger(\vec{x})\right) \exp\left(\int_S d\vec{x} \sum_{i=1}^N j_i(\vec{x}) \psi_i(\vec{x})\right) | V, B, \{\alpha_i\} \rangle}{\langle V, B, \{\alpha_i\} | V, B, \{\alpha_i\} \rangle} \tag{5.13}$$

We can write this functional in the operator representation with

$$\mathcal{Z}_{j',j} = \operatorname{tr}\left[\widehat{B} \otimes \widehat{B}^* \exp\left\{\int_{-T/2}^{T/2} \mathrm{d}\tau \mathbb{T}_{j',j}(\tau) - \int_{S} \mathrm{d}\vec{x} \sum_{k=1}^{N} j_k(\vec{x}) j_k'(\vec{x})\right\}\right], \tag{5.14}$$

which we have used to introduce the definition of the transfer operator with sources $\mathbb{T}_{j',j}(\tau)$ given by

$$\begin{split} \mathbb{T}_{j',j}(\tau) &= \int_{S} d\vec{x} \left(-\mathcal{H}(\tau,\vec{x}) \otimes \mathbb{I} - \mathbb{I} \otimes \mathcal{H}^{*}(\tau,\vec{x}) \right. \\ &+ \sum_{i=1}^{N} (\alpha_{i}[\tau,\vec{x},\hat{\phi}(\vec{x}),\hat{\pi}(\vec{x})] + j'_{i}(\vec{x})) \otimes (\alpha_{i}[\tau,\vec{x},\hat{\phi}(\vec{x}),\hat{\pi}(\vec{x})]^{*} + j_{i}(\vec{x})) \bigg) \,. \end{split} \tag{5.15}$$

One can intuitively think of the transfer operator $\mathbb T$ as the operator that generates the time evolution of both the 'bra' and the 'ket' part of the correlator simultaneously between a time τ and $\tau+d\tau$. A couple of examples are now in order.

First, the norm of $|V,B,\alpha\rangle$ in the denominator of Equation 5.14 will be computed in the operator representation as

$$\langle V, B, \{\alpha_i\} | V, B, \{\alpha_i\} \rangle = \operatorname{tr} \left[\hat{B} \otimes \hat{B}^* \, \mathcal{T} \exp \left(\int_{-\frac{T}{2}}^{\frac{T}{2}} d\tau \, \mathbb{T}(\tau) \right) \right], \tag{5.16}$$

where the source-less transfer operator \mathbb{T} has been introduced

$$\mathbb{T}(\tau) = \int_{S} d\vec{x} \left(-\mathcal{H}(\tau, \vec{x}) \otimes \mathbb{I} - \mathbb{I} \otimes \mathcal{H}^{*}(\tau, \vec{x}) + \sum_{i=1}^{N} \alpha_{i} [\tau, x, \hat{\phi}(\vec{x}), \hat{\pi}(\vec{x})] \otimes \alpha_{i} [\tau, \vec{x}, \hat{\phi}(\vec{x}), \hat{\pi}(\vec{x})]^{*} \right). \tag{5.17}$$

We see that the norm of a state is nothing but the expectation value of the identity operator, therefore performing the trace over the evolution of the virtual space without any insertion of the coupling functions α_i 's.

Our second example is a simple 2-body correlator of the physical theories, e.g.,

$$\left\langle \psi_i^{\dagger}(x)\psi_k(y)\right\rangle = \frac{\delta}{\delta j_i'(x)} \frac{\delta}{\delta j_k(y)} \mathcal{Z}_{j',j} \bigg|_{j_k,j_i'=0}. \tag{5.18}$$

This correlator will be computed using the operator representation of the virtual space as

$$\begin{split} \left\langle \psi_i^\dagger(x) \psi_k(y) \right\rangle &= \operatorname{tr} \left[\widehat{B} \otimes \widehat{B}^* \mathcal{M}_{T/2,\tau_2}(\mathbb{I} \otimes \alpha_i^* [\tau_2, \vec{x}, \widehat{\phi}(\vec{x}), \widehat{\pi}(\vec{x})]) \mathcal{M}_{\tau_2,\tau_1} \right. \\ & \times \left. (\alpha_k [\tau_1, \vec{y}, \widehat{\phi}(\vec{y}), \widehat{\pi}(\vec{y})] \otimes \mathbb{I}) \mathcal{M}_{\tau_1, -T/2} \right], \end{split} \tag{5.19}$$

where $x=(\tau_2,\vec{x})$ and $y=(\tau_1,\vec{y})$ and $\mathcal{M}_{u,v}=\mathcal{T}\exp\left[\int_v^u d\tau \mathbb{T}(\tau)\right]$, the propagator operator of the virtual theory in the virtual field theory. We can interpret Equation (5.19) the same way that we interpreted Equation (5.12), in which each physical field is implemented in the virtual space trace through the couplings α_i 's.

With these tools, in [224], some correlators of simple quadratic and quartic bosonic theories were numerically studied. The authors showed that the manifold of Gaussian cTNSs provides arbitrarily accurate approximations to the ground states of the quadratic Hamiltonians and decent estimates for quartic ones at weak coupling. Additionally, since they captured the short-distance behavior of the theories in a very precise manner, they showed that Gaussian cTNSs even allow one to renormalize away simple divergences variationally. As of today, this result is the only one that provides evidence that cTNS is an advantageous numerical tool with which to study further QFTs.

This lack of exploration stands in contrast to the many studies performed with cMPS such as [217],[225] or [216], which are made possible because cMPSs are parametrized by finite matrices, and can therefore more easily be variationally optimized. Given how it was shown in [185] that cTNS reduces to cMPS in the 1-dimensional limit, is it somehow possible to harness the numerical power of cMPS to study higher dimensional systems described by cTNS?

As we have seen in Chapter 2, this question already has an answer in the context of PEPS. In [125], the authors provided an exact duality transformation between the bulk of a quantum spin system, described by a PEPS, and its boundary given as an MPS. The duality associates to every region a Hamiltonian on the boundary, in such a way that the bulk's entanglement spectrum corresponds to the boundary Hamiltonian's excitation spectrum. In short, for every PEPS, there exists a dual description in terms of its boundary MPS. Finally, our question is, under which conditions can we find a similar result for cTNS?

5.2 THE BULK-BOUNDARY CORRESPONDENCE OF CTNS

5.2.1 FIXED POINTS OF THE TRANSFER OPERATOR AND ITS LINDBLAD FORM

To tackle the question, let us first understand the transfer operator's structure, specifically its fixed point. We will assume that \mathbb{T} is τ -independent and that it has a single

non-degenerate eigenstate λ_0 that has the biggest positive real part. If $|R_0\rangle$ and $|L_0\rangle$ are the respective right and left eigenvectors such that

$$\mathbb{T}|R_0\rangle = \lambda_0|R_0\rangle \ (L_0|\mathbb{T} = (L_0|\overline{\lambda_0}), \tag{5.20}$$

then

$$e^{T\mathbb{T}} = \sum_j e^{T\lambda_j} |R_j| (L_j| = e^{T\lambda_0} \sum_j e^{T(\overline{\lambda_j - \lambda_0})} |R_j| (L_j| = e^{T\lambda_0} \sum_j \zeta_j^T |R_j| (L_j|, \quad \text{(5.21)})$$

with $|\zeta_i| < 1$. Therefore, in the limit $T \to \infty$ we get

$$e^{T\mathbb{T}} \to e^{T\lambda_0} |R_0\rangle(L_0|, \tag{5.22}$$

and as a result, the computation of the norm of cTNS would be reduced to

$$||V, B, \{\alpha_i\}\rangle||^2 = e^{T\lambda_0}(L_0|\hat{B} \otimes \hat{B}^*|R_0), \tag{5.23}$$

in the fixed-point limit. If $\mathcal H$ is bounded from below, then one can rescale the Hamiltonian of the virtual cTNS without loss of generality to make $\lambda_0=0$. The most important concept to take away from this computation is that the fixed-point limit replaces the computation of the trace of cTNS with the correlator of the fixed points of the transfer operator. This procedure significantly reduces the complexity of the computation of any correlator with cTNS, but of course, the complexity of the computation gets relegated to finding such fixed points.

As will be shown in [3], one can show that a cTNS is in Lindblad form if

$$\int_{S} d\vec{x} \mathcal{H}(\vec{x}) + \mathcal{H}^*(\vec{x}) = \int_{S} d\vec{x} \sum_{i=1}^{N} \alpha_i^* \alpha_i.$$
 (5.24)

in which case the coupling functions α_i correspond to the jump operators of the Lindbladian. Working on the basis of the Lindbladian would provide us with certain analytical guarantees about the behavior of the fixed points, such as their existence as groundstates of local gapped Hamiltonians under certain conditions [226]. However, working on the basis in which the cTNS has the Lindblad form comes with caveats.

Let us see this problem using an example: the real massive boson. We consider here the bosonic virtual field theory with a single real bosonic species given by the Hamiltonian

$$\mathsf{H}_{fb} = \int_{S} d\vec{x} : \mathcal{H}_{fb}(\vec{x}) :, \tag{5.25}$$

with

$$\mathcal{H}_{fb}(\vec{x}) = \frac{[\hat{\pi}(\vec{x})]^2}{2} + \frac{[\nabla \hat{\phi}(\vec{x})]^2}{2} + \frac{1}{2}m^2[\hat{\phi}(\vec{x})]^2, \tag{5.26}$$

and where : : is the normal ordering with respect to the momentum modes.

The goal is to find α_i s.t. the cTNS is in the Lindblad form. It is the case if and only if

$$2H_{fb} = \int_{S} d\vec{x} \sum_{i=1}^{N} \alpha_i^* \alpha_i, \qquad (5.27)$$

where $\alpha_i=\alpha_i[\vec{x},\hat{\phi}(\vec{x}),\hat{\pi}(\vec{x})]$, because we assume the bosonic field to be real $\hat{\phi}^*=\hat{\phi}$. Because the theory is quadratic and thus free, we can use the momentum expansion of the operators, which is given by

$$\hat{\phi}(\vec{x}) = \frac{1}{(2\pi)^{\frac{d-1}{2}}} \int \frac{d\vec{k}}{\sqrt{2\omega(\vec{k})}} \left(e^{i\vec{k}\cdot\vec{x}} \tilde{\phi}(\vec{k}) + e^{-i\vec{k}\cdot\vec{x}} \tilde{\phi}^*(\vec{k}) \right), \tag{5.28}$$

and

$$\hat{\pi}(\vec{x}) = \frac{1}{i(2\pi)^{\frac{d-1}{2}}} \int d\vec{k} \sqrt{\frac{\omega(\vec{k})}{2}} \left(e^{i\vec{k}\cdot\vec{x}} \tilde{\phi}(\vec{k}) - e^{-i\vec{k}\cdot\vec{x}} \tilde{\phi}^*(\vec{k}) \right), \tag{5.29}$$

with $\omega(\vec{k}) = \sqrt{\vec{k}^2 + m^2}$.

The next step is to insert both Equations (5.28) and (5.29) into Equation (5.27). The first step is then to compute

$$\int_{S} d\vec{x} \left[\pi(\vec{x}) \right]^{2} = \int d\vec{k} \frac{\omega(\vec{k})}{2} \left(\tilde{\phi}(\vec{k}) \tilde{\phi}^{*}(\vec{k}) + \tilde{\phi}^{*}(\vec{k}) \tilde{\phi}(\vec{k}) - \tilde{\phi}(\vec{k}) \tilde{\phi}(-\vec{k}) - \tilde{\phi}^{*}(\vec{k}) \tilde{\phi}^{*}(-\vec{k}) \right), \tag{5.30}$$

as well as

$$\int_{S} d\vec{x} \left([\nabla \hat{\phi}(\vec{x})]^{2} + m^{2} [\hat{\phi}(\vec{x})]^{2} \right)
= \int d\vec{k} \frac{\omega(\vec{k})}{2} \left(\tilde{\phi}(\vec{k}) \tilde{\phi}(-\vec{k}) + \tilde{\phi}(\vec{k}) \tilde{\phi}^{*}(\vec{k}) + \tilde{\phi}^{*}(\vec{k}) \tilde{\phi}(\vec{k}) + \tilde{\phi}^{*}(\vec{k}) \tilde{\phi}^{*}(-\vec{k}) \right),$$
(5.31)

so that then the Hamiltonian is written as

$$2\int_{S} d\vec{x} \,\mathcal{H}_{fb}(\vec{x}) = \int d\vec{k} \,\omega(\vec{k}) \left(\tilde{\phi}^{*}(\vec{k}) \tilde{\phi}(\vec{k}) + \tilde{\phi}(\vec{k}) \tilde{\phi}^{*}(\vec{k}) \right), \tag{5.32}$$

and therefore

$$2H_{fb} = \int d\vec{k} \, 2\omega(\vec{k}) \tilde{\phi}^*(\vec{k}) \tilde{\phi}(\vec{k}). \tag{5.33}$$

From (5.29) and (5.28) we can deduce that the momentum modes are given by

$$\tilde{\phi}(\vec{k}) = \sqrt{\frac{\omega(\vec{k})}{2}} \frac{1}{(2\pi)^{\frac{d-1}{2}}} \int_{S} d\vec{x} \hat{\phi}(\vec{x}) e^{-i\vec{k}\cdot\vec{x}} + \frac{i}{\sqrt{2\omega(\vec{k})}} \frac{1}{(2\pi)^{\frac{d-1}{2}}} \int_{S} d\vec{x} \hat{\pi}(\vec{x}) e^{-i\vec{k}\cdot\vec{x}}, \quad (5.34)$$

and

$$\tilde{\phi}^*(\vec{k}) = \sqrt{\frac{\omega(\vec{k})}{2}} \frac{1}{(2\pi)^{\frac{d-1}{2}}} \int_S d\vec{x} \hat{\phi}(\vec{x}) e^{i\vec{k}\cdot\vec{x}} - \frac{i}{\sqrt{2\omega(\vec{k})}} \frac{1}{(2\pi)^{\frac{d-1}{2}}} \int_S d\vec{x} \vec{\pi}(\vec{x}) e^{i\vec{k}\cdot\vec{x}}.$$
 (5.35)

Then, inserting these expressions into Equation (5.33) one gets

$$2H_{fb} = \int_{S} d\vec{x} \hat{\pi}(\vec{x})^{2} + \frac{1}{(2\pi)^{d-1}} \int d\vec{k} \int_{S^{2}} d\vec{x} d\vec{y} \left\{ \omega(\vec{k})^{2} \hat{\phi}(\vec{x}) \hat{\phi}(\vec{y}) e^{i\vec{k}\cdot(\vec{x}-\vec{y})} + i\omega(\vec{k}) [\hat{\phi}(\vec{x}), \hat{\pi}(\vec{y})] e^{i\vec{k}\cdot(\vec{x}-\vec{y})} \right\}.$$
(5.36)

To satisfy the requirement that the above expression can be presented in the form $\int_S d\vec{x} \sum_{i=1}^N \alpha_i^* \alpha_i$, it is enough to take N=1 and $\alpha=\alpha_1$ being of the form

$$\alpha = i\hat{\pi}(\vec{x}) + \int_{S} d\vec{y} I(\vec{x} - \vec{y}) \hat{\phi}(\vec{y}), \tag{5.37}$$

with some real-valued symmetric kernel $I(\vec{r})$. By an explicit use of this ansatz, we easily get

$$I(\vec{r}) = \frac{1}{(2\pi)^{d-1}} \int d\vec{k} \,\omega(\vec{k}) e^{i\vec{k}\cdot\vec{r}} = -\kappa \frac{mK_1(m|\vec{r}|)}{|\vec{r}|},\tag{5.38}$$

where K_1 is the modified Bessel function of the second type and κ a numerical constant. Finally,

$$\alpha = i\hat{\pi}(\vec{x}) - m\kappa \int_{S} d\vec{y} \, \frac{K_1(m|\vec{x} - \vec{y}|)}{|\vec{x} - \vec{y}|} \hat{\phi}(\vec{y}), \tag{5.39}$$

and this is the Lindblad operator for the free massive boson. Here, we see that the coupling operator in the Lindblad form is highly non-local, and therefore, it will be tough to provide any details about the fixed point of such a highly non-local open QFT. Interestingly, this choice of basis for this model has already been used in the context of cMPS [227] to provide a relativistic use-case scenario, even though it was derived in a completely different way.

5.2.2 THE TRANSFER OPERATOR IN HAMILTONIAN FORM

We have seen that the Lindblad form of cTNS yields highly non-local couplings, which does not simplify the task of finding the fixed points of \mathbb{T} , regardless of the analytical guarantees about the properties of the fixed points. To simplify this task, we attempt to interpret the transfer operator \mathbb{T} instead as a new Hamiltonian on the double bosonic Fock space, which we denote by $\mathcal{H}_{\mathbb{T}}$ and call the boundary hamiltonian, following the standard approach known from quantum theory. Before discussing the general problem of which bulk virtual Hamiltonians in cTNS form yield neat boundary Hamiltonian forms for the transfer operator, we begin with some motivating results.

THE SINE-GORDON AND TODA MODELS AS BOUNDARY HAMILTONIANS

We start from the operator representation of cTNS as shown in Equation (5.9). Our first choice will be that the virtual QFT is a single virtual massless free real ($\hat{\phi}(\vec{x}) = \hat{\phi}^*(\vec{x})$) boson, and therefore D=1. The Hamiltonian then reads

$$\mathcal{H}_0(\vec{x}) = \frac{[\hat{\pi}(\vec{x})]^2}{2} + \frac{[\nabla \hat{\phi}(\vec{x})]^2}{2}.$$
 (5.40)

To fully specify the cTNS, we also need to choose the couplings to the physical theory α_i 's, and this is the key choice that achieves the interesting bulk-boundary correspondence. We will choose the virtual field theory to be coupled to a physical theory consisting of two physical species. Therefore, we choose the last term of the exponent of Equation (5.9) to be

$$\sum_{i=1}^{2} \alpha_{i} [\hat{\phi}(\vec{x})] \psi_{i}^{\dagger}(\tau, \vec{x}) = \mu e^{i\beta\hat{\phi}(\vec{x})} \psi_{1}^{\dagger}(\tau, \vec{x}) + \mu e^{-i\beta\hat{\phi}(\vec{x})} \psi_{2}^{\dagger}(\tau, \vec{x}), \tag{5.41}$$

where $\beta, \mu \in \mathbb{R}$. With this specific coupling, the transfer operator of Equation (5.17) becomes

$$\begin{split} \mathbb{T} &= \int_{S} d\vec{x} \left(-\mathcal{H}_{0}(\vec{x}) \otimes \mathbb{1} - \mathbb{1} \otimes \mathcal{H}_{0}^{*}(\vec{x}) + \sum_{i=1}^{2} (\alpha_{i} [\hat{\phi}(\vec{x})]) \otimes (\alpha_{i} [\hat{\phi}(\vec{x})])^{*} \right) \\ &= \int_{S} d\vec{x} \left(-\mathcal{H}_{0}(\vec{x}) \otimes \mathbb{1} - \mathbb{1} \otimes \mathcal{H}_{0}^{*}(\vec{x}) + \mu^{2} e^{i\beta\hat{\phi}(\vec{x})} \otimes e^{-i\beta\hat{\phi}(\vec{x})} + \mu^{2} e^{-i\beta\hat{\phi}(\vec{x})} \otimes e^{i\beta\hat{\phi}(\vec{x})} \right). \end{split} \tag{5.42}$$

IN what follows, we introduce the notation $\mathcal{O}^1 = \mathcal{O} \otimes \mathbb{1}$ and $\mathcal{O}^2 = \mathbb{1} \otimes \mathcal{O}$. Thus, we can rewrite Equation (5.42)

$$\mathbb{T} = \int_{S} d\vec{x} \left(-\mathcal{H}_{0}^{1}(\vec{x}) - \mathcal{H}_{0}^{2*}(\vec{x}) + \mu^{2} e^{i\beta(\hat{\phi}^{1}(\vec{x}) - \hat{\phi}^{2}(\vec{x}))} + \mu^{2} e^{-i\beta(\hat{\phi}^{1}(\vec{x}) - \hat{\phi}^{2}(\vec{x}))} \right), \tag{5.43}$$

which leads to

$$\mathbb{T} = \int_{S} d\vec{x} \left(-\mathcal{H}_{0}^{1}(\vec{x}) - \mathcal{H}_{0}^{2*}(\vec{x}) + 2\mu^{2} \cos \beta (\hat{\phi}^{1}(\vec{x}) - \hat{\phi}^{2}(\vec{x})) \right). \tag{5.44}$$

The transfer operator acts on the doubled Fock space of the virtual QFT. By defining a new basis for the joint Fock space as $\hat{\phi}^{\pm}=\frac{1}{\sqrt{2}}(\hat{\phi}^1\pm\hat{\phi}^2)$ and using the hermiticity of $\hat{\phi}$, we see that the transfer matrix becomes

$$\mathbb{T} = \int_{S} d\vec{x} \left(-\mathcal{H}_{0}^{+}(\vec{x}) - \mathcal{H}_{sG}^{-}(\vec{x}) \right). \tag{5.45}$$

with the sine-Gordon Hamiltonian

$$\mathcal{H}_{sG}^{-}(\vec{x}) = \mathcal{H}_{0}^{-}(\vec{x}) - 2\mu^{2}\cos\left(\beta\sqrt{2}\hat{\phi}^{-}(\vec{x})\right). \tag{5.46}$$

We have positively written the transfer operator in terms of known Hamiltonians on the coupled Fock space. The specific choice of α_i 's led to the factorization of the two spaces into a free boson part and a sine-Gordon part. Thanks to this factorization, some of the correlators of the original field theory can now be easily computed via this specific cTNS representation. A good example would be given by

$$\langle \psi_{1}(\tau_{1},\vec{y})\psi_{2}^{\dagger}(\tau_{2},\vec{x})\rangle_{\text{Phys}} = \text{Tr}\left[\widehat{B}\otimes\widehat{B}^{*}\mathcal{M}_{T/2,\tau_{2}}\alpha_{2}^{2^{*}}(\tau_{2},\vec{x})\mathcal{M}_{\tau_{2},\tau_{1}}\alpha_{1}^{1}(\tau_{1},\vec{y})\mathcal{M}_{\tau_{1},-T/2}\right] \xrightarrow{T\to\infty} \\ \mu^{2}\langle e^{i\beta\hat{\phi}^{2}(\tau_{1},\vec{x})}e^{i\beta\hat{\phi}^{1}(\tau_{2},\vec{y})}\rangle_{sG\otimes0} = \mu^{2}\langle e^{i\frac{\beta}{\sqrt{2}}\hat{\phi}^{+}(\tau_{1},\vec{x})}e^{i\frac{\beta}{\sqrt{2}}\hat{\phi}^{+}(\tau_{2},\vec{y})}\rangle_{0}\langle e^{i\frac{\beta}{\sqrt{2}}\hat{\phi}^{-}(\tau_{1},\vec{x})}e^{i\frac{\beta}{\sqrt{2}}\hat{\phi}^{-}(\tau_{2},\vec{y})}\rangle_{sG}. \tag{5.47}$$

Equation (5.47) is the main result of this section, and its central message is that the computation of a physical correlator splits into two known correlators of the fixed-point theory of the cTNS. This result solidifies our intuition that cTNS can be used to gain insight analytically into complicated QFTs by using a smart choice of the virtual space. In this specific case, the free boson correlator of vertex operators is known from CFT. At the same time, in the sine-Gordon theory we can compute analytically some of the vertex operator correlators using the Fateev-Lukyanov-Zamolodchikov-Zamolodchikov (FLZZ) formulas [228] or make use of the Relativistic Continuous Matrix Product States (RCMPS) [225, 227] to do it numerically.

The previous example can be generalized straightforwardly to more general Kac-Moody algebras, as we show now. Let then $\mathfrak g$ be a Kac-Moody algebra of rank r with Cartan subalgebra $\mathfrak h$ equipped with an inner product $\langle\cdot,\cdot\rangle$ induced by the Killing form [209]. Since dim $\mathfrak h=r$, let $\tilde\alpha_1,\ldots,\tilde\alpha_r$ denote simple roots and $\{n_i\}_{i=1}^r$ be the corresponding set of Kac labels. We define

$$\alpha_i[\hat{\phi}(\vec{x})] = \frac{m}{\beta} \sqrt{n_i} e^{i\beta \langle \tilde{\alpha}_i, \hat{\phi}(\vec{x}) \rangle}. \tag{5.48}$$

Then

$$\sum_{i=1}^{r} \alpha_{i}[\hat{\phi}(\vec{x})] \otimes \alpha_{i}[\hat{\phi}(\vec{x})]^{*} = \frac{m^{2}}{\beta^{2}} \sum_{i=1}^{r} n_{i} e^{i\beta \langle \tilde{\alpha}_{i}, \hat{\phi}^{1}(\vec{x}) - \hat{\phi}^{2}(\vec{x}) \rangle}. \tag{5.49}$$

Again, introducing $\phi^{\pm}=\frac{1}{\sqrt{2}}\left(\phi^1\pm\phi^2\right)$ we see that the transfer matrix becomes

$$\mathbb{T} = \int_{S} d\vec{x} \left(-\mathcal{H}_{0+}(\vec{x}) - \mathcal{H}_{T-}(\vec{x}) \right), \tag{5.50}$$

where $\mathcal{H}_{T-}(\vec{x})$ is now the Toda Hamiltonian [229] in the ϕ^- field, which again is another analytically tractable QFT.

It is natural to ask now, how general is this procedure of constructing a boundary virtual Hamiltonian out of the virtual QFT of a cTNS?

GENERIC BOUNDARY HAMILTONIAN OF CTNS

We would like to determine when a given boundary Hamiltonian $\mathcal{H}_{\mathbb{T}}(\vec{x})$ can be represented as

$$\mathcal{H}_{\mathbb{T}} = \mathcal{H} \otimes \mathbb{1} + \mathbb{1} \otimes \mathcal{H} - \sum_{k} \alpha_{k} \otimes \alpha_{k}^{*}, \tag{5.51}$$

for a certain bulk Hamiltonian $\mathcal{H}=\mathcal{H}_0+V$, and a family of bulk couplings $\{\alpha_k\}$. Moreover, motivated by the sine-Gordon example, we demand that there exists a linear change of variables such that the Hamiltonian $\mathcal{H}_{\mathbb{T}}$ splits into two distinct terms, each depending exclusively on one of the variables such that we can still retain some analytical power over the resulting correlators. Mainly, for D=1, we denote $\phi^1=\phi\otimes\mathbb{I}$ and $\phi^2=\mathbb{1}\otimes\phi$, and ask about a linear transformation $S:(\phi^1,\phi^2)\to(\phi^+,\phi^-)$ to a new variables (ϕ^+,ϕ^-) such that

$$\mathcal{H}_{\mathbb{T}} = \mathcal{G}_{+}(\phi^{+}) + \mathcal{G}_{-}(\phi^{-}), \tag{5.52}$$

where again both \mathcal{G}_+ and \mathcal{G}_- are bosonic Hamiltonians in the corresponding variables. Let us denote the right-hand side of (5.51) by $F(\phi^1,\phi^2)$, and have a nondegenerate linear transformation $S:(\phi^1,\phi^2)\to(\phi^+,\phi^-)$ parameterized by

$$\begin{cases} \phi^{+} = \alpha \phi^{1} + \beta \phi^{2}, \\ \phi^{-} = \gamma \phi^{1} + \delta \phi^{2} \end{cases}, \qquad \alpha \delta \neq \beta \gamma.$$
 (5.53)

To begin constraining this transformation, we will demand that both bulk and boundary Hamiltonians have the bosonic kinetic terms,

$$F(\phi^1,\phi^2) = \mathcal{H}_0(\phi^1) + \mathcal{H}_0(\phi^2) + \tilde{F}(\phi^1,\phi^2), \qquad \mathcal{G}_\pm(\phi_\pm) = \mathcal{H}_0(\phi_\pm) + V_\pm(\phi_\pm), \quad \textbf{(5.54)}$$

and also that

$$F(\phi^{1}, \phi^{2}) = \mathcal{G}_{+}(\phi^{+}) + \mathcal{G}_{-}(\phi^{-}), \tag{5.55}$$

We can condense all the previous conditions as

$$\begin{cases} \mathcal{H}_{0}(\phi^{1}) + \mathcal{H}_{0}(\phi^{2}) = \mathcal{H}_{0}(\phi_{+}) + \mathcal{H}_{0}(\phi_{-}) \\ \tilde{F}(\phi^{1}, \phi^{2}) = V_{+}(\phi_{+}) + V_{-}(\phi_{-}). \end{cases} \tag{5.56}$$

The first of these conditions implies that $\alpha^2+\gamma^2=1=\beta^2+\delta^2$ and $\alpha\beta+\gamma\delta=0$. Therefore

$$\begin{pmatrix} \phi^+ \\ \phi^- \end{pmatrix} = \begin{pmatrix} \cos \varphi & \cos \theta \\ \sin \varphi & \sin \theta \end{pmatrix} \begin{pmatrix} \phi^1 \\ \phi^2 \end{pmatrix}, \text{ with } \varphi, \theta \text{ satisfying } \cos(\theta - \varphi) = 0. \tag{5.57}$$

The second condition implies that either $\theta = \varphi + \frac{\pi}{2}$, in which case,

$$\begin{pmatrix} \phi^{+} \\ \phi^{-} \end{pmatrix} = \begin{pmatrix} \cos \varphi & -\sin \varphi \\ \sin \varphi & \cos \varphi \end{pmatrix} \begin{pmatrix} \phi^{1} \\ \phi^{2} \end{pmatrix}, \tag{5.58}$$

or $\theta = \varphi - \frac{\pi}{2}$ and

$$\begin{pmatrix} \phi^+ \\ \phi^- \end{pmatrix} = \begin{pmatrix} \cos \varphi & \sin \varphi \\ \sin \varphi & -\cos \varphi \end{pmatrix} \begin{pmatrix} \phi^1 \\ \phi^2 \end{pmatrix}. \tag{5.59}$$

In the second case, let us parameterize $\varphi \to 2\varphi$. Then, the first choice of angles corresponds to a rotation \mathcal{R}_{φ} by an angle φ , while the second one is a reflection \mathcal{P}_{φ} about a line through the origin which makes an angle φ with the horizontal axis. All such transformations give us the group O(2) of isometries of the plane.

Since $\sum\limits_k \alpha_k \otimes \alpha_k^* = \sum\limits_k (\alpha_k \otimes \mathbb{1})(\mathbb{1} \otimes \alpha_k^*)$, the remaining condition in Equation (5.56) is

$$V(\phi^1) + V(\phi^2) - \sum_k \alpha_k(\phi^1) \alpha_k^*(\phi^2) = V_+(\phi^+) + V_-(\phi^-). \tag{5.60} \label{eq:5.60}$$

For D > 1, we denote the variables by

$$\phi_i^1 = \phi_i \otimes \mathbb{1}, \qquad \phi_i^2 = \mathbb{1} \otimes \phi_i, \qquad i = 1, \dots, D. \tag{5.61}$$

The new boundary fields are then denoted by $\tilde{\phi}_k$ with $k=1,\dots,2D$. Repeating the previous arguments we deduce that the transformation between them must be an isometry so that it belongs to O(2D). Any such matrix can be parametrized as

$$\operatorname{diag}(\mathcal{R}_{\varphi_1}, \dots, \mathcal{R}_{\varphi_K}, \underbrace{\pm 1, \dots, \pm 1}_{L \text{ times}}), \tag{5.62}$$

with 2K + L = 2D.

Now that we know what kind of transformations are allowed in the space of virtual fields such that a kinetic term is preserved, can we find the α_i 's such that a specific theory is recovered in the boundary?

Let us demand, for instance, that the boundary recovers a generic ϕ^n theory, which would correspond to

$$V_{+}(\phi^{+}) = \frac{m^{2} (\phi^{+})^{2}}{2}, \qquad V_{-}(\phi^{-}) = \frac{m^{2} (\phi^{-})^{2}}{2} + \frac{\lambda^{n}}{n!} (\phi^{-})^{n}, \qquad (5.63)$$

we have even allowed possible mass terms for the bosonic boundary field theories, as these would still allow us to retain analytical control over many correlators. We demand that the virtual bulk Hamiltonian $\mathcal H$ is also described by a free bosonic theory, and we have to find then possible α 's that could satisfy (5.51). Since the mass term is preserved by any of the O(2) maps $(\phi^1,\phi^2)\to (\phi^+,\phi^-)$, it remains to find α_l 's such that

$$\sum_{l} \alpha_{l}(\phi^{1}) \alpha_{l}^{*}(\phi^{2}) = -\frac{\lambda^{n}}{n!} (\phi^{-})^{n}.$$
 (5.64)

Since $\phi^-=a\phi^1+b\phi^2$ with $a^2+b^2=1$ (with $a=\sin\varphi$, $b=\cos\varphi$ for rotations, and $a=\sin2\varphi$, $b=-\cos2\varphi$ for reflections), the right-hand side of Equation (5.64) can be written as

$$\sum_{k=0}^{n} \beta_k(a,b) (\phi^1)^k (\phi^2)^{n-k} \ , \ \beta_k(a,b) = -\frac{\lambda^n}{n!} \binom{n}{k} a^k b^{n-k} \in \mathbb{R}$$
 (5.65)

One can then look for solutions to our problem within a certain class of functionals α_l 's. We concentrate here on the ones that admit a Laurent-type ansatz decomposition. Mainly, we assume that $\alpha_l(\phi) = \sum_{k \in \mathbb{Z}} \alpha_{l,k} \phi^k$ with some complex parameters $\alpha_{l,k}$. Then

$$\sum_{l} \alpha_{l}(\phi^{1}) \alpha_{l}(\phi^{2})^{*} = \sum_{l} \sum_{k,p \in \mathbb{Z}} \alpha_{l,k} \alpha_{l,p}^{*}(\phi^{1})^{k}(\phi^{2})^{p} = \sum_{k \in \mathbb{Z}} \left[\sum_{p \in \mathbb{Z}} \left(\sum_{l} \alpha_{l,k} \alpha_{l,p}^{*} \right) (\phi^{2})^{p} \right] (\phi^{1})^{k}.$$
(5.66)

We immediately notice that k (and p) have to be restricted to $0, \dots, n$. Furthermore, for every $k, p = 0, \dots, n$ we have to have

$$\sum_{l} \alpha_{l,k} \alpha_{l,p}^* = \beta_k \delta_{n-k,p}.$$
 (5.67)

In particular, for every $k=m\neq\frac{n}{2}$ we have $\sum_{l}|\alpha_{l,k}|^2=0$. For n odd this means that $\alpha_{l,k}=0$, for every l and k, which leads to a contradiction. Thus the only option left is that n=2q is even. Then we have $\alpha_{l,k\neq q}=0$, for arbitrary l. The only coefficient of α_l that is potentially nonzero is $\alpha_{l,q}$, and is subject to $\sum_{l}|\alpha_{l,q}|^2=\beta_q$. Then, in particular, $\sum_{l}\alpha_{l}(\phi^1)\alpha_{l}^*(\phi^2)$ contains only a single monomial $(\phi^1\phi^2)^q$, which leads to contradiction with (5.65).

In summary, there exists no set of α_i 's that can be written as a formal power series, such that a bosonic bulk theory can exactly become a boundary bosonic ϕ^n theory. There is however a way to allow for a ϕ^n boundary starting from a bosonic bulk, and for that, it is mandatory that the boundary splits into two ϕ^n theories.

If we consider instead the following boundary Hamiltonian

$$\mathcal{H}_{\mathbb{T}} = \mathcal{H}_{0}^{+} + \mathcal{H}_{0}^{-} + \frac{m^{2}}{2}(\phi^{+})^{2} + \mu(\phi^{+})^{n} + \frac{m^{2}}{2}(\phi^{-})^{2} + \mu(\phi^{-})^{n}$$
(5.68)

with $\mu \in \mathbb{R}$, then we will be able to find a bulk theory that reproduces this boundary. We begin by parametrizing the orthogonal transformation $S \in O(2)$ by

$$\begin{cases} \phi^{+} = \cos \varphi \phi^{1} + \epsilon \sin \varphi \phi^{2}, \\ \phi^{-} = \sin \varphi \phi^{1} - \epsilon \cos \varphi \phi^{2}, \end{cases}$$
 (5.69)

where $\epsilon = \pm 1$. In the above parametrization, we have

$$\mathcal{H}_{\mathbb{T}} = \mathcal{H}_{0}^{1} + \mathcal{H}_{0}^{2} + \frac{m^{2}}{2} \left[(\phi^{1})^{2} + (\phi^{2})^{2} \right] + 2\mu \sum_{k=n \, (\text{mod } 2)} \binom{n}{k} \cos^{k} \varphi \sin^{n-k} \varphi(\phi^{1})^{k} (\phi^{2})^{n-k}. \tag{5.70}$$

To satisfy

$$V(\phi^1) + V(\phi^2) - \sum_{l} \alpha_l(\phi^1) \alpha_l^*(\phi^2) = 2\mu \sum_{k=n \, (\text{mod } 2)} \binom{n}{k} \cos^k \varphi \sin^{n-k} \varphi(\phi^1)^k (\phi^2)^{n-k} \quad \textbf{(5.71)}$$

we have to have 2|n. This condition arises as a consequence of our demand for a symmetric decomposition of the polynomials in terms of the potentials for both ϕ^1 and ϕ^2 . Then, in order to generate the appropriate cross-terms, $\alpha_l(\phi) = \zeta_l \phi^{\frac{n}{2}}$, which in turn enforces that n=4. But then $\sum\limits_{l} |\zeta_l|^2 = 2\mu \cos^{\frac{n}{2}} \varphi \sin^{\frac{n}{2}} \varphi$ and $V(\phi) = v_n \phi^n$ and $v_n = 2\mu \cos^n \varphi = 2\mu \sin^n \varphi$. Therefore this means that the only allowed transformations $S \in O(2)$ are the ones that satisfy $\cos \varphi = \varepsilon \sin \varphi$, which forces that $\varphi = \frac{\pi}{4}$. Furthermore, we see that μ has to be non-positive since under the above conditions, we have $\sum\limits_{l} |\zeta_l|^2 = \frac{\pi}{4} \sin^{\frac{n}{2}} \varphi \cos^{\frac{n}{2}} \varphi$

 $\frac{\mu}{2^{\frac{n}{2}-1}}$. In that case, the remaining condition implies that n=4 and $V(\phi)=\frac{-|\mu|}{2^{\frac{n}{4}-1}}\phi^4$.

So far, we have presented a setting in which we could provide a bulk cTNS with a desired fixed point and one in which it was not possible. Indeed, the more freedom we introduce into the ansatz using α_i 's and V's, the easier it becomes to reproduce a target boundary Hamiltonian, at the cost of complicating the bulk cTNS. There is a lot of arbitrariness in which functions can or can not be reproduced generically. To make more accurate statements, we will attempt to study this situation more systematically in the upcoming section.

5.2.3 A GENERIC APPROACH TO THE BULK-BOUNDARY PROBLEM

We have seen that we must determine some baselines for both the boundary and the bulk Hamiltonian to start providing more accurate statements about their relationship. We then begin by demanding the following structure of the boundary Hamiltonian

$$\mathcal{H}_{\mathbb{T}}(\phi^+,\phi^-) = \mathcal{H}_0(\phi^+) + \mathcal{H}_0(\phi^-) + V_{\mathbb{T}}(\phi^+,\phi^-), \tag{5.72}$$

such that the potential $V_{\mathbb{T}}$ is given by

$$V_{\mathbb{T}}(\phi^+,\phi^-) = V(\phi^1) + V(\phi^2) - \sum_l \alpha_l(\phi^1)\alpha_l(\phi^2)^*, \tag{5.73}$$

where (ϕ^1,ϕ^2) is related to (ϕ^+,ϕ^-) through an orthogonal transformation $S\in O(2D)$. The corresponding bulk Hamiltonian corresponding to these choices is the cTNS Hamiltonian found in Equation (5.10). Because we demand that the kinetic term is preserved before and after the orthogonal transformation, the question on which two Hamiltonians can be mapped reduces to finding $V_{\mathbb{T}}$, V and α_l such that Equation (5.73) is satisfied.

One can interpret finding these solutions in two directions. Choose a cTNS, and therefore a V and α_l 's, and then see what boundary theory arises, hopefully leading to a fixed point where some correlators can be computed. Alternatively, choose a boundary theory for which analytical control is guaranteed, providing $V_{\mathbb{T}}$, and then

find the functions V and α_l 's. The latter option is our choice of interpretation. To put Equation (5.73) in a more mathematically simple notation, we are looking for a class of functions g, β_i , such that given an f, the following equation is satisfied

$$(f\circ S)(x,y)=g(x)+g(y)-\sum_i\beta_i(x)\beta_i(y)^* \ x,y\in\mathbb{R}^D, \tag{5.74}$$

where f plays the role of $V_{\mathbb{T}}$, g of V, β_i of α_l and x,y of ϕ^1,ϕ^2 . We will assume that all of these functions have convergent Taylor series representations and use the following notation for the orthogonal transformation $\begin{pmatrix} x' \\ y' \end{pmatrix} = S \begin{pmatrix} x \\ y \end{pmatrix}$. For simplicity, we will also assume that there is only a finite amount of coupling functions, that is l=0,...,N and a single bosonic species in the cTNS ansatz, therefore D=1.

If we parametrize the transformation S by

$$S = \begin{pmatrix} \cos \varphi & \epsilon \sin \varphi \\ \sin \varphi & -\epsilon \cos \varphi \end{pmatrix}, \qquad \epsilon = \pm 1, \ \varphi \in [0, 2\pi), \tag{5.75}$$

then the left-hand-side of (5.74) is a function of $(x',y')=(x\cos\varphi+y\epsilon\sin\varphi,x\sin\varphi-y\epsilon\cos\varphi)$. If one then assumes the aforementioned Taylor expansions, then the l.h.s reads

$$(f\circ S)(x,y)=\sum_{k,l\geq 0}f_{k,l}(x\cos\varphi+y\epsilon\sin\varphi)^k(x\sin\varphi-y\epsilon\cos\varphi)^l, \tag{5.76}$$

with some coefficients $f_{k,l} \in \mathbb{R}$, where the reality of the coefficients is imposed due to the hermiticity of the boundary Hamiltonian. Using the well-known binomial expansion, the above formula can be expressed in the following form:

$$(f \circ S)(x,y) = \sum_{k,l>0} \sum_{n=0}^{k} \sum_{m=0}^{l} \eta(k,l,n,m) x^{n+m} y^{k+l-(n+m)}, \tag{5.77}$$

where

$$\eta(k,l,n,m) = f_{k,l} \binom{k}{n} \binom{l}{m} (-1)^{l-m} \epsilon^{k+l-(n+m)} \cos^{n+l-m} \varphi \sin^{m+k-n} \varphi \in \mathbb{R}. \quad \textbf{(5.78)}$$

To deal with the r.h.s of Equation (5.74), we again perform Taylor expansions of the corresponding functions. Expanding $\beta_i(x)=\sum\limits_{k\geq 0}b_{i,k}x^k$ with $b_{i,k}\in\mathbb{C}$ and $g(x)=\sum\limits_{k\geq 0}g_kx^k$ with $g_k\in\mathbb{R}$ then the r.h.s becomes

$$g(x) + g(y) - \sum_{i} \beta_{i}(x)\beta_{i}(y)^{*} = \sum_{k \geq 0} g_{k}(x^{k} + y^{k}) + \sum_{k,l \geq 0} B_{k,l}x^{k}y^{l} \ , \ B_{k,l} = -\sum_{i=1}^{N} b_{i,k}b_{i,l}^{*} \in \mathbb{R}$$
 (5.79)

Equations (5.77) and (5.79) are the key Equations for all future computations. Our goal will be now to understand the minimal ingredients needed in both the bulk and the boundary in order to obtain anything non-trivial. To do so, we depart from the simplest examples and slowly increase their complexity until anything non-trivial can emerge. Our first simplest example will be to assume that the bulk potentials are simply set to 0 and that there is a single coupling α in the cTNS.

POTENTIAL-LESS BULK WITH A SINGLE COUPLING

Since we are assuming that the bulk potential is simply g=0 and that there is only one coupling α , the condition that we need to solve is given by

$$\sum_{k,l\geq 0} \sum_{n=0}^{k} \sum_{m=0}^{l} \eta(k,l,n,m) x^{n+m} y^{k+l-(n+m)} = \sum_{k,l\geq 0} B_{k,l} x^k y^l. \tag{5.80}$$

Denoting $\eta_0 = \eta(0,0,0,0)$, and observing that

$$\eta_0 = \begin{cases} (f \circ S)(x, -x\epsilon \cot \varphi), & \sin \varphi \neq 0, \\ (f \circ S)(x, x\epsilon \tan \varphi), & \cos \varphi \neq 0, \end{cases}$$
 (5.81)

we infer that, for all n > 0,

$$0 = \sum_{k+l=n} B_{k,l} \epsilon^l \left\{ \frac{(-\cot \varphi)^l}{\tan^l \varphi} \right\}, \text{ for } \begin{cases} \sin \varphi \neq 0, \\ \cos \varphi \neq 0, \end{cases}$$
 (5.82)

and $B_{0,0}=\eta_0$. Defining $\tilde{b}_l=b_l\rho(l)$ with

$$\rho(l) = \epsilon^l \begin{cases} (-\cot \varphi)^l, & \sin \varphi \neq 0, \\ \tan^l \varphi, & \cos \varphi \neq 0, \end{cases}$$
 (5.83)

the above condition takes the form

$$\forall n > 0 \quad \sum_{k+l=n} b_k \tilde{b}_l^* = 0.$$
 (5.84)

We first assume that φ is such that we can indeed freely use the above formulas, i.e., $\sin \varphi \neq 0$ and $\cos \varphi \neq 0$. We will consider the remaining cases separately later.

To gather intuition on how to solve this set of equations, we first look at its behavior for low n and then increasingly raise it. For n = 1, this yields:

$$b_0 \tilde{b_1^*} + b_1 \tilde{b}_0^* = 0 \tag{5.85}$$

First, we show that if $b_0=0$, then also $\forall k>0$ $b_k=0$. Indeed, if $b_0=0$, then by considering (5.84) with n=2, we infer that $b_1\tilde{b}_1^*=0$. As long as our condition on φ is satisfied, we infer that $b_1=0$. Seeing the structure of this last set of equations, we can proceed by induction.

Suppose that all b_0, b_1, \dots, b_{n-1} vanish and consider (5.84) with the parameter 2n, i.e.

$$b_0\tilde{b}_{2n}^* + b_1\tilde{b}_{2n-1}^* + \dots + b_{n-1}\tilde{b}_{n+1}^* + b_n\tilde{b}_n^* + b_{n+1}\tilde{b}_{n-1}^* + \dots + b_{2n-1}\tilde{b}_1^* + b_2\tilde{b}_0^* = 0.$$
 (5.86)

By the inductive hypothesis, this equation reduces to $|b_n|^2 \rho(n) = 0$, so that also $b_n = 0$ since $\rho \neq 0$ under the assumptions on φ . Therefore, it suffices to assume $b_0 \neq 0$.

Let us now write all the b_k 's in their polar decompositions, i.e. $b_k = |b_k|e^{i\theta_k}$. Assuming $b_0 \neq 0$, from (5.85) we get that either $b_1 = 0$, or

$$e^{2i(\theta_1 - \theta_0)} = -\rho(1),$$
 (5.87)

and the latter implies that $|\rho(1)|=1$. Suppose now $b_1=0$. Then considering (5.84) with n=2 we infer that either $b_2=0$ or $|\rho(2)|=1$. As an inductive hypothesis, suppose that $b_1=...=b_n=0$ and take (5.84) with the parameter n+1. It then reduces to

$$b_0 \tilde{b}_{n+1}^* + b_{n+1} \tilde{b}_0^* = 0. {(5.88)}$$

Therefore, either $b_{n+1}=0$ or $|\rho(n+1)|=1$. As a result, either $b_k=0$ for all k>0, or there exists l>0 such that $|\rho(l)|=1$.

In the former case we end up with the conclusion that $\beta(x)=b_0=$ const, so that $(f\circ S)(x,y)=-|b_0|^2<0$, while the latter, since $\rho(l)=\rho(1)^l$, leads to the conclusion that $|\rho(1)|=1$, that is, only transformations with either $|\cot\varphi|=1$ or $|\tan\varphi|=1$ are allowed. In fact, in both cases, this is the same condition, leading to

$$\varphi \in \left\{ \frac{\pi}{4}, \frac{3\pi}{4}, \frac{5\pi}{4}, \frac{7\pi}{4} \right\}. \tag{5.89}$$

The corresponding transformations $S = S_{\epsilon}(\varphi)$ are

$$S_{+}\left(\frac{\pi}{4}\right) = \frac{1}{\sqrt{2}} \begin{pmatrix} 1 & 1 \\ 1 & -1 \end{pmatrix}, \quad S_{-}\left(\frac{\pi}{4}\right) = \frac{1}{\sqrt{2}} \begin{pmatrix} 1 & -1 \\ 1 & 1 \end{pmatrix},$$

$$S_{+}\left(\frac{3\pi}{4}\right) = \frac{1}{\sqrt{2}} \begin{pmatrix} -1 & 1 \\ 1 & 1 \end{pmatrix}, \quad S_{-}\left(\frac{3\pi}{4}\right) = \frac{1}{\sqrt{2}} \begin{pmatrix} -1 & -1 \\ 1 & -1 \end{pmatrix},$$

$$S_{+}\left(\frac{5\pi}{4}\right) = \frac{1}{\sqrt{2}} \begin{pmatrix} -1 & -1 \\ -1 & 1 \end{pmatrix}, \quad S_{-}\left(\frac{3\pi}{4}\right) = \frac{1}{\sqrt{2}} \begin{pmatrix} -1 & 1 \\ -1 & -1 \end{pmatrix},$$

$$S_{+}\left(\frac{7\pi}{4}\right) = \frac{1}{\sqrt{2}} \begin{pmatrix} 1 & -1 \\ -1 & -1 \end{pmatrix}, \quad S_{-}\left(\frac{7\pi}{4}\right) = \frac{1}{\sqrt{2}} \begin{pmatrix} 1 & 1 \\ -1 & 1 \end{pmatrix}.$$

$$(5.90)$$

Therefore, in this case, the function f depends only on either x-y or x+y. In summary, we have proven that in the absence of bulk potentials, the only possible non-trivial solution is that the boundary potentials depend exclusively on one of the variables.

Let us briefly comment on the case in which we could not move the trigonometric functions to the r.h.s in Equation (5.82). For $\sin\varphi=0$, the only allowed transformations are $S=\begin{pmatrix}\epsilon'&0\\0&\epsilon''\end{pmatrix}$ with $\epsilon',\epsilon''=\pm 1$, corresponding to $(x,y)\mapsto (\epsilon'x,\epsilon''y)$. Similarly,

for
$$\cos \varphi = 0$$
, we have $S = \begin{pmatrix} 0 & \epsilon' \\ \epsilon'' & 0 \end{pmatrix}$ with $\epsilon', \epsilon'' = \pm 1$, and $(x,y) \mapsto (\epsilon'y, \epsilon''x)$. In both

these cases, the transformation reduces to a trivial relabeling of the names of functions, which will exclude them from our considerations.

It remains, therefore, to explicitly study transformations leading to the variables x-y and x+y. We start with the x-y case. This means that $(f\circ S_-)(x-y)=P(x-y)$ for some function P. Writing this explicitly,

$$P(x-y) = \sum_{k \ge 0} p_k (x-y)^k = \sum_{k \ge 0} \sum_{n=0}^k p_k \binom{k}{n} (-1)^{k-n} x^n y^{k-n}, \qquad p_k \in \mathbb{R}, \qquad \textbf{(5.91)}$$

so that the equation we have to solve takes the form

$$\sum_{k\geq 0} \sum_{n=0}^k p_k \binom{k}{n} (-1)^{k-n} x^n y^{k-n} = \sum_{k,l\geq 0} B_{k,l} x^k y^l. \tag{5.92}$$

First, taking y = x, the left-hand-side is simply p_0 , and for all n > 0 we have to have

$$\sum_{k+l=n} B_{k,l} = 0, (5.93)$$

while $p_0 = B_{0,0} = -|b_0|^2$. The system of equations (5.93) is in this case equivalent to

$$\begin{cases} \sum\limits_{k+l=n} \mathrm{Re}(b_k^*b_l) = 0, & n = 2m+1, \quad m \geq 0, \\ \sum\limits_{k+l=n} \mathrm{Re}(b_k^*b_l) + \frac{1}{2}|b_m|^2 = 0, & n = 2m, \quad m > 0. \end{cases} \tag{5.94}$$

Therefore, there exists a sequence $\kappa = (\kappa_n)_{n=1}^{\infty} \subset \mathbb{R}$ s.t.

$$\sum_{\substack{k+l=n\\k< l}} b_k^* b_l = i\kappa_n - \frac{1}{2} |b_m|^2 \delta_{n,2m}. \tag{5.95}$$

Since $B_{k,l} = -b_k b_l^*$, the above equation can be equivalently written as

$$\sum_{\substack{k+l=n\\k>l}} B_{k,l} = -\frac{1}{2} B_{m,m} \delta_{n,2m} - i\kappa_n.$$
 (5.96)

This leads to at most one family of solutions for $B_{k,l}=B_{k,l}(\kappa,B_{0,0})$ parameterized by a sequence κ of real numbers, and a non-positive number $B_{0,0}$ (since $B_{0,0}=-|b_0|^2=p_0$). If $p_0=0$, then $b_0=0$ and therefore all b_k must vanish. On the other hand, from (5.92) we get

$$(-1)^{l} p_{k+l} \binom{k+l}{n} = B_{k,l}, {(5.97)}$$

and since p_n is a purely real quantity for all n, it must happen that $B_{k,l} \in \mathbb{R}$, for all k,l, which leads to contradiction with (5.96) unless $b_m = \kappa_{2m} = 0$, for all m > 0. Therefore, the only potential solution is of the form $\beta(x) = b_0 = \sqrt{-p_0}e^{i\theta}$ and $P(x-y) = p_0$, with $\theta \in [0,2\pi)$ and $p_0 \leq 0$.

Now we consider the situation with $(f\circ S)(x,y)=Q(x+y)$ with some polynomial Q. In this case $\rho(k)=(-1)^k$, for n=2m+1 with $m\geq 0$ the condition on $\widetilde{B}_{k,l}=B_{k,l}\rho(l)$ reads

$$\operatorname{Im}\left(\sum_{\substack{k+l=2m+1\\k< l}} B_{k,l}\right) = 0, \tag{5.98}$$

so that $\sum_{k+l=2m+1} B_{k,l} \equiv \kappa_{2m+1} \in \mathbb{R}$. Similarly, for n=2m with m>0 we get

$$\operatorname{Im}\left(\sum_{\substack{k+l=2m\\k< l}} B_{k,l}\right) + \frac{(-1)^m}{2} |b_m|^2 = 0, \tag{5.99}$$

hence

$$\sum_{\substack{k+l=2m\\k< l}} B_{k,l} = \kappa_{2m} + i \frac{(-1)^m}{2} |b_m|^2, \tag{5.100}$$

with $\kappa_{2m}\in\mathbb{R}$. Comparing Q(x+y) with $\sum\limits_{k,l\geq 0}B_{k,l}x^ky^l$ we infer that $\forall k,l\ B_{k,l}\in\mathbb{R}$. As a result, for all m>0, we have $b_m=0$.

To summarize, whenever the bulk Hamiltonian contains no potentials, and there is only a single coupling to the physical field, the only possible allowed transformations of variables restrict the boundary potential to exclusively depend on one of the fixed-point variables. Furthermore, the only permitted solution in this case is with constant β and f. This example shows how important it is to either include virtual bulk potentials or several couplings in order to be able to describe anything other than the trivial scenario. These last two scenarios are the ones that show the positive examples presented above with the ϕ^4 bulk theory or the sine-Gordon fixed-point.

POTENTIAL-FULL BULK WITH A SINGLE COUPLING

Let us then increase the complexity one more step by allowing the bulk to have non-trivial potentials as well as several couplings to the physical field theory. Here we assume that the function f is of the form f(x',y')=h(x')+l(y'), where both functions h and l are allowed to be non-constant. With $S \in O(2)$ as in (5.75), we have

$$\begin{split} (f\circ S)(x,y) &= \sum_{k\geq 0} h_k (x\cos\varphi + y\epsilon\sin\varphi)^k + \sum_{k\geq 0} l_k (x\sin\varphi - y\epsilon\cos\varphi)^k \\ &= \sum_{k\geq 0} \sum_{n=0}^k \binom{k}{n} \Big[h_k \cos^n\varphi \epsilon^{k-n} \sin^{k-n}\varphi + l_k \sin^n\varphi (-1)^{k-n}\epsilon^{k-n} \cos^{k-n}\varphi \Big] x^n y^{k-n}. \end{split}$$

Therefore, Equations (5.74),(5.77) and (5.79) take the form

$$\begin{pmatrix} a+b \\ a \end{pmatrix} \left[h_{a+b} \cos^a \varphi \sin^b \varphi \epsilon^b + l_{a+b} \sin^a \varphi \cos^b \varphi (-1)^b \epsilon^b \right] = g_a \delta_{b,0} + g_b \delta_{a,0} + B_{a,b}.$$
 (5.102)

We first remark that a=b=0 leads to $h_0+l_0=2g_0+B_{0,0}$. Then, taking $a\neq b=0$ we end up with

$$h_a \cos^a \varphi + l_a \sin^a \varphi = g_a + B_{a,0}, \tag{5.103}$$

while for $b \neq a = 0$ we get

$$h_b \sin^b \varphi \epsilon^b + l_b \cos^b \varphi (-1)^b \epsilon^b = g_b + B_{0,b}. \tag{5.104}$$

Comparing these two conditions and making use of the hermiticity, we have

$$h_a(\cos^a\varphi-\sin^a\varphi\epsilon^a)+l_a(\sin^a\varphi-(-\epsilon)^a\cos^a\varphi)=0. \tag{5.105}$$

This equation was derived under the assumption that a > 0; however, it also holds identically for a = 0, so we can make use of it for any $a \ge 0$.

At this point, one can distinguish two cases here:

1. There exists (φ,ϵ) such that $\cos^a\varphi=\epsilon^a\sin^a\varphi$, for all $a\geq 0$, or such that $\cos^a\varphi=(-\epsilon)^a\sin^a\varphi$, for all $a\geq 0$. Both of them can be unified to the existence of $\widetilde{\varphi}$ s.t. $\cos\widetilde{\varphi}=\pm\sin\widetilde{\varphi}$. The solutions in the second case can be easily obtained from the first one by simply replacing (h_a,l_a,ϵ) by $(l_a,h_a,-\epsilon)$. Hence, we can consider only the first scenario without the loss of generality.

2. There exists (φ, ϵ) such that for some $a \ge 0$ we have either $\cos^a \varphi \ne \epsilon^a \sin^a \varphi$ or $\cos^a \varphi \ne (-\epsilon)^a \sin^a \varphi$.

From now on, we will assume that we find ourselves under the first case. First, the condition $\cos^a \varphi = \epsilon^a \sin^a \varphi$ applied in (5.105) implies that

$$l_a \sin^a \varphi (1 - (-1)^a) = 0. {(5.106)}$$

For a even this does not lead to any further restrictions on the coefficient l_a . However, since under our assumption $\sin\varphi_1\neq 0$, we infer that for a odd, a=2p+1, this leads to the constraint: $l_{2p+1}=0$. From (5.103) we then get

$$h_{2p+1} = \frac{\epsilon}{\sin^{2p+1}\varphi}(g_{2p+1} + B_{2p+1,0}). \tag{5.107}$$

Taking a = b = p in (5.102) we end up with

$$\forall p \ge 0 \quad h_{2p} + (-1)^p l_{2p} = \frac{B_{p,p} + 2g_p \delta_{p,0}}{\binom{2p}{p} \cos^{2p} \varphi}. \tag{5.108}$$

We now analyze (5.102). For $a, b \neq 0$, it is equivalent to

$$\binom{a+b}{a} \epsilon^{a+b} \sin^{a+b} \varphi \Big(h_{a+b} + (-1)^b l_{a+b} \Big) = B_{a,b}.$$
 (5.109)

Applying it for the pair $(a,b) \rightsquigarrow (a+1,2k)$ gives

$$h_{2k+a+1} + l_{2k+a+1} = \frac{B_{a+1,2k}}{\binom{2k+a+1}{a+1} \epsilon^{a+1} \sin^{2k+a+1} \varphi},$$
(5.110)

while for $(a, b) \rightsquigarrow (a, 2k + 1)$ we have

$$h_{2k+a+1} - l_{2k+a+1} = \frac{B_{a,2k+1}}{\binom{2k+a+1}{a}\epsilon^{a+1}\sin^{2k+a+1}\varphi}.$$
 (5.111)

As a result,

$$h_{2k+a+1} = \frac{1}{2\epsilon^{a+1} \sin^{2k+a+1} \varphi} \left[\frac{B_{a+1,2k}}{\binom{2k+a+1}{a+1}} + \frac{B_{a,2k+1}}{\binom{2k+a+1}{a}} \right], \tag{5.112}$$

and

$$l_{2k+a+1} = \frac{1}{2\epsilon^{a+1} \sin^{2k+a+1} \varphi} \left[\frac{B_{a+1,2k}}{\binom{2k+a+1}{a+1}} - \frac{B_{a,2k+1}}{\binom{2k+a+1}{a}} \right]. \tag{5.113}$$

Since under our assumptions $l_{\mathrm{odd}}=0$, the latter equation leads to

$$B_{2p+1,2k} = B_{2p,2k+1} \frac{\binom{2k+2p+1}{2p+1}}{\binom{2k+2p+1}{2p}} = \frac{2k+1}{2p+1} B_{2p,2k+1},$$
 (5.114)

therefore, the former one reduces to

$$h_{2p+2k+1} = \frac{\epsilon B_{2p,2k+1}}{\binom{2k+2p+1}{2p} \sin^{2k+2p+1} \varphi}.$$
 (5.115)

Comparing with (5.107) with $p \rightsquigarrow p + k$, we have

$$\frac{B_{2p+2k,1}}{2p+1} = g_{2p+2k+1} + B_{2p+2k+1,0}. (5.116)$$

In particular, the expression $\frac{g_{2p+2k+1}+B_{2p+2k+1,0}}{B_{2p+2k+1}}$ is k-independent, and

$$1 = \frac{g_1 + B_{1,0}}{B_{1,1}} = \frac{g_3 + B_{3,0}}{B_{3,1}} = \frac{g_5 + B_{5,0}}{B_{5,1}} = \dots$$
 (5.117)

Next, from (5.109) we get for all a, b > 0,

$$\frac{B_{a,b}}{B_{b,a}} = \frac{h_{a+b} + (-1)^b l_{a+b}}{h_{a+b} + (-1)^a l_{a+b}}.$$
(5.118)

There are four cases for (a,b): (even, even), (odd, odd), (odd, even), (even, odd). For the first two of them, the above ratio is trivially equal to 1. For the remaining ones, however, we have $a+b\in 2\mathbb{Z}+1$, but then $l_{a+b}=0$, and again the ratio is equal to 1. As a result, $B_{a,b}=B_{b,a}$ for all a,b>0. From (5.103) and (5.104), due to the hermiticity of the remaining terms, we also have $B_{a,0}=B_{0,a}$ for all a>0. Therefore, $B_{a,b}=B_{b,a}$ for all $a,b\geq 0$.

This symmetry, together with (5.110), introduces a constraint on the transformation S. Mainly, the parameter ϵ has to satisfy $\epsilon^{a+1}=1$ for all $a\geq 0$, i.e. only $\epsilon=1$ is allowed.

As we have seen in this section, there are many constraints amongst all the coefficients. Still, the exploration of this set of Equations is not yet complete and constitutes the content of our upcoming work [3]. To establish further constraints, one can begin by demanding that N=1 alongside non-trivial bulk potentials. Our explorations so far point us towards the conclusion that in order to allow for non-trivial solutions, the series expansion of the couplings α needs to contain no zero terms, as otherwise, all the constraints lead only to finite polynomials, but more work is needed to set this result in stone.

5.3 OUTLOOK

In this chapter, we have presented continuous Tensor Networks as an ansatz designed to tackle physical QFTs by coupling them to a virtual QFT in the same spirit as Tensor Networks. Although being a proper generalization of the already known cMPS to higher dimensions, much less is understood either numerically or analytically about the ansatz or its use-case scenarios.

In this chapter, we have focused our efforts on trying to study theoretically when using a cTNS can be advantageous in order to study complicated QFTs. Guided by

an example in which a correlator of a complicated coupled physical bosonic field theory could be computed as a fixed-point correlator of a specific cTNS, we sought to understand what is the general structure behind this phenomenology.

Although this is an ongoing study, we have so far understood the minimal ingredients a cTNS must have to exhibit non-trivial behaviour at its fixed point. These ingredients are either non-trivial bulk potentials or several independent couplings to the physical theory. Our current efforts are devoted to fully understand the latter ones to provide more useful scenarios for cTNS.

Future directions include the completion of the aforementioned results, as well as the usage of the numerical approach of cMPS to efficiently describe the cases in which an analytical expression for the fixed-point correlator exists. Possible extensions include the development of a consistent fermionic cTNS, as well as possible implementations of cTNS on curved space-times.

ACKNOWLEDGMENTS

I have been extremely fortunate to enjoy the support of a myriad of different people throughout the journey that this thesis has been, both scientifically and personally. First and foremost, I am deeply thankful for being able to learn from and work with my supervisor Ignacio Cirac. I feel very honored to have been able to learn from your scientific thinking and have always left our discussions inspired and motivated to keep discovering. I deeply value your guidance and support as a mentor, as well as the very inspiring environment that you have created at MPQ, from which we all benefit and that I have felt very safe in.

On the same wavelength, I feel extremely lucky to have been able to work with my co-supervisor Germán Sierra. Our discussions have always renewed and strengthened my motivation and desire to keep working on very hard problems. I have learned a lot from your amazing intuition and scientific demeanor, and look forward to all our future discussions. I am very thankful for all your visits at MPQ as well as your patience with all my mistakes.

I also wish to extend my gratitude to my co-authors and the postdocs that have served a guiding role through these last years. Firstly, my thanks go to Antoine Tilloy for being my first guide when I arrived at MPQ, and from whom I learned a lot about field theory. Secondly, to Arkadiusz Bochniak, for allowing me to participate in a very enjoyable and active in-person collaboration from which I have gained a lot. Finally, to Adrián Franco Rubio, for always being that person that I could reach to discuss any detail about my projects, no matter how small. From common scientific interests to a good friend, I hope our scientific paths continue to intertwine.

I also wish to acknowledge the many opportunities I have had to travel to conferences and workshops, and all the inspiring people I have met in them. I wish to give a special regard to José Garre, Alberto Ruiz, Anne Nielsen and Ivan Kukuljan as some of those people that have always made me look forward to fruitful scientific discussions.

This thesis would sound and look very different where it not for proofreaders. I want to extend my heartfelt thanks to Patrick Emonts, Jiri Guth-Jarkovsky, Germán Sierra, Arkadiusz Bochniak, Adrián Franco Rubio and Marc Serra. Thank you very much for taking the time and care to go through the different parts of this thesis, and leaving it better than it previously was.

I wish to extend my gratitude to all the secretaries of the theory group, Andrea Angione, Regina Jasny and Andrea Kluth. Thank you all for always making all administrative problems seem small thanks to your efficiency and willingness to help, I deeply appreciate you. Likewise, I want to extend this gratitude to Sonya Gzyl from IMPRS-QST. Not only have I been very fortunate to receive their grant for the first years of this PhD, but Sonya has been an amazing support and point of contact for all of us IMPRS students. Thank you for all the amazing work you do in helping us create great scientific events, we are very lucky to work with you.

Throughout these years at MPQ, I have been fortunate to meet and interact with a lot of beautiful people. The incredible atmosphere at MPQ would not be what it is where

it not for all of you. Firstly, to my first office mates ever, David Stephen, Caroline de Groot and Jiri Guth. You all made the office a warm space in which to discuss physics, politics or whatever crossed our minds. You three helped in creating such a safe and fun space that I deeply valued. A special warm regard goes to David Stephen, for not only being an invaluable friend with whom to spend countless hours, but also a paramount support who helped me keep myself grounded and safe in difficult times.

Secondly, the second iteration of the office, Maxine Luo, Xiehang Yu and Marianna Cruppi. I have enjoyed our office mates dinners, and a special warm and heartfelt thanks goes to Marianna. I feel very glad to have found within you, yet another invaluable support with whom to talk about whatever was needed. I hope that through the years, regardless of the distance, we keep finding on one another the distinct warmth feeling of being understood.

Lastly, to all of you across the corridors. To Flavio Baccari, I hope your cheeky funny sarcasm remains always sharp. To Julian Bender, for being the best Oktoberfest wingman one could ask for. To Arthur Christianen, for sharing the passion for great fantasy stories. To Eduardo Sanchez, for acting as the best mentor I could have asked for upon my arrival at MPQ. To Tommasso Guaita, for always being a great person to talk to and the savior of the seminar. To Miguel Bello, for sharing with me my passion for live music. To Patrick Emonts, for being an incredible friend, support and teammate. No matter the absurdity of the task, you know you can always can count on me. To Giacomo Giudice and Samantha, for allowing me to share my passion for snowboarding and mountaineering with them.

To Alvaro Alhambra, for being a genuinely amazing person and sharing adventures both in and outside of the mountains. To David Castells, for always being willing to lend a hand, as well as to our many late night chats in the office. To Maria Cea, for being a great house-neighbor and friend. To Denise Cocchiarella, for a great switch riding session and to more fun in the slopes. To Marta Florido, for our shared experience in writing a book, as well as future concerts. To Miguel Frias, for the many adventures we have shared in the mountains, you have been a great friend with whom to ride. To Guillermo Gonzalez, for allowing me to poison your taste in series and the many adventures in the snow and online. You both have been a big source of smiles and laughter that I deeply value.

To Rajah Nutakki, for being an amazing co-organizer and friend. To Vjosa Blakaj, for being a great thesis-writing teammate with whom to share frustrations through these last months. To Yifan Jia, for the shared songs and episodes at Benasque. To Reinis Irmejs, for being a great person to ride along, and to the many senseless posts we share. To Pavel Kos, for being a very inspiring scientist, hiker and skier from whom to learn. To Sirui Lu, for trusting me in our mountain and sports adventures. To Irene Papaefstathiou, for being a good friend through the pandemic and sharing harmless gossip.

To Benjamin Schiffer, for being a great hackathon organizer and another person with whom to share snow adventures. To Yorgos Styliaris, for being one of the most inspiring postdocs that I have had the pleasure to meet. To Erickson Tjoa, for our late night and weekend chats. To Dominik Wild, for being a great friend with whom to share mountain, music and also being a very inspiring postdoc. To Esther Cruz Rico, for being a great friend and partner-in-crime through the many nights in Benasque. To Jordi Tura, for being a familiar face upon my arrival at MPQ, and co-founder of the Garching CDR.

A lot of the support I have received also comes from people who are much more far away. First and foremost, to the CM-crew. To Gerard Cassola, Adri, Berny, Jon Ander and Laia Gasull, in all of our nights I have found a haven to rest, laugh and share lots of joy with all of you. I wish that there still are many adventures that await us online in the future. To the Pseudofisics, which although I have been further away, I deeply care and value all of you. A warm thanks goes to Maria Flors, for the many weekends we have shared in these foreign lands. To the friends from AEC, it is always a joy for me to come back to see our relationships strong. A special regards goes to Mikel Gorostidi and Clara Vidal, you two are extremely important for me. To Marc Enzo, being able to share time with you on my visits back home is always a highlight. To Gerard Vaquer, for keeping me connected with the musical side of myself that I so deeply cherish.

A very warm thanks also goes to my housemates Lux Hengel and Christina Schuh. Our flat in Eching has been the most enjoyable house-sharing experiences I have ever had, and I deeply cherish all the moments we have shared through the last 5 years. I want to extend a heartfelt thanks to my grandfather, who inspired me to develop my passion for science and discovery. I also wish to acknowledge all the artists that enrich my life with their art, music and games.

Lastly, I want to thank both my parents for their invaluable support and allowing me to live a very privileged life. Without you, I would never have been in a position to pursue science, and for that I will forever be grateful. I can not put into words how important my sister, Laia Gasull, has been throughout these last years. Through all challenges, I have always found an invaluable support in you, and I hope that I have been able to reciprocate it. Another invaluable friend and support in my life is Marc Serra, without whom I would probably be much more lost today. I feel very privileged to consider you one of my best friends, and I hope that we live many adventures in the future.

To finalize, these last years have not only been a journey of scientific discovery, but a journey of personal growth. In this sense, I wish to give my heartfelt thanks to the mental health professionals who have aided me. Thank you for helping me nurture and develop the tools to better understand myself. All of the people mentioned in these acknowledgments have left a footprint in my path, no matter how big or small. To those whose path has departed from mine, know that I carry with me the footprints you have left, not only as a memento, but also as a promise to remain true to all of which we have shared and valued together.



BIBLIOGRPAHY

- [1] Albert Gasull, J. Ignacio Cirac, and German Sierra. "Field Tensor Networks: Theorems, proofs and an exact representation of a 2 dimensional chiral gapped state." In: *ArXiv* (2025), In preparation.
- [2] Albert Gasull et al. "Symmetries and field tensor network states". In: *Phys. Rev. B* 107 (15 Apr. 2023), p. 155102. DOI: 10.1103/PhysRevB.107.155102.
- [3] Albert Gasull, Arkadiusz Bochniak, and J. Ignacio Cirac. "Bulk-boundary correspondance in continuous Tensor Network states". In: *ArXiv* (2025), In preparation.
- [4] Paolo Molignini et al. "Crossdimensional universality classes in static and periodically driven Kitaev models". In: *Phys. Rev. B* 103 (18 May 2021), p. 184507. DOI: 10.1103/PhysRevB.103.184507.
- [5] Roger Penrose. Emperor's New Mind. Oxford University Press UK, 1999.
- [6] N. H. March et al. "The Many-Body Problem in Quantum Mechanics". In: American Journal of Physics 37.1 (Jan. 1969), pp. 116–116. DOI: 10.1119/ 1.1975378. eprint: https://pubs.aip.org/aapt/ajp/articlepdf/37/1/116/10113860/116_1_online.pdf.
- [7] Michael A. Nielsen and Isaac L. Chuang. *Quantum Computation and Quantum Information: 10th Anniversary Edition*. Cambridge University Press, 2010.
- [8] Matthew B. Hastings and Tohru Koma. "Spectral Gap and Exponential Decay of Correlations". In: *Communications in Mathematical Physics* 265.3 (Apr. 2006), pp. 781–804. DOI: 10.1007/s00220-006-0030-4.
- [9] M. Fannes, B. Nachtergaele, and R. F. Werner. "Finitely correlated states on quantum spin chains". In: *Communications in Mathematical Physics* 144.3 (Mar. 1992), pp. 443–490. DOI: 10.1007/BF02099178.
- [10] Ignacio Cirac et al. *Matrix Product States and Projected Entangled Pair States:* Concepts, Symmetries, and Theorems. 2021. arXiv: 2011.12127 [quant-ph].
- [11] Román Orús. "A practical introduction to tensor networks: Matrix product states and projected entangled pair states". In: *Annals of Physics* 349 (2014), pp. 117–158. DOI: https://doi.org/10.1016/j.aop.2014.06.013.
- [12] Jacob C Bridgeman and Christopher T Chubb. "Hand-waving and interpretive dance: an introductory course on tensor networks". In: *Journal of Physics A: Mathematical and Theoretical* 50.22 (May 2017), p. 223001. DOI: 10.1088/1751-8121/aa6dc3.
- [13] Alexander Müller-Hermes, J Ignacio Cirac, and Mari Carmen Bañuls. "Tensor network techniques for the computation of dynamical observables in one-dimensional quantum spin systems". In: *New Journal of Physics* 14.7 (July 2012), p. 075003. DOI: 10.1088/1367-2630/14/7/075003.

- [14] F. Verstraete, J. J. García-Ripoll, and J. I. Cirac. "Matrix Product Density Operators: Simulation of Finite-Temperature and Dissipative Systems". In: *Phys. Rev. Lett.* 93 (20 Nov. 2004), p. 207204. DOI: 10.1103/PhysRevLett.93. 207204.
- [15] Norbert Schuch, David Pérez-García, and Ignacio Cirac. "Classifying quantum phases using matrix product states and projected entangled pair states". In: *Physical Review B* 84.16 (Oct. 2011). DOI: 10.1103/physrevb.84.165139.
- [16] Norbert Schuch et al. "Topological Order in the Projected Entangled-Pair States Formalism: Transfer Operator and Boundary Hamiltonians". In: *Physical Review Letters* 111.9 (Aug. 2013). DOI: 10.1103/physrevlett.111.090501.
- [17] Shuo Yang et al. "Chiral Projected Entangled-Pair State with Topological Order". In: *Physical Review Letters* 114.10 (Mar. 2015). DOI: 10.1103/physrevlett.114.106803.
- [18] P. C. Hohenberg and B. I. Halperin. "Theory of dynamic critical phenomena". In: *Rev. Mod. Phys.* 49 (3 July 1977), pp. 435–479. DOI: 10.1103/RevModPhys.49.435.
- [19] Michael E. Fisher. "Renormalization group theory: Its basis and formulation in statistical physics". In: *Rev. Mod. Phys.* 70 (2 Apr. 1998), pp. 653–681. DOI: 10.1103/RevModPhys.70.653.
- [20] R Folk and G Moser. "Critical dynamics: a field-theoretical approach". In: *Journal of Physics A: Mathematical and General* 39.24 (May 2006), R207. DOI: 10. 1088/0305-4470/39/24/R01.
- [21] G. Vidal et al. "Entanglement in Quantum Critical Phenomena". In: *Phys. Rev. Lett.* 90 (22 June 2003), p. 227902. DOI: 10.1103/PhysRevLett.90. 227902.
- [22] G. Vidal. "Entanglement Renormalization". In: *Phys. Rev. Lett.* 99 (22 Nov. 2007), p. 220405. DOI: 10.1103/PhysRevLett.99.220405.
- [23] Klaus von Klitzing. "The quantized Hall effect". In: *Rev. Mod. Phys.* 58 (3 July 1986), pp. 519–531. DOI: 10.1103/RevModPhys.58.519.
- [24] Avi Karsenty. "A Comprehensive Review of Integrated Hall Effects in Macro-, Micro-, Nanoscales, and Quantum Devices". In: *Sensors* 20.15 (2020). DOI: 10.3390/s20154163.
- [25] Klaus von Klitzing. "Developments in the quantum Hall effect". In: *Philosophical Transactions of the Royal Society A: Mathematical, Physical and Engineering Sciences* 363.1834 (2005), pp. 2203–2219. DOI: 10.1098/rsta.2005.1640. eprint: https://royalsocietypublishing.org/doi/pdf/10.1098/rsta.2005.1640.
- [26] Tsuneya Ando, Yukio Matsumoto, and Yasutada Uemura. "Theory of Hall Effect in a Two-Dimensional Electron System". In: *Journal of the Physical Society of Japan* 39.2 (1975), pp. 279–288. DOI: 10.1143/JPSJ.39.279. eprint: https://doi.org/10.1143/JPSJ.39.279.
- [27] Jun-ichi Wakabayashi and Shinji Kawaji. "Hall Effect in Silicon MOS Inversion Layers under Strong Magnetic Fields". In: *Journal of the Physical Society of Japan* 44.6 (1978), pp. 1839–1849. DOI: 10.1143/JPSJ.44.1839. eprint: https://doi.org/10.1143/JPSJ.44.1839.

- [28] K. v. Klitzing, G. Dorda, and M. Pepper. "New Method for High-Accuracy Determination of the Fine-Structure Constant Based on Quantized Hall Resistance". In: *Phys. Rev. Lett.* 45 (6 Aug. 1980), pp. 494–497. DOI: 10.1103/PhysRevLett.45.494.
- [29] D. J. Thouless. "Quantization of particle transport". In: *Phys. Rev. B* 27 (10 May 1983), pp. 6083–6087. DOI: 10.1103/PhysRevB.27.6083.
- [30] K. S. Novoselov et al. "Room-Temperature Quantum Hall Effect in Graphene". In: *Science* 315.5817 (Mar. 2007), pp. 1379–1379. DOI: 10.1126/science. 1137201.
- [31] D. R. Yennie. "Integral quantum Hall effect for nonspecialists". In: *Rev. Mod. Phys.* 59 (3 July 1987), pp. 781–824. DOI: 10.1103/RevModPhys.59.781.
- [32] Chetan Nayak et al. "Non-Abelian anyons and topological quantum computation". In: *Reviews of Modern Physics* 80.3 (2008), pp. 1083+. DOI: 10.1103/revmodphys.80.1083.
- [33] Mohsin Iqbal et al. "Non-Abelian topological order and anyons on a trappedion processor". In: *Nature* 626.7999 (Feb. 2024), pp. 505–511. DOI: 10.1038/s41586-023-06934-4.
- [34] J. Dubail and N. Read. "Tensor network trial states for chiral topological phases in two dimensions and a no-go theorem in any dimension". In: *Physical Review B* 92.20 (Nov. 2015). DOI: 10.1103/physrevb.92.205307.
- [35] Xiang Li et al. *Strict area law entanglement versus chirality*. 2024. arXiv: 2408. 10306 [quant-ph].
- [36] Gregory Moore and Nicholas Read. "Nonabelions in the fractional quantum hall effect". In: *Nuclear Physics B* 360.2 (1991), pp. 362–396. DOI: https://doi.org/10.1016/0550-3213(91)90407-0.
- [37] P. Di Francesco, P. Mathieu, and D. Senechal. *Conformal Field Theory*. Graduate Texts in Contemporary Physics. New York: Springer-Verlag, 1997. DOI: 10. 1007/978-1-4612-2256-9.
- [38] Edward Witten. "Quantum field theory and the Jones polynomial". In: *Communications in Mathematical Physics* 121.3 (1989), pp. 351–399.
- [39] Daniel C. Cabra and Gerardo L. Rossini. "Explicit Connection Between Conformal Field Theory and 2+1 Chern–Simons Theory". In: *Modern Physics Letters A* 12.23 (1997), pp. 1687–1697. DOI: 10.1142/S0217732397001722. eprint: https://doi.org/10.1142/S0217732397001722.
- [40] Jens Fjelstad et al. *Uniqueness of open/closed rational CFT with given algebra of open states*. 2008. arXiv: hep-th/0612306 [hep-th].
- [41] Jørgen Ellegaard Andersen and Kenji Ueno. *Construction of the Witten-Reshetikhin-Turaev TQFT from conformal field theory*. 2014. arXiv: 1110.5027 [math.QA].
- [42] Jürgen Fuchs, Christoph Schweigert, and Alessandro Valentino. "Bicategories for Boundary Conditions and for Surface Defects in 3-d TFT". In: *Communications in Mathematical Physics* 321.2 (May 2013), pp. 543–575. DOI: 10.1007/s00220-013-1723-0.

- [43] Juan Maldacena. "The Large N Limit of Superconformal Field Theories and Supergravity". In: *International Journal of Theoretical Physics* 38.4 (1999), pp. 1113–1133. DOI: 10.1023/a:1026654312961.
- [44] J. Ignacio Cirac and Germán Sierra. "Infinite matrix product states, conformal field theory, and the Haldane-Shastry model". In: *Phys. Rev. B* 81 (10 Mar. 2010), p. 104431. DOI: 10.1103/PhysRevB.81.104431.
- [45] Anne E. B. Nielsen, Germán Sierra, and J. Ignacio Cirac. "Violation of the area law and long-range correlations in infinite-dimensional-matrix product states". In: *Phys. Rev. A* 83 (5 May 2011), p. 053807. DOI: 10.1103/PhysRevA.83.053807.
- [46] Ivan Glasser et al. "Construction of spin models displaying quantum criticality from quantum field theory". In: *Nuclear Physics B* 886 (2014), pp. 63–74. DOI: https://doi.org/10.1016/j.nuclphysb.2014.06.016.
- [47] Ivan Glasser et al. "Exact parent Hamiltonians of bosonic and fermionic Moore–Read states on lattices and local models". In: 17.8 (Aug. 2015), p. 082001. DOI: 10.1088/1367-2630/17/8/082001.
- [48] Benedikt Herwerth et al. "Excited states in spin chains from conformal blocks". In: *Phys. Rev. B* 91 (23 June 2015), p. 235121. DOI: 10.1103/PhysRevB. 91.235121.
- [49] Benedikt Herwerth et al. "Bosonic Gaussian states from conformal field theory". In: *Physical Review B* 98.11 (Sept. 2018). DOI: 10.1103/physrevb. 98.115156.
- [50] Anne E B Nielsen, J Ignacio Cirac, and Germán Sierra. "Quantum spin Hamiltonians for the SU(2)k WZW model". In: *Journal of Statistical Mechanics: Theory and Experiment* 2011.11 (Nov. 2011), P11014. DOI: 10 . 1088 / 1742 5468/2011/11/P11014.
- [51] N. Read. "Compactly supported Wannier functions and algebraic < mml:math xmlns:mml = "http://www.w3.org/1998/Math/-MathML" > < mml:mi > K < / mml:mi > < / mml:math > -theory". In: *Physical Review B* 95.11 (Mar. 2017). DOI: 10.1103/physrevb.95.115309.
- [52] Norbert Schuch et al. "Computational Complexity of Projected Entangled Pair States". In: *Phys. Rev. Lett.* 98 (14 Apr. 2007), p. 140506. DOI: 10.1103/PhysRevLett.98.140506.
- [53] Yuki Takeuchi, Yasuhiro Takahashi, and Seiichiro Tani. "Hardness of efficiently generating ground states in postselected quantum computation". In: *Phys. Rev. Res.* 3 (1 Mar. 2021), p. 013213. DOI: 10 . 1103 / PhysRevResearch.3.013213.
- [54] Matthias Troyer and Uwe-Jens Wiese. "Computational Complexity and Fundamental Limitations to Fermionic Quantum Monte Carlo Simulations". In: *Phys. Rev. Lett.* 94 (17 May 2005), p. 170201. DOI: 10.1103/PhysRevLett.94. 170201.
- [55] Bruno Nachtergaele and Robert Sims. "Lieb-Robinson Bounds and the Exponential Clustering Theorem". In: *Communications in Mathematical Physics* 265.1 (Mar. 2006), pp. 119–130. DOI: 10.1007/s00220-006-1556-1.

- [56] David Gosset and Yichen Huang. "Correlation Length versus Gap in Frustration-Free Systems". In: *Physical Review Letters* 116.9 (Mar. 2016). DOI: 10.1103/physrevlett.116.097202.
- [57] Bruno Nachtergaele and Robert Sims. "Lieb-Robinson Bounds and the Exponential Clustering Theorem". In: *Communications in Mathematical Physics* 265.1 (Mar. 2006), pp. 119–130. DOI: 10.1007/s00220-006-1556-1.
- [58] Jutho Haegeman et al. "Variational matrix product ansatz for dispersion relations". In: *Phys. Rev. B* 85 (10 Mar. 2012), p. 100408. DOI: 10 . 1103 / PhysRevB.85.100408.
- [59] Carlos Fernández-González et al. "Gapless Hamiltonians for the Toric Code Using the Projected Entangled Pair State Formalism". In: *Physical Review Letters* 109.26 (Dec. 2012). DOI: 10.1103/physrevlett.109.260401.
- [60] C. Fernández-González et al. "Frustration Free Gapless Hamiltonians for Matrix Product States". In: *Communications in Mathematical Physics* 333.1 (Nov. 2014), pp. 299–333. DOI: 10.1007/s00220-014-2173-z.
- [61] L. D. Landau. "On the theory of phase transitions". In: Zh. Eksp. Teor. Fiz. 7 (1937). Ed. by D. ter Haar, pp. 19–32. DOI: 10.1016/B978-0-08-010586-4.50034-1.
- [62] J M Kosterlitz and D J Thouless. "Ordering, metastability and phase transitions in two-dimensional systems". In: *Journal of Physics C: Solid State Physics* 6.7 (Apr. 1973), p. 1181. DOI: 10.1088/0022-3719/6/7/010.
- [63] Horst L. Stormer, Daniel C. Tsui, and Arthur C. Gossard. "The fractional quantum Hall effect". In: *Rev. Mod. Phys.* 71 (2 Mar. 1999), S298–S305. DOI: 10. 1103/RevModPhys.71.S298.
- [64] X. G. Wen. "Vacuum degeneracy of chiral spin states in compactified space". In: *Phys. Rev. B* 40 (10 Oct. 1989), pp. 7387–7390. DOI: 10.1103/PhysRevB. 40.7387.
- [65] X. G. WEN. "TOPOLOGICAL ORDERS IN RIGID STATES". In: International Journal of Modern Physics B 04.02 (1990), pp. 239–271. DOI: 10.1142 / S0217979290000139. eprint: https://doi.org/10.1142 / S0217979290000139.
- [66] X. G. Wen and Q. Niu. "Ground-state degeneracy of the fractional quantum Hall states in the presence of a random potential and on high-genus Riemann surfaces". In: *Phys. Rev. B* 41 (13 May 1990), pp. 9377–9396. DOI: 10.1103/PhysRevB.41.9377.
- [67] A. J. Coleman. "Necessary Conditions for N-Representability of Reduced Density Matrices". In: *Journal of Mathematical Physics* 13.2 (Feb. 1972), pp. 214–222. DOI: 10.1063/1.1665956. eprint: https://pubs.aip.org/aip/jmp/article-pdf/13/2/214/19145282/214_1_online.pdf.
- Verstraete. [68] Yi-Kai Liu, Matthias Christandl, and F. Computational Complexity of the < mml:math "Ouantum xmlns:mml = "http://www.w3.org/1998/Math/MathML" display = "inline"> < mml:mi > N < / mml:mi > < / mml:math > -Representability Problem: QMA Complete". In: Physical Review Letters 98.11 (Mar. 2007). DOI: 10.1103/physrevlett.98.110503.

- [69] M. B. Hastings. "Solving gapped Hamiltonians locally". In: *Phys. Rev. B* 73 (8 Feb. 2006), p. 085115. DOI: 10.1103/PhysRevB.73.085115.
- [70] F. Verstraete et al. "Criticality, the Area Law, and the Computational Power of Projected Entangled Pair States". In: *Phys. Rev. Lett.* 96 (22 June 2006), p. 220601. DOI: 10.1103/PhysRevLett.96.220601.
- [71] F. Verstraete and J. I. Cirac. "Matrix product states represent ground states faithfully". In: *Phys. Rev. B* 73 (9 Mar. 2006), p. 094423. DOI: 10 . 1103 / PhysRevB.73.094423.
- [72] V Zauner et al. "Symmetry breaking and the geometry of reduced density matrices". In: *New Journal of Physics* 18.11 (Nov. 2016), p. 113033. DOI: 10.1088/1367-2630/18/11/113033.
- [73] Charles H. Bennett et al. "Mixed-state entanglement and quantum error correction". In: *Physical Review A* 54.5 (Nov. 1996), pp. 3824–3851. DOI: 10.1103/physreva.54.3824.
- [74] Martin B. Plenio and S. Virmani. *An introduction to entanglement measures*. 2006. arXiv: quant-ph/0504163 [quant-ph].
- [75] Dardo Goyeneche et al. "Absolutely maximally entangled states, combinatorial designs, and multiunitary matrices". In: *Phys. Rev. A* 92 (3 Sept. 2015), p. 032316. DOI: 10.1103/PhysRevA.92.032316.
- [76] Xiao-Lan Zong et al. "Monogamy of Quantum Entanglement". In: *Frontiers in Physics* 10 (June 2022). DOI: 10.3389/fphy.2022.880560.
- [77] Carlton M. Caves, Christopher A. Fuchs, and Rüdiger Schack. "Unknown quantum states: The quantum de Finetti representation". In: *Journal of Mathematical Physics* 43.9 (Sept. 2002), pp. 4537–4559. DOI: 10.1063/1.1494475.
- [78] Matthew B. Hastings. *Gapped Quantum Systems: From Higher Dimensional Lieb-Schultz-Mattis to the Quantum Hall Effect*. 2021. arXiv: 2111.01854 [math-ph].
- [79] Eugenio Bianchi et al. "Volume-Law Entanglement Entropy of Typical Pure Quantum States". In: *PRX Quantum* 3.3 (July 2022). DOI: 10 . 1103 / prxquantum.3.030201.
- [80] Hyejin Ju et al. "Entanglement scaling in two-dimensional gapless systems". In: *Phys. Rev. B* 85 (16 Apr. 2012), p. 165121. DOI: 10.1103/PhysRevB.85. 165121.
- [81] Pasquale Calabrese and John Cardy. "Entanglement entropy and quantum field theory". In: 2004.06 (June 2004), P06002. DOI: 10 . 1088 / 1742 5468 / 2004/06/p06002.
- [82] Xie Chen, Zheng-Cheng Gu, and Xiao-Gang Wen. "Local unitary transformation, long-range quantum entanglement, wave function renormalization, and topological order". In: *Physical Review B* 82.15 (Oct. 2010). DOI: 10.1103/physrevb.82.155138.
- [83] M. Born and V. Fock. "Beweis des Adiabatensatzes". In: *Zeitschrift fur Physik* 51.3-4 (Mar. 1928), pp. 165–180. DOI: 10.1007/BF01343193.

- [84] Xie Chen, Zheng-Cheng Gu, and Xiao-Gang Wen. "Classification of gapped symmetric phases in one-dimensional spin systems". In: *Physical Review B* 83.3 (Jan. 2011). DOI: 10.1103/physrevb.83.035107.
- [85] F. D. M. Haldane. "Nonlinear Field Theory of Large-Spin Heisenberg Antiferromagnets: Semiclassically Quantized Solitons of the One-Dimensional Easy-Axis Néel State". In: *Phys. Rev. Lett.* 50 (15 Apr. 1983), pp. 1153–1156. DOI: 10.1103/PhysRevLett.50.1153.
- [86] F.D.M. Haldane. "Continuum dynamics of the 1-D Heisenberg antiferromagnet: Identification with the O(3) nonlinear sigma model". In: *Physics Letters A* 93.9 (1983), pp. 464–468. DOI: https://doi.org/10.1016/0375-9601(83) 90631-X.
- [87] Ian Affleck and F. D. M. Haldane. "Critical theory of quantum spin chains". In: *Phys. Rev. B* 36 (10 Oct. 1987), pp. 5291–5300. DOI: 10.1103/PhysRevB. 36.5291.
- [88] I Affleck. "Quantum spin chains and the Haldane gap". In: *Journal of Physics: Condensed Matter* 1.19 (May 1989), p. 3047. DOI: 10.1088/0953-8984/1/19/001.
- [89] Shantanu Mishra et al. "Observation of fractional edge excitations in nanographene spin chains". In: *Nature* 598.7880 (2021), pp. 287–292.
- [90] Xie Chen, Zheng-Xin Liu, and Xiao-Gang Wen. "Two-dimensional symmetry-protected topological orders and their protected gapless edge excitations". In: *Physical Reviews B* 84.23, 235141 (Dec. 2011), p. 235141. DOI: 10.1103/PhysRevB.84.235141. arXiv: 1106.4752 [cond-mat.str-el].
- [91] Xie Chen et al. "Symmetry protected topological orders and the group cohomology of their symmetry group". In: *Physical Reviews B* 87.15, 155114 (Apr. 2013), p. 155114. DOI: 10.1103/PhysRevB.87.155114. arXiv: 1106.4772 [cond-mat.str-el].
- [92] Zheng-Cheng Gu and Xiao-Gang Wen. "Symmetry-protected topological orders for interacting fermions: Fermionic topological nonlinear sigma models and a special group supercohomology theory". In: *Physical Review B* 90.11 (Sept. 2014). DOI: 10.1103/physrevb.90.115141.
- [93] Norbert Schuch, Ignacio Cirac, and David Pérez-García. "PEPS as ground states: Degeneracy and topology". In: *Annals of Physics* 325.10 (2010), pp. 2153–2192. DOI: https://doi.org/10.1016/j.aop.2010.05.008.
- [94] Yoshiko Ogata. *Classification of symmetry protected topological phases in quantum spin chains.* 2021. arXiv: 2110.04671 [math-ph].
- [95] Michael A. Levin and Xiao-Gang Wen. "String-net condensation: A physical mechanism for topological phases". In: *Physical Review B* 71.4 (Jan. 2005). DOI: 10.1103/physrevb.71.045110.
- [96] Laurens Lootens et al. "Matrix product operator symmetries and intertwiners in string-nets with domain walls". In: *SciPost Physics* 10.3 (Mar. 2021). DOI: 10.21468/scipostphys.10.3.053.
- [97] W. P. Su, J. R. Schrieffer, and A. J. Heeger. "Soliton excitations in polyacetylene". In: *Phys. Rev. B* 22 (4 Aug. 1980), pp. 2099–2111. DOI: 10.1103/PhysRevB.22.2099.

- [98] M. Nakahara. Geometry, topology and physics. 2003.
- [99] Alexander Altland and Martin R. Zirnbauer. "Nonstandard symmetry classes in mesoscopic normal-superconducting hybrid structures". In: *Physical Reviews B* 55.2 (Jan. 1997), pp. 1142–1161. DOI: 10.1103/PhysRevB.55.1142. arXiv: cond-mat/9602137 [cond-mat].
- [100] Alexei Kitaev, Vladimir Lebedev, and Mikhail Feigel'man. "Periodic table for topological insulators and superconductors". In: *AIP Conference Proceedings*. AIP, 2009. DOI: 10.1063/1.3149495.
- [101] K. v. Klitzing, G. Dorda, and M. Pepper. "New Method for High-Accuracy Determination of the Fine-Structure Constant Based on Quantized Hall Resistance". In: *Phys. Rev. Lett.* 45 (6 Aug. 1980), pp. 494–497. DOI: 10.1103/PhysRevLett.45.494.
- [102] Eduardo Fradkin. *Field Theories of Condensed Matter Physics*. 2nd ed. Cambridge University Press, 2013.
- [103] D. J. Thouless et al. "Quantized Hall Conductance in a Two-Dimensional Periodic Potential". In: *Phys. Rev. Lett.* 49 (6 Aug. 1982), pp. 405–408. DOI: 10. 1103/PhysRevLett.49.405.
- [104] Qian Niu, D. J. Thouless, and Yong-Shi Wu. "Quantized Hall conductance as a topological invariant". In: *Phys. Rev. B* 31 (6 Mar. 1985), pp. 3372–3377. DOI: 10.1103/PhysRevB.31.3372.
- [105] A.Yu. Kitaev. "Fault-tolerant quantum computation by anyons". In: *Annals of Physics* 303.1 (2003), pp. 2–30. DOI: https://doi.org/10.1016/S0003-4916(02)00018-0.
- [106] R de-Picciotto et al. "Direct observation of a fractional charge". In: *Physica B: Condensed Matter* 249-251 (1998), pp. 395–400. DOI: https://doi.org/10.1016/S0921-4526(98)00139-2.
- [107] June-Young M. Lee and H. -S. Sim. "Non-Abelian anyon collider". In: *Nature Commun.* 13.1 (2022), p. 6660. DOI: 10.1038/s41467-022-34329-y. arXiv: 2202.03649 [cond-mat.mes-hall].
- [108] Mohsin Iqbal et al. "Non-Abelian topological order and anyons on a trappedion processor". In: *Nature* 626.7999 (2024), pp. 505–511. DOI: 10 . 1038 / s41586-023-06934-4. arXiv: 2305.03766 [quant-ph].
- [109] M. Ruelle et al. "Comparing Fractional Quantum Hall Laughlin and Jain Topological Orders with the Anyon Collider". In: *Phys. Rev. X* 13.1 (2023), p. 011031. DOI: 10.1103/PhysRevX.13.011031.
- [110] James Nakamura et al. "Direct observation of anyonic braiding statistics". In: *Nature Phys.* 16.9 (2020), pp. 931–936. DOI: 10.1038/s41567-020-1019-1. arXiv: 2006.14115 [cond-mat.mes-hall].
- [111] H. Bartolomei et al. "Fractional statistics in anyon collisions". In: *Science* 368.6487 (2020), pp. 173–177. DOI: 10.1126/science.aaz5601. arXiv: 2006.13157 [cond-mat.mes-hall].
- [112] R. B. Laughlin. "Anomalous Quantum Hall Effect: An Incompressible Quantum Fluid with Fractionally Charged Excitations". In: *Phys. Rev. Lett.* 50 (18 May 1983), pp. 1395–1398. DOI: 10.1103/PhysRevLett.50.1395.

- [113] G. S. Canright and S. M. Girvin. "Anyons, the quantum Hall effect, and two-dimensional superconductivity". In: *Int. J. Mod. Phys. B* 3 (1989), pp. 1943–1963. DOI: 10.1142/S0217979289001263.
- [114] Samuel Bieri and Jürg Fröhlich. "Physical principles underlying the quantum Hall effect". In: *Comptes Rendus. Physique* 12.4 (May 2011), pp. 332–346. DOI: 10.1016/j.crhy.2011.02.001.
- [115] Shiing-Shen Chern and James Simons. "Characteristic Forms and Geometric Invariants". In: *Annals of Mathematics* 99.1 (1974), pp. 48–69.
- [116] J. Frohlich and C. King. "The Chern-Simons Theory and Knot Polynomials". In: *Commun. Math. Phys.* 126 (1989), p. 167. DOI: 10.1007/BF02124336.
- [117] Spencer D. Stirling. *Abelian Chern-Simons theory with toral gauge group, modular tensor categories, and group categories.* 2008. arXiv: 0807.2857 [hep-th].
- [118] N. Read and G. Moore. "Fractional Quantum Hall Effect and Nonabelian Statistics". In: *Progress of Theoretical Physics Supplement* 107 (1992), pp. 157–166. DOI: 10.1143/ptps.107.157.
- [119] Mitsutoshi Fujita et al. "Fractional quantum Hall effect via holography: Chern-Simons, edge states and hierarchy". In: *Journal of High Energy Physics* 2009.06 (June 2009), pp. 066–066. DOI: 10.1088/1126-6708/2009/06/066.
- [120] Jürgen Fuchs et al. *Algebraic structures in two-dimensional conformal field theory*. 2023. arXiv: 2305.02773 [math.QA].
- [121] Ingo Runkel et al. *Topological and conformal field theory as Frobenius algebras*. 2006. arXiv: math/0512076 [math.CT].
- [122] Steven R. White. "Density matrix formulation for quantum renormalization groups". In: *Phys. Rev. Lett.* 69 (19 Nov. 1992), pp. 2863–2866. DOI: 10.1103/PhysRevLett.69.2863.
- [123] Guifré Vidal. "Efficient Classical Simulation of Slightly Entangled Quantum Computations". In: *Phys. Rev. Lett.* 91 (14 Oct. 2003), p. 147902. DOI: 10. 1103/PhysRevLett.91.147902.
- [124] Norbert Schuch et al. "Entropy Scaling and Simulability by Matrix Product States". In: *Phys. Rev. Lett.* 100 (3 Jan. 2008), p. 030504. DOI: 10 . 1103/PhysRevLett.100.030504.
- [125] J. Ignacio Cirac et al. "Entanglement spectrum and boundary theories with projected entangled-pair states". In: *Physical Review B* 83.24 (June 2011). DOI: 10.1103/physrevb.83.245134.
- [126] Hui Li and F. D. M. Haldane. "Entanglement Spectrum as a Generalization of Entanglement Entropy: Identification of Topological Order in Non-Abelian Fractional Quantum Hall Effect States". In: *Physical Review Letters* 101.1 (July 2008). DOI: 10.1103/physrevlett.101.010504.
- [127] Frank Pollmann et al. "Entanglement spectrum of a topological phase in one dimension". In: *Phys. Rev. B* 81 (6 Feb. 2010), p. 064439. DOI: 10 . 1103/PhysRevB.81.064439.
- [128] D. Pérez-García et al. "String Order and Symmetries in Quantum Spin Lattices". In: *Phys. Rev. Lett.* 100 (16 Apr. 2008), p. 167202. DOI: 10.1103/PhysRevLett.100.167202.

- [129] M. B. Hastings. "Solving gapped Hamiltonians locally". In: *Physical Review B* 73.8 (Feb. 2006). DOI: 10.1103/physrevb.73.085115.
- [130] Alexei Kitaev and John Preskill. "Topological Entanglement Entropy". In: *Phys. Rev. Lett.* 96 (11 Mar. 2006), p. 110404. DOI: 10.1103/PhysRevLett.96. 110404.
- [131] José Garre-Rubio, Sofyan Iblisdir, and David Pérez-García. "Symmetry reduction induced by anyon condensation: A tensor network approach". In: *Phys. Rev. B* 96 (15 Oct. 2017), p. 155123. DOI: 10.1103/PhysRevB.96.155123.
- [132] Henrik Dreyer, J. Ignacio Cirac, and Norbert Schuch. "Projected entangled pair states with continuous virtual symmetries". In: *Phys. Rev. B* 98 (11 Sept. 2018), p. 115120. DOI: 10.1103/PhysRevB.98.115120.
- [133] Dominic J. Williamson et al. "Matrix product operators for symmetry-protected topological phases: Gauging and edge theories". In: *Phys. Rev. B* 94 (20 Nov. 2016), p. 205150. DOI: 10.1103/PhysRevB.94.205150.
- [134] Oliver Buerschaper. "Twisted injectivity in projected entangled pair states and the classification of quantum phases". In: *Annals of Physics* 351 (Dec. 2014), pp. 447–476. DOI: 10.1016/j.aop.2014.09.007.
- [135] Mehmet Burak Şahinoğlu et al. "Characterizing Topological Order with Matrix Product Operators". In: *Annales Henri Poincaré* 22.2 (Jan. 2021), pp. 563–592. DOI: 10.1007/s00023-020-00992-4.
- [136] W. Kohn. "Analytic Properties of Bloch Waves and Wannier Functions". In: *Phys. Rev.* 115 (4 Aug. 1959), pp. 809–821. DOI: 10.1103/PhysRev.115.809.
- [137] Christian Brouder et al. "Exponential Localization of Wannier Functions in Insulators". In: *Phys. Rev. Lett.* 98 (4 Jan. 2007), p. 046402. DOI: 10.1103/PhysRevLett.98.046402.
- [138] Juraj Hasik et al. "Simulating Chiral Spin Liquids with Projected Entangled-Pair States". In: *Phys. Rev. Lett.* 129 (17 Oct. 2022), p. 177201. DOI: 10.1103/PhysRevLett.129.177201.
- [139] Didier Poilblanc, J. Ignacio Cirac, and Norbert Schuch. "Chiral topological spin liquids with projected entangled pair states". In: *Physical Review B* 91.22 (June 2015). DOI: 10.1103/physrevb.91.224431.
- [140] Nikita Sopenko. "Chiral topologically ordered states on a lattice from vertex operator algebra". In: *Adv. Theor. Math. Phys.* 28.1 (2024), pp. 1–35. DOI: 10. 4310/ATMP.2024.v28.n1.a1. arXiv: 2301.08697 [cond-mat.strel].
- [141] Gong Cheng et al. Exact fixed-point tensor network construction for rational conformal field theory. 2024. arXiv: 2311.18005 [cond-mat.str-el].
- [142] Xiang Li et al. *Strict area law entanglement versus chirality*. 2024. arXiv: 2408. 10306 [quant-ph].
- [143] Steven Weinberg. *The Quantum Theory of Fields*. Cambridge University Press, 1995.
- [144] H. Leutwyler. *Goldstone Bosons*. 1994. arXiv: hep-ph/9409422 [hep-ph].

- [145] N. W. Ashcroft and N. D. Mermin. Solid State Physics. Holt-Saunders, 1976.
- [146] Alexander Altland and Ben D. Simons. *Condensed Matter Field Theory*. 2nd ed. Cambridge University Press, 2010.
- "Anyons and Conformal Field Theories". In: *Anyons: Quantum Mechanics of Particles with Fractional Statistics*. Berlin, Heidelberg: Springer Berlin Heidelberg, 1992, pp. 123–131. DOI: 10.1007/978-3-540-47466-1_9.
- [148] Paul Ginsparg. Applied Conformal Field Theory. 1988. arXiv: hep-th/9108028 [hep-th].
- [149] Krzysztof Gawedzki. *Conformal field theory: a case study*. 1999. arXiv: hep-th/9904145 [hep-th].
- [150] Gregory Moore and Nathan Seiberg. "Classical and quantum conformal field theory". In: *Communications in Mathematical Physics* 123.2 (1989), pp. 177–254.
- [151] Matthias R Gaberdiel. "An introduction to conformal field theory". In: *Reports on Progress in Physics* 63.4 (Mar. 2000), pp. 607–667. DOI: 10.1088/0034-4885/63/4/203.
- [152] Peter Goddard. "MEROMORPHIC CONFORMAL FIELD THEORY". In: Jan. 1989.
- [153] Richard E. Borcherds. "Vertex algebras, Kac-Moody algebras, and the Monster". In: *Proceedings of the National Academy of Sciences* 83.10 (1986), pp. 3068–3071. DOI: 10.1073/pnas.83.10.3068. eprint: https://www.pnas.org/doi/pdf/10.1073/pnas.83.10.3068.
- [154] Richard E. Borcherds. "Monstrous moonshine and monstrous Lie superalgebras." In: *Inventiones mathematicae* 109.2 (1992), pp. 405–444.
- [155] Igor Frenkel, James Lepowsky, and Arne Meurman. *Vertex operator algebras and the Monster*. English. Vol. 134. Pure and Applied Mathematics. United States: Academic Press, 1988.
- [156] Yongchang Zhu. "Zhu Y.: Modular invariance of characters of vertex operator algebras. J. Amer. Math. Soc. 9(1), 237-302". In: *Journal of the American Mathematical Society* 9 (Jan. 1996). DOI: 10.1090/S0894-0347-96-00182-8.
- [157] Victor G. Kac. "Vertex algebras for beginners". In: 1997.
- [158] R. Haag. Local quantum physics: Fields, particles, algebras. Springer, 1992.
- [159] Antony J. Wassermann. "Operator Algebras and Conformal Field Theory". In: *International Congress of Mathematicians*. 1995. DOI: 10.1007/978-3-0348-9078-6_89.
- [160] Fabrizio Gabbiani and Jurg Frohlich. "Operator algebras and conformal field theory". In: *Commun. Math. Phys.* 155 (1993), pp. 569–640. DOI: 10.1007/BF02096729.
- [161] Denis Bernard. "On the Wess-Zumino-Witten Models on the Torus". In: *Nucl. Phys. B* 303 (1988), pp. 77–93. DOI: 10.1016/0550-3213(88)90217-9.
- [162] Denis Bernard. "On the Wess-Zumino-Witten Models on Riemann Surfaces". In: *Nucl. Phys. B* 309 (1988), pp. 145–174. DOI: 10.1016/0550-3213(88) 90236-2.

- [163] Yongchang Zhu. "Global vertex operators on Riemann surfaces". In: *Communications in Mathematical Physics* 165 (Oct. 1994). DOI: 10.1007/BF02099421.
- [164] Krzysztof Gawędzki. "SU(2) WZW theory at higher genera". In: *Communications in Mathematical Physics* 169.2 (May 1995), pp. 329–371. DOI: 10.1007/bf02099476.
- [165] Robbert Dijkgraaf, Erik P. Verlinde, and Herman L. Verlinde. "C = 1 Conformal Field Theories on Riemann Surfaces". In: *Commun. Math. Phys.* 115 (1988), pp. 649–690. DOI: 10.1007/BF01224132.
- [166] John L. Cardy. "Boundary conditions, fusion rules and the Verlinde formula". In: *Nuclear Physics B* 324.3 (1989), pp. 581–596. DOI: https://doi.org/10.1016/0550-3213(89)90521-X.
- [167] John Cardy. "Boundary conformal field theory". In: *arXiv preprint hep-th/0411189* (2004).
- [168] David C. Lewellen. "Sewing constraints for conformal field theories on surfaces with boundaries". In: *Nucl. Phys. B* 372 (1992), pp. 654–682. DOI: 10.1016/0550-3213(92)90370-Q.
- [169] G. Pradisi, A. Sagnotti, and Ya S. Stanev. "Planar duality in SU(2) WZW models". In: *Phys. Lett. B* 354 (1995), pp. 279–286. DOI: 10.1016/0370-2693(95)00532-P. arXiv: hep-th/9503207.
- [170] G. Pradisi, A. Sagnotti, and Ya. S. Stanev. "The Open descendants of nondiagonal SU(2) WZW models". In: *Phys. Lett. B* 356 (1995), pp. 230–238. DOI: 10.1016/0370-2693(95)00840-H. arXiv: hep-th/9506014.
- [171] A. M. Polyakov. "Conformal Symmetry of Critical Fluctuations". In: Письма в ЖЭТФ 12 (12 1970), p. 538.
- [172] David Poland, Slava Rychkov, and Alessandro Vichi. "The conformal bootstrap: Theory, numerical techniques, and applications". In: *Reviews of Modern Physics* 91.1 (Jan. 2019). DOI: 10.1103/revmodphys.91.015002.
- [173] G.M. Tuynman and W.A.J.J. Wiegerinck. "Central extensions and physics". In: *Journal of Geometry and Physics* 4.2 (1987), pp. 207–258. DOI: https://doi.org/10.1016/0393-0440(87)90027-1.
- [174] Andrea Cappelli and Jean-Bernard Zuber. *A-D-E Classification of Conformal Field Theories*. 2009. arXiv: 0911.3242 [hep-th].
- [175] Erik Verlinde. "Fusion rules and modular transformations in 2D conformal field theory". In: *Nuclear Physics B* 300 (1988), pp. 360–376. DOI: https://doi.org/10.1016/0550-3213(88)90603-7.
- [176] Y Z Huang. "Geometric interpretation of vertex operator algebras." In: *Proceedings of the National Academy of Sciences* 88.22 (1991), pp. 9964–9968. DOI: 10.1073/pnas.88.22.9964. eprint: https://www.pnas.org/doi/pdf/10.1073/pnas.88.22.9964.
- [177] J. Wess and B. Zumino. "Consequences of anomalous ward identities". In: *Physics Letters B* 37.1 (1971), pp. 95–97. DOI: https://doi.org/10.1016/0370-2693(71)90582-X.

- [178] Edward Witten. "Global aspects of current algebra". In: *Nuclear Physics B* 223.2 (1983), pp. 422–432. DOI: https://doi.org/10.1016/0550-3213(83) 90063-9.
- [179] Matthias Blau and George Thompson. "Derivation of the Verlinde formula from Chern-Simons theory and the G/G model". In: *Nuclear Physics B* 408.2 (Nov. 1993), pp. 345–390. DOI: 10.1016/0550-3213(93)90538-z.
- [180] G. Vidal et al. "Entanglement in Quantum Critical Phenomena". In: *Phys. Rev. Lett.* 90 (22 June 2003), p. 227902. DOI: 10.1103/PhysRevLett.90. 227902.
- [181] J. Dubail and N. Read. "Tensor network trial states for chiral topological phases in two dimensions and a no-go theorem in any dimension". In: *Phys. Rev. B* 92 (20 Nov. 2015), p. 205307. DOI: 10.1103/PhysRevB.92.205307.
- [182] T. B. Wahl et al. "Projected Entangled-Pair States Can Describe Chiral Topological States". In: *Phys. Rev. Lett.* 111 (23 Dec. 2013), p. 236805. DOI: 10.1103/PhysRevLett.111.236805.
- [183] B. Pirvu et al. "Matrix product states for critical spin chains: Finite-size versus finite-entanglement scaling". In: *Physical Review B* 86.7 (Aug. 2012). DOI: 10. 1103/physrevb.86.075117.
- [184] F. Verstraete and J. I. Cirac. "Continuous Matrix Product States for Quantum Fields". In: *Phys. Rev. Lett.* 104 (19 May 2010), p. 190405. DOI: 10.1103/PhysRevLett.104.190405.
- [185] Antoine Tilloy and J. Ignacio Cirac. "Continuous Tensor Network States for Quantum Fields". In: *Phys. Rev. X* 9 (2 May 2019), p. 021040. DOI: 10.1103/PhysRevX.9.021040.
- [186] Anne E. B. Nielsen et al. "Field tensor network states". In: *Phys. Rev. B* 103 (15 Apr. 2021), p. 155130. DOI: 10.1103/PhysRevB.103.155130.
- [187] F. D. M. Haldane. "Exact Jastrow-Gutzwiller resonating-valence-bond ground state of the spin- $\frac{1}{2}$ antiferromagnetic Heisenberg chain with $1/r^2$ exchange". In: *Phys. Rev. Lett.* 60 (7 Feb. 1988), pp. 635–638. DOI: 10.1103/PhysRevLett. 60.635.
- [188] B. Sriram Shastry. "Exact solution of an S = 1/2 Heisenberg antiferromagnetic chain with long-ranged interactions". In: *Phys. Rev. Lett.* 60 (7 Feb. 1988), pp. 639–642. DOI: 10.1103/PhysRevLett.60.639.
- [189] V. Kalmeyer and R. B. Laughlin. "Equivalence of the resonating-valence-bond and fractional quantum Hall states". In: *Phys. Rev. Lett.* 59 (18 Nov. 1987), pp. 2095–2098. DOI: 10.1103/PhysRevLett.59.2095.
- [190] R.B Laughlin. "Spin hamiltonian for which quantum hall wavefunction is exact". In: *Annals of Physics* 191.1 (1989), pp. 163–202. DOI: https://doi.org/10.1016/0003-4916(89)90339-4.
- [191] I. Stakgold and M.J. Holst. *Green's Functions and Boundary Value Problems*. Pure and Applied Mathematics: A Wiley Series of Texts, Monographs and Tracts. Wiley, 2011.
- [192] H.A. Schwarz. In: Journal für die reine und angewandte Mathematik 1869.70 (1869), pp. 105–120. DOI: doi:10.1515/crll.1869.70.105.

- [193] E. B. Christoffel. "Sul problema delle temperature stazionarie e la rappresentazione di una data superficie". In: *Annali di Matematica Pura ed Applicata* (1867-1897) 1 (1867), pp. 89–103.
- [194] R.S. Strichartz. *A Guide To Distribution Theory And Fourier Transforms*. World Scientific Publishing Company, 2003.
- [195] I. S. Gradshteyn and I. M. Ryzhik. *Table of integrals, series, and products*. Seventh. Elsevier/Academic Press, Amsterdam, 2007, pp. xlviii + 1171.
- [196] Martin Gaven Iwaniec Tadeusz. "Riesz transforms and related singular integrals." In: *Journal für die reine und angewandte Mathematik* 473 (1995), pp. 25–58.
- [197] Frederick W. King. *Hilbert Transforms*. Encyclopedia of Mathematics and its Applications. Cambridge University Press, 2009.
- [198] Dang Vu Giang. "Finite Hilbert transforms". In: *Journal of Approximation Theory* 200 (2015), pp. 221–226. DOI: https://doi.org/10.1016/j.jat. 2015.08.001.
- [199] Jiangsheng You and Gengsheng L Zeng. "Explicit finite inverse Hilbert transforms". In: *Inverse Problems* 22.3 (May 2006), p. L7. DOI: 10.1088/0266-5611/22/3/L01.
- [200] M. Fannes, B. Nachtergaele, and R. F. Werner. "Finitely correlated states on quantum spin chains". In: *Communications in Mathematical Physics* 144.3 (1992), pp. 443–490.
- [201] Frank Pollmann et al. "Symmetry protection of topological phases in one-dimensional quantum spin systems". In: *Phys. Rev. B* 85 (7 Feb. 2012), p. 075125. DOI: 10.1103/PhysRevB.85.075125.
- [202] Xie Chen, Zheng-Cheng Gu, and Xiao-Gang Wen. "Classification of gapped symmetric phases in one-dimensional spin systems". In: *Phys. Rev. B* 83 (3 Jan. 2011), p. 035107. DOI: 10.1103/PhysRevB.83.035107.
- [203] M. Sanz et al. "Matrix product states: Symmetries and two-body Hamiltonians". In: *Phys. Rev. A* 79 (4 Apr. 2009), p. 042308. DOI: 10.1103/PhysRevA.79.042308.
- [204] Xie Chen, Zheng-Cheng Gu, and Xiao-Gang Wen. "Classification of gapped symmetric phases in one-dimensional spin systems". In: *Phys. Rev. B* 83 (3 Jan. 2011), p. 035107. DOI: 10.1103/PhysRevB.83.035107.
- [205] Ruben Verresen, Nick G. Jones, and Frank Pollmann. "Topology and Edge Modes in Quantum Critical Chains". In: *Physical Review Letters* 120.5 (Jan. 2018). DOI: 10.1103/physrevlett.120.057001.
- [206] Ruben Verresen, Roderich Moessner, and Frank Pollmann. "One-dimensional symmetry protected topological phases and their transitions". In: *Phys. Rev. B* 96 (16 Oct. 2017), p. 165124. DOI: 10.1103/PhysRevB.96.165124.
- [207] Ruben Verresen et al. "Gapless Topological Phases and Symmetry-Enriched Quantum Criticality". In: *Phys. Rev. X* 11 (4 Dec. 2021), p. 041059. DOI: 10. 1103/PhysRevX.11.041059.

- [208] Anne E B Nielsen, J Ignacio Cirac, and Germán Sierra. "Quantum spin Hamiltonians for the SU(2) kWZW model". In: 2011.11 (Nov. 2011), P11014. DOI: 10.1088/1742-5468/2011/11/p11014.
- [209] Brian C Hall. "An elementary introduction to groups and representations". In: *arXiv preprint math-ph/0005032* (2000).
- [210] V. Bargmann. "On Unitary Ray Representations of Continuous Groups". In: *Annals of Mathematics* 59.1 (1954), pp. 1–46.
- [211] Chanchal K. Majumdar and Dipan K. Ghosh. "On Next-Nearest-Neighbor Interaction in Linear Chain. I". In: *Journal of Mathematical Physics* 10.8 (Aug. 1969), pp. 1388–1398. DOI: 10.1063/1.1664978.
- [212] Steven A. Kivelson, Daniel S. Rokhsar, and James P. Sethna. "Topology of the resonating valence-bond state: Solitons and high- T_c superconductivity". In: *Phys. Rev. B* 35 (16 June 1987), pp. 8865–8868. DOI: 10.1103/PhysRevB. 35.8865.
- [213] M. Sanz et al. "Matrix product states: Symmetries and two-body Hamiltonians". In: *Phys. Rev. A* 79 (4 Apr. 2009), p. 042308. DOI: 10.1103/PhysRevA.79.042308.
- [214] Frank Pollmann et al. "Symmetry protection of topological phases in onedimensional quantum spin systems". In: *Phys. Rev. B* 85 (7 Feb. 2012), p. 075125. DOI: 10.1103/PhysRevB.85.075125.
- [215] Jutho Haegeman et al. "Calculus of continuous matrix product states". In: *Physical Review B* 88.8 (Aug. 2013). DOI: 10.1103/physrevb.88.085118.
- [216] Benoît Tuybens et al. "Variational Optimization of Continuous Matrix Product States". In: *Phys. Rev. Lett.* 128 (2 Jan. 2022), p. 020501. DOI: 10 . 1103 / PhysRevLett.128.020501.
- [217] Damian Draxler et al. "Continuous matrix product states with periodic boundary conditions and an application to atomtronics". In: *Physical Review B* 95.4 (Jan. 2017). DOI: 10.1103/physrevb.95.045145.
- [218] Jutho Haegeman et al. "Entanglement Renormalization for Quantum Fields in Real Space". In: *Phys. Rev. Lett.* 110 (10 Mar. 2013), p. 100402. DOI: 10.1103/PhysRevLett.110.100402.
- [219] Adrián Franco-Rubio and Guifré Vidal. "Entanglement and correlations in the continuous multi-scale entanglement renormalization ansatz". In: *Journal of High Energy Physics* 2017.12 (Dec. 2017). DOI: 10.1007/jhep12(2017)129.
- [220] Su-Kuan Chu et al. "Scale-Invariant Continuous Entanglement Renormalization of a Chern Insulator". In: *Physical Review Letters* 122.12 (Mar. 2019). DOI: 10. 1103/physrevlett.122.120502.
- [221] Adrián Franco-Rubio. "Entanglement renormalization for quantum fields with boundaries and defects". In: *Phys. Rev. B* 104 (12 Sept. 2021), p. 125131. DOI: 10.1103/PhysRevB.104.125131.
- [222] David Jennings et al. "Continuum tensor network field states, path integral representations and spatial symmetries". In: *New J. Phys.* 17.6 (2015), p. 063039. DOI: 10.1088/1367-2630/17/6/063039. arXiv: 1212.3833 [quant-ph].

- [223] David Jennings et al. "Continuum tensor network field states, path integral representations and spatial symmetries". In: *New Journal of Physics* 17.6 (June 2015), p. 063039. DOI: 10.1088/1367-2630/17/6/063039.
- [224] Teresa D. Karanikolaou, Patrick Emonts, and Antoine Tilloy. "Gaussian continuous tensor network states for simple bosonic field theories". In: *Phys. Rev. Research* 3 (2 Apr. 2021), p. 023059. DOI: 10.1103/PhysRevResearch.3.023059.
- [225] Antoine Tilloy. "Relativistic continuous matrix product states for quantum fields without cutoff". In: *Phys. Rev. D* 104 (9 Nov. 2021), p. 096007. DOI: 10.1103/PhysRevD.104.096007.
- [226] Raz Firanko, Moshe Goldstein, and Itai Arad. "Area law for steady states of detailed-balance local Lindbladians". In: *Journal of Mathematical Physics* 65.5 (May 2024), p. 051901. DOI: 10.1063/5.0167353. eprint: https://pubs.aip.org/aip/jmp/article-pdf/doi/10.1063/5.0167353/19952691/051901_1_5.0167353.pdf.
- [227] Antoine Tilloy. *Relativistic continuous matrix product states for quantum fields without cutoff.* 2021. arXiv: 2102.07741 [quant-ph].
- [228] Vladimir Fateev et al. "Expectation values of local fields in the Bullough-Dodd model and integrable perturbed conformal field theories". In: *Nuclear Physics B* 516.3 (Apr. 1998), pp. 652–674. DOI: 10.1016/s0550-3213(98)00002-9.
- [229] V.A Fateev and A.V Litvinov. "Correlation functions in conformal Toda field theory I". In: *Journal of High Energy Physics* 2007.11 (Nov. 2007), pp. 002–002. DOI: 10.1088/1126-6708/2007/11/002.